

**DEVELOPMENT OF PHOTOREDOX CATALYSIS-MEDIATED
FUNCTIONALIZATION METHODS FOR ARENES AND OLEFINS**

Megan Elizabeth Schutzbach-Horton

A dissertation submitted to the faculty at the University of North Carolina at Chapel Hill in
partial fulfillment of the requirements for the degree of Doctor of Philosophy in the
Department of Chemistry.

Chapel Hill
2020

Approved by:

David A. Nicewicz

Jeffrey S. Johnson

Abigail S. Knight

Frank A. Leibfarth

Marcey L. Waters

© 2020
Megan Elizabeth Schutzbach-Horton
ALL RIGHTS RESERVED

ABSTRACT

Megan Elizabeth Schutzbach-Horton: DEVELOPMENT OF PHOTOREDOX CATALYSIS-MEDIATED FUNCTIONALIZATION METHODS FOR ARENES AND OLEFINS
(Under the direction of David A. Nicewicz)

I. Introduction to Organic Photoredox Catalysis

This chapter provides a brief discussion of relevant photophysical properties and the thermodynamics of photoinduced electron transfer. The development of acridinium ion catalysts and their use by our lab is also included.

II. Development of Photoredox Catalysis-Mediated Methods for the Hydrofunctionalization of Glycols

Efforts to-date on the development of glycol hydrofunctionalization methods using acridinium-mediated photoredox catalysis are summarized. This work includes data obtained by Heqing Sun on the use of *exo*-glycols as substrates in a hydroalkoxylation reaction. The latter portion of the chapter summarizes efforts towards the use of *endo*-glycols as substrates in a variety of hydrofunctionalization methods, including hydroamination and hydroalkoxylation reactions.

III. Development of a Photoredox-Mediated Method for the Anti-Markovnikov Hydroazidation of Activated Olefins

This chapter discusses the use of acridinium-mediated photoredox catalysis in the development of an anti-Markovnikov hydroazidation method that is complementary to existing work. Using mild conditions that feature the use of TMSN₃ and TFE, we report the synthesis of 31 organic azides in yields ranging from 22 – 98%.

IV. Development of a Method for the Nucleophilic Defluorination of Electron-Neutral and Electron-Rich Fluoroarenes

In this chapter, the development of a general method for the use of electron-neutral and electron-rich fluoro(hetero)arenes as substrates in a CRA-S_NAr reaction is discussed. Using both an acridinium catalyst, as well as a novel xanthylium catalyst, conditions were developed for 78 examples of nucleophilic defluorination in a manner that is complementary to existing S_NAr chemistry.

ACKNOWLEDGEMENTS

The success of my graduate studies is the result of so many individuals beyond myself. I have had the privilege of interacting with so many incredible human beings over the course of my undergraduate/graduate studies and would be remiss if I didn't acknowledge that support. First, I would like to thank my advisor, Dave Nicewicz, for the opportunity to work in his lab for the last five years. Dave: I cannot tell you how much I appreciate the opportunity to learn and grow as a scientist under your guidance. I appreciate your commitment to ensuring that I succeed and your support of my professional goals.

To my committee: Thank you for your willingness to support me over the course of my graduate studies. I appreciate the guidance in terms of research, as well as professional matters. I am so incredibly thankful to find myself in a department that values graduate students as much as the Chemistry Department at UNC does. I can't tell you how grateful I am for the greetings in the hallways, conversations in passing, and general interest in my well-being. Knowing that I have the support of so many incredible faculty members has made graduate school so much more bearable.

To my coworkers: I am so grateful to have surrounded myself with all of you incredible scientists. When I first joined the lab, I was afraid that I wouldn't fit in because everyone was so "normal". That fear was soon put to rest when Cole Cruz convinced Cortney Cavanaugh to show me her velociraptor impersonation. Turns out, "normal" is vastly overrated. Everyone that I've interacted with over the years has brightened my world in so many ways. I am constantly in awe of the insane amount of talent that is possessed by the

members of the group, and I have appreciated all of the fruitful discussions I've had with colleagues over the years. I am so grateful for the love and support that you all have shown me over the last five years. Thank you for eating all of my gluten free baked goods and being good sports about being forced to draw for Secret Santa on November 1st.

To my friends: There is no way that I would have made it through graduate school without your fierce friendship and support. You have been such incredible supporters along this crazy, bumpy road. To keep things short, I will simply say thank you again. Know that this accomplishment is as much yours as it is mine because each and every one of you believed in me when I couldn't believe in myself.

To my family: Mom and Dad, this is for you. Thank you for believing in me from the beginning and seeing me through the rough patches. Everyone thinks that you have to be a genius to go to graduate school, but the truth is that hard work and dedication get you so much farther than sheer intelligence. Thank you for teaching me how to work hard and see things through to the end. There is no doubt in my mind that all of my strengths and abilities were inherited from you, and I am so grateful for your love and support. Ben: Thank you for reminding me to laugh and that I will never be as smart as you. I find that I am constantly in need of your reminders to take myself less seriously and enjoy life.

Matthew Charles: Thank you for finding me. I am so incredibly grateful for the opportunity to experience life with you. Your endless optimism and huge heart are a constant joy. Thank you for supporting me and giving me strength to tackle life's challenges. There is no one else that I would rather be on this crazy adventure with. I love you endlessly.

Graduate school has undoubtedly been the most challenging experience of my life thus far. If you had asked me during the early days (okay, pretty much any day), I would

have sworn to you that I was always on the verge of failing out. But thanks to the support of my colleagues, friends, family, etc., I found the strength to push through. Special shout out to SSRI's, buckets of coffee, and murder-related podcasts for helping me get by as well.

SSDGM.

PREFACE

A portion of the work discussed in Chapter 2 was carried out by Heqing Sun, an alumnus of the Nicewicz group. Heqing carried out initial work on the functionalization of glycals with external olefins and preliminary investigations on substrates with internal olefins. His work provided extensive insight into the behavior of glycals in our acridinium-mediated hydrofunctionalization systems. I am grateful for all of the support he provided while at UNC and beyond.

The work discussed in Chapter 3 was performed in collaboration with Nicholas Onuska and José Rosario Collazo. Nicholas and I worked on initial reaction optimization, and the three of us explored the substrate scope for this transformation.

Chapter 4 was a collaboration with Vincent Pistrutto. Vincent worked on the defluorination of electron-neutral fluoroarenes using pyrazole as a nucleophile, as well as the defluorination of electron-rich fluoro(hetero)arenes using nitrogenous nucleophiles. I had the privilege of exploring the scope of azole nucleophiles for the defluorination of electron-neutral fluoroarenes, as well as the defluorination of electron-rich fluoro(hetero)arenes using carboxylic acid nucleophiles.

*I dedicate this dissertation to every woman who was
ever told that she would never succeed.*

“Nevertheless, she persisted”

TABLE OF CONTENTS

CHAPTER 1: INTRODUCTION TO ORGANIC PHOTOREDOX CATALYSIS	1
1.1 Introduction.....	1
1.2 Organic Photoredox Catalysis Background	2
1.2.1 Photophysics of Organic Photoredox Catalysis	2
1.2.2 Exploring the Thermodynamics of Photoinduced Electron Transfer (PET).....	8
1.2.3 Use of Acridinium Salts as Organic Photoredox Catalysts.....	12
1.3 Prior Nicewicz Lab Work	20
1.3.1 Development of Olefin Hydrofunctionalization Reactions	20
1.3.2 Development of Cation-Radical-Accelerated Nucleophilic Aromatic Substitution Reactions	24
1.4 Conclusions.....	26
CHAPTER 2: DEVELOPMENT OF PHOTOREDOX CATALYSIS-MEDIATED METHODS FOR THE HYDROFUNCTIONALIZATION OF GLYCALs	28
2.1 Introduction.....	28
2.1.1 Glycosides and Their Importance	28
2.1.2 Synthesis of Aminoglycosides <i>via</i> Polar Chemistry	32
2.1.3 Synthesis of Deoxyglycosides <i>via</i> Polar Chemistry	38
2.1.4 Synthesis of Glycomimetics <i>via</i> Polar Chemistry.....	42
2.1.5 Synthesis of Glycosides and Glycomimetics <i>via</i> Photoredox/Photoacid Catalysis	54
2.1.6 Extension of Photoredox Catalysis to the Synthesis of Novel Glycosides	64

2.2 Results and Discussion	65
2.2.1 Previous Work.....	65
2.2.2 Method Development.....	70
2.2.3 Computational Studies	102
2.3 Conclusions.....	102
2.4 Future Work	102
2.5 Acknowledgements.....	103
CHAPTER 3: DEVELOPMENT OF A PHOTOREDOX-MEDIATED METHOD FOR THE ANTI-MARKOVNIKOV HYDROAZIDATION OF ACTIVATED OLEFINS.....	104
3.1 Introduction.....	104
3.1.1 Importance of Hydroazidation Products	104
3.1.2 Previous Hydroazidation Methods.....	107
3.2 Results and Discussion	115
3.2.1 Development of Hydroazidation Method	115
3.3 Conclusions.....	127
3.4 Acknowledgements.....	128
CHAPTER 4: DEVELOPMENT OF A METHOD FOR THE NUCLEOPHILIC DEFLUORINATION OF ELECTRON-NEUTRAL AND ELECTON-RICH FLUOROARENES	129
4.1 Introduction.....	129
4.1.1 Importance of Nucleophilic Aromatic Substitution	129
4.1.2 Previous Defluorination Methods	135
4.2 Results and Discussion	144
4.2.1 Defluorination of Electron-Neutral Fluoroarenes Using Azoles as Nucleophiles	144

4.2.2 Intramolecular Defluorination of Electron-Neutral Fluoroarenes Using Carboxylic Acids as Nucleophiles	152
4.2.3 Defluorination of Electron-Rich Fluoroarenes Using Nitrogenous Nucleophiles.....	157
4.2.4 Defluorination of Electron-Rich Fluoroarenes Using Carboxylic Acids as Nucleophiles.....	168
4.2.5 Computational Studies	178
4.3 Conclusions.....	180
4.4 Future Work	180
4.5 Acknowledgements.....	180
APPENDIX A: EXPERIMENTAL DATA FOR CHAPTER 2.....	181
A.1 General Experimental Information	181
A.2 Synthesis of Photoredox Catalysts and Substrates.....	183
A.3 General Procedure for Hydrofunctionalization of <i>Exo</i> - and <i>Endo</i> -Glycals and Characterization of Products.....	199
APPENDIX B: EXPERIMENTAL DATA FOR CHAPTER 3	213
B.1 General Experimental Information	213
B.2 Catalyst and Substrate Synthesis.....	216
B.3 Characterization of Hydroazidation Products	227
APPENDIX C: EXPERIMENTAL DATA FOR CHAPTER 4	243
C.1 General Experimental Information	243
C.2 Electrochemical and Photophysical Methods	244
C.3 Synthesis and Characterization of Catalysts and Substrates	254
C.4 Experimental Procedures and Characterization of Reaction Products.....	270
REFERENCES	321

LIST OF FIGURES

Figure 1-1. Molecular Orbital Depiction of Photoinduced Electron Transfer	3
Figure 1-2. Jablonski Diagram Showing Possible Pathways After Excitation	3
Figure 1-3. Molecular Orbital Depictions of PET Scenarios	6
Figure 1-4. Molecular Orbital Depiction of Back Electron Transfer	7
Figure 1-5. Examples of Ground State Oxidation Potentials of Organic Molecules	11
Figure 1-6. Examples of Organic Photoredox Catalysts	11
Figure 1-7. Representative Examples of Acridinium Salts	12
Figure 1-8. Acridinium Salt Deactivation By Nucleophilic Addition	13
Figure 1-9. Charge Transfer State of Fukuzumi's Acridinium Salt	13
Figure 1-10. Catalyst Deactivation <i>Via</i> Nucleophilic Addition to Acridine Core	17
Figure 1-11. Robust Acridinium Salt Developed by Nicewicz and Coworkers	18
Figure 1-12. Novel Acridinium Salts Synthesized by Nicewicz and Coworkers	19
Figure 2-1. Carbohydrate-Containing Biologically Relevant Molecules	29
Figure 2-2. Aminoglycoside-Containing Pharmaceuticals	30
Figure 2-3. Examples of Biologically Relevant Deoxyglycosides	30
Figure 2-4. Examples of Pharmaceuticals Containing Glycomimetics	31
Figure 2-5. General Scheme Depicting Glycomimetics with Novel Linkages	43
Figure 2-6. Rationale for Exclusive Formation of <i>Z</i> -Olefins	56
Figure 2-7. Generation of Charge Transfer State of 9-Mesityl Acridiniums	56
Figure 2-8. Novel and Commercial Photoacid Catalysts	57
Figure 2-9. Conformational Studies on Tri- <i>O</i> -Acetyl Glycals	74
Figure 2-10. Redesigned Glycal Substrate	77

Figure 2-11. Catalyst Key for Table 2-10	82
Figure 2-12. Tentative Stereochemical Assignments for Hydroamination Products.....	84
Figure 2-13. Rationale for Nucleophile Approach.....	84
Figure 2-14. H-Atom Donor Key for Table 2-16.....	94
Figure 3-1. Biologically Relevant Compounds Possessing Nitrogenous Functionality	104
Figure 3-2. Kinetic Data for Azide Addition Into Styrenyl Cation Radicals.....	116
Figure 4-1. (Hetero)arenes Possessing Biologically Relevant Properties.....	129
Figure 4-2. (Hetero)aromatic Natural Products of Interest to the Synthetic Community ...	130
Figure 4-3. Photoredox Catalyst Key for Table 4-2.....	148
Figure 4-4. NPA Values for Ground State and Cation Radical of 4-Fluoroanisole.....	179
Figure 4-5. NPA Values for 2-Chloro-4-Fluoroanisole	180
Figure C-1. CV of 4-Fluorotoluene	245
Figure C-2. CV of 3,4-Dimethyl-fluorobenzene	246
Figure C-3. CV of 2,6-Dimethyl-fluorobenzene	247
Figure C-4. CV of 2-Fluoro-5-trifluoromethylanisole.....	248
Figure C-5. CV of 4-Fluoroanisole.....	249
Figure C-6. Absorption and Emission Spectra for Catalyst A	250
Figure C-7. CV of Catalyst A	251
Figure C-8. Absorption and Emission Spectra for Catalyst C	252
Figure C-9. CV of Catalyst C	252
Figure C-10. Absorption and Emission Spectra for Catalyst D	253
Figure C-11. CV of Catalyst D	254
Figure C-12. Racemic HPLC Trace for Standard of 4.38	312

Figure C-13. HPLC Trace of Enantiopure 4.38	312
Figure C-14. Ground State and Excited State NPA Values for Substrates.....	319
Figure C-15. Additional NPA Data for Substrates	320

LIST OF SCHEMES

Scheme 1-1. Fukuzumi's Aerobic Bromination Method and Representative Scope	14
Scheme 1-2. Proposed Mechanism for Aerobic Bromination	15
Scheme 1-3. Representative Scope of Transformations Featuring Acridinium Catalysts	16
Scheme 1-4. Select Methods Developed by Nicewicz and Coworkers.....	21
Scheme 1-5. Proposed Mechanism for Anti-Markovnikov Hydrofunctionalization	22
Scheme 1-6. Disulfide Crossover Experiment	23
Scheme 1-7. Summary of CRA-S _N Ar Methods Developed by Nicewicz and Coworkers.....	25
Scheme 1-8. Proposed Mechanistic Pathway for CRA-S _N Ar Methods	26
Scheme 2-1. General Strategies for Derivatization of Glycosides	32
Scheme 2-2. Strategies for the Synthesis of Aminoglycosides	33
Scheme 2-3. Giese's Synthesis of Aminoglycosides	34
Scheme 2-4. Azidonitration of Peracetylated Galactal Derivative.....	35
Scheme 2-5. Azidonitration of Peracetylated Glucal Derivative	35
Scheme 2-6. Carreira's Synthesis of Aminoglycosides Using Mn Catalysis.....	37
Scheme 2-7. DuBois' Synthesis of Aminoglycosides Using Rh Catalysis	38
Scheme 2-8. Representative Methods for Deoxyglycoside Synthesis	39
Scheme 2-9. Gagné's Synthesis of Deoxyglycosides and Linear Carbohydrates	41
Scheme 2-10. Synthesis of Deoxyglycosides Using Boron Catalysis.....	42
Scheme 2-11. Strategies for the Synthesis of Novel Linkages.....	43
Scheme 2-12. Routes Used to Synthesize C-Glycosides.....	44
Scheme 2-13. Walczak's Methods for the Synthesis of C-Glycosides	46
Scheme 2-14. Radical-Mediated Methods for the Synthesis of C-Glycosides	47

Scheme 2-15. Langer's Synthesis of Indol- <i>N</i> -Glycoside	48
Scheme 2-16. Synthesis of <i>N</i> -Linked Glycopeptides from Glycosyl Azides.....	49
Scheme 2-17. Synthesis of Disaccharides with <i>N</i> -Linkages	50
Scheme 2-18. Transition Metal-Mediated Synthesis of <i>S</i> -Glycosides	51
Scheme 2-19. Sequential Synthesis of <i>S</i> -Oligosaccharides.....	52
Scheme 2-20. Radical-Mediated Synthesis of <i>S</i> -Glycosides.....	53
Scheme 2-21. Photoredox-Mediated Trifluoromethylation of <i>Exo</i> -Glycals	55
Scheme 2-22. Model Reaction for Photoredox-Mediated Glycosylation	58
Scheme 2-23. Scope of <i>Endo</i> -Glycal Substrates in Photoredox-Mediated Glycosylation.....	59
Scheme 2-24. Scope of Alcohol Nucleophiles in Photoredox-Mediated Glycosylation.....	61
Scheme 2-25. Substrate Scope for Synthesis of <i>C</i> -Glycosides	63
Scheme 2-26. Oxidized Byproduct and Proposed Mechanism of Formation	72
Scheme 2-27. Proposed Mechanism for Hydrofunctionalization of <i>Endo</i> -Glycals	97
Scheme 3-1. Divergent Reactivity Stemming From Organoazides.....	105
Scheme 3-2. Synthesis of Alkyl Azides <i>via</i> S _N 2 Pathway	105
Scheme 3-3. Use of the Mitsunobu Reaction to Synthesize Azides.....	106
Scheme 3-4. Use of Alkyl Azide Intermediates in the Synthesis of Natural Products	106
Scheme 3-5. Mechanistic Possibilities for Lewis Acid-Mediated Hydroazidation.....	108
Scheme 3-6. Surface-Mediated Hydroazidation of Olefins	109
Scheme 3-7. Conditions and Scope for Cobalt-Catalyzed Hydroazidation of Olefins	110
Scheme 3-8. Modern Methods for the Hydroazidation of Olefins	111
Scheme 3-9. Electrochemical Methods for the Synthesis of Alkyl Azides.....	112
Scheme 3-10. Photoredox Catalysis-Mediated Hydroazidation of <i>N</i> -Phenyl Amides.....	113

Scheme 3-11. Anti-Markovnikov Hydroazidation of Unactivated Olefins.....	114
Scheme 3-12. Azide Reactivity Influenced by Solvent Identity	117
Scheme 3-13. Mechanistic Proposal for the Formation of Thiol-Ene Byproduct	118
Scheme 3-14. Substrate Scope for the Anti-Markovnikov Hydroazidation.....	125
Scheme 3-15. Mechanistic Proposal for Hydroazidation of Olefins	126
Scheme 4-1. Mechanistic Possibilities for S _N Ar Reaction	131
Scheme 4-2. Orbital Alignment for Concerted S _N Ar Pathway	132
Scheme 4-3. Computational Determination of Meisenheimer Intermediate	133
Scheme 4-4. Regioselectivity Challenges Associated with Benzyne	133
Scheme 4-5. Early Example of S _N Ar with Unactivated Fluoroarene Substrate	136
Scheme 4-6. Formation of Aryl Ethers <i>via</i> S _N Ar with Fluoroarene Substrates	137
Scheme 4-7. Ru-Catalyzed Amination of Unactivated Fluoroarenes	138
Scheme 4-8. Representative Scope for <i>N</i> -Arylation of Nitrogenous Heterocycles.....	139
Scheme 4-9. Representative Scope for Aliphatic Amination of Fluoroarenes.....	141
Scheme 4-10. Synthesis of Vortioxetine <i>via</i> S _N Ar with Fluoroarene.....	142
Scheme 4-11. Representative Scope for DDQ-Mediated S _N Ar with Fluoroarenes	143
Scheme 4-12. Fluoroarene Scope for Nucleophilic Defluorination with Pyrazole	150
Scheme 4-13. Scope of Azoles Compatible with Defluorination Conditions	151
Scheme 4-14. Substrate Scope for Intramolecular Defluorination Reaction	156
Scheme 4-15. Fluoroanisole Derivatives Compatible with Defluoroamination	162
Scheme 4-16. Scope of Fluoroarenes Compatible with Defluoroamination	164
Scheme 4-17. Heterofluoroarene Scope Compatible with Defluoroamination Conditions .	165
Scheme 4-18. Amine Nucleophile Scope for Defluoroamination Reaction.....	167

Scheme 4-19. Fluoroanisole Derivatives Compatible with Defluorooxygenation.....	173
Scheme 4-20. Scope of Fluoroarenes Compatible with Defluorooxygenation Conditions..	175
Scheme 4-21. Heterofluoroarenes Compatible with Defluorooxygenation	176
Scheme 4-22. Carboxylic Acid Nucleophile Scope	177
Scheme A-1. Synthesis of 2.29	187
Scheme A-2. Synthesis of 2.30	190
Scheme A-3. Synthesis of 2.32	190
Scheme A-4. Synthesis of 2.34	191
Scheme C-1. Synthesis of 4.54	262
Scheme C-2. Synthesis of 4.57	264
Scheme C-3. Synthesis of 4.63	268

LIST OF TABLES

Table 2-1. Representative Examples of Glycal Functionalization	36
Table 2-2. Solvent Screen for Hydroalkoxylation of <i>Exo</i> -Glycal	66
Table 2-3. Condition Optimization for Hydroalkoxylation of <i>Exo</i> -Glycal	67
Table 2-4. Additional Optimization for Hydroalkoxylation of <i>Exo</i> -Glycal	68
Table 2-5. Nucleophile Scope for Hydrofunctionalization of <i>Exo</i> -Glycals	69
Table 2-6. Initial Solvent Screen for Hydroamination of <i>Endo</i> -Glycal	71
Table 2-7. Base Loading and Identity Screen for Hydroamination of <i>Endo</i> -Glycal	73
Table 2-8. Reactivity Screen for Hydrofunctionalization of <i>Endo</i> -Glycal	76
Table 2-9. Optimization with Redesigned Glycal Substrate	79
Table 2-10. Catalyst and Base Optimization for Hydroamination of <i>Endo</i> -Glycal	81
Table 2-11. Initial Optimization Using Triflamide as a Nucleophile	85
Table 2-12. Optimization Using Ammonium Carbamate as a Nucleophile	86
Table 2-13. Initial Optimization Using Methanol as a Nucleophile	88
Table 2-14. Catalyst and Base Loading Screen for Hydroalkoxylation of <i>Endo</i> -Glycal	89
Table 2-15. Base Identity Screen for Hydroalkoxylation of <i>Endo</i> -Glycal	91
Table 2-16. H-Atom Donor Screen for Hydroalkoxylation of <i>Endo</i> -Glycal	93
Table 2-17. Optimization of Acridinium-Mediated Glycosylation	95
Table 2-18. Further Condition Optimization for Acridinium-Mediated Glycosylation	96
Table 2-19. Attempts at Difunctionalization of <i>Endo</i> -Glycals	99
Table 2-20. Hydrofunctionalization of Disiloxane-Protected <i>Endo</i> -Glycal	101
Table 3-1. Initial Reaction Optimization of the Hydroazidation of Indene	115
Table 3-2. Optimization of Azide Loading	119

Table 3-3. Optimization of Acridinium Salt Loading	120
Table 3-4. Initial Results for the Hydroazidation of Unsubstituted Styrenes	121
Table 3-5. H-Atom Donor Screen for Unsubstituted Styrenes	122
Table 3-6. H-Atom Donor Loading Screen for Unsubstituted Styrenes	123
Table 3-7. Effect of More Reactive H-Atom Donor on Various Terminal Styrenes	124
Table 4-1. Initial Catalyst Screen to Observe Reactivity	145
Table 4-2. Reaction Optimization for Defluorination of 4-Fluorotoluene with Pyrazole....	147
Table 4-3. Optimization for Defluorooxygenation of 4-Fluorotoluene	153
Table 4-4. Reaction Optimization for Intramolecular Defluorination	155
Table 4-5. Reaction Optimization for Defluorination with Ammonium Carbamate	159
Table 4-6. Reaction Optimization for Defluorination with Benzyl Amine.....	161
Table 4-7. Identification of Optimal Base for Defluorination with Benzoic Acid	168
Table 4-8. Identification of Optimal Catalyst for Defluorooxygenation	170
Table 4-9. Reaction Optimization with 4-Fluoroanisole as the Model Substrate	172

LIST OF ABBREVIATIONS

α	Alpha
β	Beta
δ	Delta
λ	Wavelength
τ	Excited State Lifetime of Fluorescence
μs	Microseconds
1,5-AF	1,5-Anhydrofructose
1,5-AG	1,5-Anhydroglucitol
A	Acceptor
Ac	Acetyl
AIBN	2,2'-Azobis(2-methylpropionitrile)
BET	Back Electron Transfer
BLEDs	Blue Light Emitting Diodes
Bn	Benzyl
Bu	Butyl
Bz	Benzoyl
CAN	Ceric Ammonium Nitrate
CFL	Compact Fluorescent Lightbulb
CRA-S _N Ar	Cation Radical-Accelerated Nucleophilic Aromatic Substitution
CT	Charge Transfer
CV	Cyclic Voltammogram
D	Donor

d	Doublet
dd	Doublet of Doublets
ddd	Doublet of Doublet of Doublets
dt	Doublet of Triplets
DCE	1,2-Dichloroethane
DCM	Dichloromethane
DEAD	Diethyl Azodicarboxylate
DIAD	Diisopropyl Azodicarboxylate
DMDC	Dimethyl Dicarboxylate
DPPA	Diphenyl Phosphoryl Azide
d.r.	Diastereomeric Ratio
E ⁺	Electrophile
e ⁻	Electron
ET	Electron Transfer
EDG	Electron Donating Group
Et	Ethyl
EWG	Electron Withdrawing Group
E _{0,0}	Excited State Energy
E _{ox}	Ground State Oxidation Potential
E _{red}	Ground State Reduction Potential
E* _{red}	Excited State Reduction Potential
F	Faraday Constant
ΔG _{ET}	Gibbs Free Energy of Electron Transfer

ΔG_{PET}	Gibbs Free Energy of Photoinduced Electron Transfer
HAT	Hydrogen Atom Transfer
Hex	Hexyl
HFIP	1,1,1,3,3,3-Hexafluoroisopropanol
HMPA	Hexamethylphosphoric Triamide
HOMO	Highest Occupied Molecular Orbital
$h\nu$	Photon
Hz	Hertz
IC	Internal Conversion
ISC	Intersystem Crossing
J	Coupling Constant
k_q	Bimolecular Quenching Constant
LDA	Lithium Diisopropylamide
LFP	Laser Flash Photolysis
LUMO	Lowest Unoccupied Molecular Orbital
MeCN	Acetonitrile
MHz	Megahertz
m	Multiplet
m -	Meta
NFSI	N-Fluorobenzenesulfonimide
nm	Nanometer
NMP	N-Methyl-2-Pyrrolidone
NMR	Nuclear Magnetic Resonance

NO	Nitric Oxide
NOESY	Nuclear Overhauser Effect Spectroscopy
NPA	Natural Population Analysis
ns	Nanosecond
Nuc.	Nucleophile
<i>o</i> -	Ortho
<i>p</i> -	Para
PET	Photoinduced Electron Transfer
PG	Protecting Group
PhCF ₃	Trifluorotoluene
PhMe	Toluene
PMN	2-Phenylmalononitrile
ppm	Parts Per Million
Pr	Propyl
q	Quartet
r.r.	Regiomic Ratio
r.t.	Room Temperature
s	Singlet
SCE	Standard Calomel Electrode
SET	Single Electron Transfer
S _N Ar	Nucleophilic Aromatic Substitution
SOMO	Singularly Occupied Molecular Orbital
S ₀	Ground State Singlet

S ₁	First Excited State Singlet
t	Triplet
tBu	Tert-Butyl
TBAF	Tetrabutylammonium Fluoride
TBS	Tert-butyl-dimethylsilyl
Tces	2,2,2-Trichloroethoxysulfonamide
TEMPO	(2,2,6,6-Tetramethylpiperidin-1-yl)oxyl
TFAA	Trifluoroacetic Anhydride
TFE	2,2,2-Trifluoroethanol
THF	Tetrahydrofuran
TLC	Thin-Layer Chromatography
TMS	Trimethylsilyl
T ₁	First Excited State Triplet
UV	Ultraviolet
V	Volt
W	Watts
X	Halogen

CHAPTER 1: INTRODUCTION TO ORGANIC PHOTOREDOX CATALYSIS

1.1 Introduction

As the need to access more complex synthetic targets becomes increasingly important, the synthetic organic community is challenged to develop novel methods for the construction of these molecules. As such, many new areas of chemistry for building up molecular complexity have been explored, including electrochemistry¹, flow chemistry², and photoredox catalysis.^{3,4} These fields offer access to transformations and molecules that have previously been difficult or impossible to achieve through traditional two-electron avenues.

In particular, the use of photoredox catalysis to facilitate the construction of challenging bonds and molecules has grown drastically over the last decade. The use of visible light to generate radicals is of great interest to the chemical community as an alternative to UV light. In contrast to UV light, visible light is only absorbed by molecules possessing extended conjugation, which allows for the selective generation of radicals in a complex reaction mixture. The generation of radicals is typically accomplished through the use of a photocatalyst that possesses extended conjugation (i.e. can absorb visible light) and can participate in electron transfer with the desired radical precursor in solution.

Common transition metal-based photoredox catalysts are polypyridyl ruthenium(II)- and iridium(III)-complexes. These compounds have been used extensively to develop transformations that proceed through the reduction of the metal center after generation of the excited state complexes *via* irradiation with visible light. These complexes are potent excited state reductants and have been discussed thoroughly in a handful of reviews.⁴⁻⁶ However,

despite their utility, transition metal-based photoredox catalysts are expensive and can be challenging to remove from crude reaction mixtures. Both of these factors limit the appeal of these complexes to the chemical industry where affordability and facile purification are two important criteria that must be met for use on large-scale processes.

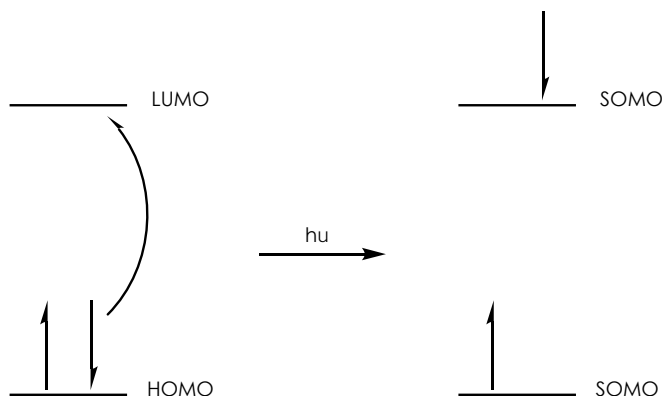
To that end, organic photoredox catalysts have become a popular alternative, as they are less prohibitively expensive and much more readily removed from reaction mixtures. This discussion will focus on the use of organic photocatalysts and the underlying principles behind their activity.

1.2 Organic Photoredox Catalysis Background

1.2.1 Photophysics of Organic Photoredox Catalysis

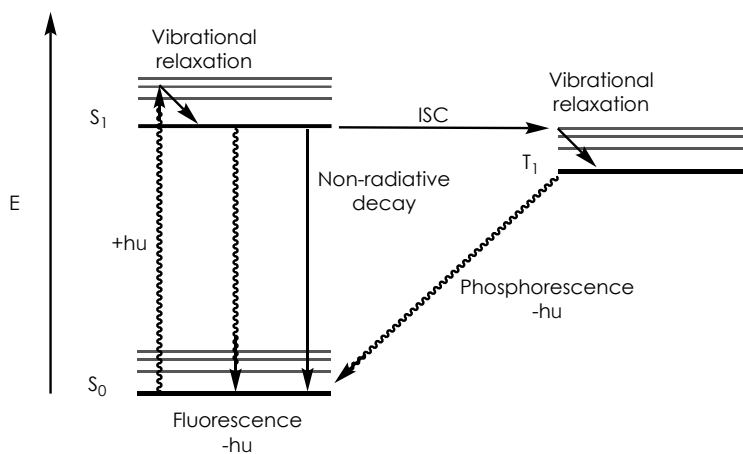
Transformations mediated by organic photoredox catalysts are lauded for the selective generation of reactive radical intermediates upon irradiation with visible light. The process of generating the open-shell intermediates involves an electron transfer (ET) event between a donor molecule and an acceptor molecule. As this process is initiated by photoexcitation *via* irradiation with visible light, it is referred to as a photoinduced electron transfer (PET). PET occurs when a photon of visible light ($h\nu$) is absorbed by an organic molecule possessing extended conjugation, in this case the photoredox catalyst. This results in the formation of an excited state photoredox catalyst when one electron in the catalyst's HOMO is promoted to its LUMO, which results in the formation of two SOMOs with differing energies (**Figure 1-1**).

Figure 1-1. Molecular Orbital Depiction of Photoinduced Electron Transfer



The promotion of an electron from the ground state (S_0) to the lowest energy singlet excited state, S_1 , is shown in the Jablonski diagram in **Figure 1-2**. It is also possible for the direct excitation of an electron into higher energy excited states, but rapid vibrational relaxation and/or ISC results in the repopulation of S_1 .

Figure 1-2. Jablonski Diagram Showing Possible Pathways After Excitation



There are multiple paths forward for the excited state species: it can undergo PET with a ground state molecule, which will be discussed shortly, or it can undergo several radiative/

non-radiative processes. Fluorescence occurs when the excited state energy is released in the form of a photon and results in the return to S_0 . Similarly, non-radiative decay, or internal conversion, also results in the return to S_0 , but in this case, the excited state energy is dissipated through different channels, including collisions with solvent molecules. Finally, the excited state species can undergo ISC, which involves the conversion of S_1 to the triplet excited state, T_1 . ISC is particularly slow, as this conversion requires one of the unpaired electrons to undergo a spin-flip, and this process is spin forbidden. Upon generation of T_1 , the loss of a photon and a spin-flip of one of the unpaired electrons results in relaxation down to S_0 .

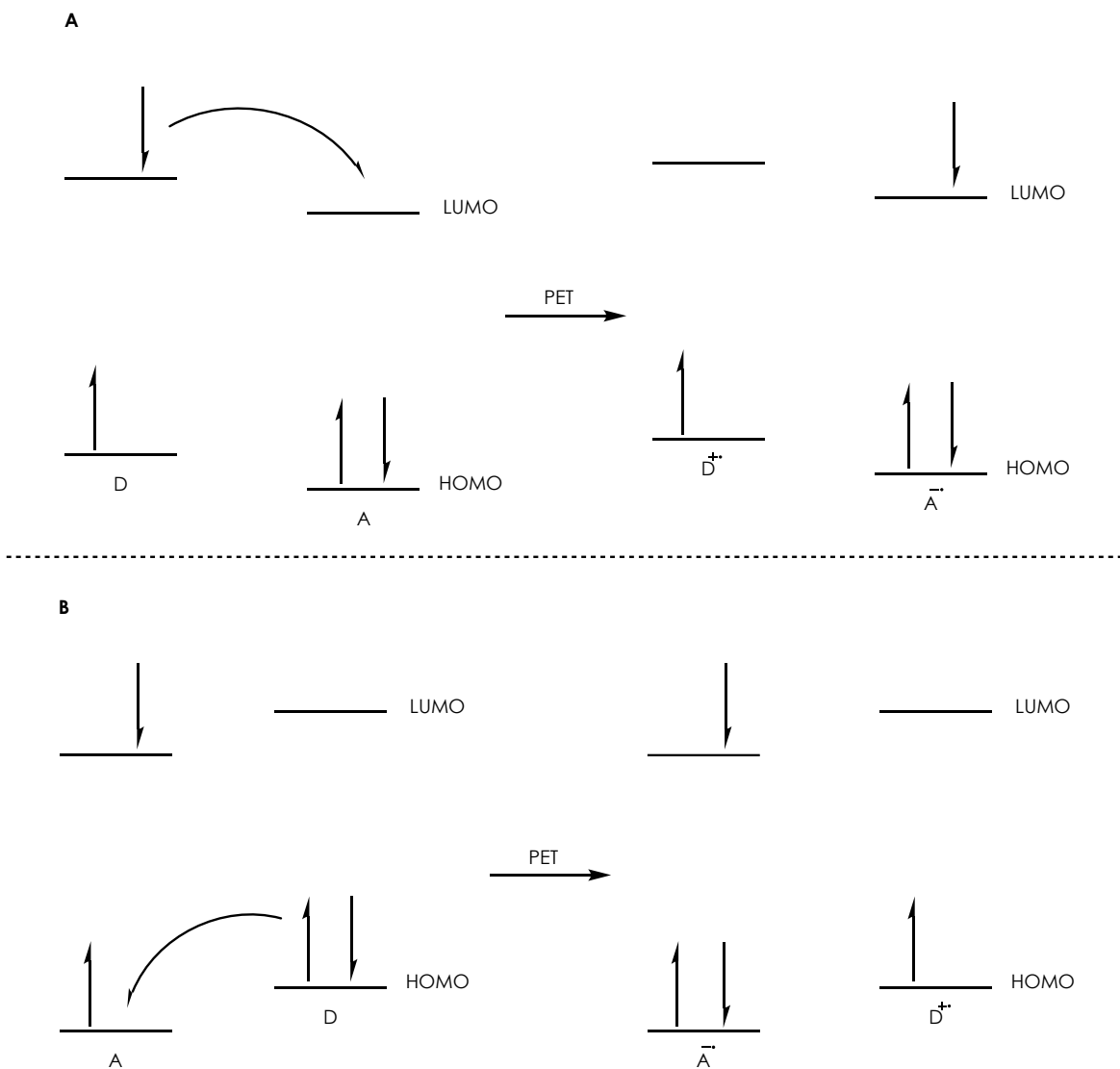
Synthetic chemists are interested in the PET pathway, as this results in productive reactivity *via* the generation of highly reactive intermediates, while other radiative and non-radiative pathways are unproductive and simply result in a return to S_0 . In order to ensure that PET has the opportunity to occur, synthetic chemists must consider several important photophysical properties of the photoredox catalyst. The first property to be taken into account before the development of photoredox catalysis-mediated transformations is the λ_{max}^{abs} , which is the local absorbance maximum for lowest energy absorption.³ This value is important, as it provides synthetic chemists with, among other things, an idea of what wavelengths of light will be absorbed by the photoredox catalyst, which allows for the selection of an appropriate source of irradiation. Additionally, knowing the λ_{max}^{abs} of a photoredox catalyst is crucial in order to ensure that the excitation of reagents other than the catalyst is kept to a minimum.³

In addition to the λ_{max}^{abs} value, synthetic chemists are interested in the excited state lifetime, τ , of the photocatalyst they wish to employ. Organic photoredox catalysts typically

possess τ values on the order of 2-20 ns, while transition metal-based photoredox catalysts have much longer τ values (300 ns – 6 μ s).^{3,7,8} For transition metal catalysts, after excitation to S_1 , rapid ISC typically occurs to form T_1 . As the decay from T_1 to S_1 is a spin forbidden process, the excited state lifetime is much longer than for organic photoredox catalysts.⁴ However, as long as the catalyst has an excited state lifetime longer than 1 ns, it is possible for it to engage in PET with a ground state molecule.³ Although, the longer the excited state lifetime of a photoredox catalyst, the more likely it is for it to encounter a ground state molecule and engage in PET.

In every ET, one molecule acts as an electron donor (D), and molecule acts as an acceptor molecule (A). **Figure 1-3** details a molecular orbital illustration for situations where the excited state catalyst acts as the donor or the acceptor.

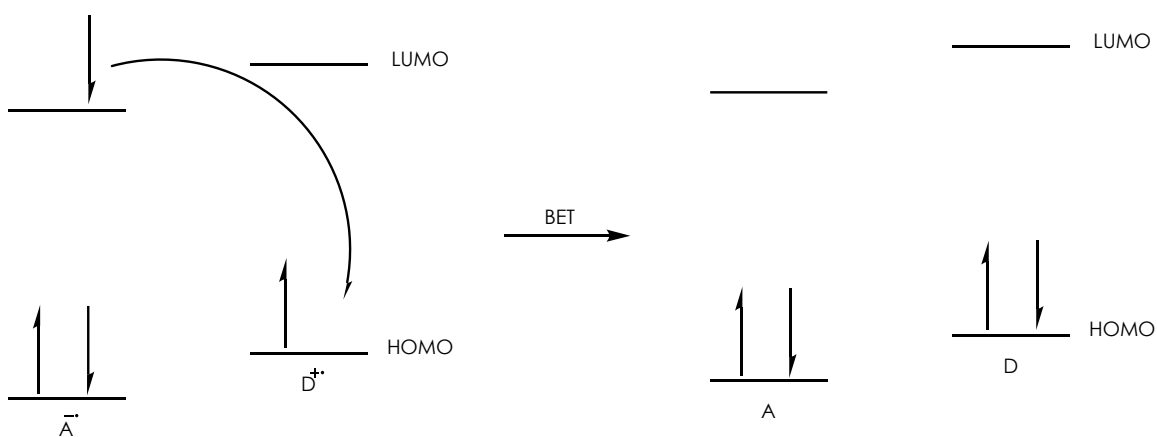
Figure 1-3. Molecular Orbital Depictions of PET Scenarios



In **Figure 1-3A**, the excited state photoredox catalyst acts as the electron donor and engages in an oxidative quenching cycle. An unpaired electron is transferred from the excited state catalyst to the lowest occupied molecular orbital, LUMO, of the ground state acceptor, or substrate. This ET event results in the formation of $D^{\bullet+}$ and $A^{\bullet-}$. **Figure 1-3B** details the

reductive quenching cycle that occurs when the excited state catalyst acts as the electron acceptor. In this pathway, ET occurs from the highest occupied molecular orbital, HOMO, of the ground state donor molecule (substrate) to the excited state acceptor molecule (catalyst) to generate A^- and D^+ . For the purposes of this report, further discussion will focus on the reductive quenching cycle. These highly reactive radical ion intermediates are the species that synthetic chemists hope to harness for the formation of novel bonds. However, in addition to the productive chemistry that can occur, there is also an unproductive event that is known to occur: back electron transfer (BET). When BET occurs, A^- donates an electron to D^+ , which results in the formation of the neutral D and A species (**Figure 1-4**).

Figure 1-4. Molecular Orbital Depiction of Back Electron Transfer



In order to encourage productive reactivity and limit BET, polar solvents can be employed as reaction media, as they result in the separation of the radical ion intermediates, which hinders BET.⁹ Although much work has been done to limit BET and promote productive pathways, PET is not guaranteed to occur between every photoredox catalyst and organic molecule, and

the next section will discuss practical considerations for identifying appropriate donor and acceptor molecules.

1.2.2 Exploring the Thermodynamics of Photoinduced Electron Transfer (PET)

In order to determine which electron donors (D) are capable of participating in PET with an electron acceptor (A), it is helpful to consider the following equation (**Equation 1-1**).

Equation 1-1. Gibbs Free Energy of Single Electron Transfer

$$\Delta G_{ET} = -F(E_{red} - E_{ox}) = -F(E_{1/2}(A/A^{-}) - E_{1/2}(D^{+}/D))$$

Equation 1-1 is used to determine the free energy of a ground state electron transfer event and provides some information on the overall thermodynamics of the proposed ET. In **Equation 1-1**, F represents Faraday's constant (23.061 kcal V⁻¹ mol⁻¹), and E_{red} and E_{ox} are the ground state redox potentials for the molecules undergoing reduction or oxidation. E_{red} is typically a negative value, as the reduction of A is thermodynamically unfavorable. Likewise, the reduction of D⁺, or E_{ox}, is a positive value, as this process is thermodynamically favorable. This term is somewhat misleading, as it describes an oxidation event, but the half-reaction is traditionally written as a reduction.

Having discussed ET generically, **Equation 1-2** is used to describe the thermodynamics of PET, which occurs when one of the components is in an excited state.

Equation 1-2. Gibbs Free Energy of Photoinduced Electron Transfer

$$\Delta G_{PET} = -F(E_{ox}(D^{+}/D) - E_{red}(A/A^{-})) - w - E_{0,0}$$

This equation resembles **Equation 1-1**, but also contains some additional terms (w and $E_{0,0}$). We note that, while in many cases, the value of w , or the solvent-dependent energy difference, is important, its relevance in photoredox catalysis-mediated transformations is much lower. Its overall impact on the value of ΔG_{PET} is negligible, and the term will be omitted moving forward.³ Hence, **Equation 1-2** can be simplified and rewritten to more clearly relate to the PET event between the excited state of a photoredox catalyst and the ground state of a substrate, as shown in **Equation 1-3**.

Equation 1-3. Modified Equation to Calculate Gibbs Free Energy of PET

$$\Delta G_{PET} = -F(E_{red}^*(cat^*/cat^{\cdot-}) - E_{ox}(sub^+/sub))$$

In this equation E_{red}^* refers to the excited state reduction potential of the photoredox catalyst in question, and E_{ox} refers to the ground state oxidation potential of the substrate. In order for a PET event to be thermodynamically favorable, E_{red}^* must be more positive than E_{ox} . This useful equation allows chemists to predict the likelihood that a PET event will occur for a given system.

In order to make use of **Equation 1-3**, several values must be determined, including E_{red}^* and E_{ox} . E_{red}^* can be calculated by **Equation 1-4** as shown below.

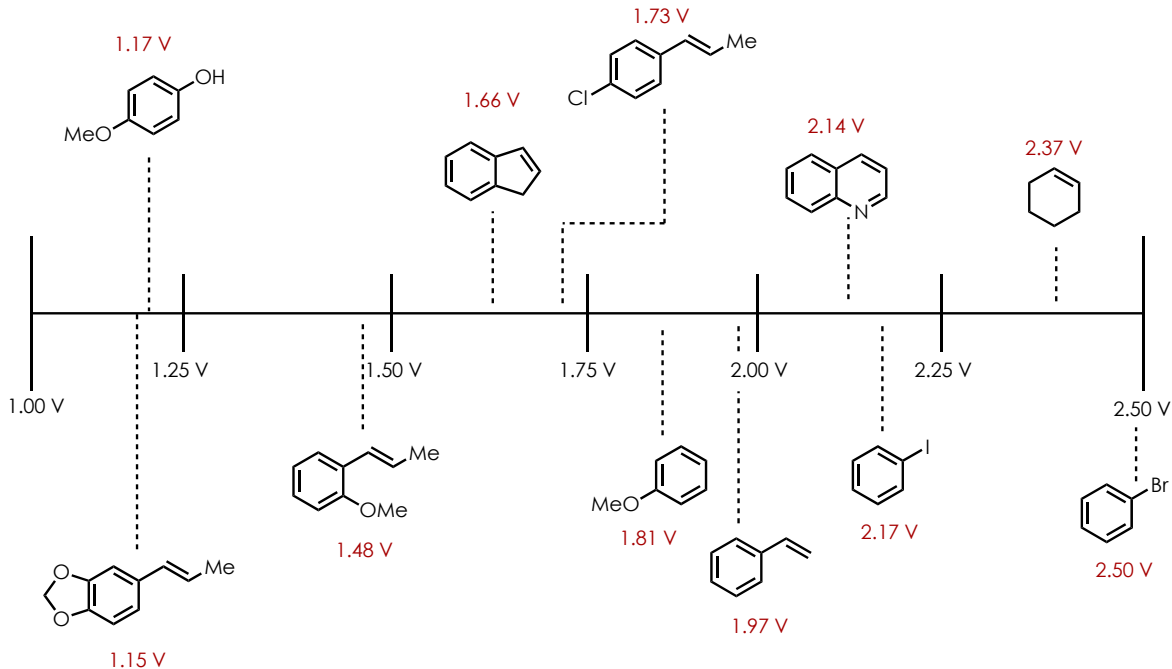
Equation 1-4. Calculation of Excited State Reduction Potential

$$E_{red}^*(cat^*/cat^{\cdot-}) = E_{red}(cat/cat^{\cdot-}) + E_{0,0}$$

E_{red}^* is equal to the ground state reduction potential of the catalyst (E_{red}) plus the excited state energy ($E_{0,0}$) of either the S_1 or T_1 state. E_{red} and E_{ox} can both be determined experimentally using cyclic voltammetry, and our lab has published an extensive collection of E_{ox} values for a variety of organic substrates.¹⁰ A computational method for calculating these values was also reported with the collection of experimental data.¹⁰ Additionally, $E_{0,0}$ can be determined through the use of fluorescence spectroscopy, and the value can be estimated by overlaying the absorption and emission spectra of the photoredox catalyst and identifying the point at which the curves intersect.

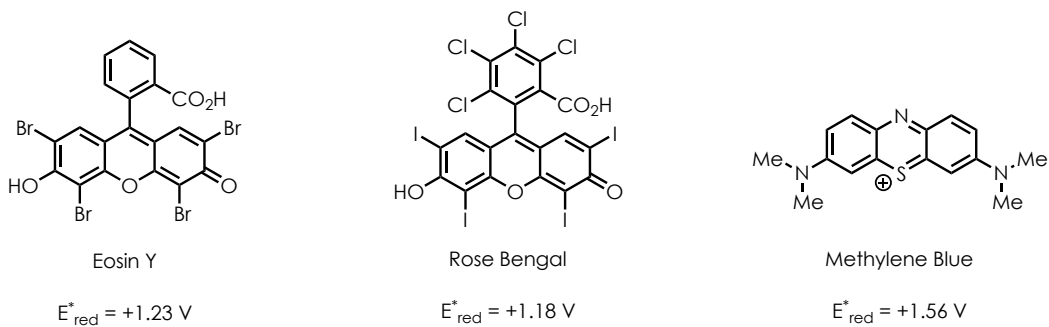
The determination of these values, E_{ox} and E_{red}^* , allows for the identification of substrates that are likely to participate in a PET event with a photoredox catalyst. As shown below in **Figure 1-5**, the ground state oxidation potentials for organic molecules is quite varied, and so the choice of photoredox catalyst is important in order to favor oxidation of the substrate while limiting any overpotential.

Figure 1-5. Examples of Ground State Oxidation Potentials of Organic Molecules



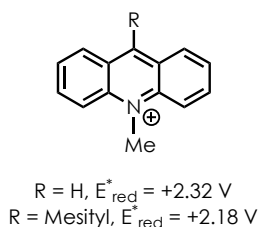
To that end, a variety of organic photoredox catalysts are shown below in **Figure 1-6**. Many of the organic molecules possess oxidation potentials that are more positive (>1.56 V vs. SCE) than the excited state reduction potentials of the organic photoredox catalysts.

Figure 1-6. Examples of Organic Photoredox Catalysts



As such, PET events are thermodynamically unfavorable and unlikely to occur, which illustrates the limitations of these catalytic systems. A solution to this dilemma is to utilize more potent excited state oxidants, and one class of such compounds are acridinium salts (**Figure 1-7**). These compounds are known to be extremely potent excited state oxidants, as shown by the E_{red}^* values in **Figure 1-7**, and their use as powerful photooxidants will be discussed in the next section.

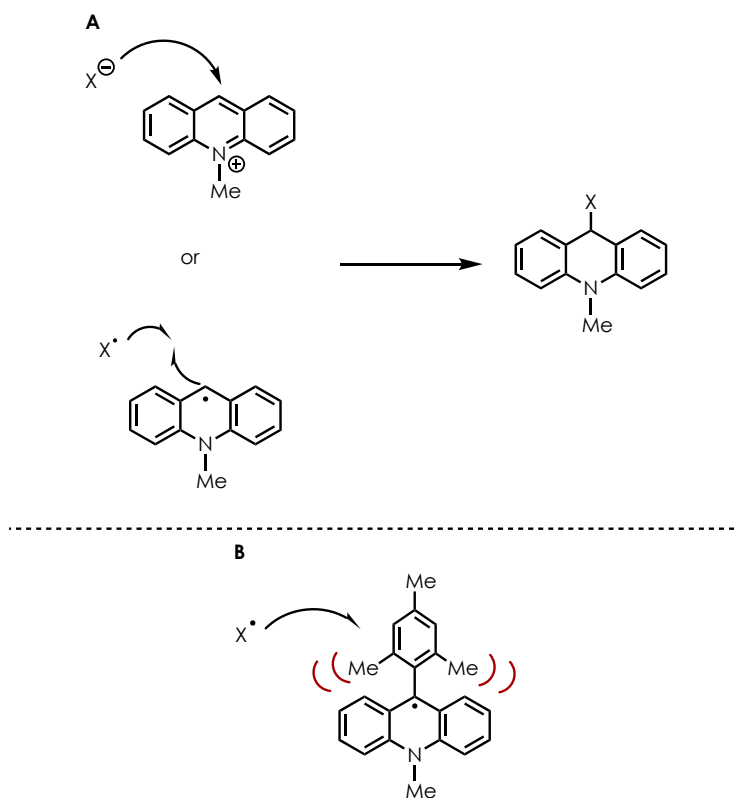
Figure 1-7. Representative Examples of Acridinium Salts



1.2.3 Use of Acridinium Salts as Organic Photoredox Catalysts

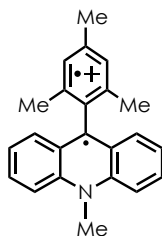
Despite the presence of acridinium ions in the literature for some time, these compounds received little use as catalysts due to their tendency to undergo nucleophilic addition at the 9-position (**Figure 1-8A**). Interest in the use of acridinium salts as catalysts began when Fukuzumi reported the synthesis of an acridinium salt with a bulky mesityl group at the 9-position, which hindered undesired nucleophilic addition (**Figure 1-8B**).¹¹

Figure 1-8. Acridinium Salt Deactivation By Nucleophilic Addition



The group was interested in this compound and its ability to access a charge transfer (CT) state through an ET between the mesityl donor and acridine acceptor (**Figure 1-9**).

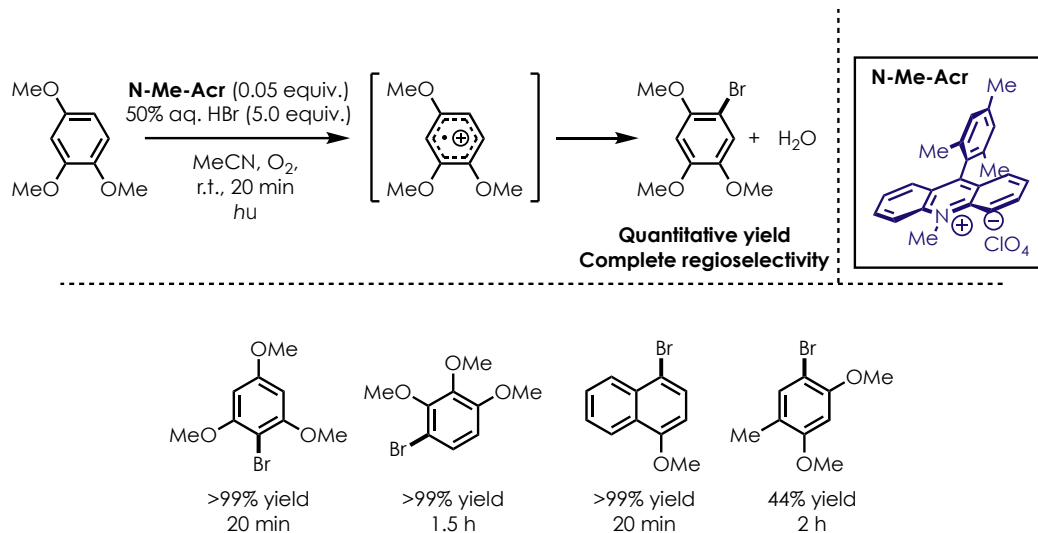
Figure 1-9. Charge Transfer State of Fukuzumi's Acridinium Salt



While the exact nature of the acridinium excited states that could be accessed was subject to much debate¹¹⁻¹⁷, the acridinium salts were determined to be potent excited state oxidants

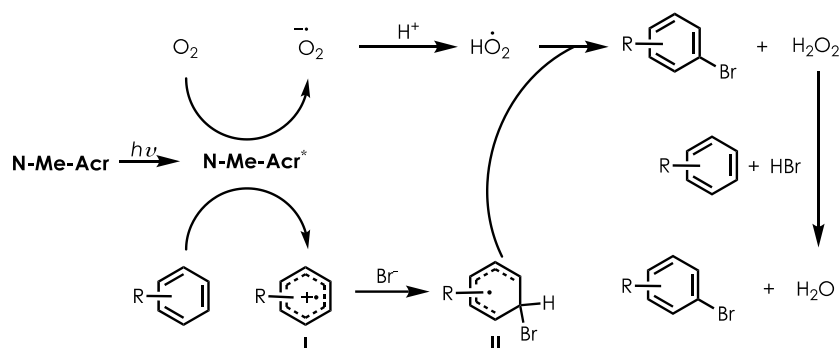
and were of interest to the synthetic community. Since the disclosure of the 9-mesityl acridinium ions, these compounds have been used in a variety of transformations, including the bromination of electron-rich arenes as shown by Fukuzumi in 2011 (**Scheme 1-1**).¹⁸

Scheme 1-1. Fukuzumi's Aerobic Bromination Method and Representative Scope



Although the scope of the reaction was relatively limited, the desired bromoarenes were synthesized in excellent yields and regioselectivities in most cases.

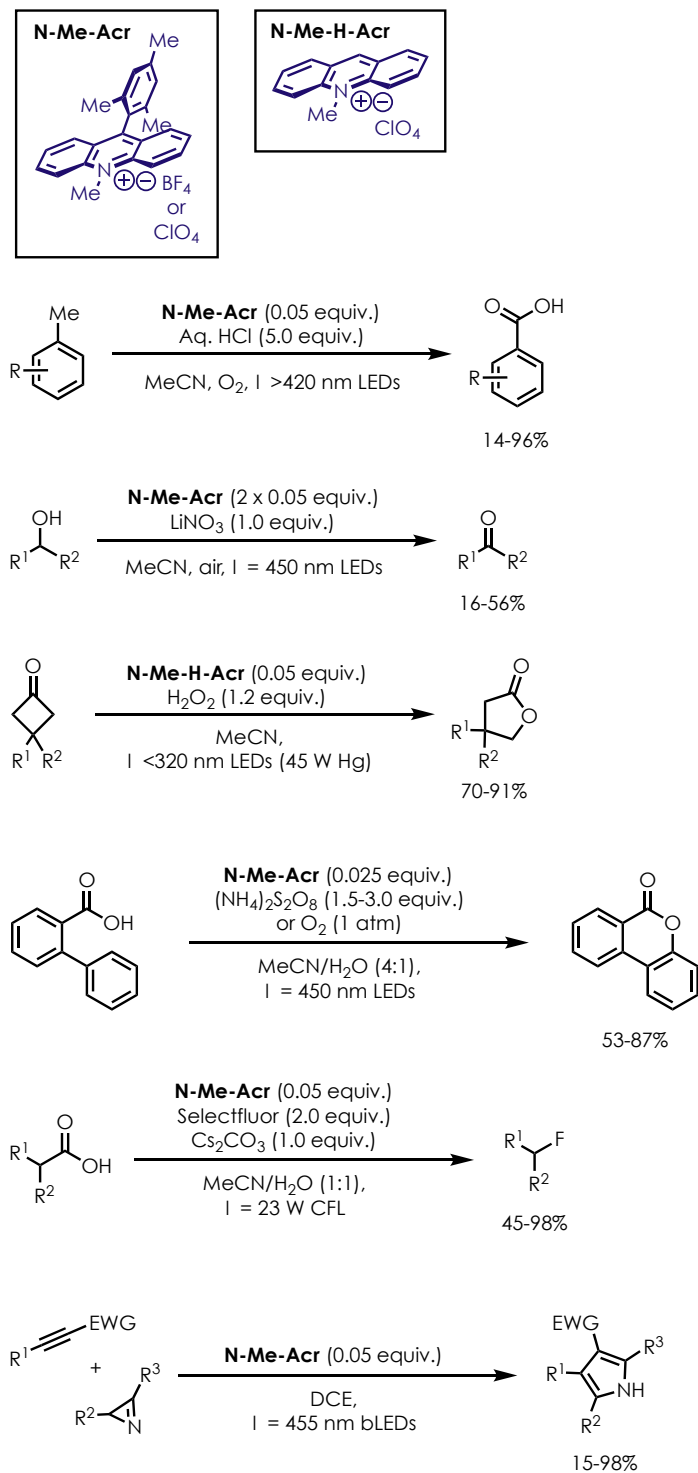
Scheme 1-2. Proposed Mechanism for Aerobic Bromination



The Fukuzumi group proposed the mechanism shown in **Scheme 1-2** as a possible pathway for their aerobic bromination reaction. Upon oxidation of the electron-rich arene substrate, the aryl cation radical, **I**, is generated and can react with the bromide anion in solution. Nucleophilic addition into **I** results in the formation of **II**, which, upon aromatization *via* interaction with HO₂⁻, forms the desired product and H₂O₂. The H₂O₂ can react with HBr and a molecule of starting material to form additional brominated arene and water. The O₂ in the system is likely responsible for turning over the catalyst by oxidation of the acridinyl radical and may also be responsible for the oxidative aromatization of **II**.

In addition to using acridinium salts as photoredox catalysts for arene functionalization, the Fukuzumi group has also reported, among other systems, a method for the oxygenation of alkenes¹⁹ and the oligomerization of fullerene.²⁰ The use of acridinium ions as photoredox catalysts has been reported by other groups as well, and **Scheme 1-3** displays a representative overview of the transformations that have been developed.^{21–26}

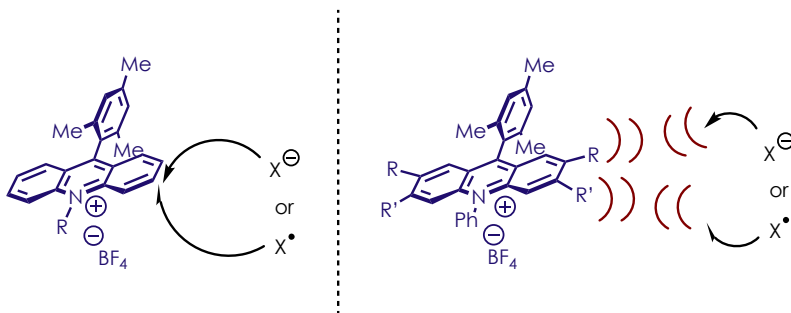
Scheme 1-3. Representative Scope of Transformations Featuring Acridinium Catalysts



As **Scheme 1-3** shows, organic photoredox catalysis mediated by acridinium salts has been used to develop methods for the synthesis of many valuable motifs. Many of the systems shown above feature mild conditions (lower reaction temperatures, no Lewis acids, etc.) when compared to traditional methods and result in the formation of densely functionalized molecules. Additionally, the majority of these transformations are completely free of transition metals, although some examples of dual acridinium/transition metal catalysis are known.^{27–32} Although this is a very limited scope, we encouraged interested parties to refer to the section on acridinium salt-mediated transformations in our review of organic photoredox catalysis, which provides a much more comprehensive discussion of this field.³

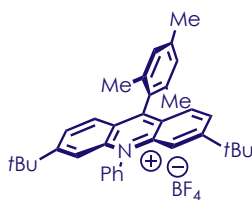
Our lab has made a great deal of progress in using acridinium salts as photoredox catalysts over the years, which will be discussed in section 1.3. Furthermore, another important contribution from the group is the development of more robust acridinium salts with varying photophysical properties. As mentioned previously, a major limitation of acridinium salts as photoredox catalysts is the susceptibility of these compounds to undergo nucleophilic addition at the 9-position. While Fukuzumi's catalyst initially presented a solution through the installation of a bulky mesityl group at the 9-position, our group realized these compounds were still prone to undergoing nucleophilic addition at other positions around the acridine core (**Figure 1-10**), which resulted in diminished catalytic activity.

Figure 1-10. Catalyst Deactivation *Via* Nucleophilic Addition to Acridine Core



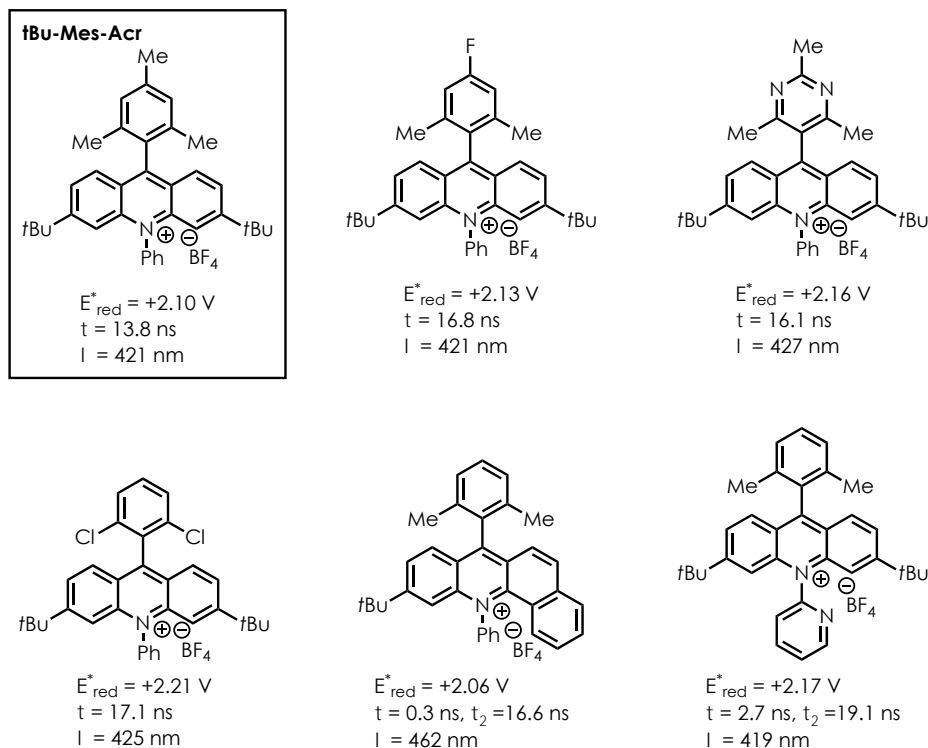
By installing bulky substituents at either the 2- and 7-positions (-R) or the 3- and 6-positions (-R'), additional degradation pathways can be hindered, which results in more robust catalysts. In particular, the acridinium salt shown in **Figure 1-11** was found to be particularly hardy and was successfully used in a variety of transformations, such as the hydrofunctionalization of olefins and the C-H functionalization of arenes.

Figure 1-11. Robust Acridinium Salt Developed by Nicewicz and Coworkers



In addition to the development of these more robust acridinium salts, our lab has also recently disclosed an operationally simple, effective route for the synthesis of acridinium salts.³³ This route is highly modular and allows for the expedient synthesis of novel acridinium catalysts. **Figure 1-12** displays some of the novel compounds synthesized *via* this route and some of the relevant photophysical data for these catalysts.

Figure 1-12. Novel Acridinium Salts Synthesized by Nicewicz and Coworkers



As shown above, these novel acridinium salts, in most cases, possessed E_{red}^* values that were considerably more potent than **tBu-Mes-Acr**, which has been used extensively by our lab.

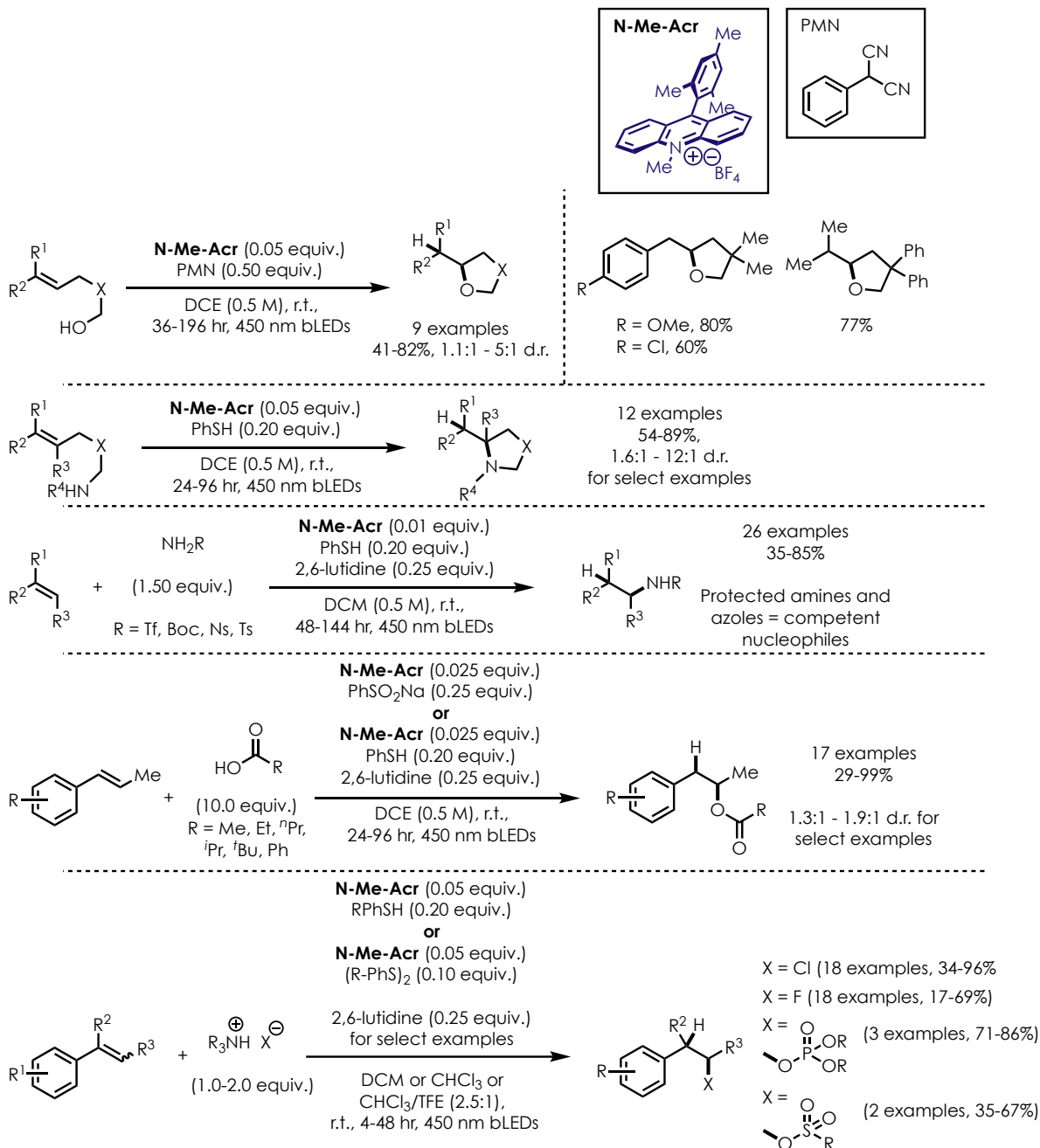
Additionally, these novel catalysts also possessed greater τ values, which means that there is a greater likelihood of a PET event occurring between the excited state catalyst and the ground state substrate. The development of this method represents a major step forward in providing access to acridinium photoredox catalysts to be used in the formation of novel bonds and important molecules.

1.3 Prior Nicewicz Lab Work

1.3.1 Development of Olefin Hydrofunctionalization Reactions

As alluded to in the previous section, our lab has long been a major player in the realm of organic photoredox catalysis featuring the use of acridinium salts. Early work from our group centered around the use of acridinium catalysts to accomplish the hydrofunctionalization of olefins. As shown below in **Scheme 1-4**, we have been able to accomplish both intra- and intermolecular transformations featuring a wide variety of nucleophiles, including, but not limited to, alkenols, amines, and halides.³⁴⁻⁴⁰

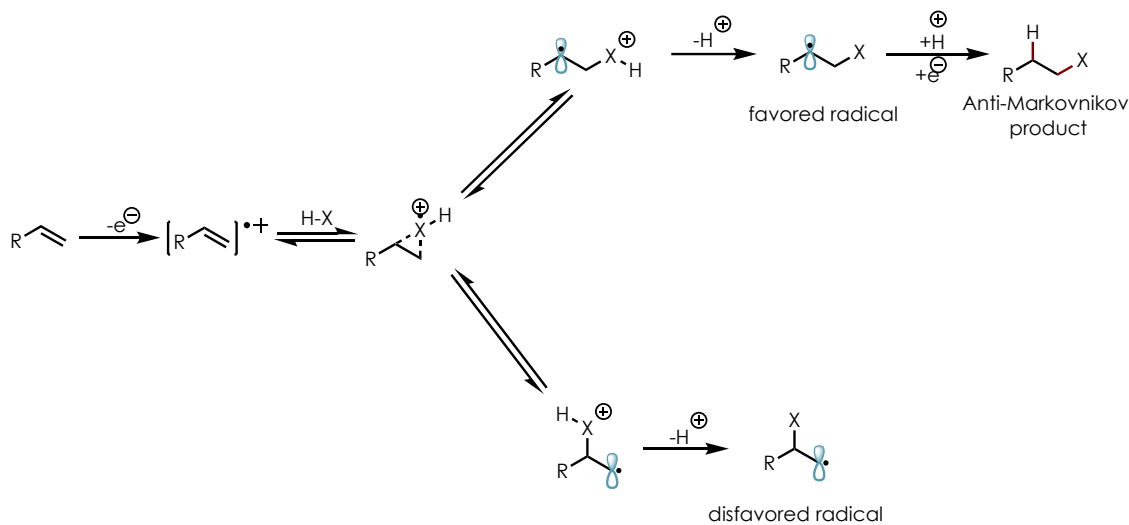
Scheme 1-4. Select Methods Developed by Nicewicz and Coworkers



These methods offer facile access to products that would be challenging to access otherwise. Additionally, the conditions employed are relatively mild, and a variety of functionality is tolerated in each case. Another exciting characteristic of these transformations is the regioselectivity, as, in all cases, the anti-Markovnikov regioisomers are

obtained. This regioselectivity renders our methods complementary to many traditional two-electron methods which yield the Markovnikov regioisomer. In order to rationalize this regioselectivity, we have proposed the following mechanistic pathway (**Scheme 1-5**).

Scheme 1-5. Proposed Mechanism for Anti-Markovnikov Hydrofunctionalization

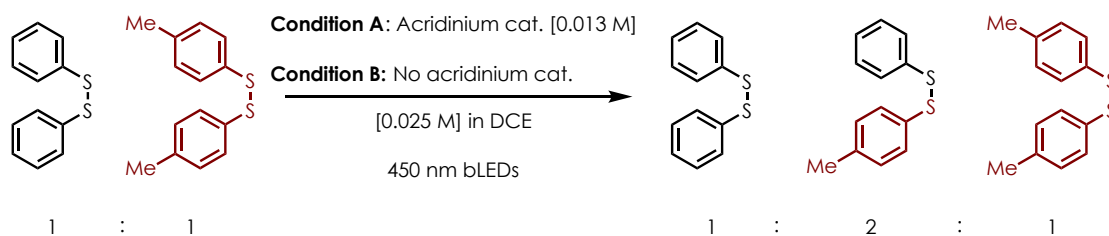


Oxidation of the olefin substrate through PET with the acridinium catalyst results in the formation of an alkene radical cation. Upon interaction with a nucleophile, it is possible for the nucleophile to undergo addition at either position. However, as shown in the top pathway, the addition of the nucleophile to the terminal position results in the formation of a more stabilized radical, which is favorable. An H-atom transfer results in the formation of the anti-Markovnikov regioisomer. As shown in the bottom pathway, addition to the position adjacent the -R group results in the formation of a less stable radical and is not the favored pathway.

An alumnus of the lab, Nathan Romero, carried out extensive mechanistic studies to support this proposed pathway.⁴¹ Using transient absorption spectroscopy, the cation radical

of anethole was detected after oxidation in the presence of an acridinium catalyst using Laser Flash Photolysis (LFP). This piece of data supports the proposed oxidation of the ground state substrate by an excited state acridinium catalyst. Additionally, in order to probe the nature of the H-atom transfer event between the HAT co-catalyst and radical intermediate, a series of experiments were conducted. As proposed by the group, HAT between the H-atom donor and favored radical intermediate furnishes the desired product, as well as generates a thiyl radical that is able to oxidize the acridine radical to regenerate the ground state acridinium catalyst. Reactivity was observed when both PhSH and (PhS)₂ were employed as HAT co-catalysts, and the group proposed that an equilibrium existed between the two compounds. As small amounts of PhSH were detected when (PhS)₂ was used as the H-atom donor, it was proposed that some sort of homolytic cleavage was responsible for the generation of the active H-atom donor.

Scheme 1-6. Disulfide Crossover Experiment



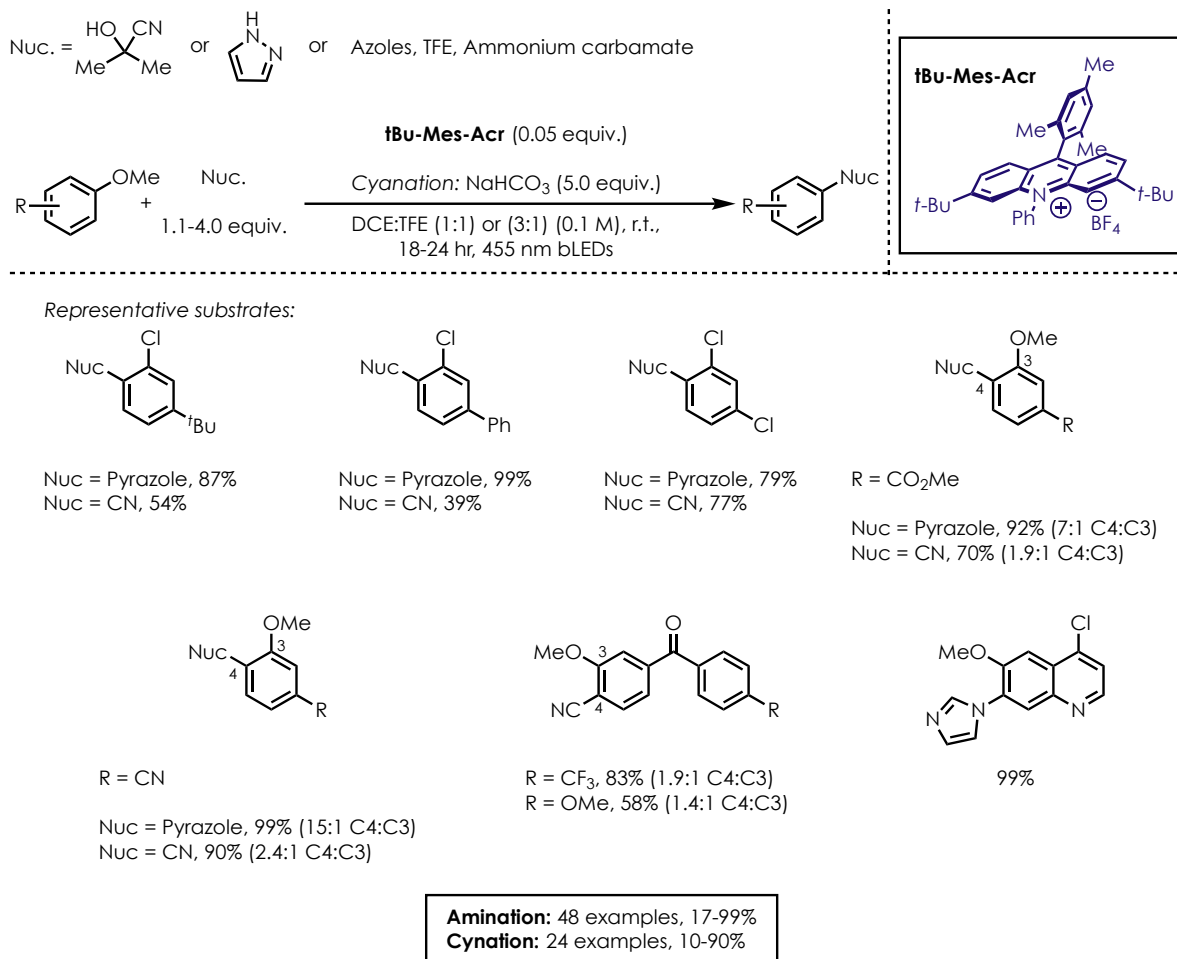
In the competition experiment shown in **Scheme 1-6**, equal amounts of (PhS)₂ and (*p*-tolS)₂ were subjected to irradiation with 450 nm blue LEDs both with and without an acridinium catalyst. In both cases, the formation of an identical mixture of products was observed. The formation of a mixed disulfide was noteworthy, as no reports of direct homolytic cleavage of an S-S bond with 450 nm light were known. However, controls run in the absence of light

and at 40 °C did not result in the formation of the mixed disulfide, indicating that the S-S bond homolysis was not thermally initiated. After confirming that thiyl radicals (PhS•) were freely present in the system, the group was interested in confirming that those species were capable of oxidizing the acridine radical to close out the photoredox catalytic cycle. Upon preparation of the acridine radical using CoCp₂, the species was exposed to PhS• generated upon excitation of (PhS)₂ *via* LFP. Transient absorption spectroscopy revealed the formation of a signal associated with the ground state acridinium catalyst, indicating that PhS• was capable of oxidizing the acridine radical. We encourage interested parties to read the full report detailing these experiments, as considerably more work was carried out that provides additional support for the proposed mechanism.⁴¹

1.3.2 Development of Cation-Radical-Accelerated Nucleophilic Aromatic Substitution Reactions

In addition to the work done on olefin hydrofunctionalization, our lab has also developed a robust research program focused on developing novel methods for the functionalization of (hetero)arenes. Several powerful methods for the C-H functionalization of arenes with nucleophiles such as azoles/ammonia, cyanide, and fluoride have been reported.^{42–46} We encourage interested parties to explore the cited reports for more information on the methods. In addition to the development of C-H arene functionalization methods, we have also reported several strategies for the use of cation radical intermediates in nucleophilic aromatic substitution reactions (S_NAr). We have termed these methods “cation radical-accelerated nucleophilic aromatic substitution” (CRA-S_NAr) reactions, and **Scheme 1-7** details the transformations.

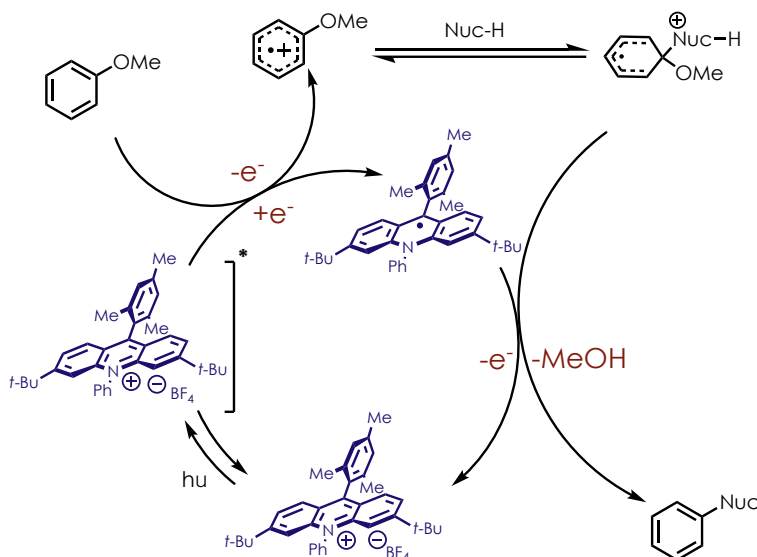
Scheme 1-7. Summary of CRA-S_NAr Methods Developed by Nicewicz and Coworkers



Methods have been developed for the use of cyano- and nitrogenous nucleophiles in our CRA-S_NAr reactions. As shown in **Scheme 1-7**, a wide variety of substrates bearing methoxy-substituents were compatible substrates in these transformations. Substrates bearing multiple methoxy-substituents were also tolerated, and excellent regioselectivity was observed when azoles were used as nucleophiles. Halides were well-tolerated in these reactions, and no evidence of dehalogenation was observed, which allows for further downstream transformations. It is noteworthy that EWGs are not required to observe

reactivity. As such, these methods are complementary to existing S_NAr conditions. A proposed mechanism for these transformations is shown below in **Scheme 1-8**.

Scheme 1-8. Proposed Mechanistic Pathway for CRA- S_NAr Methods



Upon excitation of the ground state acridinium catalyst to generate the excited state species, PET between the catalyst and the ground state substrate can occur. This affords the arene cation radical and the acridine radical. The arene cation radical can be intercepted by the nucleophile to afford an intermediate that strongly resembles the Meisenheimer intermediate observed in traditional S_NAr reaction. Subsequent extrusion of MeOH and reduction by the acridine radical results in the formation of both the desired product and the ground state acridinium catalyst.

1.4 Conclusions

Organic photoredox catalysis has emerged as a powerful strategy for the construction of complex molecules and important bonds (e.g. C-O, C-N, C-X, C-C, etc.). A basic

understanding of the photophysical and thermodynamic concepts associated with PET events allows for the selection of appropriate photoredox catalysts and substrate classes. As such, many groups, including ours, have successfully developed methods for the functionalization of small molecules, as well as the synthesis of biologically relevant targets. A brief overview of our lab's work was discussed in this section, and the subsequent chapters detail efforts made to extend the use of organic photoredox catalysis to develop novel transformations featuring olefins and fluoro(hetero)arenes.

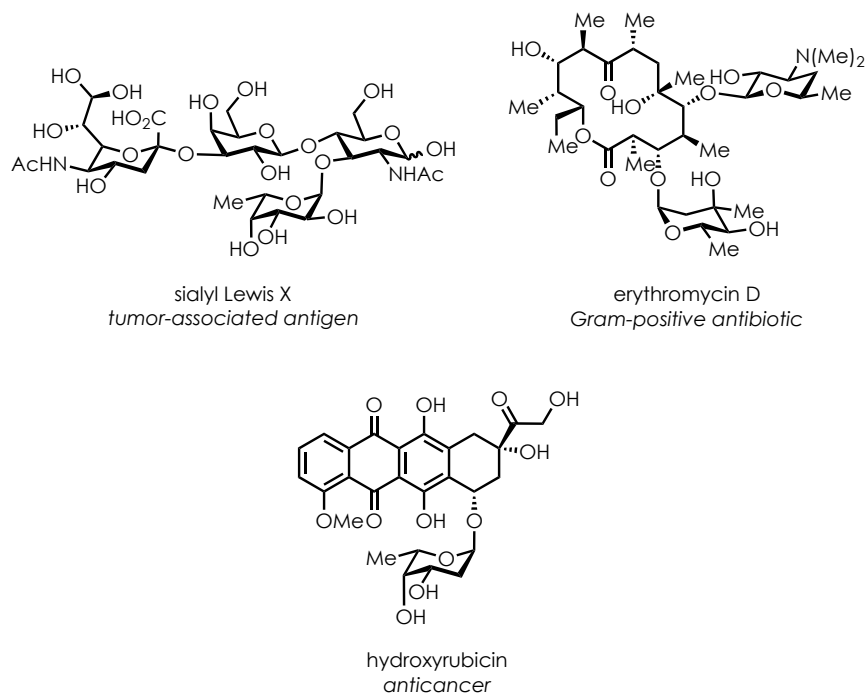
CHAPTER 2: DEVELOPMENT OF PHOTOREDOX CATALYSIS-MEDIATED METHODS FOR THE HYDROFUNCTIONALIZATION OF GLYCALS

2.1 Introduction

2.1.1 Glycosides and Their Importance

Carbohydrates are a class of molecules that have a presence in many areas of modern life. Perhaps the first thing that comes to mind for some is their role in our diets, but carbohydrates also play an important part in the realm of biologically active natural products. The rich biology and chemistry associated with these molecules has been well documented over the years, and several of these compounds with important biological activity are shown in **Figure 2-1**.⁴⁷

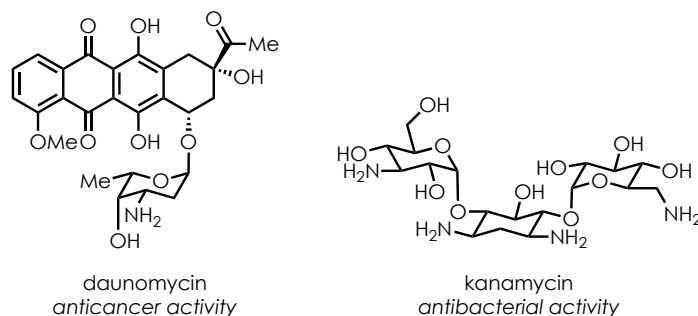
Figure 2-1. Carbohydrate-Containing Biologically Relevant Molecules



As these compounds have such important functions, it is unsurprising that so much attention has been devoted to their synthesis and derivatization. The field of carbohydrate chemistry is broad in nature, and in the interest of brevity, we have chosen to focus this discussion on a small set of compounds that are of interest to the community and our lab. In particular, the classes of glycosides that will be discussed are aminoglycosides, deoxyglycosides, and glycomimetics.

Aminoglycosides are compounds in which one or more of the hydroxyl groups have been replaced by amine functionality; as shown in **Figure 2-1**, sialyl Lewis X contains several examples of aminoglycosides. The biological importance of aminoglycosides is well documented, and these compounds have been shown to possess anticancer, antifungal, and antibiotic properties (**Figure 2-2**).⁴⁸ Additionally, they also play an important role in glycoproteins through the sensing of enzymes⁴⁹, antibodies⁵⁰, and lectins.⁵¹

Figure 2-2. Aminoglycoside-Containing Pharmaceuticals



Deoxyglycosides are carbohydrates that are lacking hydroxyl groups at one or more positions around the ring. 1-deoxyglycosides lack substitution at the C1-position, and these glycosides have been shown to possess important biological activity. The 1-deoxyglycoside, 1,5-anhydro-D-glucitol (1,5-AG) (**Figure 2-3**), is a naturally occurring compound that has been used to monitor glycemic variability and historic blood sugar trends.⁵² Additionally, 1,5-anhydro-D-fructose (1,5-AF) (**Figure 2-3**), is another 1-deoxyglycoside that serves as a precursor to compounds with antimicrobial properties.⁵³

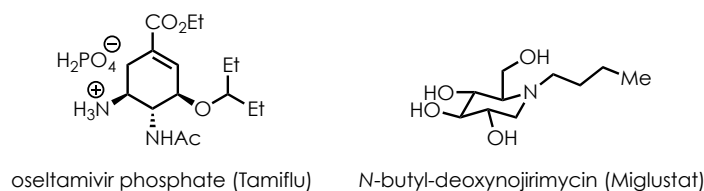
Figure 2-3. Examples of Biologically Relevant Deoxyglycosides



The third class of compounds that are particularly interesting are glycomimetics, which are molecules that closely resemble the structure of carbohydrates but possess some modifications. Glycomimetics are often the subject of study, as many of these compounds

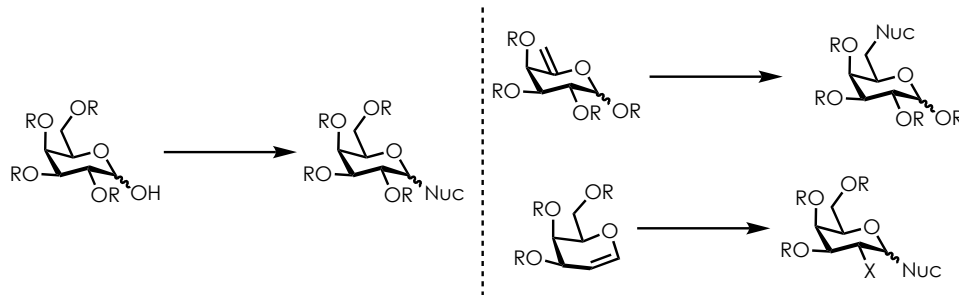
have displayed important biological activities. As shown in **Figure 2-4**, oseltamivir phosphate, is a well-known antiviral medication that is a carbocyclic variant of the sialic acids, which are carbohydrates located on the surface of human cells.⁵⁴ Another glycomimetic with interesting biological activity is Miglustat, which is an iminosugar analogue of D-glucose (**Figure 2-4**). Miglustat is used to treat type 1 Gaucher disease and type C Niemann-Pick disease, which are rare lysosomal storage disorders.⁵⁴

Figure 2-4. Examples of Pharmaceuticals Containing Glycomimetics



Because these classes of glycosides are involved in so many important biological functions and display such a wide variety of activities, their synthesis and derivatization is an important challenge to address. The synthesis of glycosides is often quite complex, and small modifications to the structure of these compounds can require the addition of several steps to the synthetic route. Much effort has been dedicated to the development of expedient methods for the synthesis of carbohydrates, and the previously mentioned classes of compounds are no exception. Broadly, glycoside synthesis and derivatization can be approached through two general strategies that are shown in **Scheme 2-1**.

Scheme 2-1. General Strategies for Derivatization of Glycosides



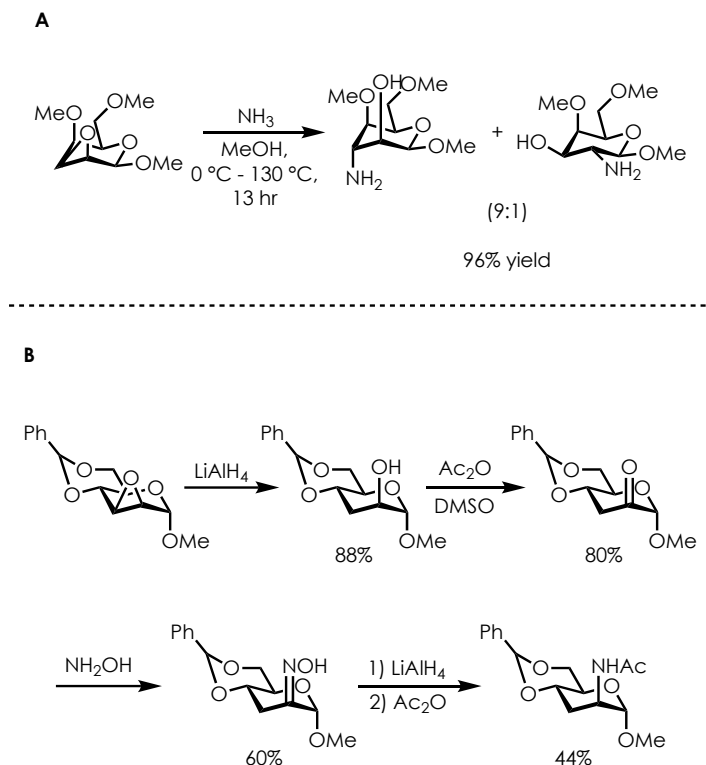
Classical carbohydrate chemistry can be employed to convert the hydroxyl group at the C1-position into a nucleofuge that can undergo nucleophilic substitution to install new functionality.⁵⁵ Conversion of the secondary hydroxyl groups into other functional handles can be accomplished through the careful selection and use of protecting groups. These routes are often lengthy with much time spent installing and removing various protecting groups, which is not an ideal strategy for the efficient synthesis and derivatization of novel glycosides/glycomimetics. The right half of the figure details the chemistry associated with glycals, which are carbohydrates possessing a unit of unsaturation. When the unit of unsaturation occurs between the C1- and C2-positions of the 6-membered pyranose units, the compound is referred to as an *endo*-glycal, and when the unit of unsaturation occurs between the C5- and C6-positions, the compound is referred to as an *exo*-glycal. Both *exo*- and *endo*-glycals have received much attention over the years, as they can be converted into a wide range of glycoside derivatives.^{56,57}

2.1.2 Synthesis of Aminoglycosides *via* Polar Chemistry

The synthesis of aminoglycosides, specifically 2-aminoglycosides, *via* either of the general pathways discussed in the previous section is well-explored.^{48,58} Epoxyglycosides have been converted to aminoglycosides through the opening of the epoxide with a variety of

nucleophiles, such as ammonia, azides or hydrides (**Scheme 2-2**), which can undergo subsequent transformations to furnish the desired products.⁴⁸

Scheme 2-2. Strategies for the Synthesis of Aminoglycosides

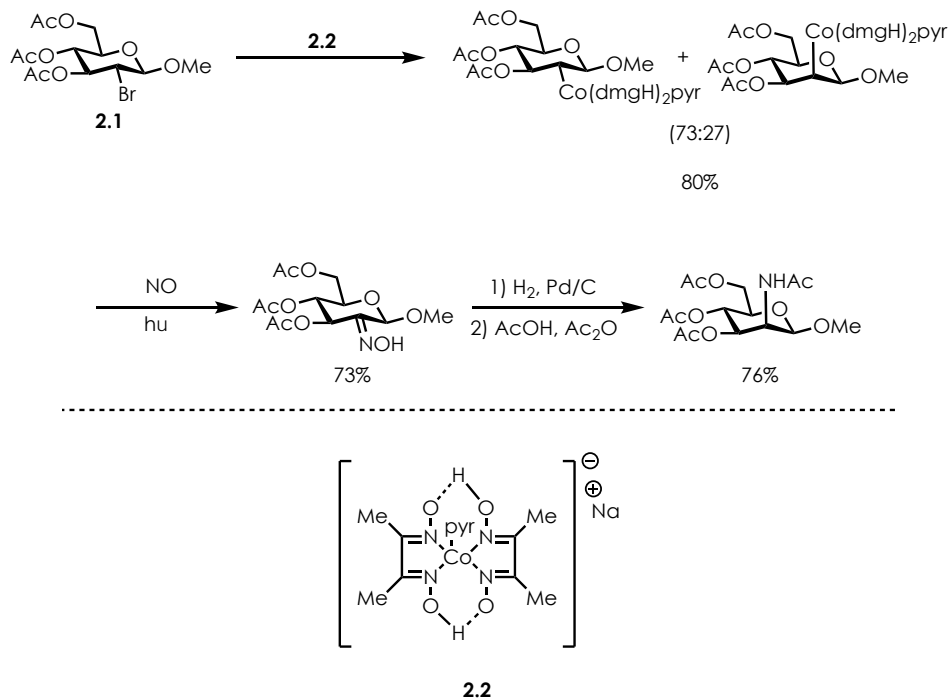


While this strategy does provide access to a variety of aminoglycosides, it suffers from several notable limitations including product mixtures (**Scheme 2-2A**)⁵⁹ and lengthy synthetic sequences (**Scheme 2-2B**).⁶⁰ Care must also be taken to ensure that other reactive functional groups in the molecule are protected to avoid the generation of undesired byproducts. Additionally, much of this early work is very limited in substrate scope, which limits its utility in the synthesis and derivatization of novel aminoglycosides.

An interesting method for the synthesis of a peracetylated mannosamine derivative was disclosed by the Giese group in 1990 (**Scheme 2-3**).⁶¹ Generation of **2.1** and subsequent exposure to a cobaloxime reagent (**2.2**) yields the desired carbohydrate-cobaloxime adduct in

good yields. Photolysis of the carbohydrate-cobaloxime adduct in the presence of NO results in the homolytic cleavage of the C-Co bond and subsequent trapping by NO to afford an intermediate bearing an oxime in good yields. Finally, hydrogenation of the oxime affords the desired aminoglycoside, mannosamine, in good overall yields. The Giese group had previously disclosed a similar method for the generation of other glycosyl bromides, which indicates that this route may be amenable to the synthesis of other aminoglycosides. Unfortunately, this method is often carried out at cryogenic temperatures and requires the installation of a halide before the desired reactivity is observed, which lengthens the reaction sequence.

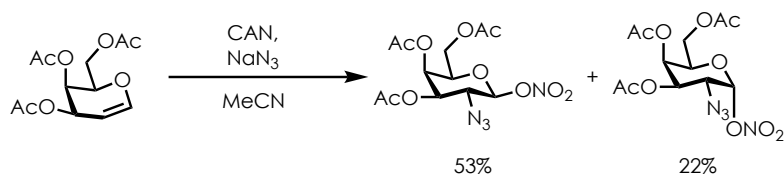
Scheme 2-3. Giese's Synthesis of Aminoglycosides



The synthesis of aminoglycosides from glycal starting materials has proven to be a popular strategy for accessing these compounds. An early example of aminoglycoside synthesis from a glycal was disclosed by the Lemieux group in 1979.⁶² The method involved

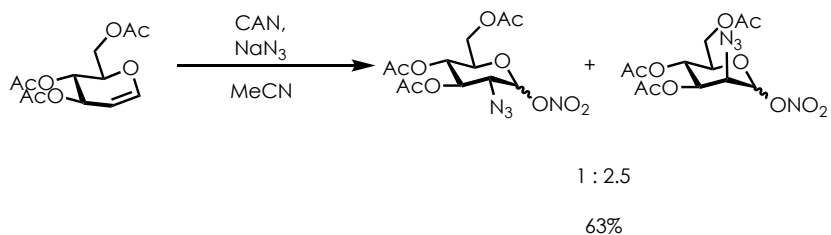
treatment of tri-*O*-acetyl-D-galactal with superstoichiometric amounts of CAN and NaN₃ to access azidonitrated glycoside products (**Scheme 2-4**) which could be further transformed into compounds with a range of functional groups at the C1-position to serve as glycosyl donors.

Scheme 2-4. Azidonitration of Peracetylated Galactal Derivative



While this method was an early proof of concept that glycals could be used as precursors to aminoglycosides, this methodology was limited to just one substrate and required superstoichiometric amounts of both CAN and NaN₃, as the transformation was not particularly efficient. Additionally, limited stereoselectivity was observed with a mixture of products formed. This initial report was followed by another in which the azidonitration of tri-*O*-acetyl-D-glucal with CAN and NaN₃ was observed (**Scheme 2-5**).⁶³ Unfortunately, less stereocontrol was observed in this example, as the equatorial nature of the C4-substituent allows for addition of the azido radical from either the top or bottom faces, whereas the axial C4-substituent in the peracetylated galactal substrate hinders addition from the top face.

Scheme 2-5. Azidonitration of Peracetylated Glucal Derivative

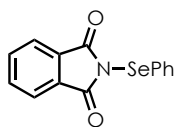


A variety of other methods have been published involving the azidofunctionalization of glycols, and a representative summary is shown in **Table 2-1**.⁶⁴⁻⁶⁸ These methods provided access to densely functionalized glycosides in typically excellent yields (entries 1-2). Unfortunately, stereocontrol was an issue for several systems, and mixtures of products were formed in almost equal amounts (entries 1-2). Entries 3 and 4 featured the use of more mild conditions, but yields of the products obtained were lower in many cases. The method described in entry 4 is noteworthy in that it is relatively general and is tolerant of more complex disaccharide substrates.

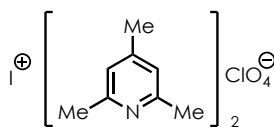
Table 2-1. Representative Examples of Glycol Functionalization

Entry	R ₁	C ₄ Orientation	Conditions	Representative Products
1	-Bn	Axial and equatorial tolerated	TMSN ₃ , TBAF, 2.3 , DCM	
2	-Bn	Equatorial	1) N ₃ I 2) P(OMe) ₃ 3) ROH, DMSO	
3	-Bn	Axial	H ₂ NSO ₂ Ph, 2.4 , DCM	
4 ^a	-Bn, Ac, Me	Axial and equatorial tolerated	2.5 , I ₂ , MeCN	

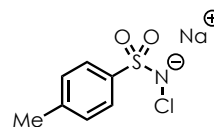
^aDisaccharide substrates tolerated in this reaction as well.



2.3



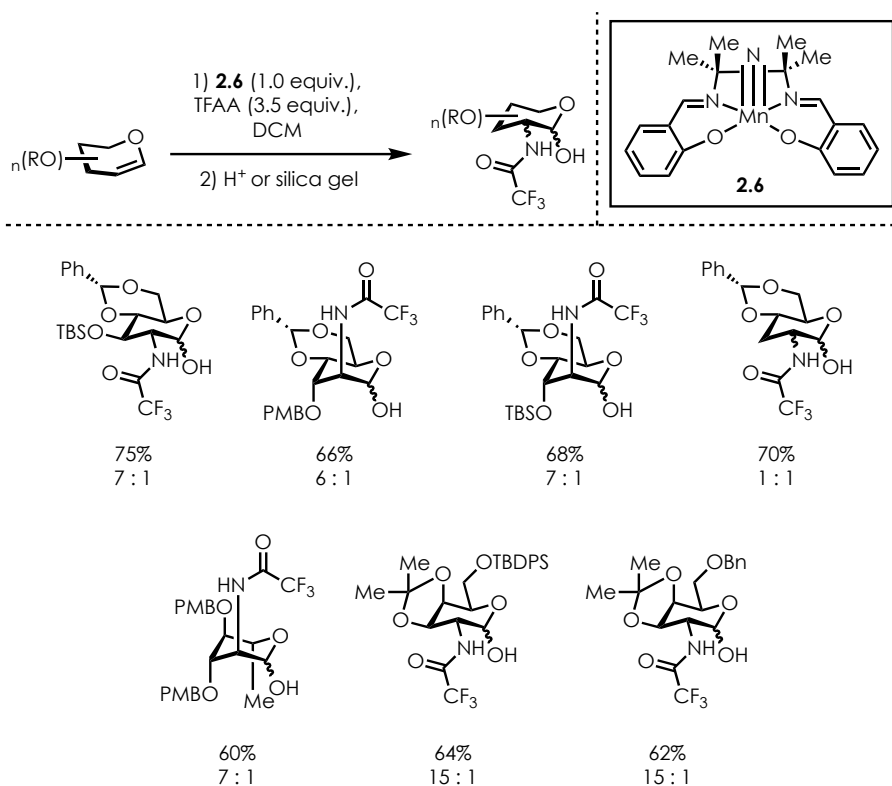
2.4



2.5

The transition metal-mediated synthesis of aminoglycosides is also well explored, and one of the earliest reports was disclosed by the Carreira group.^{69,70} The group was able to develop conditions for the manganese-mediated nitrogen transfer to a family of glycols using a Mn(saltmen) catalyst (**Scheme 2-6**).

Scheme 2-6. Carreira's Synthesis of Aminoglycosides Using Mn Catalysis

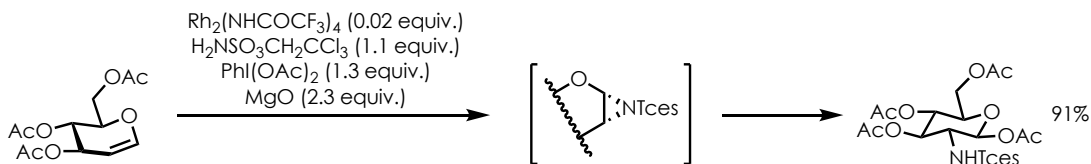


The method was tolerant of a variety of protecting groups, including silyl ethers and acetonides. Yields of the desired products were quite good, and moderate to excellent selectivities were observed in most cases.

DuBois was able to extend a previously disclosed method for the rhodium-catalyzed aziridination of alkenes to the functionalization of glycols (**Scheme 2-7**).⁷¹ The method resulted in the formation of the desired aminoglycoside in excellent yields and selectivities with exclusive formation of the β-anomer observed. Although the original method for the

aziridination of olefins was quite broad, only one glycal substrate was shown to be compatible with the conditions.

Scheme 2-7. DuBois' Synthesis of Aminoglycosides Using Rh Catalysis



While there has been much attention given to the development of methods for the synthesis of 2-aminoglycosides, many of these methods display limited scopes. Additionally, in many cases, reaction sequences comprised of several steps were necessary to effect the desired transformation. There remains a need for a general method to efficiently synthesis 2-aminoglycosides in an expedient manner.

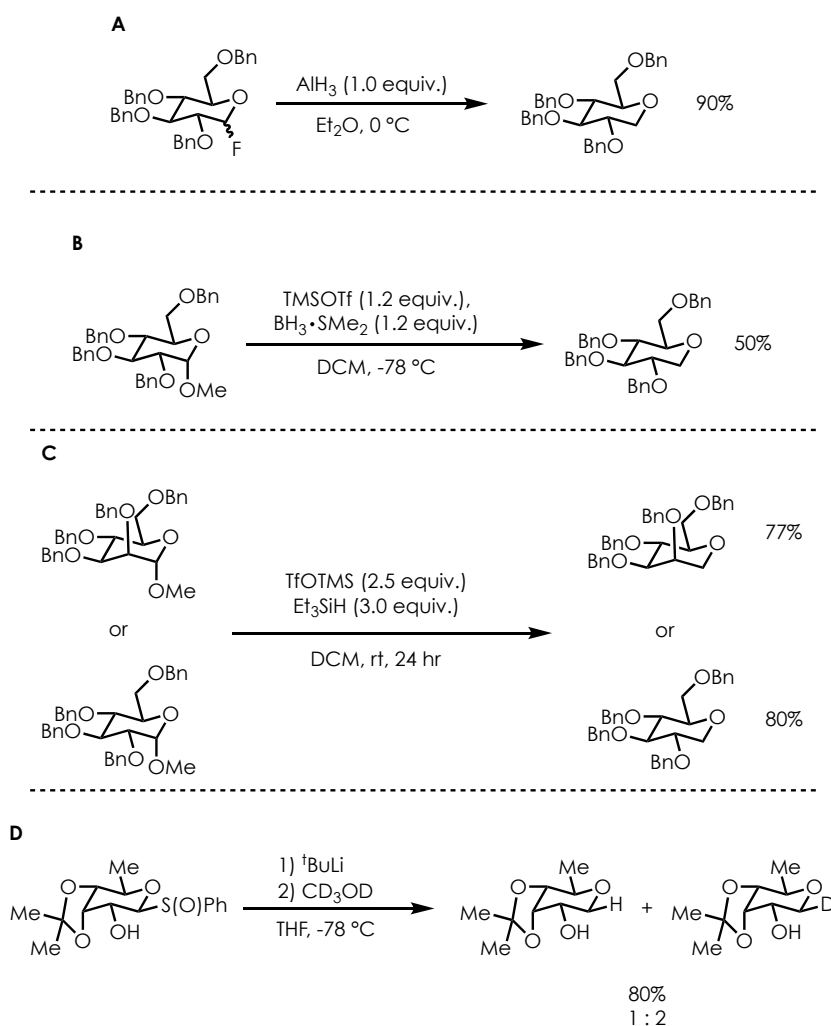
2.1.3 Synthesis of Deoxyglycosides via Polar Chemistry

As with aminoglycosides, the facile synthesis of deoxyglycosides has received a significant amount of attention over the years. The selective removal of one hydroxyl group is a challenge that is typically overcome by careful installation of protecting groups to prevent reactivity of all other reactive functional groups. Although numerous methods have been reported for the synthesis of 2-, 3-, and 4-deoxyglycosides^{72–74}, the synthesis of 1-deoxyglycosides is far less explored. As discussed earlier, 1-deoxyglycosides have been shown to have important biological activities, so their synthesis and derivatization is of interest to the chemical community.

Many of the reports for synthesizing 1-deoxyglycosides in the literature involve the use of strongly basic or reducing reagents in superstoichiometric amounts (**Scheme 2-8**).^{75–79}

The Nicolaou group reported a range of transformations to showcase the utility of glycosyl fluorides, as these compounds had received significantly less attention than other glycosyl halides (**Scheme 2-8A**).⁷⁵ Among these was the use of stoichiometric aluminum hydride to convert the perbenzylated glucose derivative to the 1-deoxyglycoside, and the desired product was formed in excellent yields.

Scheme 2-8. Representative Methods for Deoxyglycoside Synthesis



Although the transformation was accomplished in excellent yields for the previously mentioned substrate, the communication was limited in nature and no other substrates were

reported. Additionally, these conditions would not be compatible with functionality that is sensitive towards strongly reducing reagents.

Another example of conditions for the synthesis of 1-deoxyglycosides was disclosed by the Hunter group as part of a method for the reduction of ketals (**Scheme 2-8B**).⁷⁷ Using TMSOTf and borane-dimethyl sulfide, they were able to convert a small selection of ketals into protected secondary alcohol in typically excellent yields. However, the sole glycoside substrate was not particularly successful in this transformation, and the desired product was only formed in a 50% yield.

Guo and Hui also reported a novel synthetic route to access a small family of C-glycosides.⁷⁶ Their route featured a Lewis acid-mediated reductive cleavage of glycosyl donors with Et₃SiH (**Scheme 2-8C**), and they were able to use both methyl α -D-glucopyranoside and methyl α -D-mannopyranoside as substrates in this transformation. Both deoxyglycoside products were formed in good yields, and the reaction was carried out at ambient temperatures. Unfortunately, superstoichiometric amounts of both the TMSOTf and Et₃SiH were required to effect this transformation.

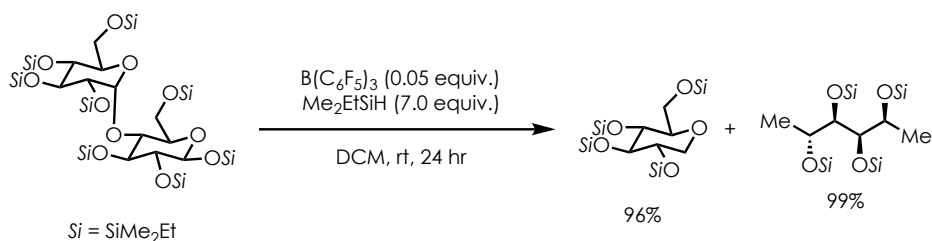
An interesting, and somewhat unexpected, synthesis of 1-deoxyglycosides was reported by the Fernández-Mayoralas group as part of their work to develop conditions for the synthesis of C-glycosides.⁷⁸ In the course of their studies, they discovered that the treatment of glycosyl phenyl sulfoxides with excess *t*BuLi and subsequent exposure to CD₃OD (**Scheme 2-8D**) resulted in a mixture of products. While formation of the expected deuterated product was observed, they also saw formation of the protonated product in a 2:1 ratio. While the main focus of their work was to expose the lithiated glycoside to a series of

electrophiles, this method proved capable of providing access to a 1-deoxyglycoside.

Unfortunately, the yield was quite poor, and only a single example was reported.

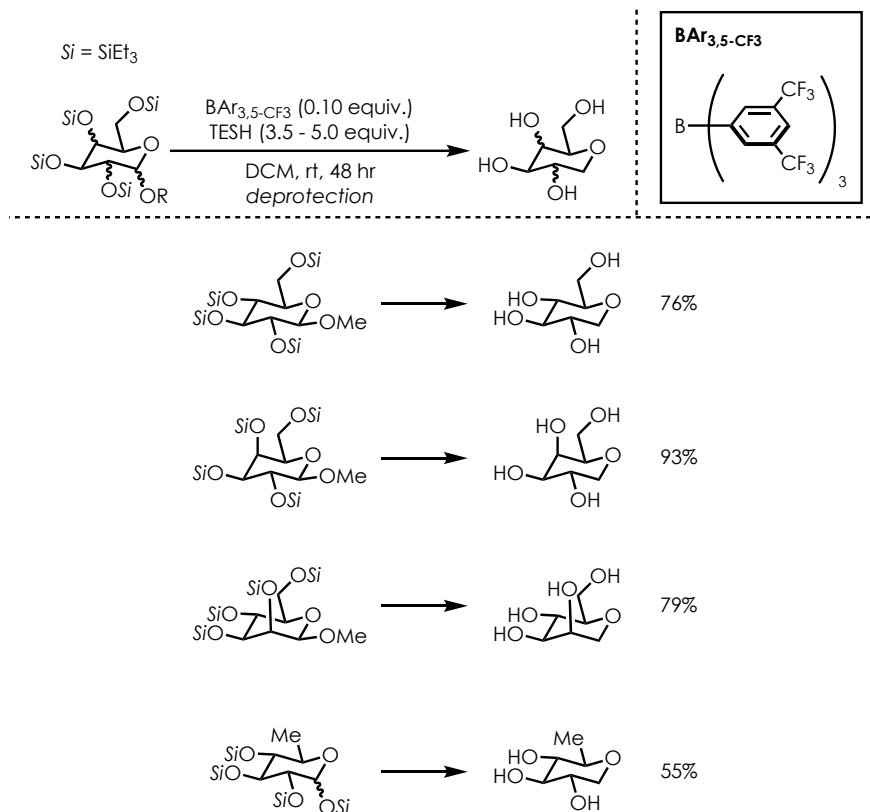
A common theme with the methods discussed above is the limited substrate scopes and superstoichiometric amounts of reagents that are required to effect the desired deoxygenation. While use of these methods could possibly be extended to other substrates, there exists a serious need for a more general strategy for the synthesis of 1-deoxyglycosides. The Gagné group has disclosed several reports of selective hydrosilylative deoxygenation reactions using boron catalysis.^{80,81} One report contained several examples of disaccharides that were converted into 1-deoxyglycosides and linear carbohydrates with an fluoroarylborane catalyst and superstoichiometric amounts of a silane reductant (**Figure 2-9**).

Scheme 2-9. Gagné's Synthesis of Deoxyglycosides and Linear Carbohydrates



Although only a few examples were shown, this system resulted in the efficient formation of the desired products, and reaction progress could easily be followed by ^{13}C NMR spectroscopy. Shortly after, the group published a related study that explored the reactivity differences between two borane catalysts.

Scheme 2-10. Synthesis of Deoxyglycosides Using Boron Catalysis



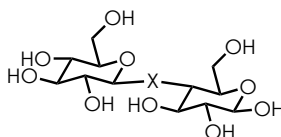
The group discovered that when persilylated glycosides were treated with BAr_{3,5}-CF₃ and Et₃SiH, they observed exocyclic C-O bond cleavage to afford 1-deoxyglycosides (**Scheme 2-10**). They reported the synthesis of a small family of 1-deoxyglycosides in moderate to excellent yields, and several other furanose substrates were tolerated as well. Although this method required the use of a large excess of Et₃SiH and prolonged reaction times, it proved to be a reasonably general method for the synthesis of 1-deoxyglycosides.

2.1.4 Synthesis of Glycomimetics *via* Polar Chemistry

The synthesis of glycomimetics, or carbohydrates with structural modifications, is a broad field, as the alterations that can be made to standard glycosides are numerous.⁸² In an

effort to keep this discussion at a reasonable length, we will focus on the synthesis of glycomimetics with novel linkages. The unusual linkages are broad in nature and can include *S*-glycosides, *C*-glycosides, and *N*-glycosides (**Figure 2-5**).

Figure 2-5. General Scheme Depicting Glycomimetics with Novel Linkages



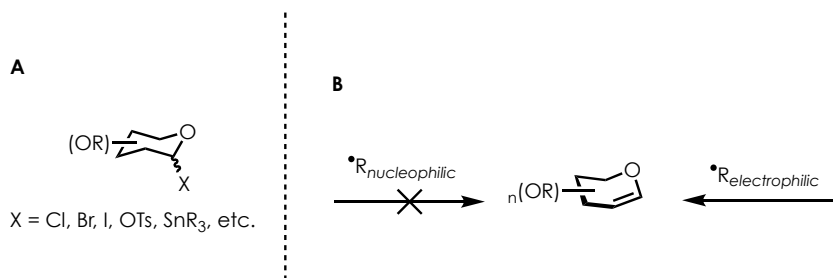
X = S : *S*-glycoside

X = NH : *N*-glycoside

X = CH₂ : *C*-glycoside

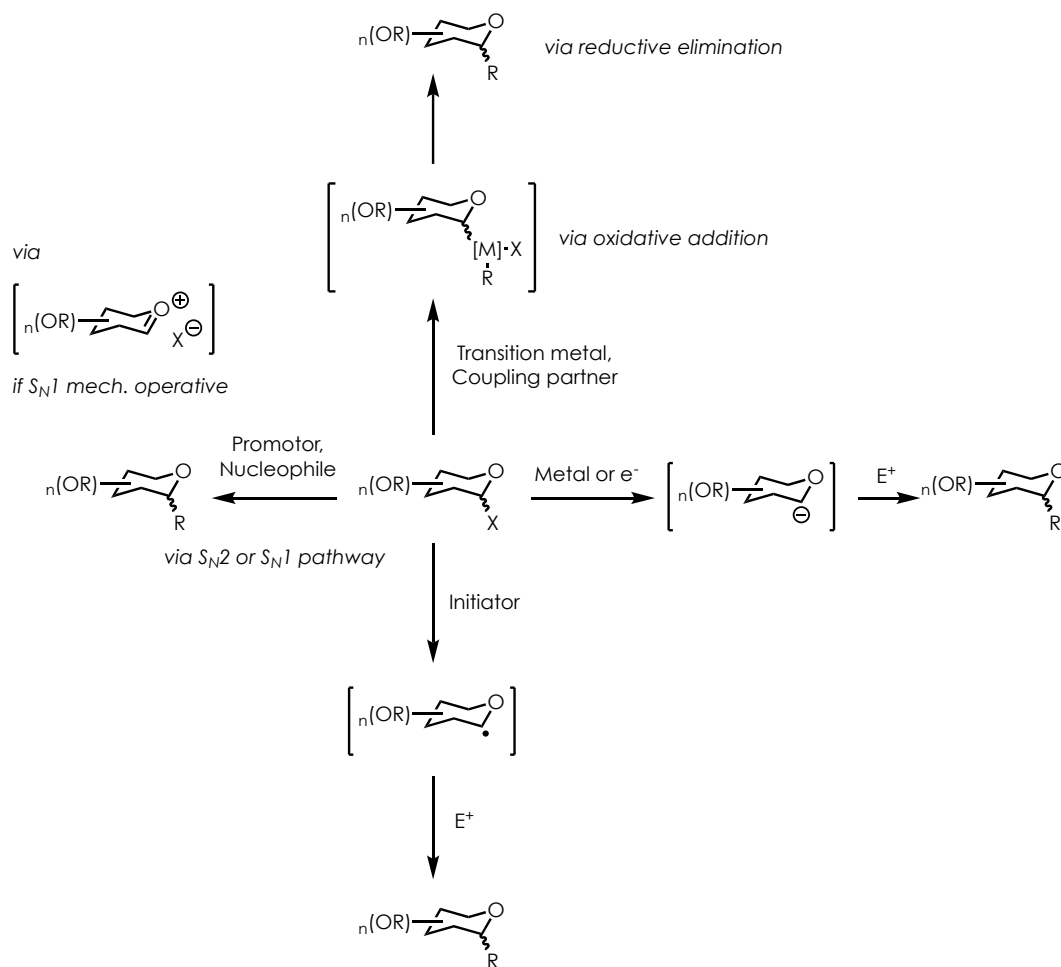
There are several strategies that can be employed to synthesize glycosides with novel linkages, and **Scheme 2-11** details the approaches that will be discussed. As **Scheme 2-11A** shows, glycosides bearing substituents such as halides or stannanes can be used in a variety of transformations, such as transition metal-mediated cross-couplings, to form novel linkages. **Scheme 2-11B** displays the other approach in which a glycal can undergo radical addition with an electrophilic radical species, such as a heteroatom radical, to form novel glycosidic linkages.

Scheme 2-11. Strategies for the Synthesis of Novel Linkages



Much work has been done to develop conditions for the construction of *C*-glycosides, and **Scheme 2-12** details the most common strategies used in these transformations. Glycosyl halides are versatile precursors to a variety of reactivity and have been shown to provide access to *C*-glycosides through transition metal-mediated cross-couplings, radical-mediated reactions, and two-electron reactions proceeding through either an S_N2 or S_N1 pathway.⁸³

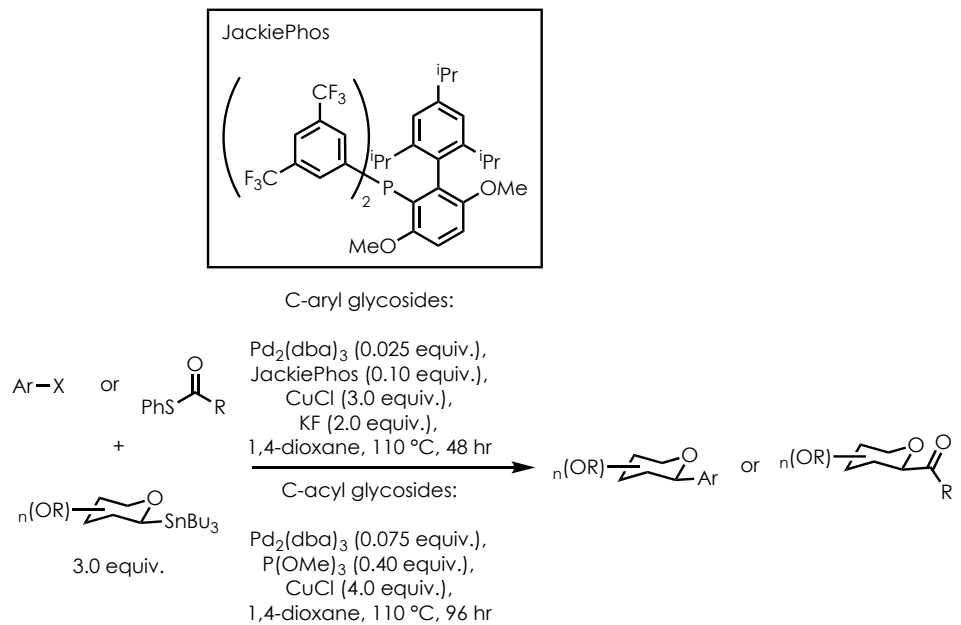
Scheme 2-12. Routes Used to Synthesize *C*-Glycosides



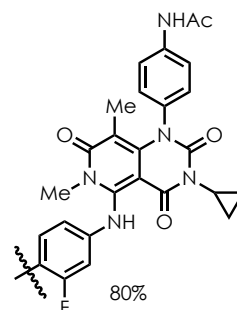
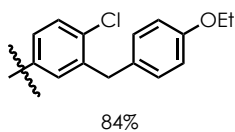
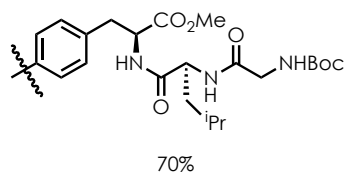
The use of transition metals has been a popular strategy in the construction of *C*-glycosides, and many groups have developed efficient methods for the synthesis of complex glycosides. One such group is the Walczak group, and they have made significant progress in the field of

C-glycoside synthesis *via* glycosyl stannanes. **Scheme 2-13** details a summary of methods they have developed to synthesize a variety of these compounds.^{84,85}

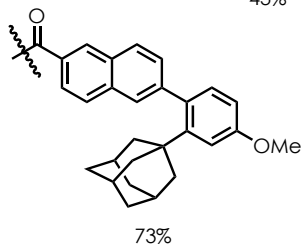
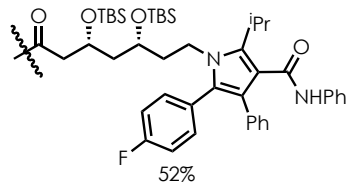
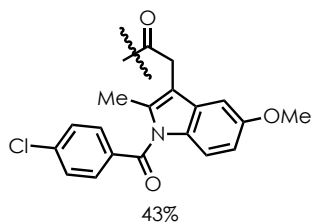
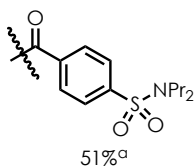
Scheme 2-13. Walczak's Methods for the Synthesis of C-Glycosides



Ar =



R =



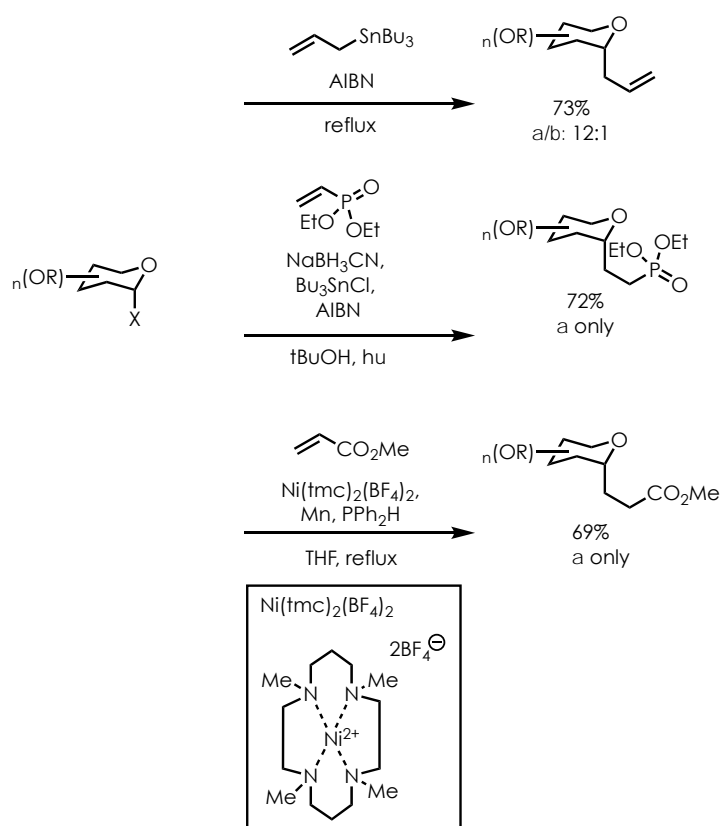
^aJackiePhos (0.30 equiv.) used instead of P(OMe)₃

Though the use of transition metal catalysis, they have been able to access a wide variety of C-glycosides in good yields and excellent stereoselectivities. In addition to the use

of simple aryl halide and acyl thioester coupling partners, they have been able to prepare many example of glycosylated pharmaceuticals and peptides, which illustrates the power of this chemistry in regards to the synthesis of novel glycomimetics. While these methods are extremely general and efficient, they do require the use of excess glycosyl stannanes, which results in the formation of tin-containing byproducts, and the reaction conditions required prolonged periods of intense heating.

The synthesis of *C*-glycosides through glycosyl radicals has also been thoroughly explored, and **Scheme 2-14** details a few of the methods that have been reported.^{86–90}

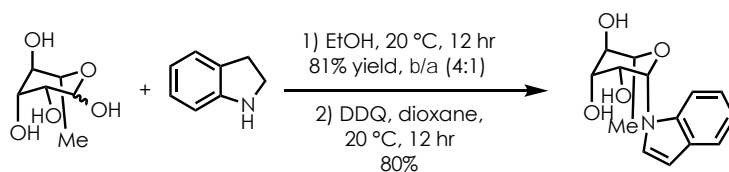
Scheme 2-14. Radical-Mediated Methods for the Synthesis of *C*-Glycosides



The generation of glycosyl radicals can be accomplished through traditional means (AIBN and heat/light) or through the use of manganese powder. These versatile intermediates can go onto react with a variety of radical acceptors to form *C*-glycosides in good yields and excellent selectivities. However, the use of tributyltin reagents is undesirable due to the toxicity of the compounds and their byproducts.

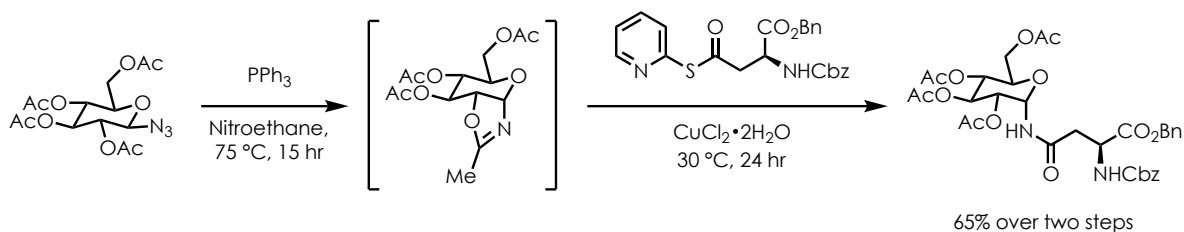
The synthesis of *N*-glycosides, or glycosides bearing linkages containing nitrogenous functionality, has been well explored over the years. *N*-glycosides bearing peptide or other nitrogenous substituents are well precedented, as the compounds often possess biological activities of great interest.⁸² In 2008, Langer disclosed a route for the synthesis of indirubin-*N*-glycosides, as related compounds have been shown to possess potent anticancer activity (**Scheme 2-15**).⁹¹ The sequence provided access to the anomerically pure indol-*N*-glycoside in just two steps and an overall yield of 65%.

Scheme 2-15. Langer's Synthesis of Indol-*N*-Glycoside



The Bernardi group has also reported the synthesis of α -*N*-glycosyl asparagine building blocks⁹² (**Scheme 2-16**), as the conformation of α -*N*-linked glycopeptides was found to be dependent on the stereochemistry of the glycoside. The facile synthesis of these glycopeptides is of interest as this behavior indicates that novel molecules with unprecedented behavior may be within the reach of the chemical community.

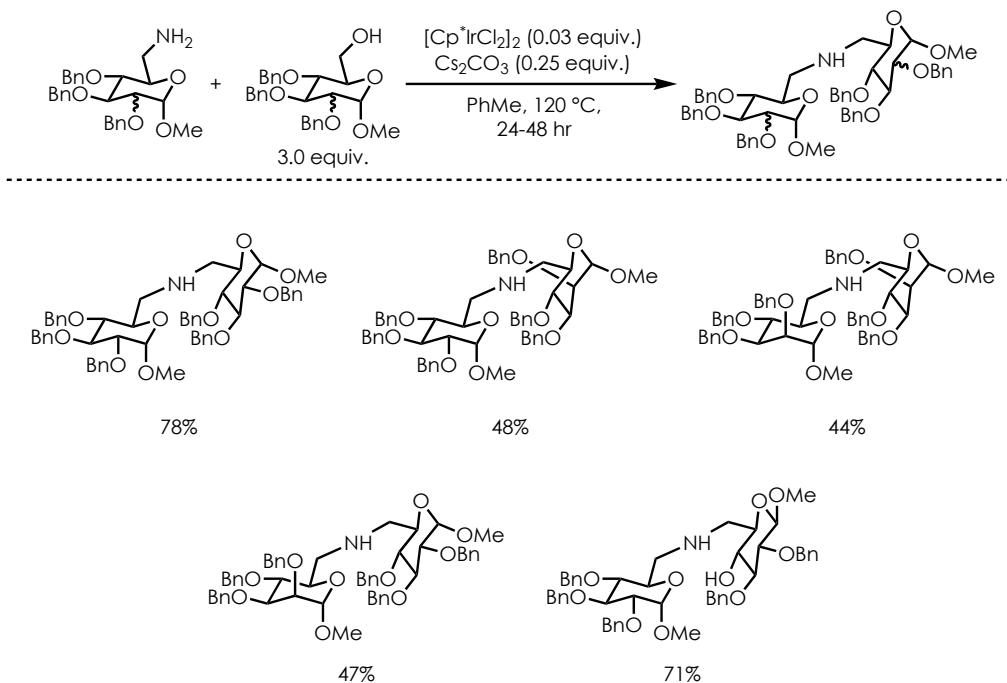
Scheme 2-16. Synthesis of *N*-Linked Glycopeptides from Glycosyl Azides



Tetra-*O*-acetyl- β -D-glucosyl azide was subjected to reductive conditions, and the resulting oxazoline intermediate was acylated using a thiopyridyl ester derivative of aspartic acid. The desired *N*-glycoside was obtained in a 65% yield (α/β : >9:1) over the two steps using mild conditions. The *N*-glycoside was then subjected to further transformations to elongate the peptide chain.

Despite all of the progress in the field of *N*-glycoside synthesis, methods for the synthesis of disaccharides with nitrogenous linkages are still mostly unknown. One method for the synthesis of these compounds was reported by Cumpstey and Mart3n-Matute in 2011 (**Scheme 2-17**) and featured the use of an iridium catalyst.⁹³ Unfortunately, only a few examples were shown, and yields of the desired disaccharides were quite varied. However, they were able to demonstrate that the system possessed excellent regioselectivity when they demonstrated the formation of a single product when both free primary and secondary hydroxyl groups were present.

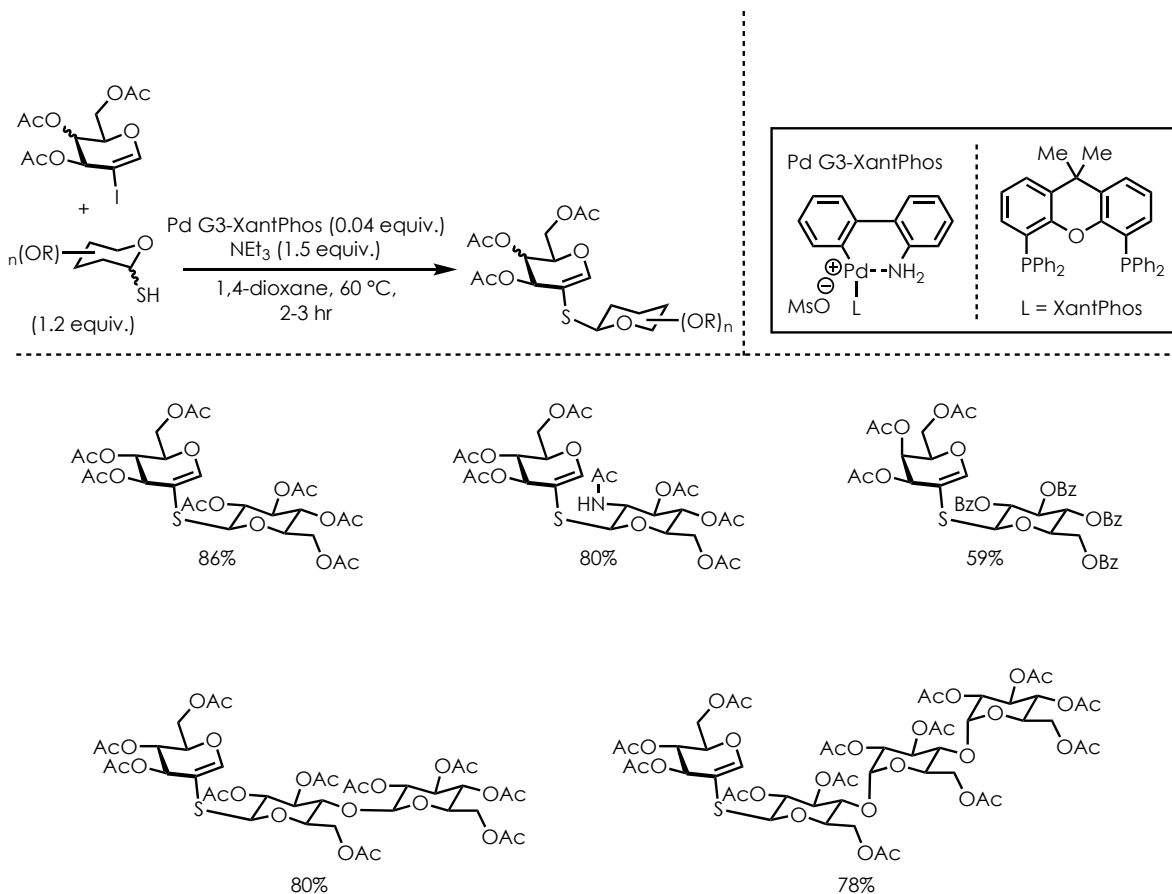
Scheme 2-17. Synthesis of Disaccharides with *N*-Linkages



S-glycosides are popular glycomimetics, as the thiol-based glycosidic linkage is considerably more stable towards hydrolysis or enzymatic degradation.⁸² As such, *S*-glycosides have been investigated as potential new therapeutics due to their enhanced stability. A popular strategy for the construction of *S*-glycosides is through the use of transition metal catalysis. Alemi and Messaoudi have reported a method for the synthesis of thio-linked glycoconjugates using a palladium-G3-Xantphos precatalyst and iodoglycals as coupling partners (**Scheme 2-18**).⁹⁴ They were able to access a variety of disaccharides and oligosaccharides with *S*-glycosidic linkages in moderate to excellent yields and with quite mild reaction conditions. The use of transition metal-mediated reactions is a powerful tool in

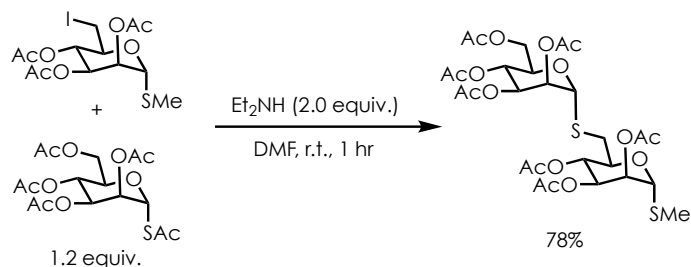
the arsenal of chemists as they look to develop methods for the construction of novel *S*-glycosides.

Scheme 2-18. Transition Metal-Mediated Synthesis of *S*-Glycosides



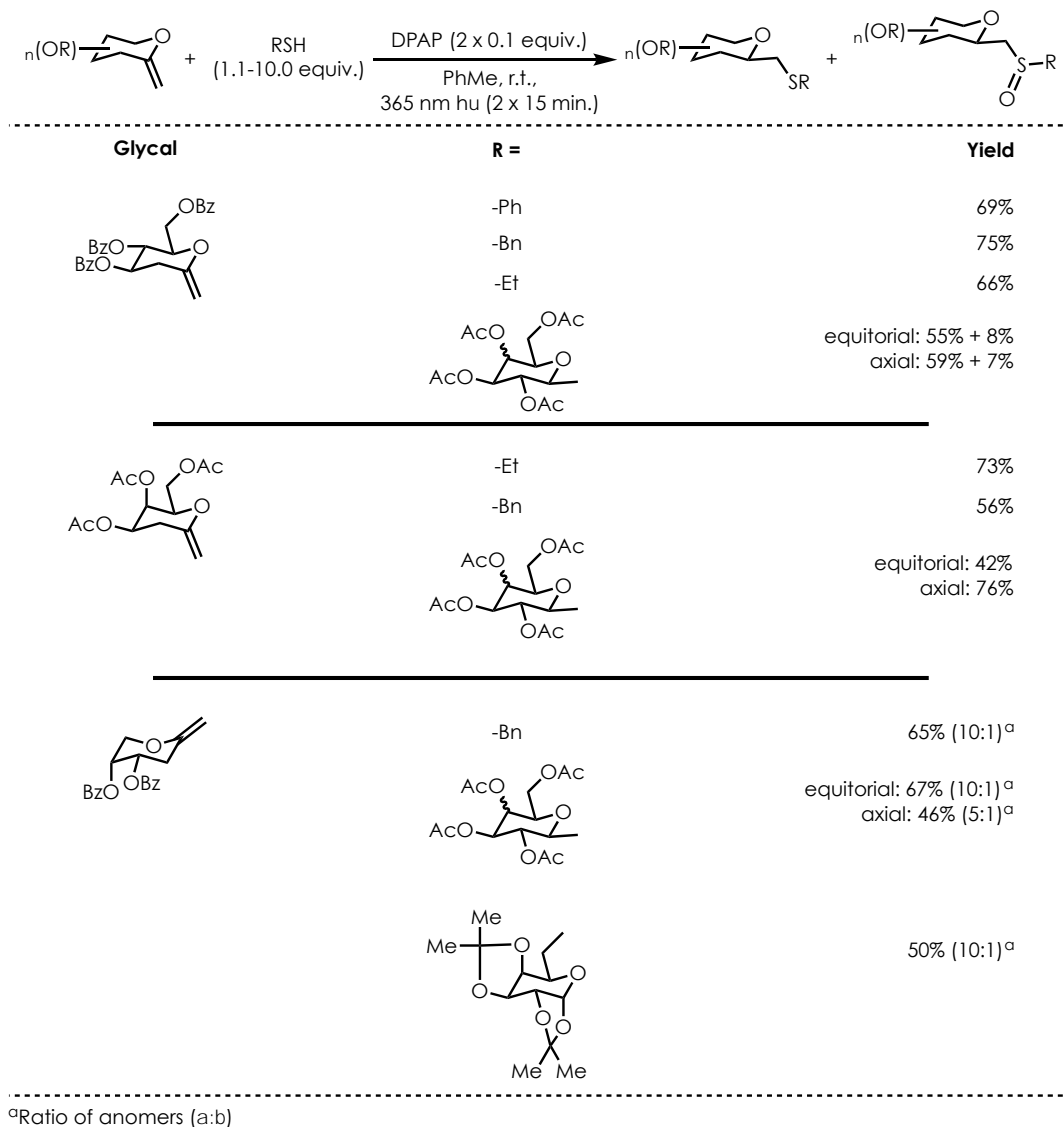
The Williams group also published a synthetic strategy for accessing *S*-oligosaccharides, and a representative example is shown in **Scheme 2-19**.⁹⁵ Treatment with diethylamine resulted in the formation of the desired disaccharide with a *S*-glycosidic linkage in good yields. Additionally, upon conversion of the primary acetate group in the product to an iodide, the sequence could be repeated to rapidly generate *S*-oligosaccharides in good yields.

Scheme 2-19. Sequential Synthesis of *S*-Oligosaccharides



Polar chemistry and transition metal-mediated reactions are not the only strategies for synthesizing *S*-glycosides. Inspired by work published by Dondoni and Marra⁹⁶ in the late 2000's (**Scheme 2-20**), Juhász and Somsák⁹⁷ recently disclosed a report in which they developed conditions for a radical-mediated thiol-ene reaction. Their system was compatible with several *exo*-glycals, and they were able to showcase a variety of thiols from which thiyl radicals could be generated. As shown in **Scheme 2-20**, yields of the desired products were generally quite good, and in most cases, excellent stereocontrol was observed. Simple thiols, such as thiophenol and ethanethiol, could be used in this reaction, as well as more complex thioglycosides. Although this method offers facile access to a small family of glycomimetics with thio-linkages, the formation of sulfoxide byproducts was often observed and, in some cases, the desired products could not be adequately purified.

Scheme 2-20. Radical-Mediated Synthesis of *S*-Glycosides



Despite all of the progress that has been made in the field of glycomimetics, many of these methods are limited in scope and plagued by mediocre yields of the desired product. Additionally, the newly formed glycosidic linkages are always located at the C1-position, which limits the number of novel compounds that can be synthesized. There still exists a need for a general method for the synthesis of glycomimetics utilizing simple starting

materials and mild reaction conditions. The ideal method would provide access to a wide range of compounds and be tolerant of a variety of functional groups.

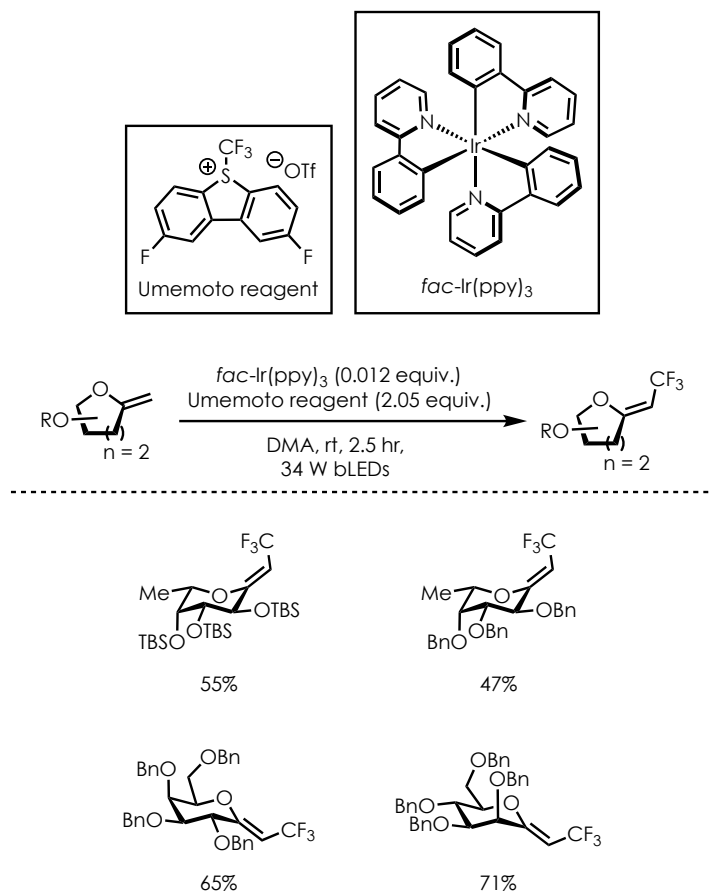
2.1.5 Synthesis of Glycosides and Glycomimetics *via* Photoredox/Photoacid Catalysis

As established in the previous sections, the synthesis of glycosides and glycomimetics using polar or classical radical chemistry has been well explored, but there are many challenges that still need to be addressed. As a result, groups have begun to investigate the use of photoredox catalysis as a potential solution to the efficient synthesis of these compounds.

The synthesis of deoxyglycosides, aminoglycosides, and glycomimetics *via* the photoredox catalysis-mediated functionalization of *exo*- and *endo*-glycals has the potential to address several of the shortcomings of the methods previously discussed. Photoredox catalysis employs relatively mild reaction conditions, and, in some cases, avoids the use of transition metals and/or hazardous reagents. However, existing examples of the use of photoredox catalysis in the synthesis of glycosides and glycomimetics are relatively limited.

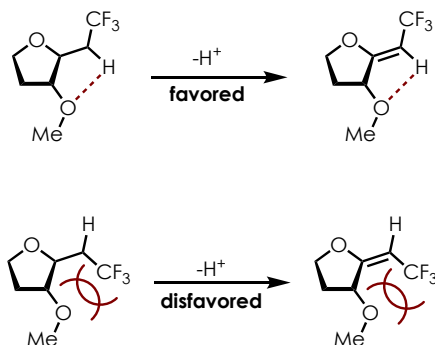
One example of *exo*-glycal functionalization that has the potential to be used *en route* to accessing glycomimetics was disclosed by the Vincent group in 2018.^{20–23} They developed an Ir-catalyzed method for the C-H trifluoromethylation of *exo*-glycals using the Umemoto reagent as the source of the trifluoromethyl radical. The method resulted in the highly diastereoselective trifluoromethylation of several *exo*-glycals, as shown in **Scheme 2-21**. The products were formed in moderate yields as a single diastereomer that featured a *Z*-olefin.

Scheme 2-21. Photoredox-Mediated Trifluoromethylation of *Exo*-Glycols



While the scope of this transformation in regard to pyranose-derived glycols was not particularly broad, the selectivity for the formation of the *Z*-olefin is extremely impressive. The group turned to computational methods and discovered that the *Z*-olefin isomer is more stable from both kinetic and thermodynamic standpoints. As shown in **Figure 2-6**, the *Z*-olefin is stabilized by intramolecular hydrogen bonding, which can occur between the adjacent alkoxy group and the olefinic proton. The *E*-olefin experiences unfavorable steric interactions between the alkoxy and trifluoromethyl groups, which results in its status as the disfavored conformer.

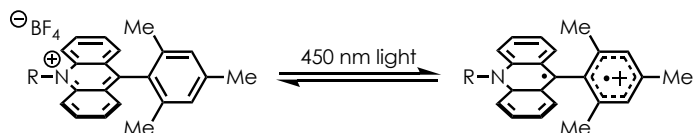
Figure 2-6. Rationale for Exclusive Formation of Z-Olefins



Although limited in scope and by moderate yields, this method shows the potential for the use of photoredox catalysis to synthesize glycomimetic precursors *via* *exo*-glycal functionalization in a highly selective manner.

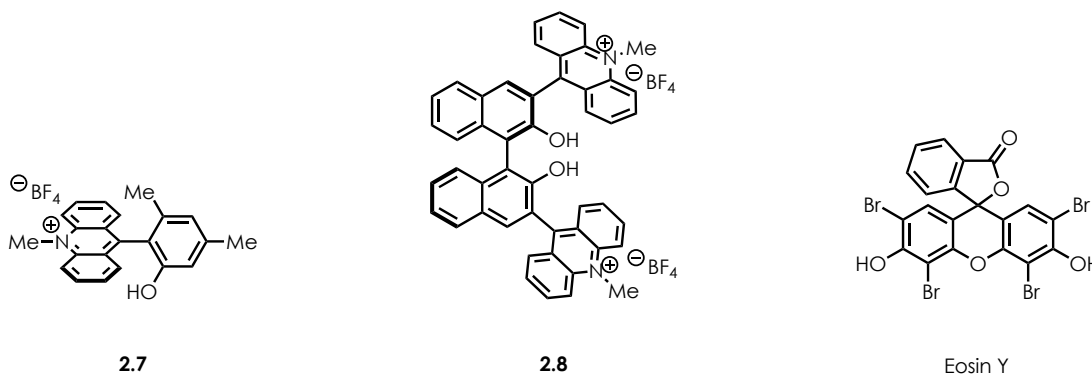
Groups are also interested in the use of *endo*-glycals as precursors of deoxyglycosides and glycomimetics, and the Wang group has disclosed a system for a photoacid-mediated glycosylation reaction.^{99,100} The group was interested in developing a mild, efficient method for the synthesis of 2-deoxyglycosides that featured the nucleophilic addition of an alcohol into an activated glycal, as this process is extremely atom economical. They sought to identify reaction conditions that provided high stereocontrol and limited the formation of Ferrier-type byproducts, which led them to consider visible light photocatalysis. Inspired by work from the Fukuzumi group¹⁸ and our lab^{33,101}, they saw the acridinium salt motif as an attractive starting point for their catalyst development.

Figure 2-7. Generation of Charge Transfer State of 9-Mesityl Acridiniums



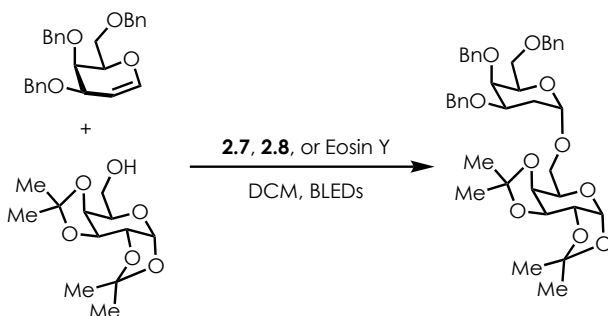
Acridinium salts with a mesityl group at the 9-position are known to undergo an ET event intramolecularly to form charge transfer states (**Figure 2-7**) upon irradiation with visible light.¹¹ These species possess potent oxidizing abilities and have been used in a wide variety of transformations, as discussed in Chapter 1. Additionally, phenolic derivatives have been shown to display increased acidity when exposed to visible light irradiation¹⁰², and the Wang group was curious if incorporating such a unit into an acridinium salt or other photoredox catalyst would result in photoacid activity. As such, they designed two novel catalysts (**2.7** and **2.8**) to evaluate alongside a commercially available photoacid, Eosin Y (**Figure 2-8**).

Figure 2-8. Novel and Commercial Photoacid Catalysts



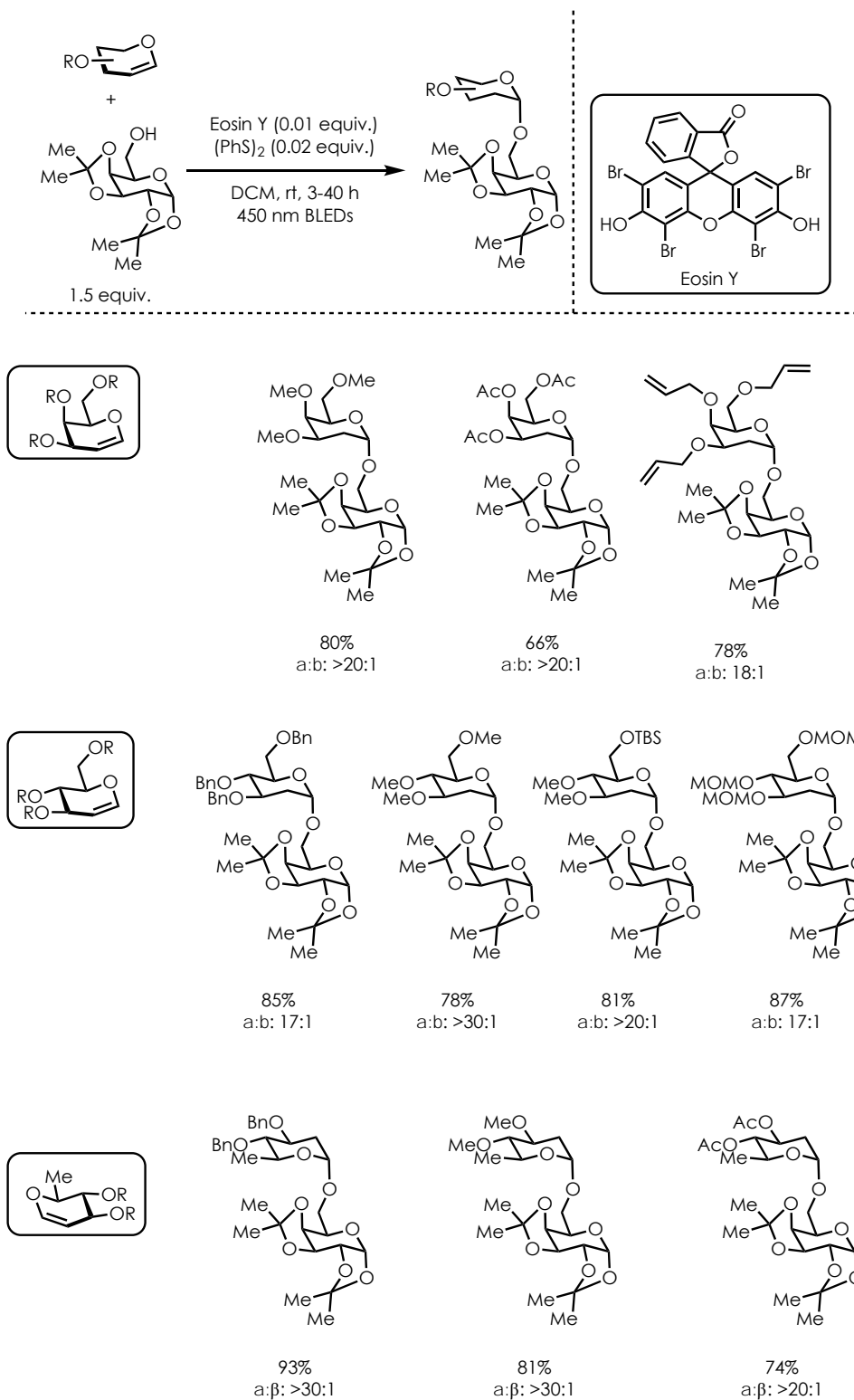
Investigation revealed that all three photoacid catalysts shown in **Figure 2-8** resulted in the formation of desired glycosylated product when used in the model reaction shown in **Scheme 2-22**, but, ultimately, eosin Y was chosen as the optimal catalyst for the transformation.

Scheme 2-22. Model Reaction for Photoredox-Mediated Glycosylation



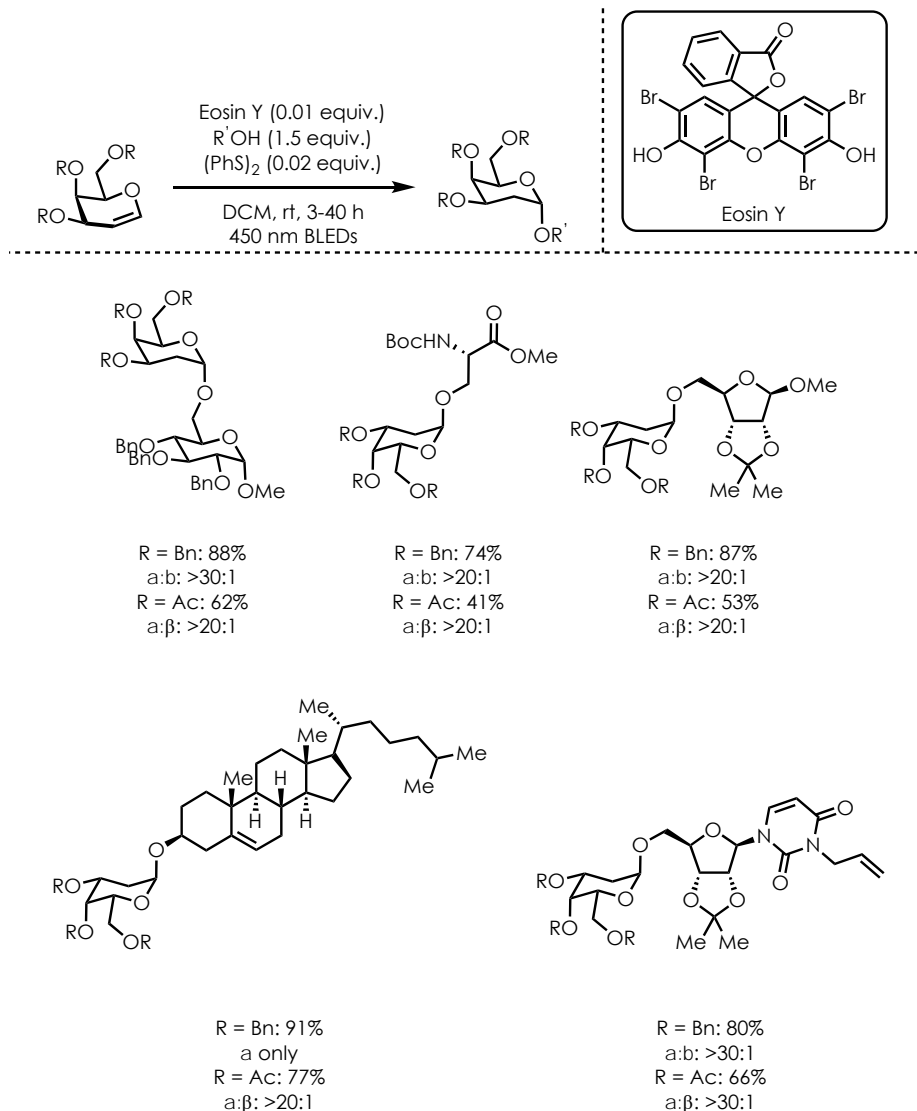
Upon determination of the optimal reaction conditions, including identifying (PhS)₂ as the most effective H-atom donor, a scope of *endo*-glycals was explored (**Scheme 2-23**). Several series of glycals, including galactals, glucals, and L-rhamnals were evaluated, and all were successful glycal donors in the glycosylation transformation. A variety of protecting groups, such as allyl ethers, silyl ethers, and benzyl ethers, were well tolerated in the transformation with the desired products formed in excellent yields. Another impressive aspect of the transformation was the excellent α -selectivity observed in all cases.

Scheme 2-23. Scope of *Endo*-Glycal Substrates in Photoredox-Mediated Glycosylation



In addition to exploring a scope of *endo*-glycals, the Wang group was also interested in determining a scope of alcohol nucleophiles. A representative scope is shown in **Scheme 2-24**, and yields of the desired products ranged from moderate to excellent. Once again, excellent α -selectivity was observed in all cases, which highlights the utility of this transformation, as such high selectivity is often not observed in glycosylation reactions. The group was especially excited that tri-*O*-acetyl galactal was such a competent substrate, as *endo*-glycals with acetoxy substituents in the 3-position are prone to Ferrier-type rearrangement, but those byproducts were not observed in this reaction. A variety of complex alcohol nucleophiles were quite successful in this transformation and shows the power of photoacid-mediated glycosylation reactions.

Scheme 2-24. Scope of Alcohol Nucleophiles in Photoredox-Mediated Glycosylation

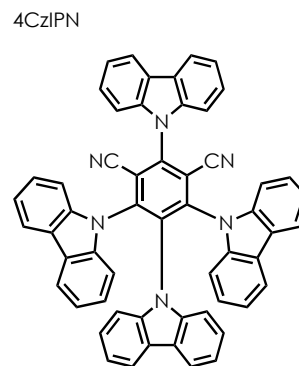
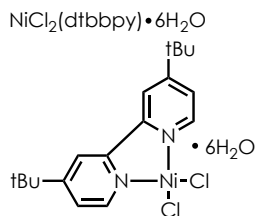
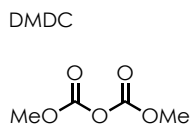
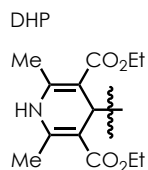
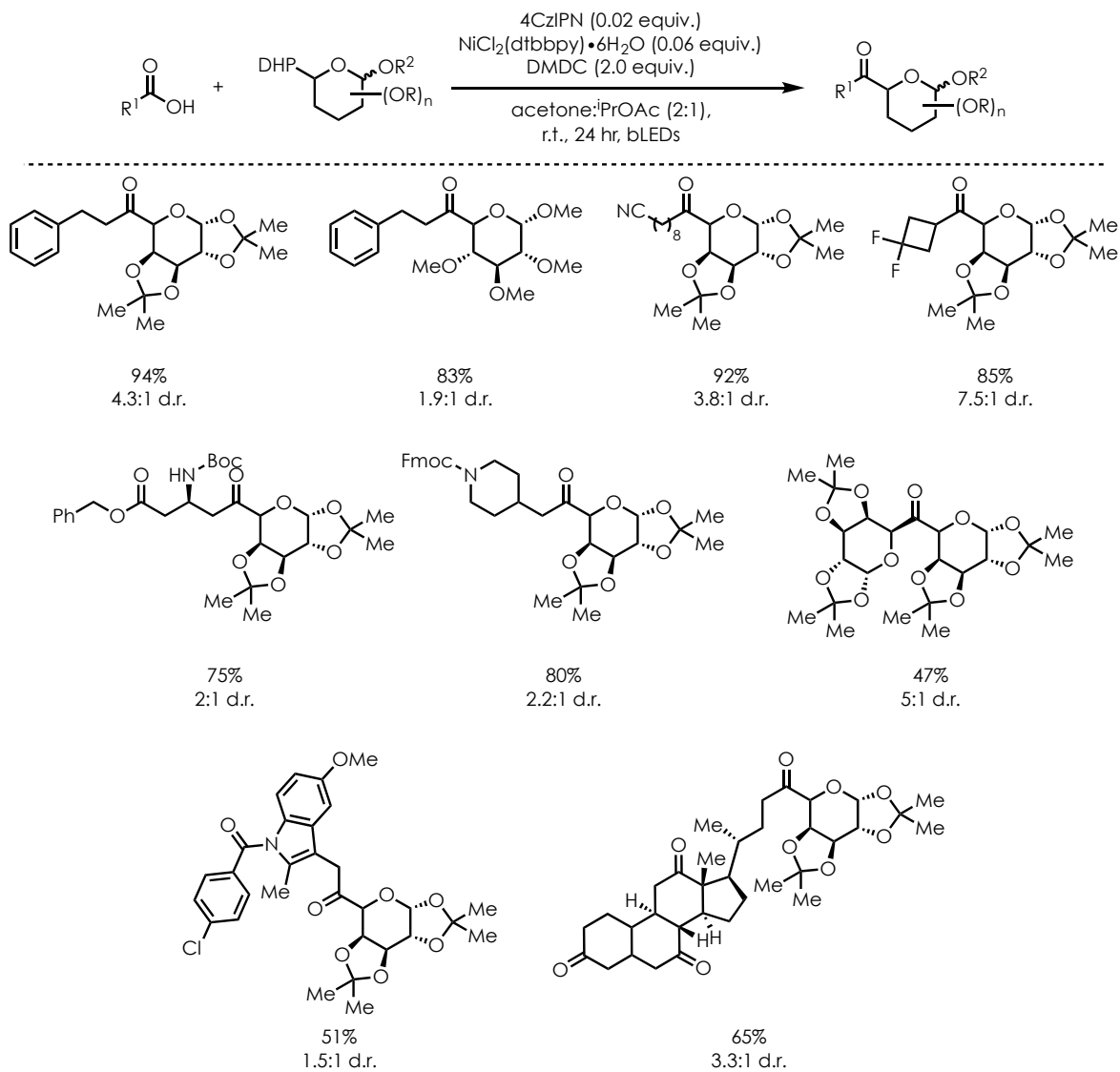


As a modified acridinium salt was employed as the catalyst for this transformation, the group was concerned with confirming that the catalyst was operating as a photoacid and not in a traditional photoredox capacity. By carrying out Stern-Volmer emission quenching experiments, they were able to confirm redox inactivity between tri-*O*-benzyl galactal and

the photoacid catalyst. Additionally, they ran several control reactions where light was excluded, the photoacid catalyst was excluded, or the disodium salt of eosin Y was used, and they observed a complete lack of reactivity in all cases. The group believed that this evidence supported their proposal that this reaction proceeded through a catalytic cycle that featured the protonation of an *endo*-glycal substrate by the excited state photoacid catalyst. Upon generation of the oxocarbenium ion intermediate, the alcohol nucleophile was able to undergo nucleophilic addition into the oxocarbenium ion to generate an intermediate that simply needed to be deprotonated to form the desired glycoside product. While an effective system for the synthesis of disaccharides, this system was limited in that only alcohol nucleophiles were explored. Additionally, reactivity occurred solely at the C1-position. The utility of this transformation would be greatly improved if other nucleophiles could be employed to synthesize glycomimetics or if conditions could be modified to access 1-deoxyglycosides.

Perhaps the most impressive use to date of photoredox catalysis in the synthesis of glycomimetics comes from the Molander group. They were able to develop conditions for the synthesis of non-anomeric *C*-acyl glycosides using tandem photoredox/nickel catalysis (**Scheme 2-25**).¹⁰³

Scheme 2-25. Substrate Scope for Synthesis of C-Glycosides



The method utilized 4CzIPN, an inexpensive organic photoredox catalyst and a Ni(II) complex to efficiently generate non-natural C-acyl glycosides. As shown by the representative scope above in **Scheme 2-25**, this system resulted in the formation of many complex C-acyl glycosides in moderate to excellent yields. Functional groups such as protected amines, cyano groups, and esters were all tolerated in this transformation with the desired C-acyl glycosides formed in excellent yields. Perhaps most impressively, complex steroidal and glycosidic carboxylic acids were compatible with the conditions employed although diminished yields of the products were observed. Unfortunately, low diastereocontrol was observed in most cases, and the system did require the use of a transition metal complex, as well as an activator.

2.1.6 Extension of Photoredox Catalysis to the Synthesis of Novel Glycosides

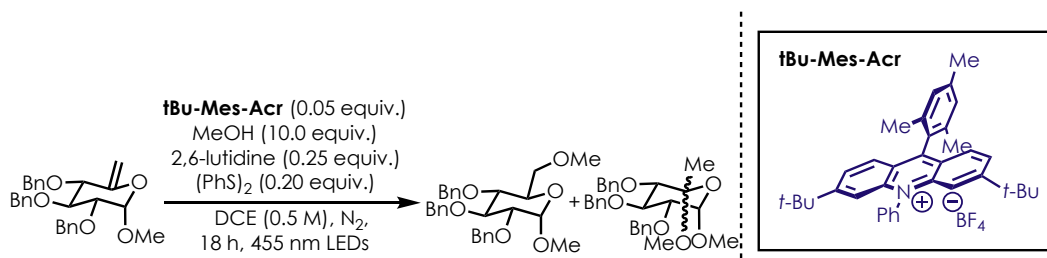
The methods discussed in the previous section detail current efforts towards the synthesis of glycosides and glycomimetics *via* the photoredox/photoacid catalysis-mediated functionalization of *exo*- and *endo*-glycals. While few in number, these methods are powerful tools in the arsenal of chemists who are interested in constructing complex glycosides/glycomimetics in a mild, efficient manner. In each method, excellent selectivities were observed, which highlights the utility of photoredox/photoacid catalysis in the realm of carbohydrate chemistry. However, one limitation of these methodologies, as well as the more traditional methods discussed previously, is the exclusive reactivity at the C1-position. While 2-deoxyglycosides are undeniably important, 1-deoxyglycosides also possess a range of important biological activities.^{104,105} The facile synthesis of glycosides and glycomimetics is of interest to the chemical biology community, as these molecules can be used for a number of important functions, such as *in vivo* bioimaging, drug design, and stability enhancement.¹⁰⁶

We believe that the opportunity remains for the development of a photoredox catalysis-mediated method to efficiently synthesize 1-deoxyglycosides, 2-aminoglycosides, and various glycomimetics. Additionally, we envision that our acridinium salt-mediated organic photoredox catalysis platform³⁴ could be extended to provide facile access to a variety of glycosides/glycomimetics that would be of interest to the synthetic and chemical biology communities.

2.2 Results and Discussion

2.2.1 Previous Work

Initial efforts in the realm of *exo*-glycal functionalization were carried out by an alumnus of the lab, Heqing Sun. His work served as the inspiration for the chemistry that will be discussed in later sections. As this work remains unpublished, a discussion of the data is provided below to summarize efforts to-date towards the hydrofunctionalization of both *exo*- and *endo*-glycals.

Table 2-2. Solvent Screen for Hydroalkoxylation of *Exo*-Glycal


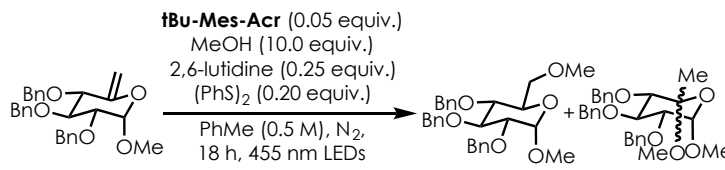
Entry ^a	Deviation from above conditions	Yield (anti-Mark. : Mark) ^b
1	None	13% : <10%
2	DCE (0.1 M)	<10% : <10%
3	EtOAc (0.5 M)	0% : 0%
4	DCM (0.5 M)	13% : <10%
5	PhCF ₃ (0.5 M)	20% : <10%
6	1,4-dioxane (0.5 M)	<10% : <10%
7	TFE (0.5 M)	0% : 0%
8	Acetone	<10% : 0%
9	CHCl ₃ (0.5 M)	14% : <10%
10	PhMe (0.5 M)	28% : <10%
11	PhMe (0.1 M)	20% : <10%
12	No tBu-Mes-Acr	0% : 0%
13	No 455 nm LEDs	0% : <10%
14	No (PhS) ₂	0% : <10%

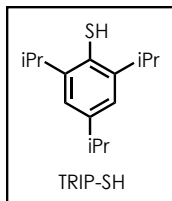
^aReactions run on a 0.10 mmol scale. ^bYields reported are ¹H NMR yields using HMDSO as an internal standard.

Work towards the development of a hydrofunctionalization method for *exo*-glycals began with the use of MeOH as a nucleophile in conjunction with a substrate derived from methyl- α -D-glucopyranoside, as shown in entry 1 of **Table 2-2**. The formation of the desired anti-Markovnikov regioisomer was observed in a 13% yield, which was a promising beginning to the functionalization of *exo*-glycals using photoredox catalysis. In addition to the formation of the desired regioisomer, a small amount (<10% yield) of the undesired Markovnikov product was formed in the course of the reaction as well. A survey of solvents (entries 2-10) revealed that toluene was the most effective reaction medium with a 28% yield of desired product formed along with trace amounts of the undesired regioisomer. It was also determined that a reaction concentration of (0.5 M) resulted in higher amounts of desired

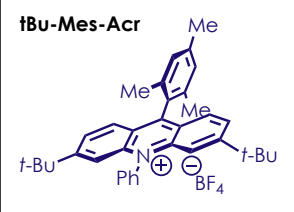
product formation than more dilute reaction concentrations (entry 11). In order to confirm that the observed reactivity was mediated by the photoredox catalyst, several control experiments were run (entries 12-14), and in the absence of **tBu-Mes-Acr**, no reactivity was observed. However, as shown in entries 13 and 14 of **Table 2-2**, some background reactivity was observed, and the undesired Markovnikov adduct was formed in trace (<10% yield) amounts.

Table 2-3. Condition Optimization for Hydroalkoxylation of *Exo*-Glycal





TRIP-SH



tBu-Mes-Acr

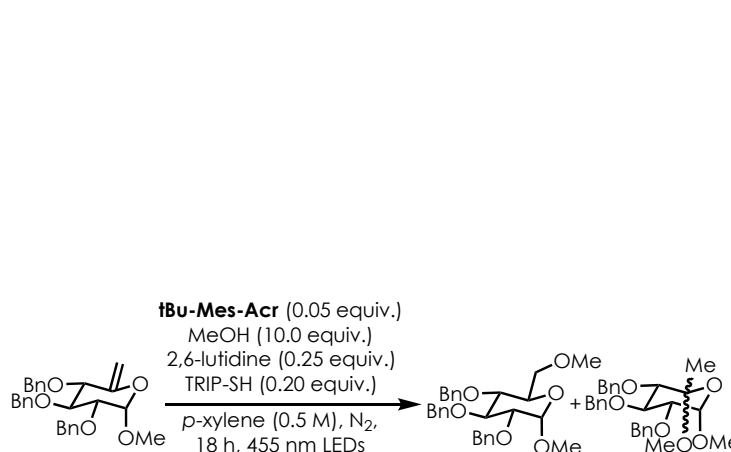
Entry ^a	Deviation from above conditions	Yield (anti-Mark. : Mark) ^b
1 ^c	None	28% : <10%
2	TRIP-SH (0.20 equiv.)	48% : 0%
3 ^d	<i>o</i> -dichlorobenzene (0.5 M)	20% : 20%
4 ^d	PhCF ₃ (0.5 M)	21% : 0%
5 ^d	<i>p</i> -xylene (0.5 M)	81% : 0%
6 ^d	<i>m</i> -dichlorobenzene (0.5 M)	27% : 0%
7 ^d	DMF (0.5 M)	<10% : 0%

^aReactions run on a 0.10 mmol scale. ^bYields reported are ¹H NMR yields using HMDSO as an internal standard. ^cEntry 1 is identical to entry 10 of **Table 2-2**. ^dTRIP-SH (0.20 equiv.) used as H-atom donor in place of (PhS)₂.

As entry 2 of **Table 2-3** shows, the use of TRIP-SH as the H-atom donor in this reaction had extremely beneficial effects, and the desired product was formed in a 48% yield. Additionally, no formation of the undesired regioisomer was observed, which was

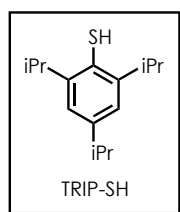
encouraging. An additional survey of solvents revealed that the use of *p*-xylene resulted in formation of the desired product in good yields and with excellent regioselectivity.

Table 2-4. Additional Optimization for Hydroalkoxylation of *Exo*-Glycal



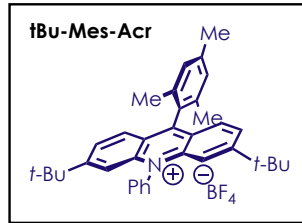
tBu-Mes-Acr (0.05 equiv.)
 MeOH (10.0 equiv.)
 2,6-lutidine (0.25 equiv.)
 TRIP-SH (0.20 equiv.)

p-xylene (0.5 M), N₂,
 18 h, 455 nm LEDs



TRIP-SH

tBu-Mes-Acr



Entry ^a	Deviation from above conditions	Yield (anti-Mark. : Mark) ^b
1	None	81% : 0%
2	(<i>p</i> -tolS) ₂ (0.20 equiv.)	53% : 0%
3	(<i>p</i> -OMe-PhS) ₂ (0.20 equiv.)	56% : 0%
4	(<i>p</i> -Cl-PhS) ₂ (0.20 equiv.)	68% : 0%
5	<i>o</i> -CO ₂ Me-PhSH (0.20)	29% : 0%
6	2,4,6-collidine (0.25 equiv.)	80% : 0%
7 ^c	3-Me-2,6-di- <i>t</i> Bu-pyridine (0.25 equiv.)	70% : 0%
8 ^c	2,6-di- <i>t</i> Bu-pyridine (0.25 equiv.)	73% : 0%
9 ^c	3,5-dimethyl-pyridine (0.25 equiv.)	53% : 0%
10 ^c	MeOH (2.0 equiv.)	<10% : 0%
11 ^c	MeOH (5.0 equiv.)	38% : 0%
12 ^c	MeOH (8.0 equiv.)	73% : 0%
13 ^c	MeOH (15.0 equiv.)	90% : 0%

^aReactions run on a 0.10 mmol scale. ^bYields reported are ¹H NMR yields using HMDSO as an internal standard. ^c2,4,6-collidine (0.25 equiv.) used as base instead of 2,6-lutidine.

As the use of TRIP-SH had resulted in a significant increase in the yield of desired product, several other H-atom donors were investigated (**Table 2-4**, entries 2-5). While several resulted in the formation of the desired product in good yields, none offered improvements over the use of TRIP-SH. Additionally, no evidence of the undesired regioisomer was observed in these trials. In order to more efficiently facilitate the

deprotonation of the nucleophile upon addition into the cation radical, a variety of bases were screened, and the use of 2,4,6-collidine (entry 6) was found to result in comparable yields of desired product, as well as an improved mass balance. The amount of MeOH used as the nucleophile was explored as well, and it was found that increasing the amount (**Table 2-4**, entry 13) resulted in the formation of the desired anti-Markovnikov product in excellent yields.

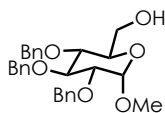
Table 2-5. Nucleophile Scope for Hydrofunctionalization of *Exo*-Glycals

TRIP-SH

tBu-Mes-Acr

Entry ^a	Deviation from above conditions	Yield (anti-Mark. : Mark) ^b
1	None	90% : 0%
2	<i>m</i> -xylene (0.5 M)	83% : 0%
3	<i>o</i> -xylene (0.5 M)	88% : 0%
4	EtOH (15.0 equiv.)	93% : 0%
5	<i>i</i> PrOH (15.0 equiv.)	83% : 0%
6	Cyclohexylmethanol (15.0 equiv.)	60% : 0%
7	Triflamide (1.5 equiv.)	26% : 0%
8	Pyrazole (1.5 equiv.)	0% : 0%
9 ^c	2.9 (1.5 equiv.)	0% : 0%

^aReactions run on a 0.10 mmol scale. ^bYields reported are ¹H NMR yields using HMDSO as an internal standard. ^c*p*-xylene (0.1 M) used as solvent system.



2.9

As shown in entries 2-3 of **Table 2-5**, the other xylene isomers were investigated as solvents in the transformation to see if any further improvements to the yield of desired product could be achieved. Both *m*- and *o*-xylene resulted in comparable yields of the desired product, but *p*-xylene was still considered a superior solvent. Satisfied with the yield of hydroalkoxylation product, other nucleophiles were employed to determine how general this system was. Both EtOH and iPrOH (**Table 2-5**, entries 4-5) were both competent nucleophiles in this system with the desired products formed in 93% and 83% respectively. Cyclohexylmethanol was also reactive in this system (entry 6), but the yields of desired product were somewhat diminished. Unfortunately, when amine nucleophiles were employed, deleterious effects or complete lack of reactivity were observed (entries 7-8). The use of a glycoside nucleophile, **2.9**, was also unsuccessful in this transformation with no reactivity observed (entry 9). The lack of reactivity observed in entries 7-9 may be due to the much lower amounts of nucleophiles that were employed in those trials.

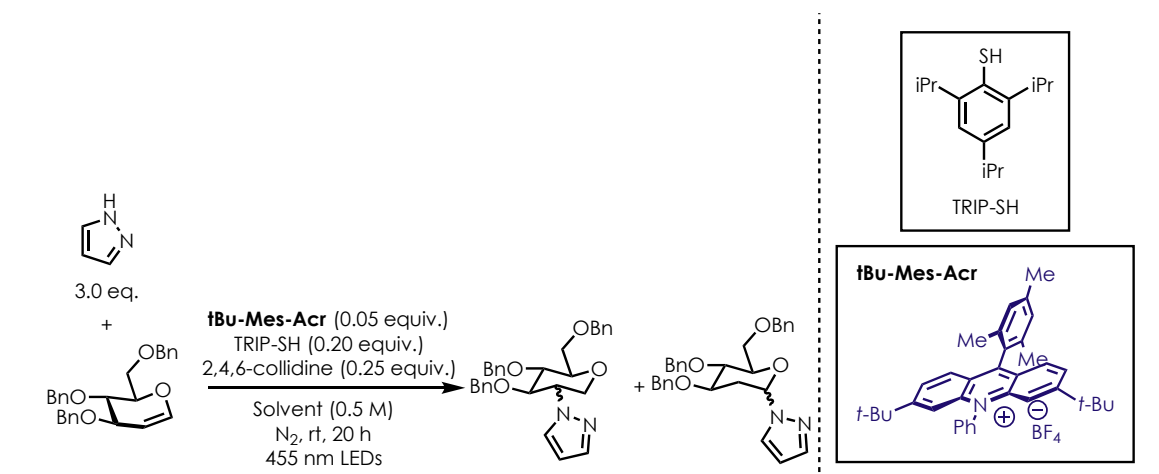
While excellent yields of hydroalkoxylated products could be obtained, the use of such large amounts of a nucleophile is undesirable and not feasible when complex nucleophiles, such as **2.9**, are employed. Efforts to reduce the amount of nucleophiles used in the glycol hydrofunctionalization system had limited success and required the addition of multiple additive. Noting that the use of such an extreme excess of nucleophile was a challenge to overcome, attention was turned towards the functionalization of *endo*-glycols.

2.2.2 Method Development

Efforts towards the development of a method for the functionalization of *endo*-glycols began by exploring the hydroamination of tri-*O*-benzyl D-glucal. As shown in **Table 2-6**, evaluating initial conditions that had been successful for the functionalization of *exo*-glycols

did not result in any significant product formation. It was not until a 9:1 mixture of CHCl₃:TFE (entry 5) was employed as the solvent system that a 24% yield of the hydroamination product was observed. Unfortunately, there appeared to be very little regioselectivity, and a 1:1 mixture of the desired anti-Markovnikov and undesired Markovnikov products was observed. Entry 7 shows that use of PhCF₃ as the reaction solvent also resulted in reactivity, but, once again, a 1:1 mixture of the desired and undesired products was formed.

Table 2-6. Initial Solvent Screen for Hydroamination of *Endo*-Glycal

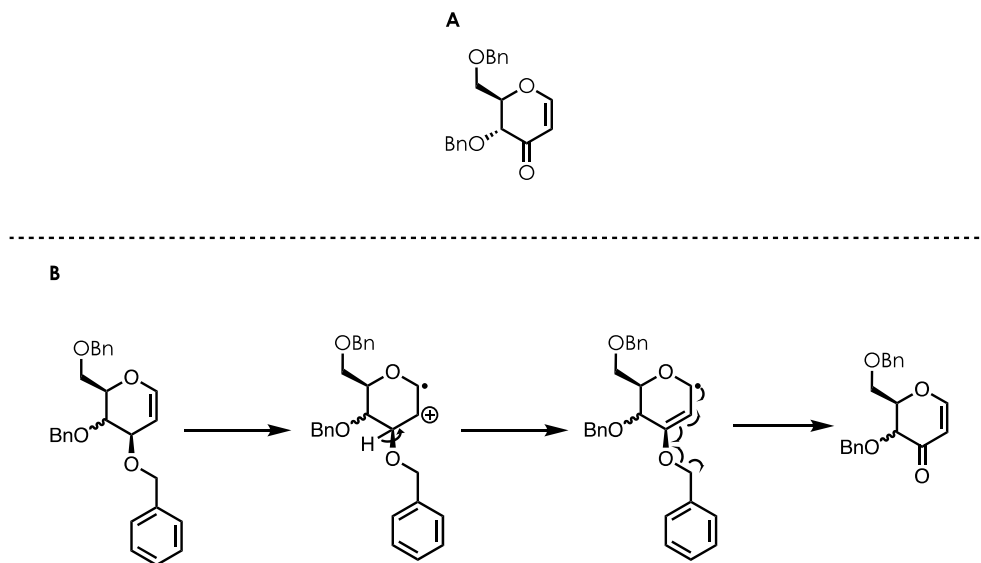


Entry ^a	Solvent	Yield (Anti-Mark : Mark) ^b
1	DCM	<10% : <10%
2	MeCN	<10% : <10%
3	o-xylene	-
4	CHCl ₃	<10% : <10%
5	CHCl ₃ :TFE (9:1)	11% : 13%
6	PhMe	-
7	PhCF ₃	17% : 17%

^aReactions run on a 0.1 mmol scale. ^b¹H NMR yields with HMDSO as an internal standard.

In addition to low yields of hydroaminated products, small amounts of unreacted starting material were observed in all cases. Analysis of the crude reaction ^1H NMR spectra was incredibly challenging, as the crude reactions were extremely messy and multiple compounds were present. In addition to the reaction components and hydroamination products, we also observed the formation of an undesired byproduct, which has been observed in other *endo*-glycal functionalization reactions (**Scheme 2-26A**). Unfortunately, this oxidized byproduct was observed to varying degrees throughout the investigations disclosed in **Table 2-6**. We proposed the mechanism in **Scheme 2-26B** to rationalize the formation of this byproduct, although no experiments were conducted to support this pathway.

Scheme 2-26. Oxidized Byproduct and Proposed Mechanism of Formation



In an effort to more effectively deprotonate the adduct formed after the addition of pyrazole into the cation radical, and to ensure that trace acid could not catalyze background reactivity, we investigated the effect of increasing the amount of base used in the reaction. As entries 1-4 in **Table 2-7** show, increasing the amount of 2,4,6-collidine used in the reaction

did not result in the formation of the desired anti-Markovnikov product to a greater degree. However, the mass balance for the reactions in entries 2 and 3 was slightly better than with lower amounts of base. Thinking that 2,4,6-collidine was not the most efficient base in the transformation, we investigated several other bases to see if the amount of desired product formed could be increased. Unfortunately, as entries 5-8 in **Table 2-7** show, none of the bases evaluated resulted in preferential formation of the desired anti-Markovnikov hydroamination product.

Table 2-7. Base Loading and Identity Screen for Hydroamination of *Endo*-Glycal

TRIP-SH

tBu-Mes-Acr

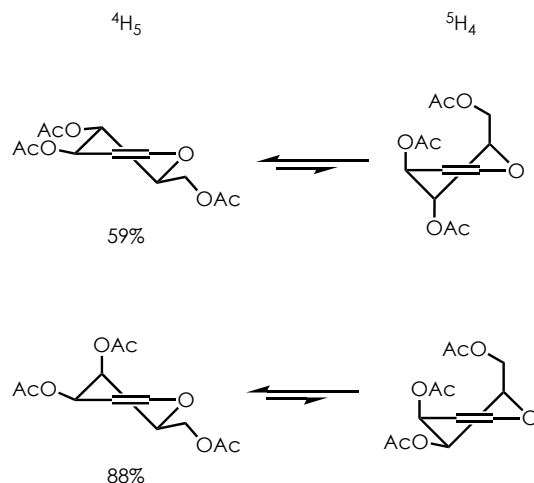
Entry ^a	Deviation from above conditions	Yield (Anti-Mark : Mark) ^b
1	None	<10% : 18%
2	0.50 equiv. 2,4,6-collidine	<10% : 16%
3	1.0 equiv. 2,4,6-collidine	<10% : 14%
4	2.0 equiv. 2,4,6-collidine	<10% : 11%
5	1.0 equiv. 2,6-lutidine	<10% : 16%
6	1.0 equiv. 3,5-lutidine	<10% : 12%
7	1.0 equiv. NaHCO ₃	<10% : 21%
8	4:1 DCM:NaHCO ₃ (sat. aq.)	<10% : 11%

^aReactions run on a 0.1 mmol scale. ^b¹H NMR yields with HMDSO as an internal standard.

Knowing that the reactivity of glycols is highly influenced by the nature of the protecting groups, we hypothesized that a substrate with different protecting groups may be

instrumental in improving the efficiency of the transformation. In addition to identifying more suitable protecting groups, several research groups have carried out complex ^1H NMR studies on families of peracetylated glycols to determine the preferred conformation of the glycols in solution.^{107,108} When tri-*O*-acetyl-*D*-glucal was examined (**Figure 2-9**), it was determined that the equilibrium lay slightly towards the left, favoring the $^4\text{H}_5$ conformation, with a molar fraction of 59%. When the glycol is in the $^4\text{H}_5$ conformation, we can envision relatively facile nucleophilic addition into the cation radical that is generated upon exposure to the excited state acridinium catalyst. However, the $^5\text{H}_4$ conformer is much more sterically congested, and may hinder addition of the nucleophile into the cation radical.

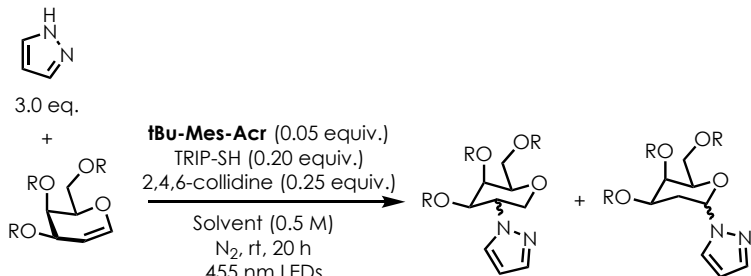
Figure 2-9. Conformational Studies on Tri-*O*-Acetyl Glycols

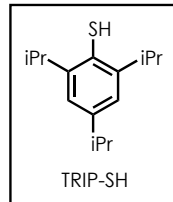


This study also revealed that tri-*O*-acetyl-*D*-galactal prefers the $^4\text{H}_5$ conformation as well, but in this case, the equilibrium lay much farther to the left with a molar fraction of 88%. We wondered if perhaps this preferential adoption of the $^4\text{H}_5$ conformer would be of use to us in

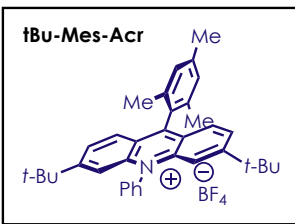
allowing a nucleophile to more easily approach the cation radical upon its generation. To this end, we prepared the perbenzylated-D-galactal substrate for evaluation.

We began by exploring the use of benzoic acid as a nucleophile (**Table 2-8**, entry 1) and discovered that only trace amounts of both the desired and undesired regioisomers were obtained. Wondering if the acidity of the nucleophile was perhaps an issue, we investigated the use of benzoate salts (entries 2-5), but, unfortunately, only small amounts of returned starting material were observed. The solubility of the benzoate salts was particularly poor, which likely contributed to the lack of desired reactivity. We also investigated the use of water as a cosolvent and nucleophile (entries 6-9), but were not able to observe the formation of either the desired or undesired products. Unfortunately, TFE was not a competent nucleophile either, as its use as either a solvent or cosolvent did not result in the formation of any hydroalkoxylated product. As noted for entries 10-12 of **Table 2-8**, the reactions were run with both catalytic and stoichiometric amounts of 2,4,6-collidine, but the higher loading of base did not result in product formation.

Table 2-8. Reactivity Screen for Hydrofunctionalization of *Endo*-Glycal




TRIP-SH



tBu-Mes-Acr

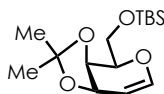
Entry ^a	R	Nucleophile (equiv.)	Solvent	Yield (Anti-Mark : Mark) ^b
1	Bn	Benzoic acid (3.0)	DCM	<10% : <10%
2	Bn	KOBz (3.0)	DCM	0%
3	Bn	NaOBz (3.0)	DCM	0%
4	Bn	LiOBz (3.0)	DCM	0%
5	Bn	NH ₄ OBz (3.0)	DCM	0%
6	Bn	H ₂ O	DCM:H ₂ O (4:1)	0%
7	Bn	H ₂ O	DCE:H ₂ O (4:1)	0%
8	Bn	H ₂ O	MeCN:H ₂ O (4:1)	0%
9	Bn	H ₂ O	CHCl ₃ :H ₂ O (4:1)	0%
10 ^c	Bn	TFE	TFE	0%
11 ^c	Bn	TFE	CHCl ₃ :TFE (9:1)	0%
12 ^c	Bn	TFE	DCE:TFE (4:1)	0%
13	TBS	Pyrazole (3.0)	DCM	<10% : 16%

^aReactions run on a 0.1 mmol scale. ^b¹H NMR yields with HMDSO as an internal standard. ^cTrial repeated with 1.0 equiv. base and same results.

We also prepared a tri-*O*-TBS-protected D-galactal derivative in an effort to explore the effects of different protecting groups on the transformation. When pyrazole was used as a nucleophile (**Table 2-8**, entry 13), we noted the formation of similar amounts of both hydroaminated regioisomers, indicating that amines were more competent nucleophiles than the others surveyed.

At this point, in addition to the limited reactivity observed, we were concerned by the varying amounts of oxidized byproduct that were formed in the trials. We designed a new substrate with an acetonide protecting group to rigidify the hydroxyl groups at the C3- and C4-positions (**Figure 2-10**). We were hopeful that this would reduce the amount of oxidative byproduct formation that occurred in the reaction and further push the equilibrium of the substrate towards the ⁴H₅ conformer.

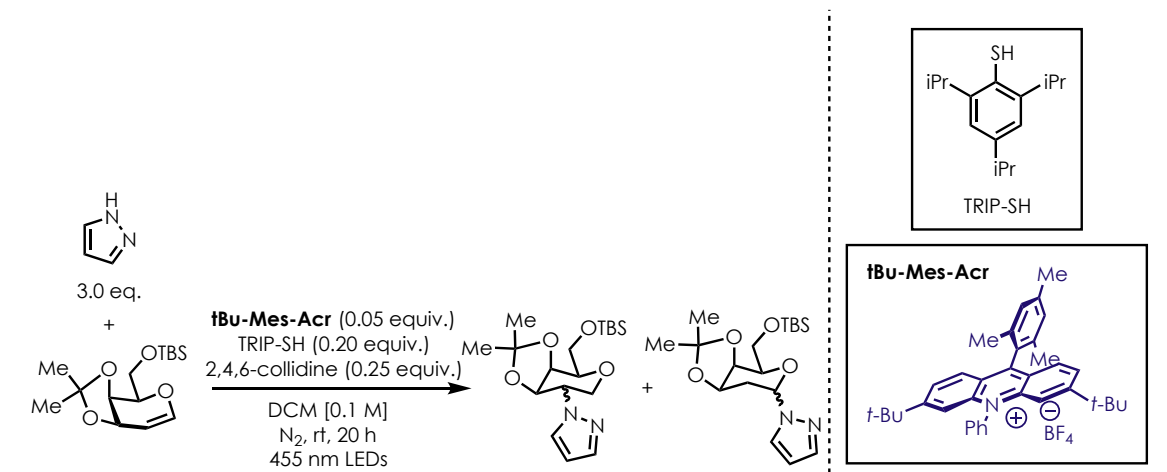
Figure 2-10. Redesigned Glycal Substrate



Upon subjecting the new substrate to the hydroamination conditions, we were delighted to observe preferential formation of the desired anti-Markovnikov product in a 26% yield (**Table 2-9**, entry 1). Additionally, none of the oxidative byproduct was formed in this reaction, supporting our substrate design hypothesis. As entries 2-6 show, both DCE and MeCN were competent solvents for this transformation with the desired product formed in 30% and 36% yields, respectively. Upon investigating the effects of reaction concentration when both DCE and MeCN were used as solvents, we discovered that a more concentrated reaction resulted in an increase in the amount of desired product formed (entries 7-12). However, we ultimately selected MeCN as the reaction solvent, as it afforded the desired product in higher yields than DCE. We also investigated the amount of pyrazole that was used in the transformation (**Table 2-9**, entries 13-15) and noted that increasing the amount of nucleophile had deleterious effects on the yield of desired product. The amount of pyrazole

used could be lowered, but the most consistent reaction yields were obtained when 3.0 equivalents were used. We explored the use of other H-atom donors in the reaction (entries 16-19) with the hypothesis that a more reactive H-atom donor could increase the amount of desired product formed through the more efficient transfer of an H-atom to prevent any unproductive pathways from occurring.

Table 2-9. Optimization with Redesigned Glycal Substrate



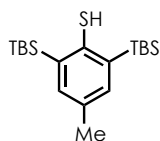
Entry ^a	Deviations from above conditions	Yield ^b (anti-Mark. : Mark.)
1	None	26% : <10%
2	DCE	30% : 11%
3	MeCN	36% : 16%
4	CHCl ₃	14% : <10%
5	TFE	<10% : <10%
6	CHCl ₃ :TFE (9:1)	13% : <10%

7	DCE (0.05 M)	20% : <10%
8	DCE (0.2 M)	30% : 10%
9	DCE (0.5 M)	36% : 12%
10	MeCN (0.05 M)	23% : 10%
11	MeCN (0.2 M)	39% : 17%
12	MeCN (0.5 M)	45% : 18%

13	1.1 equiv. pyrazole	44% : 18%
14	5.0 equiv. pyrazole	38% : 14%
15	10.0 equiv. pyrazole	39% : 14%

16	PhSH (0.20 equiv.)	34% : 13%
17	(PhS) ₂ (0.10 equiv.)	27% : <10%
18	2.10 (0.20 equiv.)	35% : 12%
19	(4-OMe-PhS) ₂ (0.10 equiv.)	24% : <10%

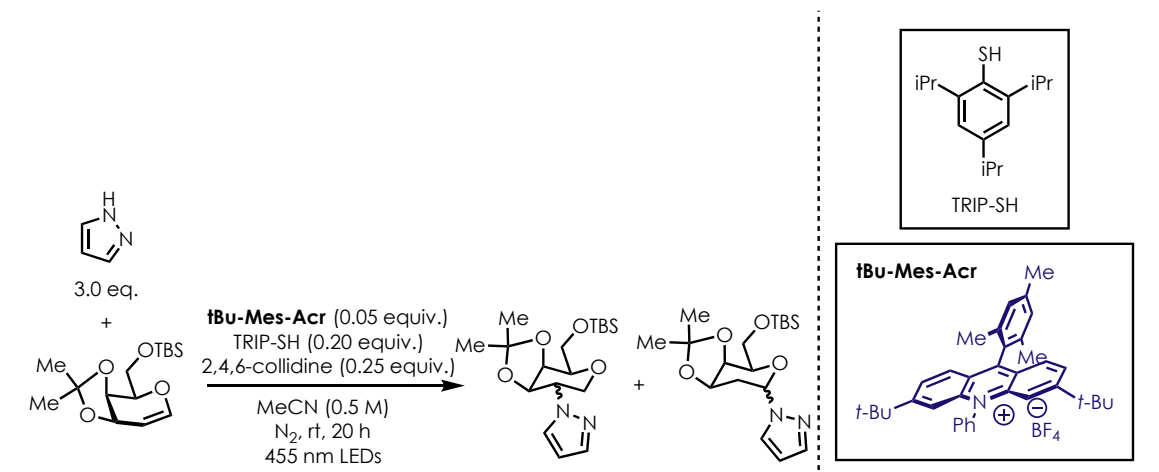
^aReactions run on 0.10 mmol scale. ^bYields are ¹H NMR yields using dimethyl terephthalate as an internal standard.



2.10

In general, we discovered that free thiols were more reactive in our hydroamination system with use of thiophenol and **2.10** resulting in higher yields of the desired product than disulfides that were evaluated.

Table 2-10. Catalyst and Base Optimization for Hydroamination of *Endo*-Glycal

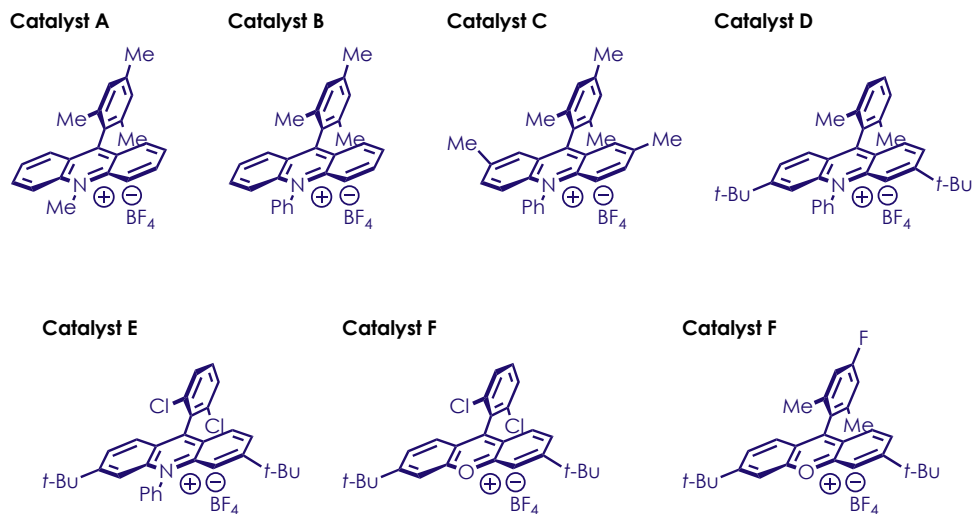


Entry ^a	Deviations from above conditions	Yield ^b (anti-Mark. : Mark.)
1 ^c	None	45% : 18%
2	0.05 equiv. Catalyst A	10% : <10%
3	0.05 equiv. Catalyst B	<10% : <10%
4	0.05 equiv. Catalyst C	<10% : <10%
5	0.05 equiv. Catalyst D	44% : 17%
6	0.05 equiv. Catalyst E	42% : 17%
7	0.05 equiv. Catalyst F	0%
8	0.05 equiv. Catalyst G	0%
9	0.025 equiv. tBu-Mes-Acr	35% : 13%
10	0.075 equiv. tBu-Mes-Acr	41% : 15%
11	0.10 equiv. tBu-Mes-Acr	38% : 13%
12	0.25 equiv. 2,6-lutidine	41% : 16%
13	0.25 equiv. 3,5-lutidine	28% : 10%
14	0.25 equiv. pyridine	29% : 10%
15	0.25 equiv. NEt ₃	17% : <10%
16	0.25 equiv. K ₂ CO ₃	0%
17	0.25 equiv. NaHCO ₃	45% : 18%
18	0.50 equiv. NaHCO ₃	46% : 17%
19	0.75 equiv. NaHCO ₃	40% : 16%
20	1.0 equiv. NaHCO ₃	38% : 15%

^aReactions run on 0.10 mmol scale. ^bYields are ¹H NMR yields using dimethyl terephthalate as an internal standard.

^cEntry 1 is equivalent to 12 of the previous table.

Figure 2-11. Catalyst Key for Table 2-10



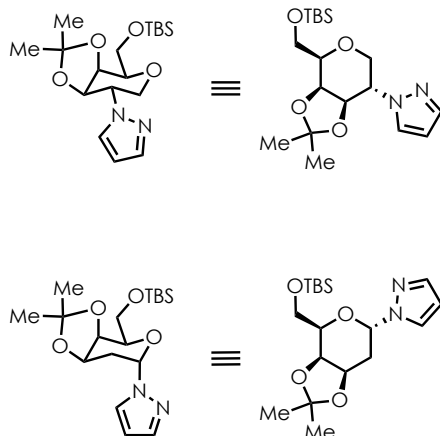
After identifying (0.5 M) MeCN as the optimal reaction solvent and concentration, we explored the use of other acridinium salts as catalysts (**Table 2-10**, entries 2-6). **Catalysts D and E (Figure 2-11)** performed comparably, while all of the others resulted in limited formation of the desired product. In addition to exploring other acridinium salts, we also evaluated two xanthylium catalysts, but no evidence of desired product formation was observed. These xanthylium catalysts are sensitive to strongly acidic or basic conditions, and bleaching of the reaction mixture was observed for the trials shown in entries 7-8. We elected to continue using **tBu-Mes-Acr** as the catalyst in the reaction, as it resulted in the most consistent yields over multiple trials. Additionally, as entries 9-11 show, decreasing or increasing the catalyst loading had deleterious effects on the yield of desired product formation.

At this point in our reaction development, yields of the desired product were moderate, so we investigated a range of bases to more efficiently facilitate the deprotonation of the distonic cation radical intermediate and to ensure that no background acid-catalyzed

reactivity occurred. As shown in 12-16, the use of bases other than 2,4,6-collidine resulted in seriously diminished yields of desired product. However, the use of NaHCO₃ resulted in yields of desired product that were comparable to those obtained with 2,4,6-collidine. A survey of NaHCO₃ loadings indicated that an increase to 0.50 equivalents resulted in a slight improvement to the amount of desired product that was formed. In the end, 2,4,6-collidine was chosen as the optimal base, but comparable results could be obtained with NaHCO₃.

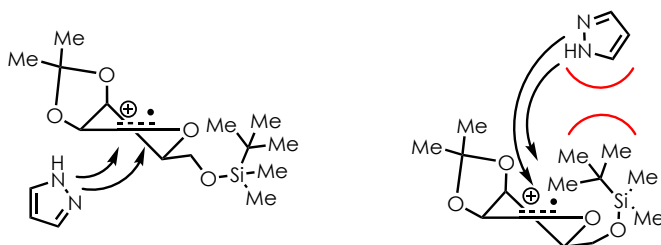
After identification of optimal reaction conditions, we set out to determine the stereochemistry of the hydroaminated products. Upon scaleup and isolation, it was discovered that, in addition to the desired anti-Markovnikov and undesired Markovnikov products, a trace amount of a minor diastereomer of the Markovnikov adduct was isolated as well. ¹H NMR spectra for these compounds were complex, so we employed 1D-NOESY experiments to elucidate the stereochemistry for these compounds. Unfortunately, due to the limited quantities of material, the 1D-NOESY experiments were relatively inconclusive. However, using coupling constants obtained through ¹H NMR spectra, we have tentatively assigned the stereochemistry of the products as shown in **Figure 2-12**.

Figure 2-12. Tentative Stereochemical Assignments for Hydroamination Products



We believe the approach of the nucleophile from the bottom face of the cation radical is dictated by the crowded steric environment hindering addition from the top face (**Figure 2-13**).

Figure 2-13. Rationale for Nucleophile Approach



Additionally, if the nucleophile were to approach the cation radical from the top face, the resulting products would experience unfavorable 1,3-diaxial interactions.

We were curious as to what other amine nucleophiles could be used successfully in this transformation and elected to investigate the use of NH_2Tf , as it had proven successful in previous hydroamination studies from our lab.

Table 2-11. Initial Optimization Using Triflamide as a Nucleophile

NH_2Tf
 3.0 eq.
 +
 tBu-Mes-Acr (0.05 equiv.)
 TRIP-SH (0.20 equiv.)
 $2,4,6\text{-collidine}$ (0.25 equiv.)
 $\xrightarrow[\text{MeCN (0.5 M)}]{\text{N}_2, \text{rt, 20 h, 455 nm LEDs}}$
 Me OTBS NHTf

Entry ^a	Deviations from above conditions	Yield ^b (anti-Mark. : Mark.)
1	None	21% : <10%
2	DCE	32% : <10%
3	DCM	42% : 13%
4	CHCl ₃	10% : <10%
5	0.25 equiv. NaHCO ₃ and DCM	10% : <10%

^aReactions run on 0.10 mmol scale. ^bYields are ¹H NMR yields using dimethyl terephthalate as an internal standard.

Upon conducting trials using a variety of solvents, we discovered that DCM (**Table 2-11**, entry 3) was the optimal solvent for this transformation with a 3:1 r.r. We briefly examined the effect of NaHCO₃ as a base in the reaction, but only deleterious effects were observed. Satisfied with the yields of hydroaminated product, we turned to explore the use of ammonium carbamate as a means to rapidly generate 2-aminoglycosides.

Table 2-12. Optimization Using Ammonium Carbamate as a Nucleophile

TRIP-SH

tBu-Mes-Acr

Entry ^a	Deviations from above conditions	Yield ^b (anti-Mark. : Mark.)
1	None	0%
2	DCE	0%
3	DCM	0%
4	CHCl ₃ :TFE (9:1)	13% : 10%
5	DCE:TFE (4:1)	22% : 18%
6 ^c	5.0 equiv. (NH ₄) ⁺ (O ₂ CNH ₂) ⁻	26% : 21%
7 ^c	7.5 equiv. (NH ₄) ⁺ (O ₂ CNH ₂) ⁻	20% : 17%
8 ^c	10.0 equiv. (NH ₄) ⁺ (O ₂ CNH ₂) ⁻	20% : 16%
9	DCE:TFE (1:1)	25% : 20%
10	DCE:TFE (2:1)	29% : 23%
11	DCE:TFE (4:1)	25% : 21%
12	DCE:TFE (10:1)	26% : 24%

^aReactions run on 0.10 mmol scale. ^bYields are ¹H NMR yields using dimethyl terephthalate as an internal standard. ^cTrials run in DCE:TFE (4:1) solvent system.

Initial investigations (**Table 2-12**, entries 1-3) were unsuccessful, and no reactivity was observed, which is likely due to the insolubility of ammonium carbamate in the solvents surveyed. Upon selecting a solvent system with one component that ammonium carbamate is soluble in (entries 4-5), we observed formation of the desired product in low yields. We determined that increasing the amount of ammonium carbamate used as a nucleophile did not result in a substantial improvement to the yield of desired product (entries 6-8). Unfortunately, we also observed formation of the undesired Markovnikov regioisomer in equivalent yields, and this 1:1 r.r. was consistent through optimization of the transformation.

In an effort to modulate the rate of release of ammonia, we examined the effects of varying amounts of TFE in the solvent system, as ammonium carbamate is readily soluble in TFE. However, as shown in entries 9-12 of **Table 2-12**, the reaction was not particularly sensitive to the amount of TFE used in the solvent system. Relatively comparable yields of the desired anti-Markovnikov regioisomer were obtained regardless of the amount of TFE used. We elected to use a 4:1 mixture of DCE:TFE as the solvent system, as this resulted in a marginally lower amount of the undesired regioisomer.

In addition to developing conditions for the facile synthesis of 2-aminoglycosides, we were curious if our method could be extended to the construction of novel glycosidic linkages. We chose to utilize methanol as a model nucleophile in order to establish whether C-O bond construction was feasible. As shown in entry 1 of **Table 2-13**, upon modifying our hydroamination conditions to feature the use of MeOH as a nucleophile, we were excited to observe formation of the hydroalkoxylated regioisomer in a 21% yield. Unfortunately, we observed preferential formation of the undesired regioisomer in a 29% yield. Increasing the amount of MeOH resulted in a substantial increase in the formation of both regioisomers of hydroalkoxylated product, but the undesired Markovnikov regioisomer was once again formed preferentially (entries 2-4). While yields for the hydroalkoxylated product were quite good, we were interested in identifying conditions for the preferential formation of the desired regioisomer. A survey of solvents (entries 5-8) revealed that the use of both DCE and DCM resulted in a 1:1 r.r. of the products, which was an improvement over the product distribution observed earlier.

Table 2-13. Initial Optimization Using Methanol as a Nucleophile

Entry ^a	Deviations from above conditions	Yield ^b (anti-Mark. : Mark.)
1	None	21% : 29%
2	1.5 equiv. MeOH	10% : 15%
3	5.0 equiv. MeOH	28% : 39%
4	10.0 equiv. MeOH	39% : 51%
5 ^c	DCE	41% : 39%
6 ^c	DCM	40% : 41%
7 ^c	CHCl ₃ :TFE (9:1)	24% : 11%
8 ^c	DCE:TFE (4:1)	38% : 24%
9 ^c	No 455 nm LEDs	0%
10 ^c	No fBu-Mes-Acr	0%
11 ^c	No 2,4,6-collidine	20% : 30%

^aReactions run on 0.10 mmol scale. ^bYields are ¹H NMR yields using dimethyl terephthalate as an internal standard.

^c10.0 equiv. MeOH used as nucleophile and DCE as the solvent.

We opted to move forward with the use of DCE, as the reaction temperatures due to the LEDs could approach the boiling point of DCM. Additionally, in order to ensure that background reactivity was not responsible for the formation of the undesired Markovnikov regioisomer, we ran several control reactions (entries 9-10) and determined that no product formation was observed in the absence of 455 nm light or acridinium catalyst. Upon running a control reaction with no base (entry 11), we observed preferential formation of the undesired regioisomer.

Concerned that trace acid generated during the course of the reaction was responsible for the formation of the undesired Markovnikov regioisomer, we ran a series of experiments with lowered loadings of acridinium catalyst to determine whether the acid was being generated from the tetrafluoroborate counterion.

Table 2-14. Catalyst and Base Loading Screen for Hydroalkoxylation of *Endo*-Glycal

TRIP-SH

tBu-Mes-Acr

Entry ^a	Deviations from above conditions	Yield ^b (anti-Mark. : Mark.)
1 ^c	None	41% : 39%
2	0.005 equiv. tBu-Mes-Acr	17% : 16%
3	0.01 equiv. tBu-Mes-Acr	37% : 36%
4	0.015 equiv. tBu-Mes-Acr	45% : 44%
5	0.02 equiv. tBu-Mes-Acr	40% : 37%
6	0.025 equiv. tBu-Mes-Acr	41% : 41%
7	0.03 equiv. tBu-Mes-Acr	45% : 43%
8	0.035 equiv. tBu-Mes-Acr	33% : 35%
9	0.04 equiv. tBu-Mes-Acr	42% : 43%
10	0.045 equiv. tBu-Mes-Acr	43% : 42%
11	0.50 equiv. 2,4,6-collidine	43% : 42%
12	0.75 equiv. 2,4,6-collidine	44% : 41%
13	1.0 equiv. 2,4,6-collidine	44% : 40%
14	2.0 equiv. 2,4,6-collidine	35% : 35%

^aReactions run on 0.10 mmol scale. ^bYields are ¹H NMR yields using dimethyl terephthalate as an internal standard.

^cEntry is identical to entry 5 of **Table 2-13**.

Entries 2-10 of **Table 2-14** detail the experiments, and we determined that lowering the amount of acridinium catalyst used in the reaction had no impact on the product distribution.

Generation of HBF_4 did not appear to be responsible for the formation of equivalent amounts of hydroalkoxylated regioisomers, and we decided to move forward with the original loading of acridinium catalyst, as there was some inconsistency with the yields of reactions run with reduced catalyst loadings. We next explored increasing the amount of base used in the reaction (entries 11-14) in an attempt to suppress the effects of trace acid generated elsewhere in the course of the reaction, but no alterations of the product distribution were observed. Additionally, upon increasing the loading of 2,4,6-collidine to superstoichiometric amounts, we observed deleterious effects to the yields of hydroalkoxylated products. We elected to move forward with a slightly increased loading of 2,4,6-collidine, as yields were marginally improved as compared to entry 1 of **Table 2-14**.

As we had established that the amount of 2,4,6-collidine used in the transformation did not have a significant impact on the product distribution, we chose to investigate the identity of base used in the reaction to determine how alternate bases would affect the outcome of the reaction.

Table 2-15. Base Identity Screen for Hydroalkoxylation of *Endo*-Glycal

TRIP-SH

tBu-Mes-Acr

Entry ^a	Deviations from above conditions	Yield ^b (anti-Mark. : Mark.)
1 ^c	None	41% : 39%
2	0.50 equiv. 2,6-lutidine	42% : 42%
3	0.50 equiv. 3,5-lutidine	37% : 36%
4	0.50 equiv. NEt ₃	0%
5	0.50 equiv. DIPEA	0%
6	0.50 equiv. NaHCO ₃	48% : 46%
7	0.50 equiv. KH ₂ PO ₄	40% : 38%
8	0.50 equiv. K ₂ HPO ₄	30% : 31%
9	0.50 equiv. K ₃ PO ₄	0%
10	0.50 equiv. NaOMe	19% : 18%
11	0.50 equiv. NaOMe in MeOH	0%
12	0.50 equiv. pyridine	35% : 34%
13	0.25 equiv. NaHCO ₃	39% : 37%
14	0.75 equiv. NaHCO ₃	45% : 42%
15	1.0 equiv. NaHCO ₃	44% : 44%
16	2.0 equiv. NaHCO ₃	47% : 46%

^aReactions run on 0.10 mmol scale. ^bYields are ¹H NMR yields using dimethyl terephthalate as an internal standard.

^cEntry is identical to entry 5 of **Table 2-13**.

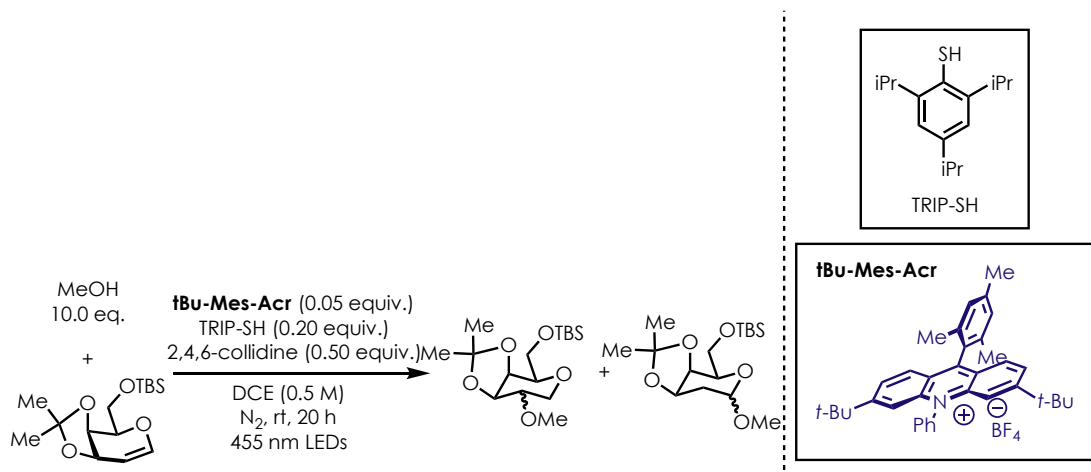
Table 2-15 (entries 2-12) detail the range of bases surveyed for our hydroalkoxylation reaction. We investigated a range of organic and inorganic bases and were dismayed to discover that none of the bases surveyed had a beneficial impact on the product distribution. In many cases (entries 2 and 6-7), we observed excellent yields of the hydroalkoxylated products, but in a ratio of 1:1. We noted the slight improvement to the yields of products

when NaHCO₃ was used as the base and chose to investigate the effect that varying amounts of NaHCO₃ had on the product distribution (entries 13-16). Unfortunately, we did not observe any change to the product distribution, and a 1:1 ratio of the two regioisomers was obtained in each trial. However, due to the improvement to reaction yield, we elected to move forward with the use of NaHCO₃ as the optimal base for this transformation.

As the generation of trace acid did not appear to be responsible for the undesirable product distribution, we wondered if slow H-atom transfer from the thiol to the glycal-nucleophile adduct allowed for reversible addition of the nucleophile into the C1- and C2-positions. We sought to probe whether an equilibration of the two regioisomers could be adjusted with the use of a more reactive H-atom donor to increase the rate of H-atom transfer. However, as shown in **Table 2-16**, the use of a variety of thiols and disulfides did not result in any alteration to the product distribution. We also investigated bulky H-atom donors (**Figure 2-14**) in an effort to hinder H-atom transfer to the C2-position. We hoped that using sterically encumbered thiols would result in preferential H-atom transfer to the C1-position and formation of the desired anti-Markovnikov product. However, as shown in entries 3-4, 7-13, and 16, the use of bulky H-atom donors had no impact on the product distribution of the reaction. Additionally, in many cases, the bulky H-atom donors also resulted in seriously diminished yields of the hydroalkoxylated regioisomers. When **2.18** (entry 13) was employed as the H-atom donor, we observed a preferential formation of the undesired regioisomer, which indicated that use of bulky H-atom donors did not necessarily hinder H-atom transfer to the C2-position. In addition to various thiols and disulfides, we also investigated the use of two compounds (entries 15 and 18) with antioxidant properties

that have been shown to possess efficient radical-trapping abilities.^{109,110} Unfortunately, neither of these compounds resulted in the formation of any hydroalkoxylated product.

Table 2-16. H-Atom Donor Screen for Hydroalkoxylation of *Endo*-Glycal

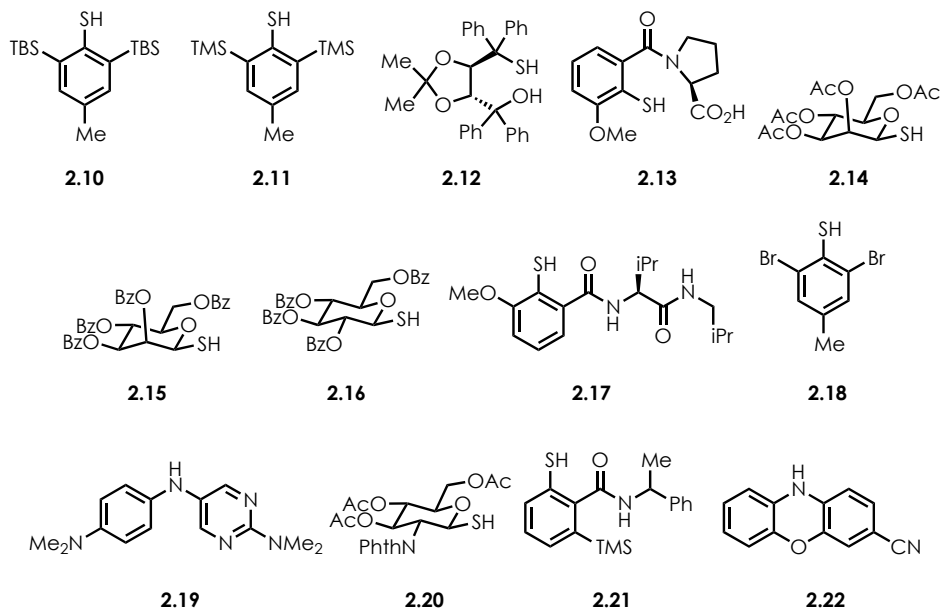


Entry ^a	Deviations from above conditions	Yield ^b (anti-Mark. : Mark.)
1 ^c	None	41% : 39%
2	0.20 equiv. PhSh	48% : 48%
3	0.20 equiv. 2.10	44% : 45%
4	0.20 equiv. 2.11	42% : 42%
5	0.20 equiv. (<i>p</i> -tolS) ₂	41% : 40%
6	0.20 equiv. (PhS) ₂	39% : 38%
7	0.20 equiv. 2.12	36% : 35%
8	0.20 equiv. 2.13	28% : 25%
9	0.20 equiv. 2.14	26% : 25%
10	0.20 equiv. 2.15	25% : 25%
11	0.20 equiv. 2.16	17% : 17%
12	0.20 equiv. 2.17	17% : 16%
13	0.20 equiv. 2.18	17% : 31%
14	0.20 equiv. (<i>p</i> -OMe-PhS) ₂	22% : 29%
15	0.20 equiv. 2.19	0%
16	0.20 equiv. 2.20	0%
17	0.20 equiv. 2.21	0%
18	0.20 equiv. 2.22	0%

^aReactions run on 0.10 mmol scale. ^bYields are ¹H NMR yields using dimethyl terephthalate as an internal standard.

^cEntry is identical to entry 5 of **Table 2-13**.

Figure 2-14. H-Atom Donor Key for Table 2-16



Puzzled by the inability to alter the ratio of product distribution, we decided to abandon the model system and explore the use of a glycoside nucleophile in our hydrofunctionalization reaction to construct novel disaccharides. We hoped that the primary alcohol portion of the nucleophile was located sufficiently far enough away from the bulk of the glycoside to avoid hindering addition to the C2-position. Unfortunately, as shown in entry 1 of **Table 2-17**, when 1,2,3,4-di-*O*-isopropylidene- α -D-galactopyranose was employed as the nucleophile, we observed a preferential formation of the undesired Markovnikov regioisomer in a 3:1 ratio. We surveyed a series of solvents that had proven to be effective reaction mediums for work discussed earlier (**Table 2-17**, entries 2-4) and discovered that DCM and CHCl_3 both resulted in the preferential formation of the undesired regioisomer. Somewhat unsurprisingly, more dilute reaction concentrations (entries 5-6 and

8-10) resulted in decreased amounts of product formation, but still only trace amounts of the desired regioisomer were observed.

Table 2-17. Optimization of Acridinium-Mediated Glycosylation

Entry ^a	Deviations from above conditions	Yield ^b (anti-Mark. : Mark.)
1 ^c	None	11% : 30%
2	DCE	0%
3	DCM	<10% : 20%
4	CHCl ₃	<10% : 28%
5	MeCN (0.05 M)	<10% : 17%
6	MeCN (0.2 M)	<10% : 38%
7	MeCN (0.5 M)	<10% : 35%
8	DCM (0.05 M)	<10% : 24%
9	DCM (0.1 M)	<10% : 29%
10	DCM (0.2 M)	<10% : 33%
11	DCM (0.5 M)	<10% : 35%

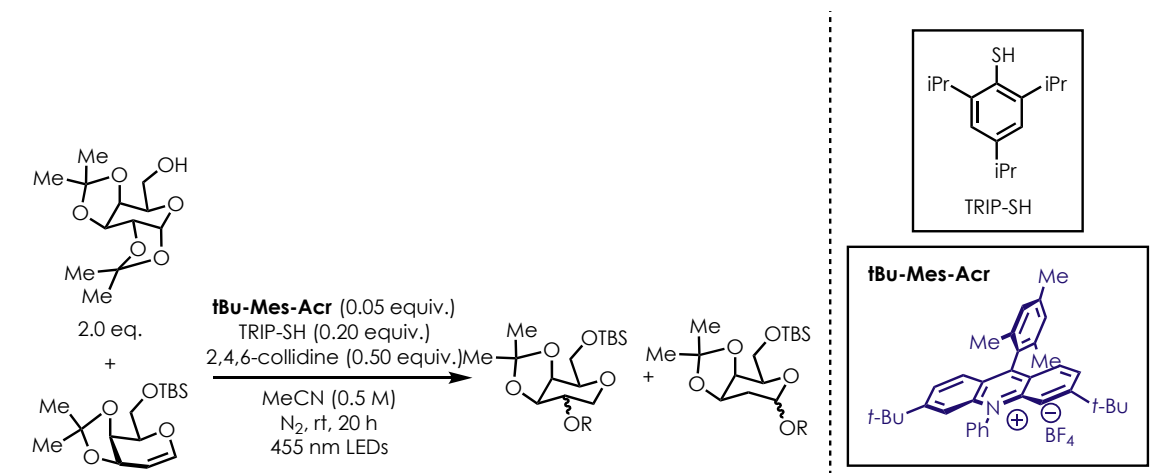
^aReactions run on 0.10 mmol scale. ^bYields are ¹H NMR yields using dimethyl terephthalate as an internal standard.

^cEntry is identical to entry 5 of **Table 2-13**.

In an effort to increase the amount of the desired regioisomer formed, we explored various loadings of base in order to more efficiently deprotonate the distonic cation radical intermediate and prevent reversible addition of the nucleophile. As shown in entries 2-5 of **Table 2-18**, increasing the amount of 2,4,6-collidine used in the reaction resulted in lower amounts of the undesired regioisomer. We elected to move forward with the use of stoichiometric base, as the use of superstoichiometric amounts did not significantly reduce

the formation of the undesired regioisomer. As NaHCO₃ had resulted in a slight increase in yields of the glycosylated products (**Table 2-18**, entry 6), we explored the use of stoichiometric NaHCO₃ in this transformation, as well as the use of other inorganic bases.

Table 2-18. Further Condition Optimization for Acridinium-Mediated Glycosylation



Entry ^a	Deviations from above conditions	Yield ^b (anti-Mark. : Mark.)
1 ^c	None	11% : 30%
2	0.25 equiv. 2,4,6-collidine	<10% : 29%
3	0.75 equiv. 2,4,6-collidine	<10% : 21%
4	1.0 equiv. 2,4,6-collidine	<10% : 17%
5	2.0 equiv. 2,4,6-collidine	<10% : 19%
6	1.0 equiv. NaHCO ₃	17% : 35%
7	1.0 equiv. K ₃ PO ₄	0%
8	1.0 equiv. K ₂ CO ₃	10% : 22%
9	1.0 equiv. Cs ₂ CO ₃	0%
10	1.0 equiv. nucleophile	11% : 38%
11	1.5 equiv. nucleophile	<10% : 41%
12	5.0 equiv. nucleophile	<10% : 54%

^aReactions run on 0.10 mmol scale. ^bYields are ¹H NMR yields using dimethyl terephthalate as an internal standard.

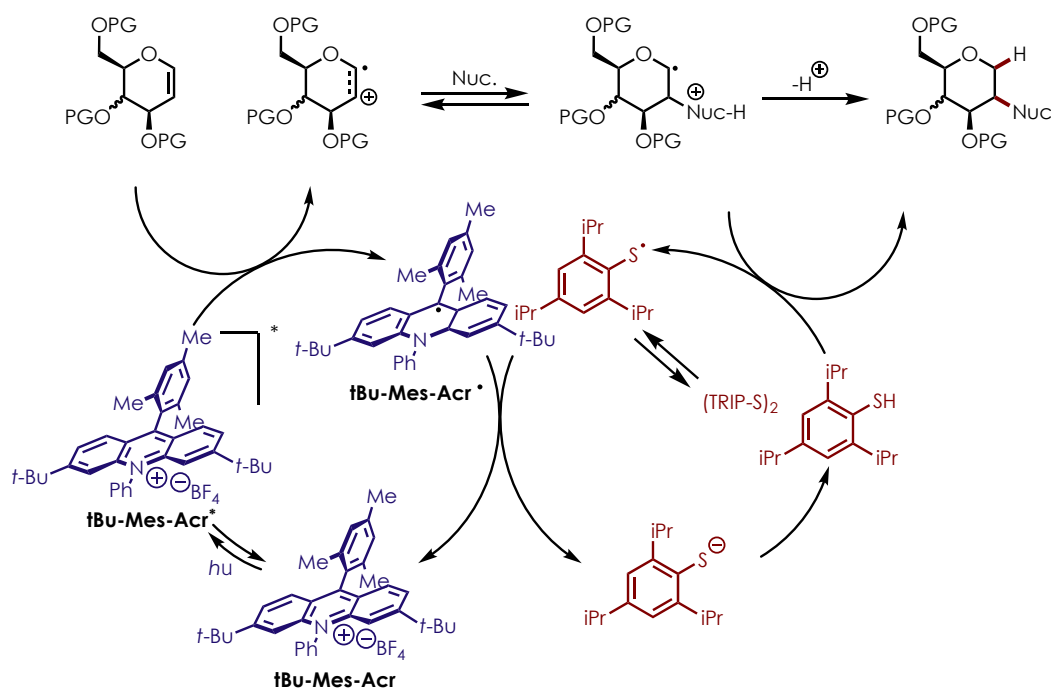
^cEntry is identical to entry 1 of **Table 2-13**.

We were pleased to discover that we observed formation of the desired anti-Markovnikov regioisomer in a 17% yield (**Table 2-18**, entry 6), but still observed preferential formation of the undesired Markovnikov regioisomer. The other bases surveyed either resulted in decreased yields of the two products or a complete lack of reactivity. Additionally, a survey

of the amount of glycoside nucleophile used in the transformation (entries 10-12) indicated that the use of greater excesses only resulted in an increase of the undesired regioisomer. We decided to pause the development of a photoredox catalysis-mediated glycosylation reaction, as the best result we observed was a 52% yield of the two regioisomers with a 2:1 r.r. favoring formation of the undesired Markovnikov adduct.

Although detailed mechanistic studies were not undertaken, we believe that this transformation proceeds in a similar manner to our previously reported hydrofunctionalization methods (**Scheme 2-27**).

Scheme 2-27. Proposed Mechanism for Hydrofunctionalization of *Endo*-Glycals



Upon excitation of **tBu-Mes-Acr** with 455 nm LEDs, the excited state catalyst, **tBu-Mes-Acr***, can participate in PET with the glycal substrate to afford the glycal cation radical species and **tBu-Mes-Acr•**. The glycal cation radical can be intercepted by the nucleophile to afford a dicationic intermediate which participates in HAT with TRIP-SH. Upon

deprotonation, the desired product is formed, the thiyl radical regenerates the ground state acridinium catalyst, and the resulting thiolate anion can undergo protonation to close the catalytic cycle.

In an effort to expand on our hydrofunctionalization method, we investigated the difunctionalization of glycals in the hopes of installing multiple functional handles for further manipulation.

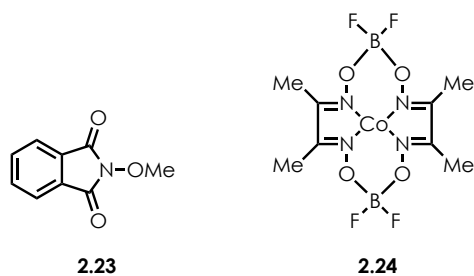
Table 2-19. Attempts at Difunctionalization of *Endo*-Glycals

TRIP-SH

tBu-Mes-Acr

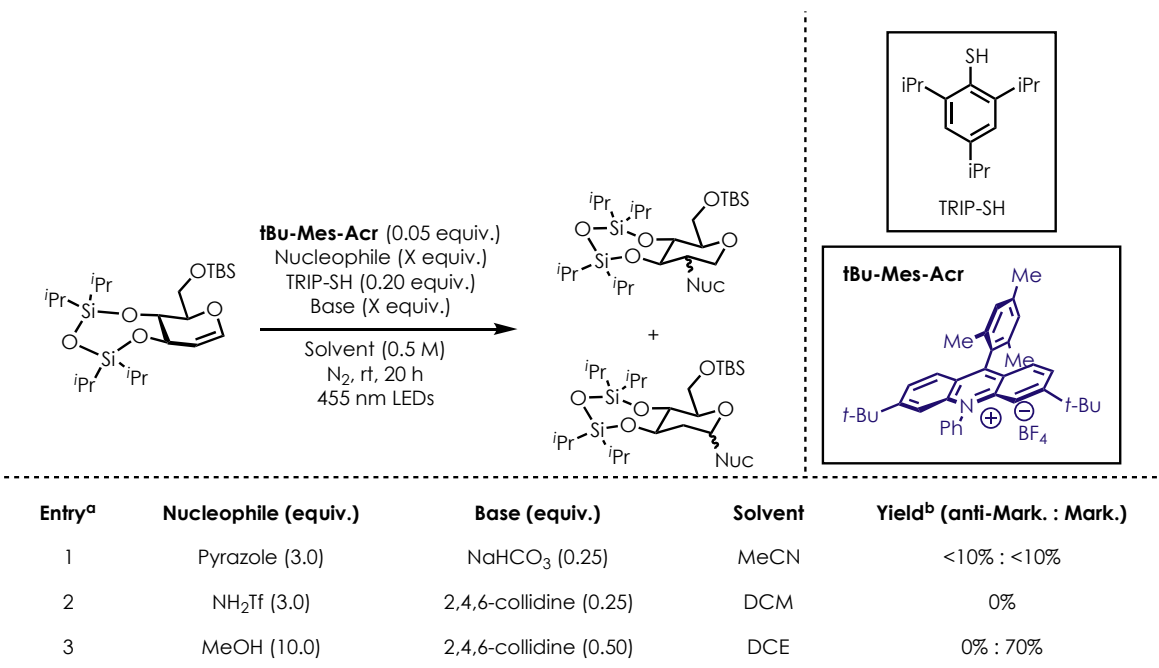
Entry ^a	Nuc. (equiv.)	Base	Additives (equiv.)	Solvent	-R	Yield ^b (anti-Mark. : Mark.)
1	Pyrazole (3.0)	2,4,6-collidine	2.23 (1.0)	MeCN	OMe	0%
2	Pyrazole (3.0)	NaHCO ₃	Methyl vinyl ketone (1.0)	MeCN	(CH ₂) ₂ C(O)Me	0%
3	Pyrazole (3.0)	NaHCO ₃	Methyl acrylate (1.0)	MeCN	(CH ₂) ₂ C(O)OMe	0%
4	Pyrazole (3.0)	NaHCO ₃	Selectfluor (1.0)	MeCN	F	0%
5	Pyrazole (3.0)	NaHCO ₃	NFSI (1.0)	MeCN	F	0%
6	MeOH (10.0)	2,4,6-collidine	2.24 (0.05)	MeCN	OMe	0%
7	MeOH (10.0)	2,4,6-collidine	2.24 (0.05)	DCE	OMe	0%
8	MeOH (10.0)	2,4,6-collidine	2.24 (0.05)	DCM	OMe	0%
9	MeOH (10.0)	No base	2.24 (0.05)	MeCN	OMe	0%
10	MeOH (10.0)	No base	2.24 (0.05)	DCE	OMe	0%
11	MeOH (10.0)	No base	2.24 (0.05)	DCM	OMe	0%

^aReactions run on 0.10 mmol scale. ^bYields are ¹H NMR yields using dimethyl terephthalate as an internal standard.



As shown in **Table 2-19**, we surveyed a range of conditions in an attempt to effect transformations ranging from fluoroaminations to dialkoxylation. Entries 1-5 details our attempts to observe reactivity with a range of radical traps, including *N*-methoxyphthalimide (**2.23**), methyl vinyl ketone, methyl acrylate, Selectfluor, and NFSI. Unfortunately, no reactivity was observed in any case, which may indicate that trapping of the radical by **2.23**, Selectfluor, and NFSI, or the radical addition into one of the Michael acceptors may be too slow to funnel the glycal-nucleophile adduct towards the desired product or that difunctionalization reagent inhibits the reaction in another way. We also sought to employ a cobalt co-catalyst (**2.24**) to effect a second oxidation event to generate a carbocation at the C1-position which can undergo nucleophilic addition by a second molecule of MeOH. As entries 6-11 show, we explored a variety of solvents for the dialkoxylation reaction, but observed no reactivity. We also investigated the effects of removing the 2,4,6-collidine from the reaction in the event that the presence of base affected the reactivity of **2.24**. As no evidence of reactivity was observed in any case, we decided not to pursue the difunctionalization of glycals any farther.

We were also interested in exploring whether other substrates with similar protecting groups could be used successfully in our hydrofunctionalization reactions. To this end, we prepared a substrate derived from D-glucal that featured a disiloxane protecting group.

Table 2-20. Hydrofunctionalization of Disiloxane-Protected *Endo*-Glycol

^aReactions run on 0.10 mmol scale. ^bYields are ¹H NMR yields using dimethyl terephthalate as an internal standard.

As shown in **Table 2-20**, we evaluated this substrate in the optimal conditions identified for use of pyrazole, triflamide, and MeOH as nucleophiles. Unfortunately, despite the similarities between this substrate and the compound we had success with, very little to no formation of desired anti-Markovnikov product was observed. Entries 1-2 show that when hydroamination conditions were applied, very little reactivity was observed. Unfortunately, when MeOH was used as a nucleophile, a 70% yield of the undesired Markovnikov regioisomer was obtained. It is possible that the size of the disiloxane protecting group hinders nucleophilic addition at the C2-position, which may explain why exclusive addition to the C1-position was observed in entry 3.

2.2.3 Computational Studies

The reactivity observed in the course of this study was not altogether what we envisioned when the exploration began. In order to better understand the preferred geometry of the ground state substrates and their cation radicals, as well as the electron density of both molecules, we have begun a computational study to further assess a small family of glycals. In collaboration with Nicholas Onuska, we seek to better understand the glycals used in this work in order to more effectively tailor reaction conditions to preferentially afford the desired anti-Markovnikov regioisomer. Computations are ongoing and will hopefully be finished shortly in order to provide a better understanding of these systems.

2.3 Conclusions

In conclusion, we have developed methods for the hydrofunctionalization of both *exo*- and *endo*-glycals as a means to access novel glycosides/glycomimetics. We report the synthesis of a small family of 1- and 2-deoxyglycosides in moderate yields (47–89%) and regioselectivities (1:1–3.2:1). The use of alcoholic and nitrogenous nucleophiles was tolerated in the systems, and we envision the extension of these methods to a broader substrate scope in the future.

2.4 Future Work

In the future, we envision the use of data obtained from computational studies to serve as a guide for further improvements to these hydrofunctionalization systems. We hope to use what we learn from the studies to expand the hydrofunctionalization of *endo*-glycals to include additional substrates and to preferentially form the desired anti-Markovnikov regioisomer in excellent yields and high diastereoselectivity. We also hope to revisit the

photoredox catalysis-mediated glycosylation reaction in order to develop a method for the facile construction of novel disaccharides.

2.5 Acknowledgements

The development of hydrofunctionalization methodologies for both *exo*- and *endo*-glycals involved assistance from many talented colleagues. Heqing Sun developed the hydrofunctionalization method for *exo*-glycals and began initial work on the functionalization of *endo*-glycals. His work provided a very solid foundation from which these studies were launched. Dr. Alexander White was also a great source of assistance during this project and provided valuable insight into reaction troubleshooting, as well as material preparation.

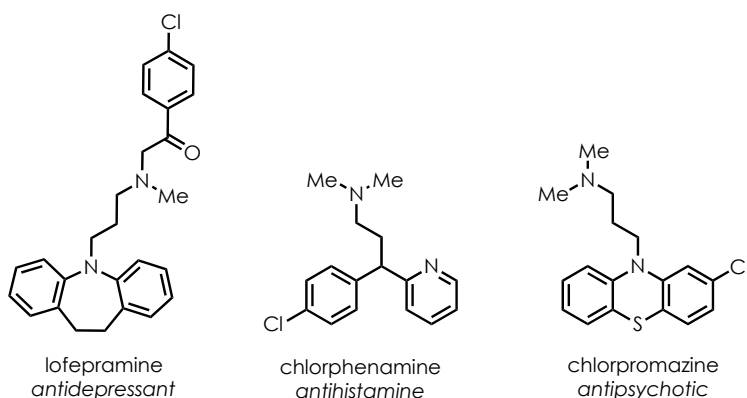
CHAPTER 3: DEVELOPMENT OF A PHOTOREDOX-MEDIATED METHOD FOR THE ANTI-MARKOVNIKOV HYDROAZIDATION OF ACTIVATED OLEFINS

3.1 Introduction

3.1.1 Importance of Hydroazidation Products

The ubiquity of nitrogenous functionality in important molecules (**Figure 3-1**), such as pharmaceuticals, agrochemicals, and functional materials, has resulted in much time being spent on the development of methods to introduce such functional groups into these molecules.

Figure 3-1. Biologically Relevant Compounds Possessing Nitrogenous Functionality

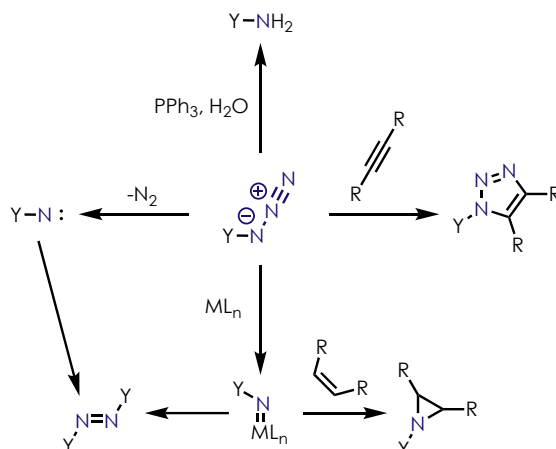


One particular group of interest is the azide, and its value lies in its versatility, as organic azides are capable of being transformed into a variety of other useful functional handles.

Scheme 3-1 showcases several of the transformations available after the installation of azide moieties into molecules. Azides can be reduced to afford an amine product, or they can be reacted with a dienophile in a [3+2] cycloaddition reaction. Additional reactivity that can be accessed from azide precursors includes the formation of nitrenes¹¹¹ or metal-imido

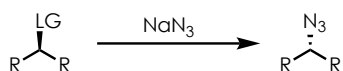
complexes.¹¹² The breadth of reactivity that can be accessed makes the introduction of azides into organic molecules an area that has received much attention from the synthetic community.

Scheme 3-1. Divergent Reactivity Stemming From Organoazides



Traditionally, azides have been incorporated into organic molecules through the use of S_N2 chemistry¹¹³ or through the use of the Mitsunobu reaction.¹¹⁴

Scheme 3-2. Synthesis of Alkyl Azides *via* S_N2 Pathway

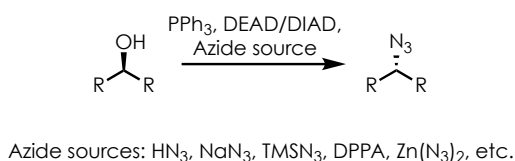


The use of S_N2 chemistry to synthesize alkyl azides (**Scheme 3-2**) has been reported since the 1930's, and numerous reviews have been written on the subject. This method involves the displacement of a nucleofuge, often a halide or pseudohalide, by an anionic azide species. The substitution proceeds with an inversion of stereochemistry, and the yields of the desired alkyl azide products are typically quite high.¹¹⁵

The Mitsunobu reaction¹¹⁶ (**Scheme 3-3**) involves the *in situ* transformation of an alcohol into an excellent leaving groups that can be displaced by a nucleophile to afford a

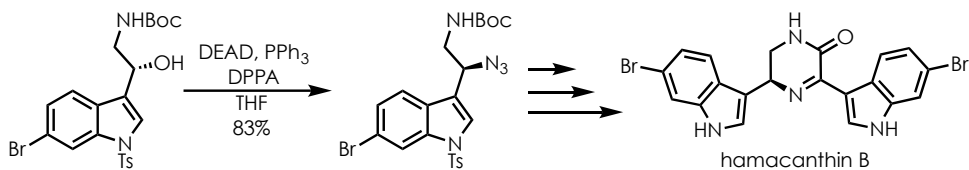
variety of functional groups, depending on the type of nucleophile employed. As the substitution step does proceed *via* an S_N2 pathway, an inversion of stereochemistry is observed at the site of reactivity. The alcohol starting material is converted into an oxyphosphonium intermediate that is extremely reactive towards nucleophilic substitution through the use of PPh₃ and an azodicarboxylate, such as DEAD or DIAD.

Scheme 3-3. Use of the Mitsunobu Reaction to Synthesize Azides



The reliability of these venerable transformations is well-known, and as such, these methods have been used as a means to install azides in the syntheses of complex natural products, such as the one shown in **Scheme 3-4**.¹¹⁷

Scheme 3-4. Use of Alkyl Azide Intermediates in the Synthesis of Natural Products

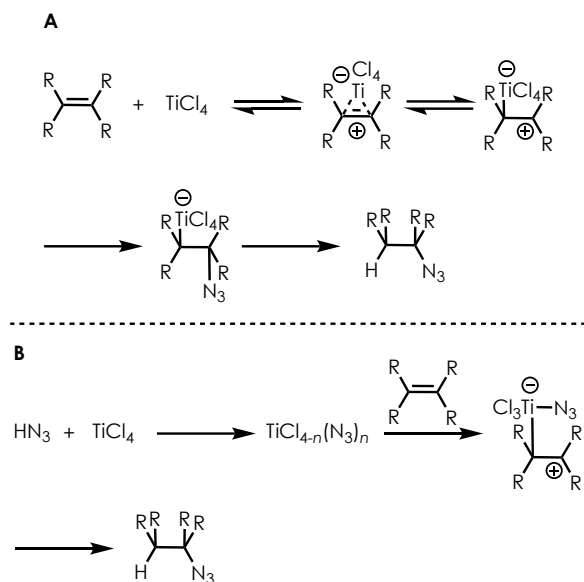


While these methods are unquestionably efficient and reliable, they rely upon the presence of preinstalled functionality, which limits the molecules to which azides can be incorporated into *via* these pathways. Additionally, the presence of other nucleophiles in the reaction, or in other steps of the synthetic route, can result in undesired reactivity and the formation of byproducts.

3.1.2 Previous Hydroazidation Methods

Over the years, many groups have worked to develop methods for introducing azides into molecules that do not require the presence of preinstalled nucleofuges. One attractive route that has received much attention is the hydroazidation of olefins. While the direct addition of HN_3 to olefins has been reported, this process is limited to cases where, following protonation, the resulting carbocation is highly stabilized.¹¹⁸ In the 1980's, much work was done to investigate the utility of Lewis acid-induced hydroazidation reactions. The Hassner group disclosed a report in which they can use either TiCl_4 or AlCl_3 to catalyze the hydroazidation of 1,1-dialkylolefins and trisubstituted olefins.¹¹⁹ While they reported the successful hydroazidation of over 20 olefins in yields ranging from poor to excellent, they noted that monoalkyl or 1,2-disubstituted olefins were almost completely unreactive in this system. The group envisioned several mechanistic pathways for this transformation, and the two options are shown in **Scheme 3-5**. In path A (**Scheme 3-5A**), the formation of a TiCl_4 -olefin π -complex or a σ -complex occurs through the interaction of the Lewis acid and the olefin. These complexes (or the protodemethylated variants) can then interact with HN_3 to afford the desired hydroazidation adduct. The other possible pathway (**Scheme 3-5B**) involves the precoordination of the TiCl_4 and the HN_3 , which is followed by complexation with the olefin, and ligand transfer to afford the hydroazidation product.

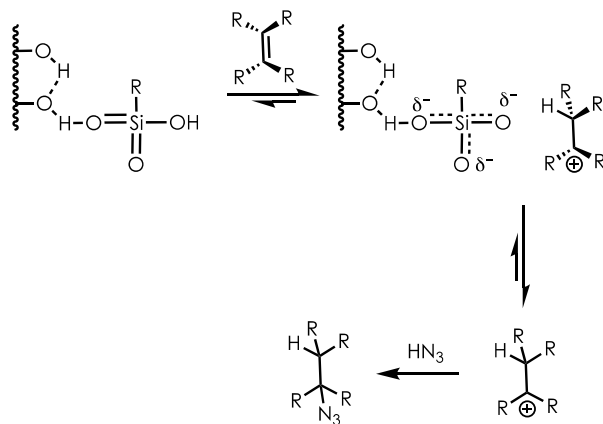
Scheme 3-5. Mechanistic Possibilities for Lewis Acid-Mediated Hydroazidation



While this method was successful, the reaction conditions employ stoichiometric TiCl_4 , as well as excess HN_3 in the presence of chlorinated solvents, which is extremely hazardous. Additionally, several classes of olefins were completely unreactive in this system, which limits how widely this reaction can be used to prepare alkyl azides.

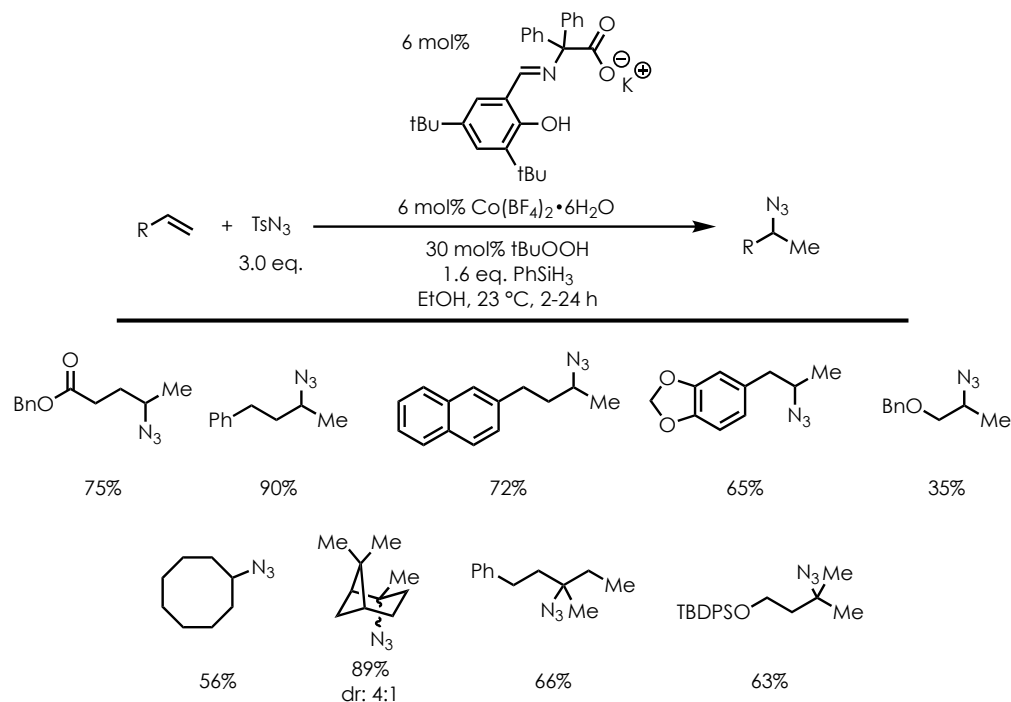
Another method for the hydroazidation of olefins was developed by the Kropp group at UNC in 1992.¹²⁰ This work makes use of HN_3 generated *in situ* to carry out the hydroazidation of a small family of cyclic olefins. By exposing TMSN_3 to SiO_2 or Al_2O_3 , along with a catalytic amount of acid, HN_3 can be generated in a manner that does not require the direct handling of the hazardous reagent. This reaction is thought to be surface-mediated through interactions between the acid catalyst and $\text{SiO}_2/\text{Al}_2\text{O}_3$, as shown in **Scheme 3-6**.

Scheme 3-6. Surface-Mediated Hydroazidation of Olefins



This early work made great advances in the field of olefin hydroazidation, but reaction scopes were often quite limited, and harsh reaction conditions were necessary. Due to the obvious issues with using HN₃, many groups have explored the use of transition metal- or radical-mediated methods for the hydroazidation of olefins. In 2005, the Carreira group developed an elegant method for the Markovnikov hydroazidation of olefins using cobalt catalysis and superstoichiometric TsN₃.¹¹⁸ The method was tolerant of functionality, such as esters and protected alcohols, and a representative scope is shown in **Scheme 3-7**. This reaction reliably provided access to the Markovnikov product when terminal olefins were employed.

Scheme 3-7. Conditions and Scope for Cobalt-Catalyzed Hydroazidation of Olefins

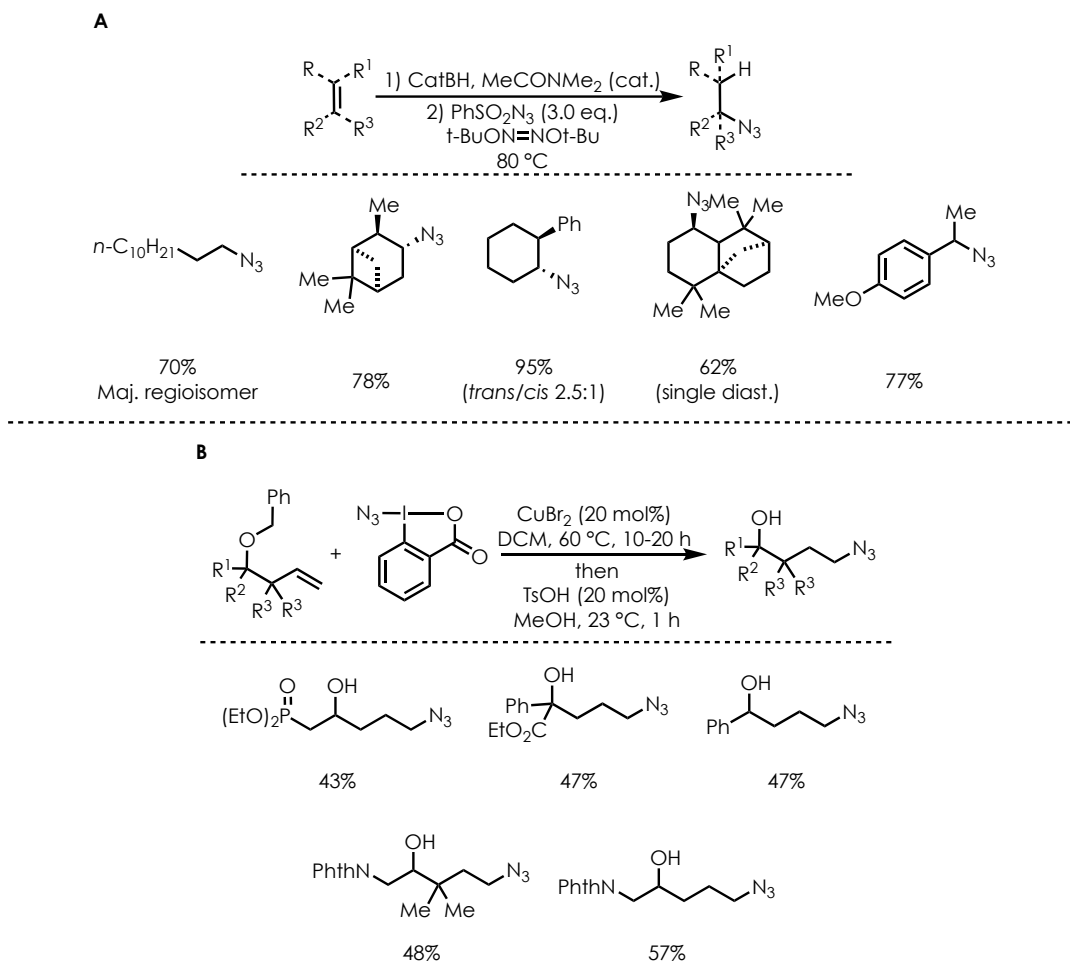


While using TsN_3 is certainly preferable to HN_3 , this reaction employed superstoichiometric amounts of the reagent, and a catalytic amount of tBuOOH was required to facilitate the initiation of the reaction, as the $\text{Co}(\text{salen})$ catalyst exhibited batch-to-batch inconsistencies without it.

Other methods for the hydroazidation of olefins have been developed by the Renaud and Chiba groups.⁸ The method developed by Renaud features a two-step hydroboration/radical-mediated azidation sequence (**Scheme 3-8A**) that begins with the hydroboration of olefins using superstoichiometric catecholborane and catalytic DMA. Upon completion of the reaction, solvent is removed, and the organoborane was treated with di-*tert*-butylhyponitrite and benzenesulfonyl azide to afford the desired alkyl azide. While this reaction sequence was successful at forming the desired products (see **Scheme 3-8A** for

representative scope), the two-step reaction sequence is cumbersome, and functional groups that are sensitive to the presence of radicals are not tolerated.

Scheme 3-8. Modern Methods for the Hydroazidation of Olefins

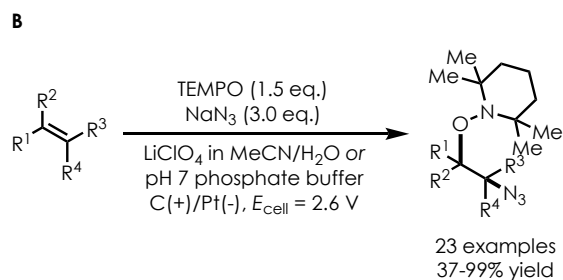
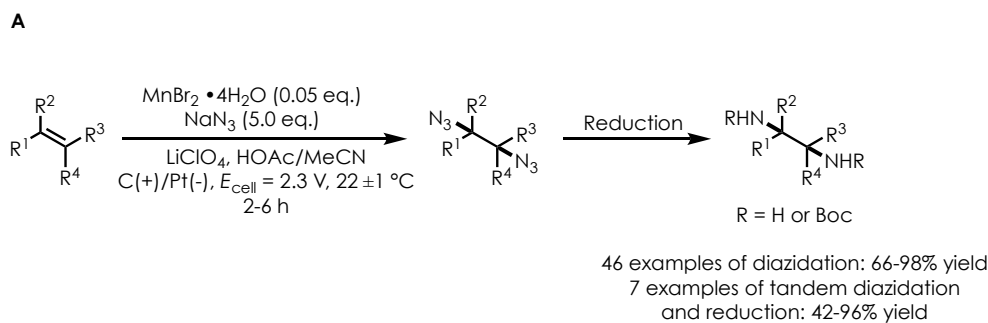


The Chiba group developed conditions for the hydroazidation of homoallylic alcohol benzyl ethers using Cu^I/Cu^{II} catalysis and a hypervalent iodine reagent. The yields of desired products were moderate, and the scope was relatively limited. Additionally, substrates had to possess a benzyl ether, as the moiety served as a traceless H-atom donor in the transformation. Unfortunately, this required an additional reaction step after the

hydroazidation in order to remove the benzyl ether and render it traceless. The necessity of a homoallylic benzyl ether as a substrate also drastically limits the scope of this transformation.

In an effort to develop more mild, general methods for the hydroazidation of olefins, the Lin group has developed electrochemical methods for the diazidation¹²³ (**Scheme 3.9A**) and azidoxygenation¹²⁴ of olefins (**Scheme 3.9B**). Their systems were tolerant of a variety of functionality, and yields were generally quite high; however, these methods required the use of superstoichiometric NaN₃. While undeniably efficient, there still exists a need for a mild hydroazidation method that does not require specialized electrochemical equipment.

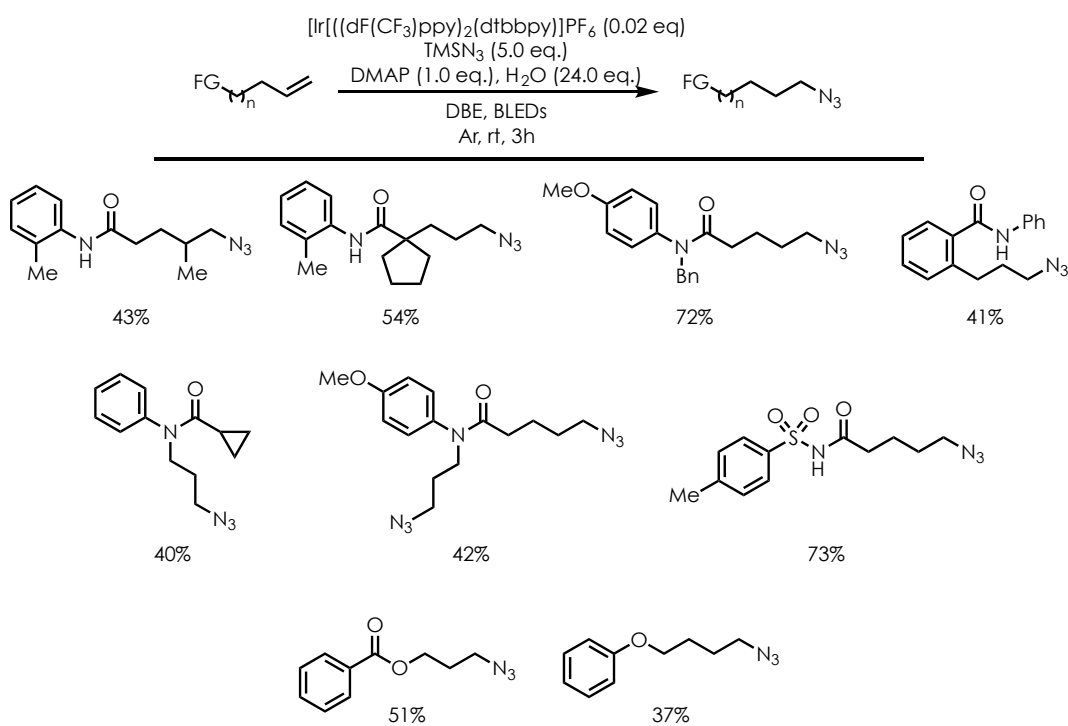
Scheme 3-9. Electrochemical Methods for the Synthesis of Alkyl Azides



More recently, the Yu group developed a method for the hydroazidation of unactivated olefins using an iridium photoredox catalyst and superstoichiometric TMSN₃.¹²⁵ While TMSN₃ is safer to handle than HN₃, the incorporation of water in the reaction conditions is designed to form HN₃ *in situ*, which necessitates caution during reaction setup

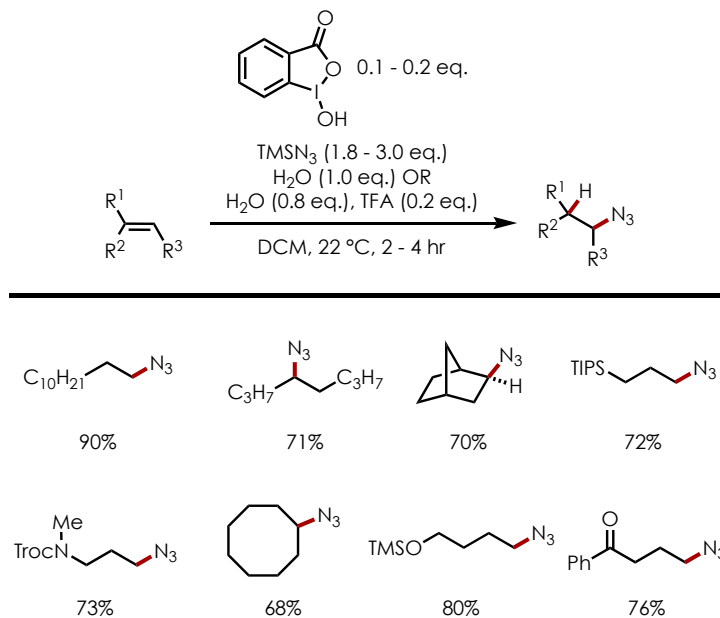
and workup. Additionally, while reaction times were quite short, and yields were quite high, the substrate scope was not particularly diverse (**Scheme 3-10**). *N*-phenyl amides comprised the majority of the scope, and substrates such as styrene, allylbenzene, and limonene were not compatible with the reaction conditions.

Scheme 3-10. Photoredox Catalysis-Mediated Hydroazidation of *N*-Phenyl Amides



Another recent example of an anti-Markovnikov hydroazidation of olefins was disclosed by the Xu group in 2019.¹²⁶ This work features the use of a catalytic amount of a benziodoxole oxidant, superstoichiometric amounts of TMSN₃, and short reaction times. **Scheme 3-11** showcases a representative scope for this transformation, and a variety of unactivated olefins were functionalized in good to excellent yields.

Scheme 3-11. Anti-Markovnikov Hydroazidation of Unactivated Olefins



This reaction was tolerant of many functional groups including amines, alcohols, carboxylic acids, and halides. Impressively, the group was able to subject several complex substrates to their hydroazidation conditions followed by a reduction/protection sequence to obtain products containing protected amines. These reactions were carried out on gram-scale to highlight the utility of this transformation. This method affords access to a wide array of organic azides in typically good yields. Notably, the reaction features low temperatures, short reaction times, and no specialized reaction equipment. However, the reaction uses DCM as a solvent, which is known to be a hazard when combined with azides. Additionally, these reaction conditions are incompatible with electron-rich, activated olefins, such as styrenes, indene, and enol ethers. While this method definitely represents progress in the area of olefin hydroazidation (mild reaction conditions, no specialized equipment, etc.), there still exists a need for the development of a mild method for the hydroazidation of activated olefins.

3.2 Results and Discussion

3.2.1 Development of Hydroazidation Method

We believed that our previously reported hydrofunctionalization systems^{35–39} could be utilized as a starting point in the development of a method for the hydroazidation of activated olefins. The hydroazidation of electron-rich styrenyl substrates is of particular interest, as the resulting products serve as precursors to a class of biologically relevant molecules known as phenethylamines.¹²⁷ We began our investigations by studying the hydroazidation of indene with NaN_3 (**Table 3-1**, entry 1) and were pleased to observe formation of the desired product in 30% yield.

Table 3-1. Initial Reaction Optimization of the Hydroazidation of Indene

Reaction scheme showing the hydroazidation of indene under conditions: tBu-Acr-BF_4 (0.05 eq.), 465 nm LEDs, 18 hr, N_2 . The product is 2-azido-2H-indene.

Structures of the catalyst and co-catalyst are shown:

- tBu-Acr-BF₄**: A zirconium-based complex with a phenyl group, a trifluoroborate counterion, and a bulky ligand system.
- TRIP-SH**: A thiol with a central phenyl ring substituted with three isopropyl groups.

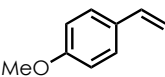
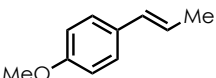
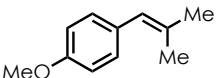
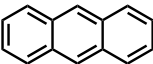
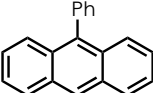
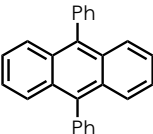
Entry ^a	Azide Source	Co-Catalyst	Additive	Solvent	Yield ^b
1	NaN_3 (2.0 eq.)	Ph_2S_2 (0.2 eq.)	TBABF_4 (1.0 eq.)	TFE (0.1 M)	30%
2	NaN_3 (2.0 eq.)	Ph_2S_2 (0.2 eq.)	TBABF_4 (1.0 eq.)	MeCN (0.1 M)	N.R.
3	TMSN_3 (2.0 eq.)	TRIP-SH (0.2 eq.)	TBABF_4 (1.0 eq.)	TFE (0.1 M)	75%
4	TMSN_3 (2.0 eq.)	TRIP-SH (0.2 eq.)	None	TFE (0.1 M)	75%

^aReactions run on 0.10 mmol scale. ^bYields determined by ^1H NMR using HMDSO as an internal standard.

In addition to the observed desired product, we also observed formation of a thiol-ene byproduct, which will be discussed in more detail shortly. Upon investigating the effects of solvent on the outcome of the reaction, we noted an extreme dependence on the identity of the solvent. As shown in entry 2 of **Table 3-1**, switching to solvents that have traditionally worked well in our hydrofunctionalization reactions, such as MeCN, resulted in no reactivity.

Various literature reports from Linda Johnston, Norman Schepp, and Danial Wayner discuss the kinetics of nucleophilic addition into styrenyl radical cations.^{128–131} Upon irradiation of a solution of a substituted styrene in TFE and exposure to an azide, the group was able to observe nucleophilic addition into the radical cation at varying rates depending on the substrate in question (**Figure 3-2**).¹²⁸

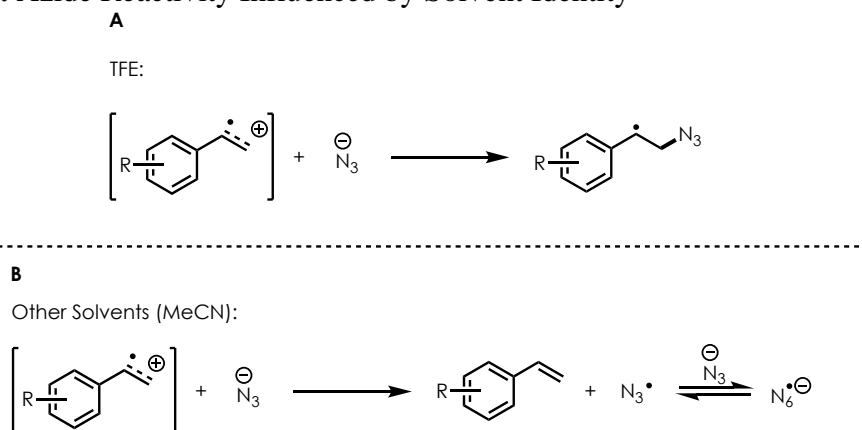
Figure 3-2. Kinetic Data for Azide Addition Into Styrenyl Cation Radicals

substrate	k_q ($10^9 \text{ M}^{-1}\text{s}^{-1}$)	
	MeCN	TFE
	42	7.0
	29	3.5
	30	1.0
	42	3.3
	28	0.45
	25	0.0043

However, when the same experiments were run in MeCN, it was noted that the addition of an azide into the radical cations proceeded at rates that are diffusion controlled ($\sim 10^{10} \text{ M}^{-1}\text{s}^{-1}$). The group originally believed that the lack of selectivity for the trials run in MeCN was due to extremely rapid addition of the azide into the various radical cations. However, upon

performing transient absorption spectroscopy, it was revealed that the benzylic radical that should be formed upon nucleophilic addition of the azide to a styrenyl radical cation was not detected. The group determined that in MeCN, ET occurs between the styrenyl radical cation and the azide (**Scheme 3-12B**).¹²⁸

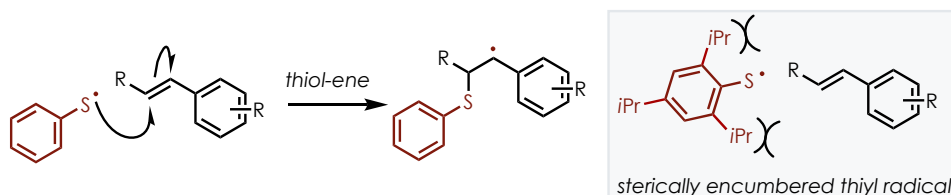
Scheme 3-12. Azide Reactivity Influenced by Solvent Identity



They were able to gather evidence *via* transient absorption spectroscopy to support this through the detection of a higher order azido radical anion species, which presumably forms through the interaction of the azidyl radical with excess azide (**Scheme 3-12B**). Transient absorption spectroscopy of the experiments in TFE, however, revealed a signal associated with the benzylic radical formed after the addition of an azide into a styrenyl radical cation (**Scheme 3-12A**). One explanation of this phenomenon involves the oxidation potentials of the azide in both MeCN and TFE. Due to the stabilizing hydrogen bonding interactions present in TFE, the apparent oxidation potential of the azide increases dramatically from (E°_{peak} (MeCN) = 0.275 V vs. Fc) to (E°_{peak} (TFE) = 0.802 V vs. Fc). Because of this increase in oxidation potential, ET between the styrenyl radical cation and the azide is no longer thermodynamically favorable, and the azide can undergo nucleophilic addition into the radical cation.¹²⁸

This data is consistent with what is observed in entries 1 and 2 in **Table 3-1**. When TFE is used as the solvent in our hydroazidation transformation, ET between the styrene radical cation and azide is not thermodynamically favorable, and productive nucleophilic addition into the radical cation is observed. Further investigations revealed that using a bulkier hydrogen atom donor, 2,4,6-triisopropylthiophenol, resulted in suppression of the undesired thiol-ene byproduct and that switching the azide source to TMSN₃ results in the formation of the desired product in 75% yield (**Table 3-1**, entry 3). The bulkier hydrogen atom donor suppressed the formation of the undesired byproduct, as the sterically hindered thiyl radical is not able to react with the styrenyl substrate (**Scheme 3-13**).

Scheme 3-13. Mechanistic Proposal for the Formation of Thiol-Ene Byproduct



At this point in the optimization, the model substrate was switched to isosafrole due to ease in interpreting NMR spectra. A brief investigation into the amount of TMSN₃ used in the reaction revealed that using only a slight excess resulted in the desired product in nearly quantitative yield (**Table 3-2**, entry 3). Although some slight inconsistencies were noted with the results, we attribute this to the uncertainties of calculating small-scale NMR yields. We found that the hydroazidation of isosafrole consistently proceeded with excellent yields using 1.25 equivalents of TMSN₃.

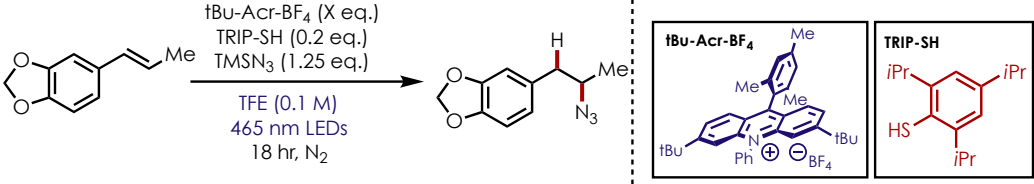
Table 3-2. Optimization of Azide Loading

Reaction scheme showing the conversion of a benzofuran derivative to an azide. Conditions: $t\text{Bu-Acr-BF}_4$ (0.05 eq.), TRIP-SH (0.2 eq.), TMSN_3 (X eq.), TFE (0.1 M), 465 nm LEDs, 18 hr, N_2 .

Entry ^a	Azide Eq.	Yield ^b
1	1.75	99%
2	1.50	77%
3	1.25	99%
4	1.00	75%

^aReactions run on 0.10 mmol scale. ^bYields determined by ¹H NMR using HMDSO as an internal standard.

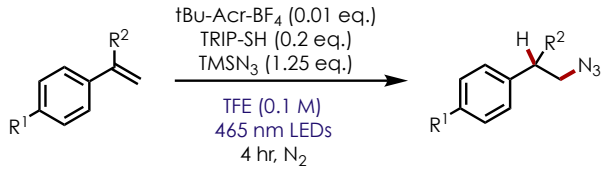
While this transformation still required a slight excess of TMSN_3 , this is a marked improvement over similar methods that require more significant excesses of azide sources. In addition to reducing the amount of azide used in the transformation, we determined that the catalyst loading could be lowered to 0.01 equivalents (**Table 3-3**, entry 4) with no reduction in the reaction yield.

Table 3-3. Optimization of Acridinium Salt Loading

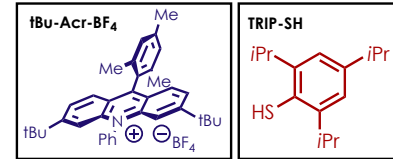
Entry ^a	Catalyst Loading (eq.)	Yield ^b
1	0.04	99%
2	0.03	99%
3	0.02	99%
4	0.01	99%

^aReactions run on 0.10 mmol scale. ^bYields determined by ¹H NMR using HMDSO as an internal standard.

Additional screening revealed that the reaction time could be reduced to just four hours, and complete consumption of starting material was observed. It was also noted that no product formation was observed in the absence of light and the acridinium photoredox catalyst. Satisfied with these conditions, we began evaluating a scope for this transformation. Upon investigating the use of unsubstituted styrenes as substrates, it became apparent that the previously identified conditions were not general, as low yields of desired products were obtained (**Table 3-4**).

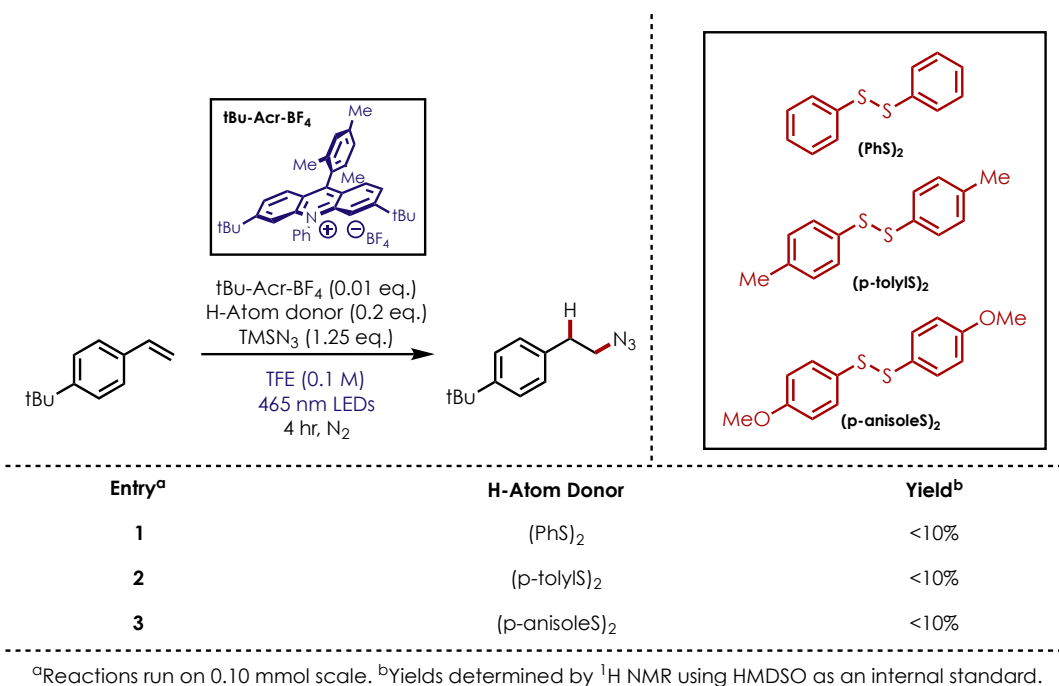
Table 3-4. Initial Results for the Hydroazidation of Unsubstituted Styrenes

Entry ^a	R ¹	R ²	Yield ^b
1	H	Me	16%
2	Cl	H	14%
3	tBu	H	14%
4	Me	H	N.R.




^aReactions run on 0.10 mmol scale. ^bYields determined by ¹H NMR using HMDSO as an internal standard.

Analysis of these reactions revealed complex mixtures that we attributed to the propensity of these molecules to polymerize to various degrees. This hypothesis is based on a method for the polymerization of styrenes with alcohol additives that was previously reported as a collaboration between the Nicewicz and You labs.¹³² After much optimization, we decided to explore the effect of different H-atom donors on the outcome of the reaction. By switching from TRIP-SH to a more reactive H-atom donor, we hoped to increase the rate of H-atom transfer and, ultimately, formation of the desired product, as well as preventing unproductive reactivity. Initially, no improvements were noted when a variety of disulfides were used as H-atom donors in the hydroazidation of 4-tert-butylstyrene (**Table 3-5**, entries 1-3).

Table 3-5. H-Atom Donor Screen for Unsubstituted Styrenes

Unfortunately, this did not result in increased yields of the desired product, so we next investigated whether increasing the amount of H-atom donor used in the reaction would facilitate formation of the desired product. Increasing the amount of H-atom donor did appear to have a beneficial impact on the outcome of the reaction. Entries 3-5 in **Table 3-6** show that using at least 0.50 equivalents of diphenyl disulfide in the reaction result in greater than 40% yield of the desired product. We then sought to confirm that this adjustment to reaction conditions would result in similar improvements for other unsubstituted styrene substrates.

Table 3-6. H-Atom Donor Loading Screen for Unsubstituted Styrenes



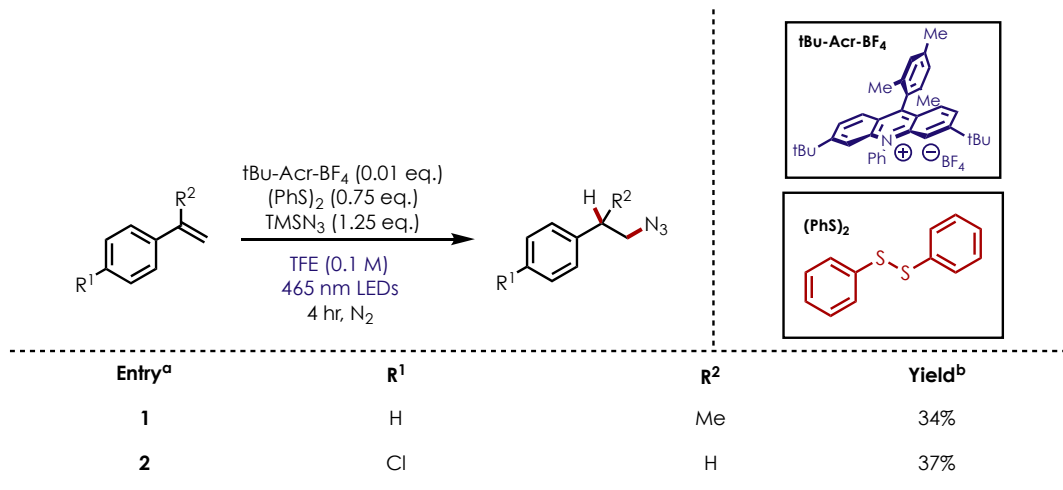
Reaction conditions:
tBu-Acr-BF₄ (0.01 eq.)
(PhS)₂ (X eq.)
TMSN₃ (1.25 eq.)
TFE (0.1 M)
465 nm LEDs
4 hr, N₂

Entry ^a	(PhS) ₂ Eq.	Yield ^b
1	0.25	14%
2	0.35	24%
3	0.50	41%
4	0.75	44%
5	1.0	44%

^aReactions run on 0.10 mmol scale. ^bYields determined by ¹H NMR using HMDSO as an internal standard.

As **Table 3-7** shows, the use of a more reactive H-atom donor, (PhS)₂, resulted in increased yields for two other terminal styrene substrates. Although these reaction yields were not as high as substrates investigated initially, we were satisfied, as terminal styrenes are challenging substrates to use in our hydrofunctionalization reactions.

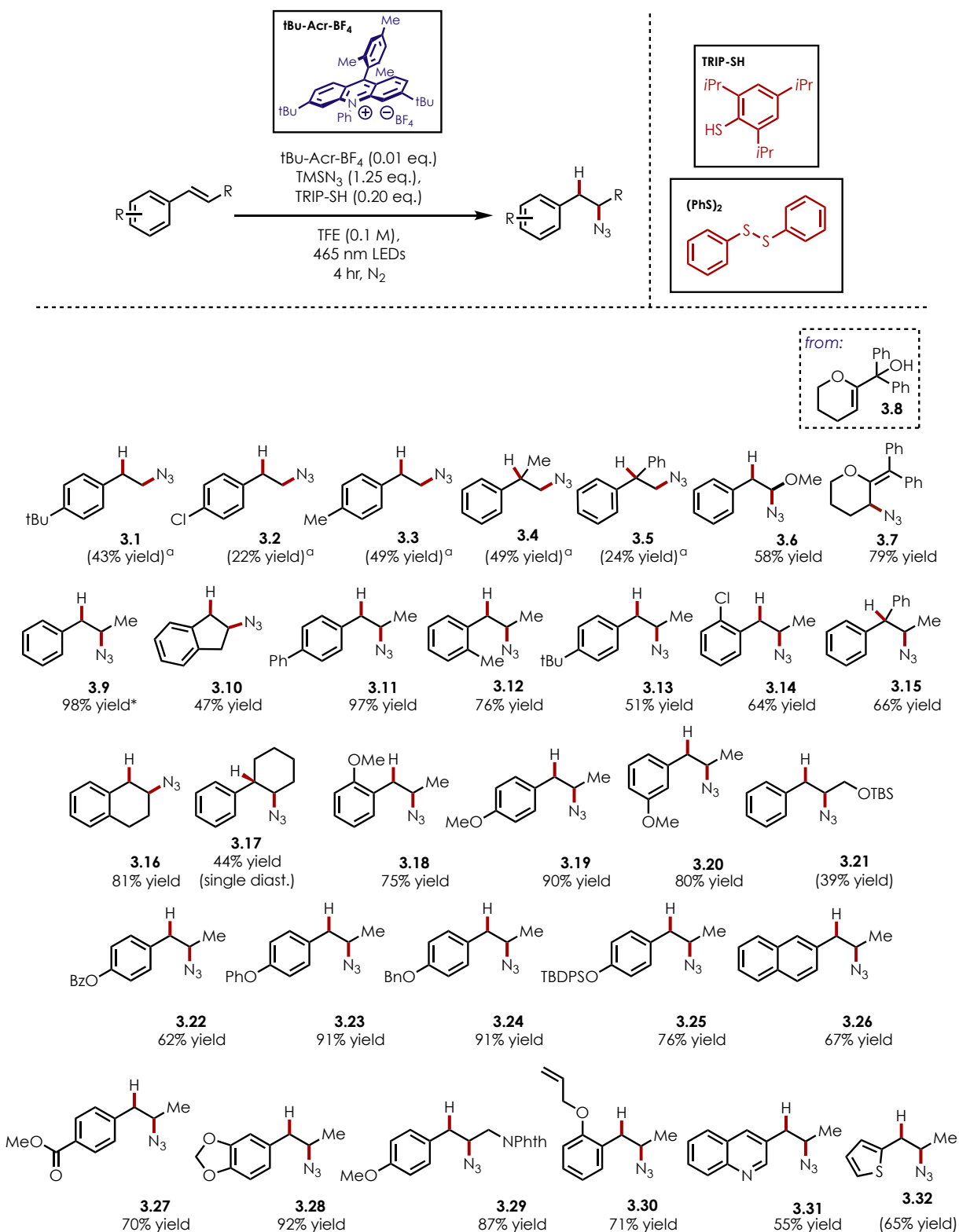
Table 3-7. Effect of More Reactive H-Atom Donor on Various Terminal Styrenes



^aReactions run on 0.10 mmol scale. ^bYields determined by ¹H NMR using HMDSO as an internal standard.

We then evaluated a scope for this transformation and were pleased to discover that our method resulted in the efficient hydroazidation of a variety of olefins (**Scheme 3-14**). A variety of *para*-substituted terminal styrenes (compounds **3.1** – **3.5**) underwent hydroazidation in moderate yields. Unfortunately, these compounds were extremely challenging to isolate, which resulted in yields being reported as ¹H NMR yields.

Scheme 3-14. Substrate Scope for the Anti-Markovnikov Hydroazidation

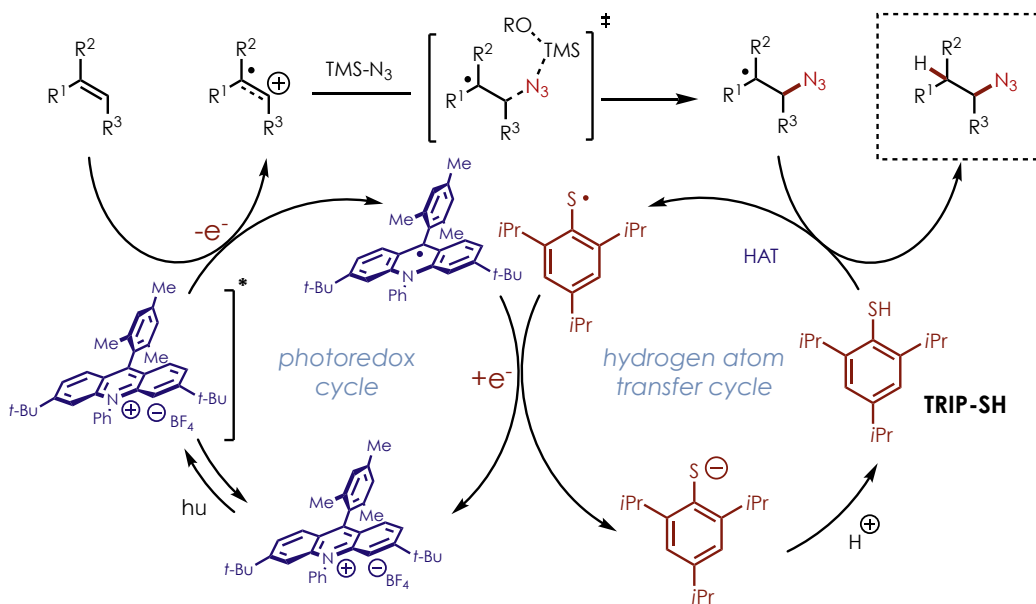


Yields reported are average of two trials on 0.5 mmol scale unless otherwise noted. Yields reported in parentheses are ¹H NMR yields using HMDSO as an internal standard. ^a0.75 eq. of (PhS)₂ used instead of TRIP-SH.

Vinyl ethers also proved to be competent substrates, and desired products were formed in good yields (compounds **3.6** and **3.7**). A variety of substitution was tolerated on derivatives of β -methylstyrene, including methyl, chloro, tert-butyl, and methoxy substituents. The presence of these groups in various positions on the arene did not appear to affect the efficiency of the transformation, as similar yields were obtained for compounds **3.18** – **3.20**. Additionally, a variety of functionality was also tolerated in the reaction, including esters, TBS-protected alcohols, and various protected phenols. This illustrates the mild, general nature of these reaction conditions and reinforces the utility of our method. These conditions were also compatible with several heterocyclic substrates, and the resulting azides were formed in good yields (compounds **3.31** and **3.32**).

Although detailed mechanistic studies were not undertaken for this project, we believe that this transformation proceeds in an analogous manner to our previously reported hydrofunctionalization reactions (**Scheme 3-15**).

Scheme 3-15. Mechanistic Proposal for Hydroazidation of Olefins



Upon irradiation of the ground state acridinium photoredox catalyst, the excited state is accessed and can undergo PET with the olefin substrate. This process generates an olefin radical cation and the reduced form of the acridinium catalyst. Nucleophilic addition of the azide into the radical cation results in the formation of a stabilized neutral, benzylic radical. As detailed investigations were not performed, it is unclear exactly what the identity of the azide nucleophile is. While it is possible that trace amounts of water in the reaction result in the formation of free azide anion, as water was not rigorously excluded during reaction setup. However, it is also possible that a termolecular transition that involves solvent-assisted desilylation/nucleophilic addition is operative, or that a more complex azide silicate species could be acting as the nucleophile. The resulting benzylic radical can then participate in hydrogen atom transfer with the TRIP-SH or $(\text{PhS})_2$ to furnish the desired product and a thiyl radical, which is capable of oxidizing the reduced acridinium catalyst. This results in the formation of the ground state acridinium catalyst and a thiolate anion, which can be protonated by solvent to close the catalytic cycle.

3.3 Conclusions

In conclusion, we were able to develop mild conditions for the hydroazidation of a large family of electron-rich olefins. This method provides access to valuable precursors of phenethylamine derivatives, which possess rich biological activities. This method does not require the use of transition metals or large excess of TMSN_3 , which serves as substantial improvements to alkene hydroazidation conditions. We feel that this method complements existing hydroazidation conditions nicely and represents a general method for the functionalization of electron-rich olefins.

3.4 Acknowledgements

This work was the result of a fruitful collaboration, and it was truly a pleasure to work on it with such fantastic colleagues. The work disclosed in this chapter was published in Synlett as part of the “9th Pacific Symposium on Radical Chemistry” cluster.¹³³

CHAPTER 4: DEVELOPMENT OF A METHOD FOR THE NUCLEOPHILIC DEFLUORINATION OF ELECTRON-NEUTRAL AND ELECTON-RICH FLUOROARENES

4.1 Introduction

4.1.1 Importance of Nucleophilic Aromatic Substitution

Perhaps one of the most well-known structural units in the realm of organic chemistry is the (hetero)aromatic ring. These compounds can be found in many important industries, such as the pharmaceutical, agrochemical, and fragrance industries (**Figure 4-1**). As well as being common features of commercially important molecules, (hetero)aromatic rings are also commonly found in many natural products that are complex synthetic targets for groups in academia (**Figure 4-2**).

Figure 4-1. (Hetero)arenes Possessing Biologically Relevant Properties

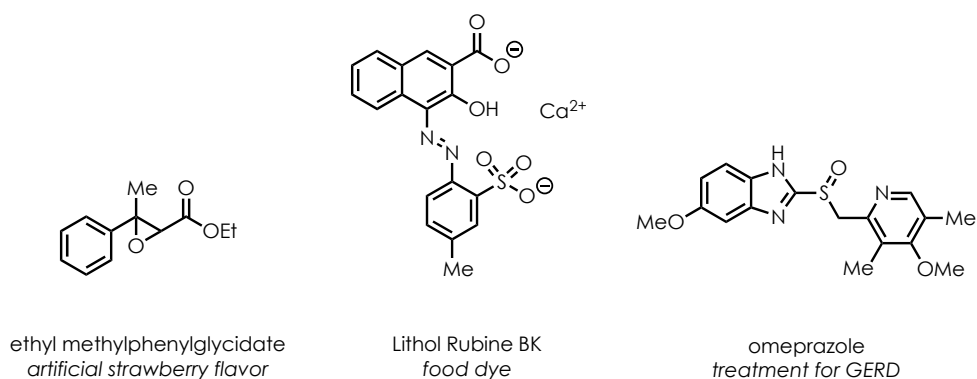
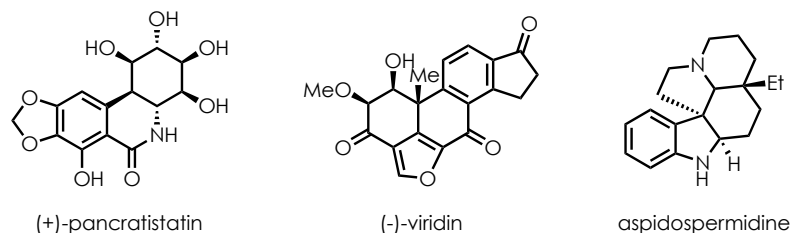


Figure 4-2. (Hetero)aromatic Natural Products of Interest to the Synthetic Community

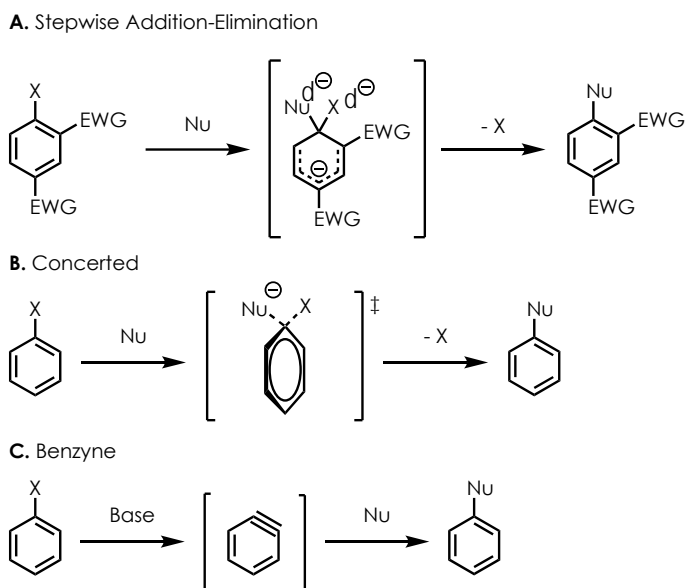


Due to the important properties of compounds containing (hetero)aromatic rings, it is unsurprising that much attention has been given to the synthesis of these compounds, especially by the pharmaceutical industry. In fact, a 2011 survey of over 3566 compounds disclosed by Pfizer, GlaxoSmithKline, and AstraZeneca revealed that 99% of the compounds contained at least one (hetero)aromatic ring.¹³⁴

One challenge that the pharmaceutical industry faces is the derivatization of compounds containing aromatic rings. In order to identify the most potent treatments, SAR studies are employed to investigate the effects of small structural changes to a compound with biological activity. However, it would be a monumental task to synthesize each compound from simple starting materials, so chemists are interested in methods for functionalizing late-stage targets to streamline the process of preparing derivatives. Unfortunately, the lack of methods that are tolerant of existing functionality and compatible with complex molecules has been cited by chemists in the pharmaceutical industry as a major challenge that needs to be addressed.¹³⁵ Ideally, substitution reactions that utilize common precursors would be employed to rapidly derivatize molecules for assessment of their biological activity.

To this end, nucleophilic aromatic substitution (S_NAr) has long been employed as a rapid method for building up complexity in (hetero)aromatic systems. As the name suggests, S_NAr involves the displacement of a nucleofuge, or leaving group, from a (hetero)arene by a nucleophile. This chemistry has a rich history with reviews on the subject published as early as 1951.¹³⁶ The reaction involves the displacement of a nucleofuge by a nucleophile and can occur *via* several mechanistic pathways (**Scheme 4-1**).

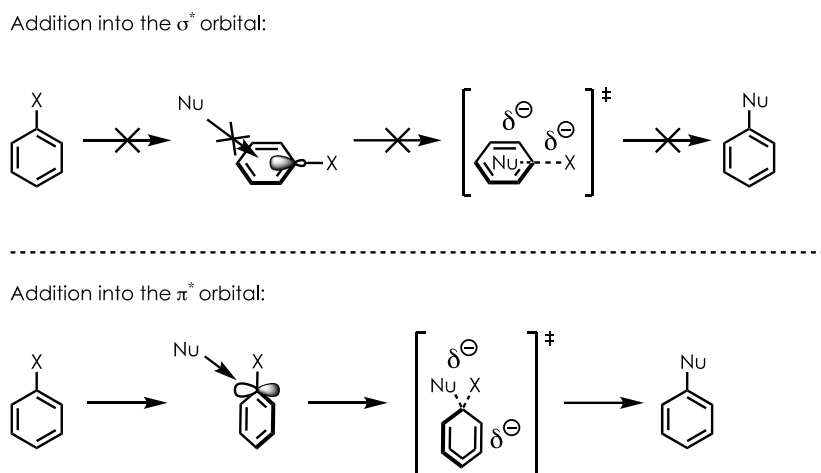
Scheme 4-1. Mechanistic Possibilities for S_NAr Reaction



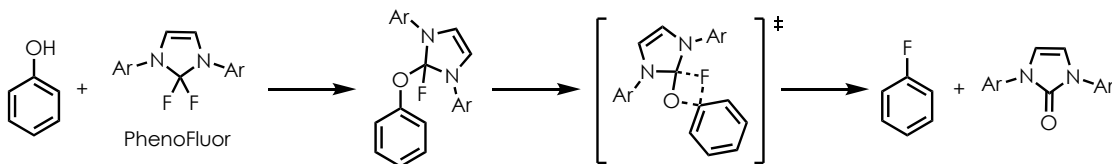
Scheme 4-1A illustrates the stepwise-addition-elimination pathway, which is typically limited to substrates with electron-withdrawing groups in the positions *ortho*- and/or *para*-positions, relative to the nucleofuge. These electron-withdrawing substituents help to stabilize the buildup of negative charge upon addition of the nucleophile to the position bearing the nucleofuge. The mechanistic pathway in **Scheme 4-1B** depicts a concerted S_NAr reaction, where an S_N2 -like pathway is operative and no significant buildup of negative charge on the arene is observed. This pathway was long thought to be extremely disfavored,

due to the alignment of the orbitals involved. The σ^* orbital of the nucleofuge is positioned so that the larger lobe points directly towards the center of the arene, which prevents concurrent addition of the nucleophile and departure of the nucleofuge (**Scheme 4-2**). However, recent reports from several groups provide compelling evidence for the existence of such a mechanistic pathway.^{137–140} Computational data from the Ritter group provides evidence of this pathway.¹³⁸ Upon examination of the reaction shown in **Scheme 4-3**, the Ritter group discovered that no Meisenheimer intermediate could be detected computationally. Their investigations revealed only the presence of a single transition state, which supported the theory that S_NAr reactions could proceed in a concerted manner.

Scheme 4-2. Orbital Alignment for Concerted S_NAr Pathway

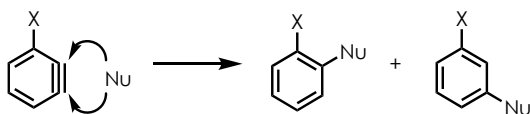


Scheme 4-3. Computational Determination of Meisenheimer Intermediate



The third S_NAr mechanistic pathway (**Scheme 4-1C**) proceeds through an electrophilic benzyne intermediate. Benzyne was first reported in the 1953 by Roberts¹⁴¹, and since then, have received significant attention by the synthetic community.^{142,143} However, the generation of benzyne typically requires preinstalled functionality and harsh conditions, which limits their utility when sensitive functional groups are present. Another limitation to the use of benzyne is the challenges in controlling the regioselectivity of product formation (**Scheme 4-4**). Although some computational studies have been carried out by Garg and Houk^{144,145} to compare several models for predicting regioselectivity of unsymmetrical benzyne, it is often quite challenging to control product formation. These factors limit the utility of benzyne in synthesis and are generally not utilized for the derivatization of biologically relevant molecules.

Scheme 4-4. Regioselectivity Challenges Associated with Benzyne



Although much work has been done to provide support for the existence of concerted S_NAr pathways, it is difficult to predict when a transformation will occur *via* a concerted mechanism without carrying out detailed studies.^{137,138} Therefore, especially in substrates

bearing EWGs, the stepwise-addition-elimination pathway is thought to be operative in most cases. Although S_NAr chemistry has been thoroughly explored and is well-understood¹⁴⁶, the necessity for EWGs located *ortho*- or *para*- relative to the nucleofuge limits the compounds which are amenable to these reaction conditions.

The pharmaceutical study discussed previously also investigated the prevalence of common EWGs that are often found in prototypical S_NAr substrates, and compounds containing aromatic nitro groups were found to be present in only 0.4% of the molecules.¹³⁴ However, aromatic substrates containing methoxy-substituents make up almost 27% of the compounds surveyed, which indicates that molecules that are more electron-rich than typical S_NAr substrates are more common in the pharmaceutical industry. As such, there exists a need for S_NAr methods that are compatible with more electron-rich arenes.

In addition to limitations due to the presence of EWGs, S_NAr substrates also must possess a nucleofuge, which is typically a halide. The previously mentioned survey of pharmaceutical compounds reveals that aryl halides are present in over 50% of the molecules included in the study, with aryl chlorides being the most common – found in 30% of the compounds.¹³⁴ However, the authors of the study note that very few of those aryl chlorides are in chemical environments that render them suitable for participation in S_NAr reactions (i.e. activated by suitable EWGs). The next most prevalent class of aryl halides in the compounds surveyed is aryl fluorides, and while fluorides are typically excellent nucleofuges in S_NAr reactions, the electronic environments of the compounds surveyed are generally not suitable for S_NAr reactions. Due to the reactivity of aryl fluorides in S_NAr reactions and their prevalence in compounds in the pharmaceutical industry, these systems represent an attractive class of targets that could be amenable to further derivatization. However, current

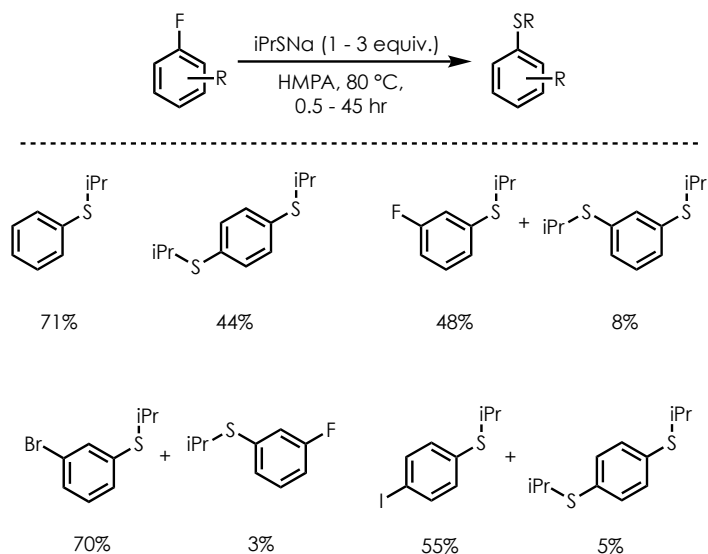
S_NAr methods are not compatible with many of these fluoroarenes, so there exists a need for the development of methods for the functionalization of electron-neutral and electron-rich fluoroarenes.

4.1.2 Previous Defluorination Methods

The functionalization of unactivated fluoroarenes has long been a challenge to the synthetic community despite the attention it has received. Methods have been reported, but suffer from many limitations including harsh reaction conditions, limited substrate compatibility, and poor yields. Early work in the field was disclosed by Huisgen and detailed the amination of simple haloarenes using lithium salts as nucleophiles.¹⁴⁷ However, fluorobenzene was the only fluoroarene that was used in the study, and the conditions required to observe desired product formation were harsh. Despite formation of *N*-phenylpiperidine in 85% yield, this method is not general and requires forcing conditions.

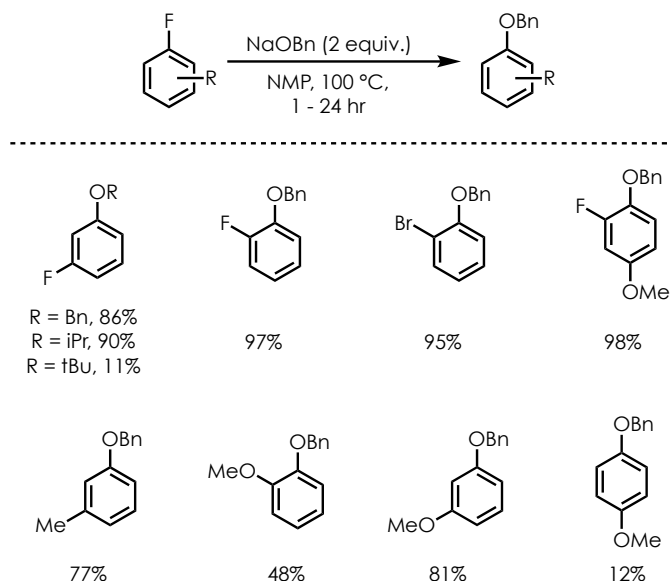
In 1979, the Tiecco group developed conditions for the functionalization of unactivated aryl halides using thiolate nucleophiles.¹⁴⁸ While the method included several examples of fluoroarenes that were successfully functionalized (**Scheme 4-5**), the reaction conditions were quite harsh and required the use of HMPA as a solvent, which is less than desirable. Although yields of the desired products were good, there were issues with disubstitution and substitution at a position occupied by another halide.

Scheme 4-5. Early Example of S_NAr with Unactivated Fluoroarene Substrate



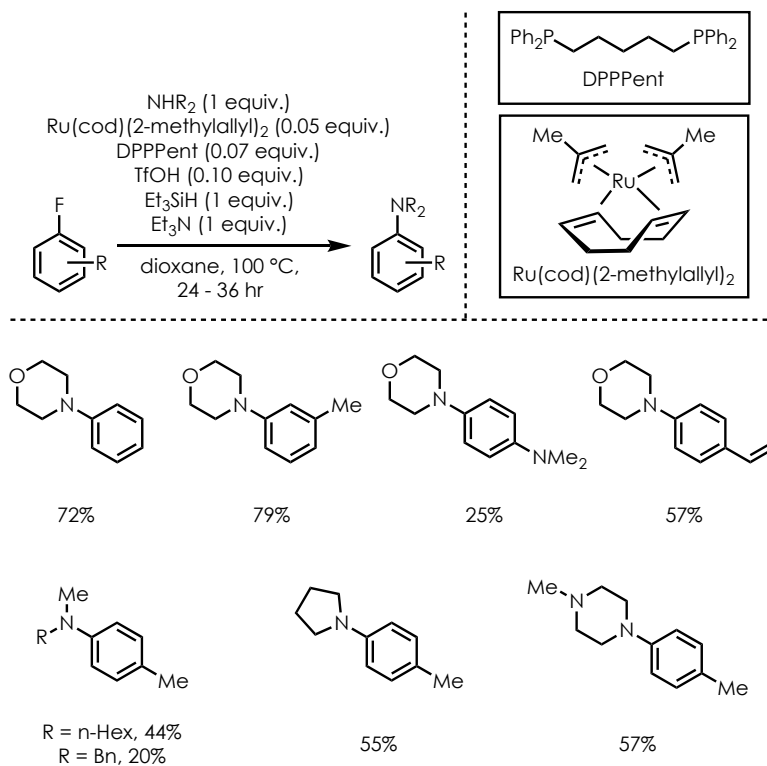
Progress in the field was made in 2006 when the Bueno group published a method for the synthesis of aromatic ethers *via* an S_NAr reaction of fluoroarenes.¹⁴⁹ While the conditions employed were still forcing, as they involved elevated reaction temperatures and alkoxide nucleophiles, a variety of fluoroarenes were competent substrates in the transformation. As shown in **Scheme 4-6**, aromatic ethers with a variety of substituents were formed in overall good yields. Additionally, a small selection of alkoxide nucleophiles was reported with the desired products formed in yields ranging from poor to excellent. In contrast to the work from Tiecco, this method featured complete chemoselectivity for the positions occupied by the fluoride substituents and no evidence of disubstitution in substrates with multiple nucleofuges. Although some aspects of the reaction conditions are not ideal, this methodology represents progress in the realm of the use of unactivated fluoroarene in S_NAr reactions.

Scheme 4-6. Formation of Aryl Ethers *via* S_NAr with Fluoroarene Substrates



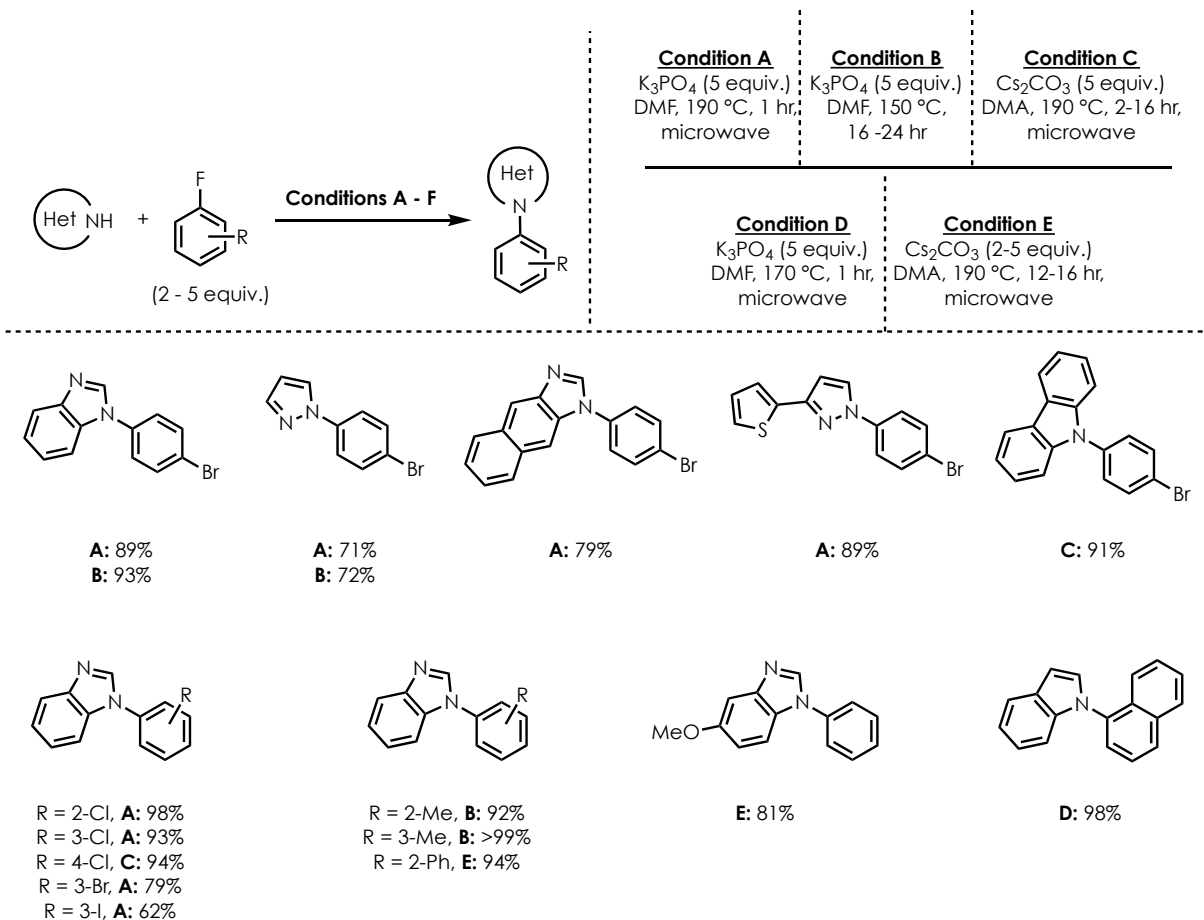
Another strategy for developing S_NAr methods that are compatible with unactivated fluoroarenes involves the use of transition metals. Many groups have reported the complexation of fluoroarenes with metals to form an η₆-arene complex, which renders the fluoroarene more electron-deficient and capable of participating in S_NAr reactions.^{150,151} However, the majority of these methods require the use of stoichiometric transition metals, which is costly and limits the applicability of these methodologies to the derivatization of pharmaceutical compounds. Recognizing the need for a catalytic method, the Shibata group developed conditions for the Ru-catalyzed amination of unactivated fluoroarenes. A partial scope is shown in **Scheme 4-7**, and a small scope of electron-rich arenes were compatible with the reaction conditions. The desired aminated products were formed in moderate yields, and a small scope of amine nucleophiles was presented as well.

Scheme 4-7. Ru-Catalyzed Amination of Unactivated Fluoroarenes



In 2012, Diness and Fairlie reported a catalyst-free method for the *N*-arylation ofazole and indole derivatives.¹⁵² In an effort to develop a method that was complementary to existing work, they sought to identify conditions that were compatible with unactivated fluoroarenes and were tolerant of other halides. As expected, in order to identify conditions that would allow selective nucleophilic addition at the site occupied by the fluoride, much investigation was required. By keeping reaction times short and carefully choosing a solvent and a base, they were able to develop several sets of conditions to carry out the *N*-arylation ofazole and indole derivatives (**Scheme 4-8**).

Scheme 4-8. Representative Scope for *N*-Arylation of Nitrogenous Heterocycles

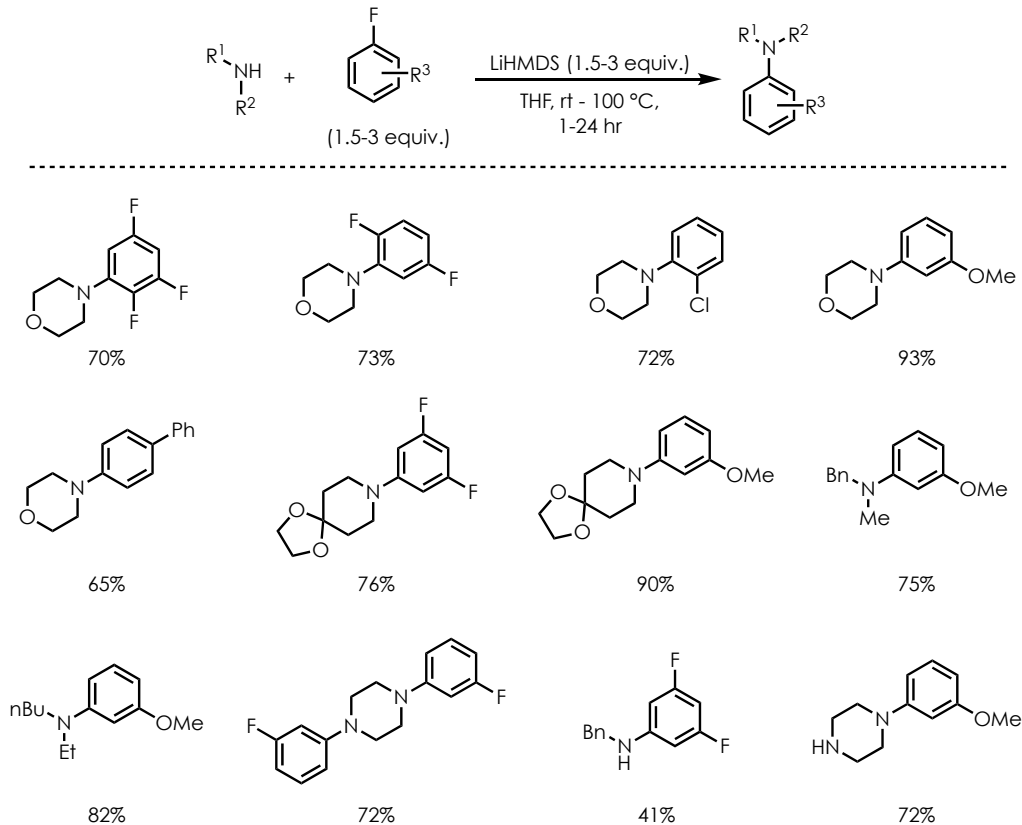


A variety of azole and indole derivatives were competent nucleophiles in the reaction, and yields were generally quite high. However, substituents on the fluoroarenes were limited to other halides or methyl groups. While it is impressive that other halide substituents were tolerated, more electron-rich groups, such as methoxy substituents, were only tolerated on the azole/indole nucleophiles. Additionally, all of the conditions required the use of harsh elements, such as high reaction temperatures or specialized reaction equipment (i.e.

microwave reactor), as well as the use of the fluoroarenes in excess. While this reaction provides access to the *N*-arylated heterocyclic products, several aspects render these conditions unsuitable for use in the late-stage derivatization of pharmaceutically relevant compounds.

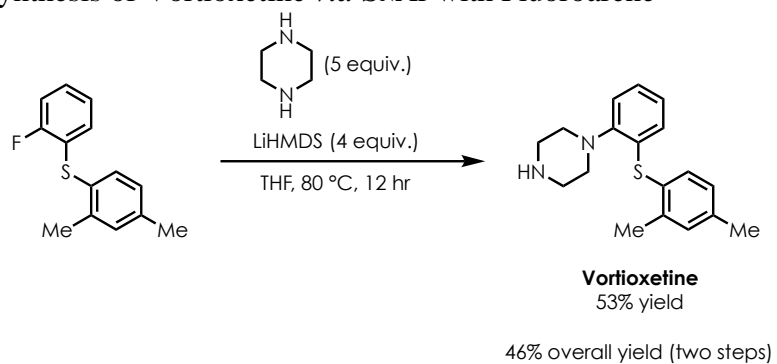
This initial report was followed by the development of a reaction that allowed aliphatic amines to serve as nucleophiles in an S_NAr reaction with unactivated fluoroarenes.¹⁵³ Initial investigations revealed that the choice of base was extremely important for this reaction, as the use of $KOtBu$ or LDA resulted in undesired reactivity. The use of $KOtBu$ resulted in the formation of an aryl ether due to the base acting as a nucleophile, while the use of LDA resulted in benzyne formation and unproductive polymerization. $LiHMDS$ proved to be a competent base for the transformation with desired aryl amines formed in good to excellent yields (**Scheme 4-9**).

Scheme 4-9. Representative Scope for Aliphatic Amination of Fluoroarenes



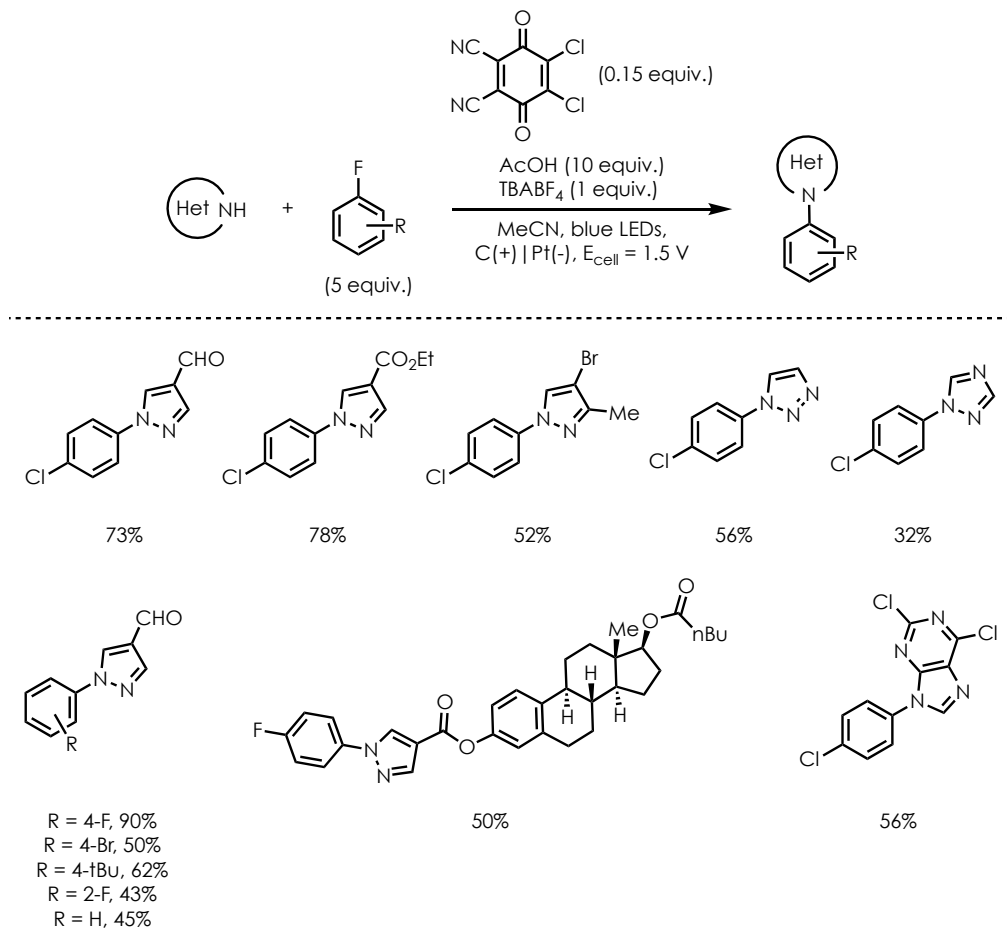
Impressively, multiple fluoride substituents are present in many substrates, and, in most cases, only one product is observed. Additionally, the presence of other halides and electron-rich substituents are well tolerated in the reaction. A variety of amines were found to be competent nucleophiles in the transformation with the desired products formed in good yields. The group was also able to use their method to synthesize the antidepressant, Vortioxetine, in just two steps with an overall yield of 46% (**Scheme 4-10**). While this method expands upon previous work by showcasing aliphatic amines as nucleophiles, the reaction conditions for this transformation are still quite harsh with temperatures reaching 100 °C and the use of a strong base to generate an anionic nucleophile. These conditions would certainly limit use of this method with more sensitive functionality.

Scheme 4-10. Synthesis of Vortioxetine *via* S_NAr with Fluoroarene



Although much work has been done to develop conditions for S_NAr reactions that are compatible with unactivated fluoroarenes, the previously discussed methods all feature limitations to their utility, including the use of strong bases and high reaction temperatures. In 2020, the Lambert group sought to address the challenge of developing an S_NAr method for unactivated fluoroarenes that featured more mild conditions, and they were able to disclose a method that requires no base and can be accomplished at ambient temperatures.¹⁵⁴

Scheme 4-11. Representative Scope for DDQ-Mediated S_NAr with Fluoroarenes



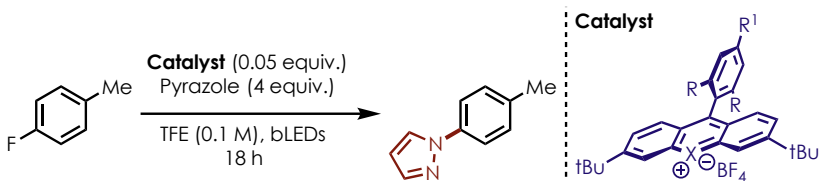
As shown in the representative scope in **Scheme 4-11**, a variety of heterocycles were competent nucleophiles in the transformation. Several nucleophiles possessed functionality for further transformations, which increases the utility of this method. A variety of substitution on the fluoroarene was well tolerated with halides and alkyl groups affording the desired products in good yields. Additionally, an impressive number of biologically relevant derivatives were showcased as nucleophiles in the reaction, which illustrates the potential use of this method in late stage functionalization.

While the Lambert group was able to develop mild conditions for the use of unactivated fluoroarenes in S_NAr reactions, there are several notable limitations. The group noted a lack of reactivity when fluoroarenes bearing alkoxy substituents were present, which prevents this method from being used with many electron-rich substrates. Additionally, this method requires the use of extremely specialized reaction equipment as detailed in the supplemental information portion of the report. In an effort to utilize both electrochemistry and photoredox catalysis, specialized glassware was crafted, which makes adoption of this method on any significant scale challenging. While the Lambert group has made great progress towards the development of an S_NAr reaction that uses unactivated fluoroarenes, we believed that the need for a method compatible with more electron-rich fluoroarenes still existed. Due to the success of our previous cation-radical-accelerated-nucleophilic aromatic substitution (CRA- S_NAr) reactions^{155,156}, we were interested in investigating whether this concept could be extended to develop a CRA- S_NAr reaction that featured a fluoride nucleofuge.

4.2 Results and Discussion

4.2.1 Defluorination of Electron-Neutral Fluoroarenes Using Azoles as Nucleophiles

We began our investigations by exploring the defluoroamination of electron-neutral fluoroarenes with azole nucleophiles. Work carried out by Vincent Pistritto used 4-fluorotoluene as a model substrate and pyrazole as the nucleophile.

Table 4-1. Initial Catalyst Screen to Observe Reactivity


Entry	R	R ¹	X	E [*] _{1/2} ^{red} (V vs. SCE)	Name of Catalyst	Yield ^a
1	Me	Me	-NPh	+2.10	Catalyst G	0%
2	Cl	H	-NPh	+2.21	Catalyst H	8%
3	Me	Me	O	+2.51	Catalyst C	<5%
4	Cl	H	O	+2.66	Catalyst D	35%
5	Me	F	O	+2.57	Catalyst A	55%

^aYields determined by ¹H NMR using HMDSO as an internal standard.

The use of acridinium catalysts (**Table 4-1**, entries 1-2) showed that very little product formation was observed using the conditions shown above. As electron transfer between the 4-fluorotoluene ($E_{\rho/2} = +2.24$ V vs. SCE) and excited state catalysts is endergonic, little reactivity is observed. A pyrylium photocatalyst ($E_{*1/2\text{red}} = +2.32$ V vs. SCE) (**Catalyst F**) resulted in product formation (37% yield), but visible degradation was observed over the course of the reaction, so the pyrylium scaffold was abandoned.

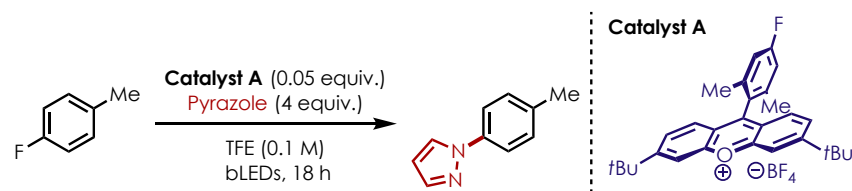
In order to achieve the nucleophilic defluorination of electron-neutral fluoroarenes with ground state reduction potentials over +2.10 V, a novel photoredox catalyst with an excited state reduction potential greater than those of the acridinium salts was necessary. To that end, our lab has recently disclosed an efficient route for the synthesis and derivatization of acridinium salts that proceeds through xanthylum salts.³³ Due to the structural similarities of xanthylum salts and pyrylium salts, we were interested in probing the photophysical properties of these compounds in an effort to develop more potent excited state oxidants (see Appendix C for detailed characterization data). These xanthylum salts were found to be extremely potent excited state oxidants ($E_{*1/2\text{red}} = > +2.5$ V vs. SCE), and their use in the

nucleophilic defluorination reaction afforded greatly increased amounts of the desired product (**Table 4-1**, entries 4-5). Interestingly, **Catalyst C** resulted in only trace amounts of desired product formation (**Table 4-1**, entry 3), which may be due to formation of a less potent charge transfer excited state. Due to the success of using **Catalyst A** to effect the defluoroamination transformation, further studies were carried out to improve the yield of the reaction.

As shown in entries 2-5 in **Table 4-2**, a variety of xanthylium and pyrylium salts were investigated as catalysts in the transformation, but none resulted in yields superior to that afforded by **Catalyst A**. In an effort to develop more efficient reaction conditions, the amount of catalyst used in the reaction was lowered to just 0.01 equivalents (**Table 4-2**, entry 6), and only slight degradation of reaction yield was observed. However, we found that increasing the amount of **Catalyst A** to 0.075 equivalents resulted a dramatic increase in reaction yield with the desired product formed in an 80% yield. Entries 9-13 of **Table 4-2** reveal the necessity of a fluorinated solvent. Much work has been carried out to study the effects of fluorinated solvents on cation radicals, and the use of a fluorinated alcoholic solvent is optimal for this transformation, as hydrogen bonding interactions with the solvent stabilize the high energy cation radicals.^{157,158} We elected to use HFIP as the sole solvent for the transformation, as a (1:1) mixture of TFE and HFIP only provided a small increase in reaction yield; entries 16-26 in **Table 4-2** were all run in HFIP. Additionally, a reaction concentration of 0.1 M was ideal, as decreasing or increasing the reaction concentration resulted in diminished yields of desired product (**Table 4-2**, entries 14-15). In an effort to reduce the amount of pyrazole that was used as a nucleophile, decreased amounts were

investigated, but only deleterious effects to the reaction yield were observed (Table 4-2, entries 16-19).

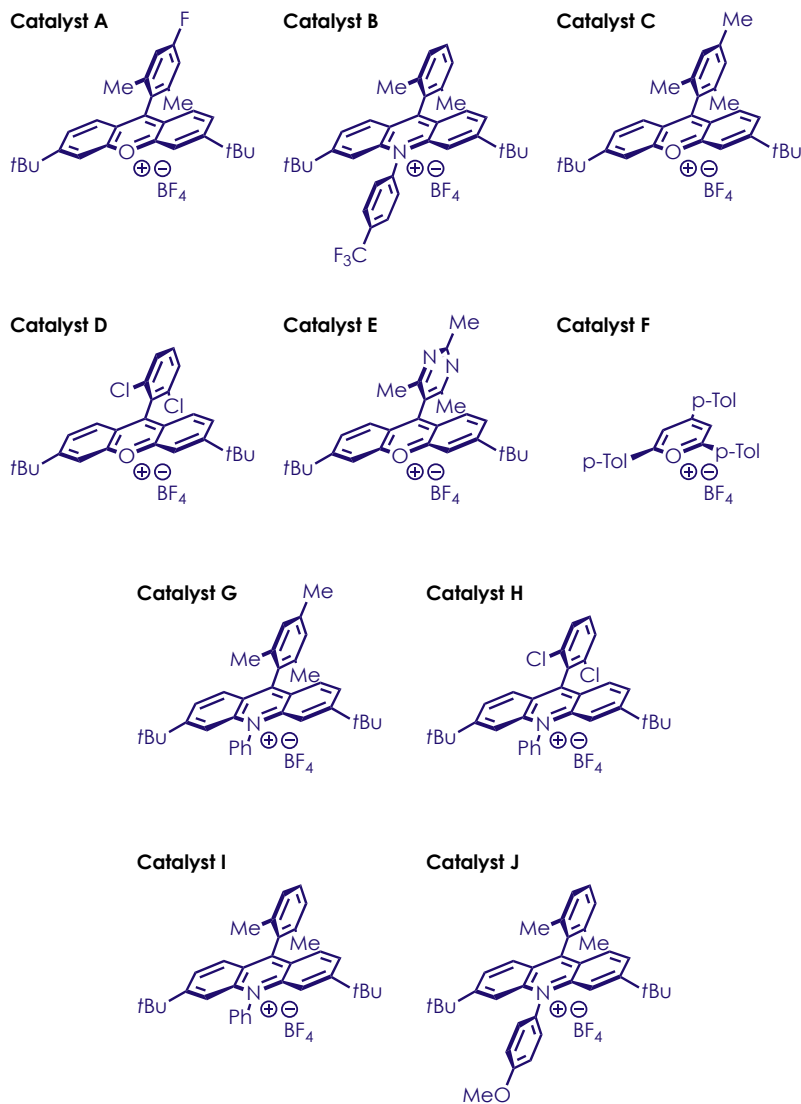
Table 4-2. Reaction Optimization for Defluorination of 4-Fluorotoluene with Pyrazole



Entry	Deviations from above conditions	Yield ^a
1	None	55%
2	Catalyst C	<5%
3	Catalyst D	35%
4	Catalyst E	9%
5	Catalyst F	37%
6	0.01 equiv. Catalyst A	48%
7	0.02 equiv. Catalyst A	54%
8	0.075 equiv. Catalyst A	80%
9	DCM	4%
10	DCE	5%
11	MeCN	10%
12	HFIP	67%
13	TFE:HFIP (1:1)	72%
14	TFE (0.075 M)	65%
15	TFE (0.150 M)	63%
16	3 equiv. pyrazole	68%
17	2.5 equiv. pyrazole	48%
18	2 equiv. pyrazole	47%
19	1 equiv. pyrazole	45%
20	456 nm Kessil lamps	63%
21	427 nm Kessil lamps	62%
22	427 nm Kessil lamps, foil barrier	82%
23	No Catalyst A	0%
24	Catalyst G ($E^*_{1/2}{}^{\text{red}} = + 2.10 \text{ V vs. SCE}$)	0%
25	Catalyst H ($E^*_{1/2}{}^{\text{red}} = + 2.21 \text{ V vs. SCE}$)	8%
26	No bLEDs	0%

^aYield determined by ¹H NMR using HMDSO as an internal standard

Figure 4-3. Photoredox Catalyst Key for Table 4-2

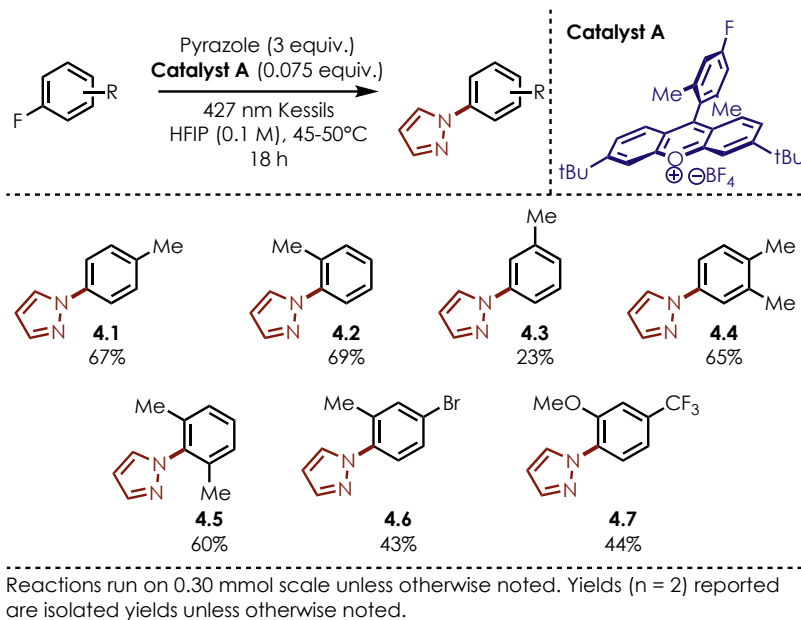


As technology improves and numerous options become available, the light source for photochemical transformation has become another reaction component that warrants serious investigation. As such, we investigated the use of Kessil brand blue LEDs in a variety of wavelengths (**Table 4-2**, entries 20-21). We discovered that this reaction did not appear to be particularly sensitive to the wavelength of light employed, but rather, the reaction setup in

relation to the LEDs. Preliminary results were obtained using two 455 nm Par38 Royal Blue Aquarium LED lamps. As shown in entry 22, when the reaction was irradiated with a singular 427 nm Kessil LED with a foil barrier on the other side (see Appendix C for photos of reaction setup), the reaction yield was improved modestly. This is likely due to the increased photon flux, as well as the thermal activation (ca. 45 – 50 °C) provided by the Kessil LEDs. An additional benefit to this is that a greater number of reactions could be run concurrently, which increases the efficiency of exploring a substrate scope. Entries 23-26 in **Table 4-2** serve as control experiments to show that in the absence of light or **Catalyst A**, no reactivity was observed. Additionally, in the presence of catalyst with an $E_{1/2\text{red}}^* < 2.5 \text{ V}$ vs. SCE, almost no reactivity was observed, which supports the unfavorable nature of the endergonic ET.

Satisfied with the yield of the desired product, we set out to identify a scope of fluoroarenes that displayed the desired reactivity when pyrazole was used as a nucleophile.

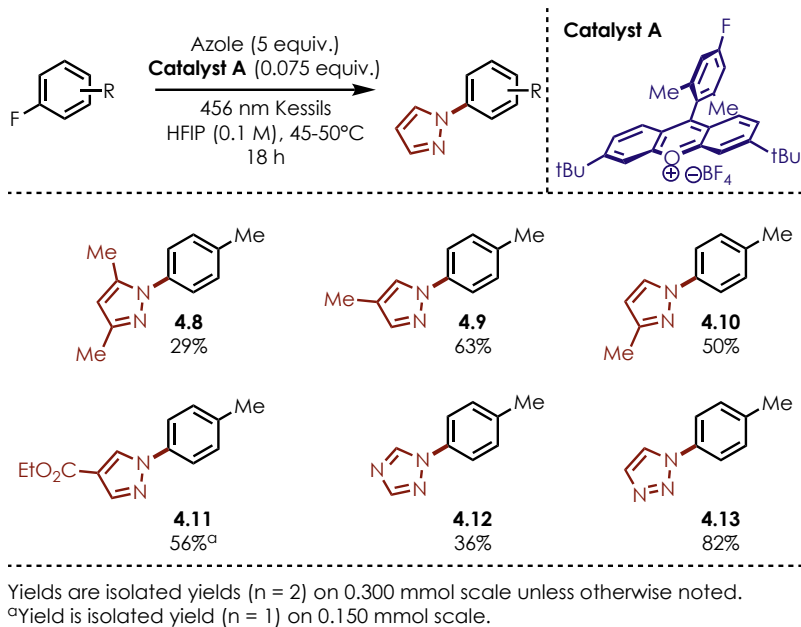
Scheme 4-12. Fluoroarene Scope for Nucleophilic Defluorination with Pyrazole



As shown in **Scheme 4-12**, a variety of fluoroarenes were tolerated in this transformation. Mono- and di-methylated fluoroarenes, **4.1-4.5**, were synthesized in yields ranging from poor to moderate. Halogenated fluoroarenes (**4.6**) were tolerated in this transformation, which is particularly exciting, as this offers a functional handle for further downstream modification. Additionally, **4.7** was obtained in moderate yields and a single product was obtained. This substrate was of particular concern for us, as previous work from the lab^{155,156} has shown the utility of methoxy substituents as capable nucleofuges. To our delight, no C-O substitution was observed for this substrate, and this effect will be discussed later in section 4.2.5.

In addition to investigating fluoroarene substrates, we were also interested in determining a scope of azole nucleophiles. By simply increasing the amount of nucleophile used in the reaction, we were able to observe defluoroamination with a variety of azoles (**Scheme 4-13**).

Scheme 4-13. Scope of Azoles Compatible with Defluorination Conditions



Mono- and di-methylated pyrazoles (**4.8-4.10**) were effective nucleophiles with yields of desired products formed in poor to moderate yields. Additionally, we were excited by the success of 4-methylpyrazole as a nucleophile, as this azole is used as a treatment for methanol and ethylene glycol poisoning.¹⁵⁹ The success of ethyl-4-pyrazole carboxylate (**4.11**) is also of note, as the pyrazole moiety is a precursor to several pesticides and antivirals.^{160,161} Triazoles were also competent nucleophiles with desired products formed in poor to excellent yields (**4.12-4.13**). Unfortunately, more complex nucleophiles, such as benzimidazole, indazole, and adenine, were unsuccessful in the transformation. However, the various biological activities possessed by aryl-substituted pyrazoles makes this nucleophilic defluorination method an attractive option for the facile preparation of this valuable motif.¹⁶²

4.2.2 Intramolecular Defluorination of Electron-Neutral Fluoroarenes Using Carboxylic Acids as Nucleophiles

Interested in exploring the use of other nucleophiles beyond azoles, we began our efforts towards a defluorooxygenation transformation by investigating the use of benzoic acid as a nucleophile and 4-fluorotoluene as a model substrate. As shown in entry 1 of **Table 4-3**, the use of NaHCO₃ as a base and a 1:1 mixture of TFE and HFIP as the solvent system resulted in just 10% yield of the desired product. Thinking that perhaps inefficient deprotonation of the nucleophile was hindering product formation, we investigated the amount of base used in the reaction (entries 2-7) and discovered that the amount of base used in the reaction did not improve the yields of desired product. We then investigated the identity of base used in the reaction to determine if a different base would improve the outcome of the reaction. As shown in entries 8-12, several inorganic bases and an organic base were examined, but no improvements to the yield of the desired product were observed.

Table 4-3. Optimization for Defluorooxygenation of 4-Fluorotoluene

Catalyst A (0.05 equiv.)
Benzoic acid (4.0 equiv.)
NaHCO₃ (2.0 equiv.)

TFE:HFIP (1:1) (0.1 M),
bLEDs, 18 h

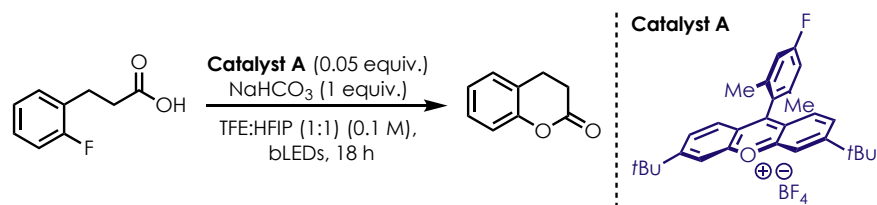
Entry	Deviations from above conditions	Yield ^a
1	None	10%
2	No NaHCO ₃	0%
3	1.0 equiv. NaHCO ₃	15%
4	3.0 equiv. NaHCO ₃	<10%
5	5.0 equiv. NaHCO ₃	<10%
6	10.0 equiv. NaHCO ₃	<10%
7	20.0 equiv. NaHCO ₃	<10%
8	Na ₂ CO ₃ instead of NaHCO ₃	<10%
9	K ₂ CO ₃ instead of NaHCO ₃	11%
10	Cs ₂ CO ₃ instead of NaHCO ₃	<10%
11	1,1,3,3-tetramethylguanidine	<10%
12	No NaHCO ₃ , TFE:HFIP:NaHCO ₃ (aq) (1:1:1)	<10%
13	1.0 equiv. benzoic acid	<10%
14	1.5 equiv. benzoic acid	<10%
15	2.0 equiv. benzoic acid	11%
16	3.0 equiv. benzoic acid	<10%
17	Sodium benzoate instead of benzoic acid	<10%
18	Potassium benzoate instead of benzoic acid	<10%
19	Lithium benzoate instead of benzoic acid	<10%
20	Ammonium benzoate instead of benzoic acid	<10%
21	Cesium benzoate instead of benzoic acid	<10%
22	Piperidinium benzoate instead of benzoic acid	<10%
23	Tetramethylpiperidinium benzoate instead of benzoic acid	0%
24	Tetrabutylammonium benzoate instead of benzoic acid	<10%

^aYield determined by ¹H NMR using HMDSO as an internal standard

We were concerned with the stability of the xanthylium catalyst when exposed to acidic conditions, so we investigated the amount of benzoic acid that was used as a nucleophile. As entries 13-16 show, even lowering the amount of benzoic acid used to just 1.0 equivalent was not able to improve the amount of desired product that was formed. A variety of benzoate

salts were used as nucleophiles (entries 17-24); however, none of the salts used were able to improve the yield of desired product. Due to the sensitivity of the xanthylium catalysts to strongly acidic or basic conditions, the use of benzoic acid as a nucleophile did not appear to be feasible. Additionally, benzoate salts, possess ground state oxidation potentials that are within the oxidizing abilities of the xanthylium catalyst (e.g. TBA benzoate: $E_{p/2} = +1.46$ V vs. SCE), which means that unproductive SET may be occurring.

In an effort to encourage the desired reactivity, we chose to explore an intramolecular defluorination transformation. We hoped that the proximity of the carboxylic acid nucleophile and fluoride nucleofuge would encourage nucleophilic defluorination. Additionally, while a CV was not obtained for the intramolecular model substrate, we believed that an alkyl carboxylic acid would be far less prone to unproductive SET events with the xanthylium catalyst.

Table 4-4. Reaction Optimization for Intramolecular Defluorination

Entry	Deviations from above conditions	Yield ^a
1	None	49%
2	2 equiv. NaHCO ₃	35%
3	Na ₂ CO ₃	<10%
4	K ₂ CO ₃	20%
5	Cs ₂ CO ₃	17%
6	2,6-lutidine	45%
7	3,5-lutidine	16%
8	2,4,6-collidine	35%
9	KH ₂ PO ₄	23%
10	K ₂ HPO ₄	40%
11	K ₃ PO ₄	12%
12	TFE	<10%
13	0.075 equiv. Catalyst A	52%
14	No Catalyst A	0%
15	No bLEDs	0%

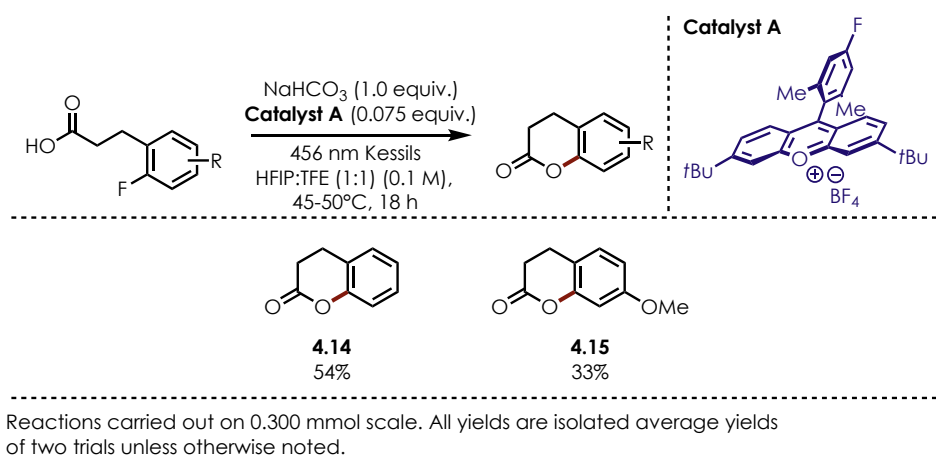
^aYield determined by ¹H NMR using HMDSO as an internal standard

We began our efforts to develop an intramolecular defluorination reaction by using 3-(2-fluorophenyl)propanoic acid as a model substrate and **Catalyst A** as the chosen photoredox catalyst. As shown in **Table 4-4**, 1.0 equivalent of NaHCO₃ afforded the optimal yield of desired product (entries 1 and 2). Additionally, a variety of organic and inorganic bases were evaluated in an attempt to identify the most efficient base for the deprotonation of the carboxylic acid nucleophile (entries 3-11), but NaHCO₃ proved to be the most effective. We found that a (1:1) mixture of TFE:HFIP was the most effective solvent for this transformation, as the exclusion of one of the components led to severely diminished yields. As we were still employing a carboxylic acid nucleophile and the reaction contained

stoichiometric amounts of NaHCO₃, we found that increasing the amount of **Catalyst A** used in the reaction increased the yield of desired product by a small amount, presumably by ensuring that active catalyst still remained after some degree of catalyst degradation (entry 13). The necessary control experiments were also performed, and no product formation was observed in the absence of **Catalyst A** or light.

Due to time constraints as a result of COVID-19, only a small substrate scope was evaluated for this transformation (**Scheme 4-14**).

Scheme 4-14. Substrate Scope for Intramolecular Defluorination Reaction



We found that scaleup and isolation of **4.14** was efficient with an average yield of 54%. We were also able to demonstrate that **4.15** could also be prepared, although the yield was somewhat diminished. Although limited in scope at this point in time, we believe that this is an efficient method for the construction of 3,4-dihydrocoumarin derivatives.

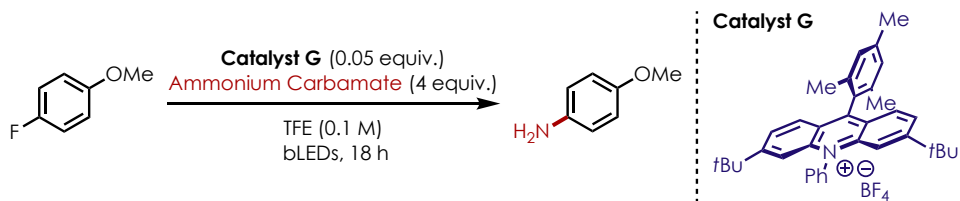
4.2.3 Defluorination of Electron-Rich Fluoroarenes Using Nitrogenous Nucleophiles

As the use of electron-rich fluoroarenes as substrates remains a challenge in the field of S_NAr chemistry, we were curious as to whether our defluorination conditions could be extended to these compounds. However, there were several obstacles to address during the development of this transformation. Our lab has previously disclosed reports of cation radical-accelerated S_NAr reactions using nitrogenous heterocycles and cyanide as nucleophiles.^{155,156} In both of these methods, methoxy-substituents serve as nucleofuges, which posed a selectivity problem for our proposed transformation. In order to develop a defluoroamination method of electron-rich fluoroarenes, identifying conditions for selective C-F bond functionalization was essential. We elected to attempt a nucleophilic defluorination reaction in the presence of methoxy-substituents to establish a baseline for selectivity between the two potential nucleofuges. Another challenge is the incompatibility of primary amine nucleophiles and xanthylium salts. Acridinium salts were chosen as catalysts for this proposed transformation, as their excited states are sufficiently potent to oxidize electron-rich fluoroarenes.

Development of the defluoroamination method was carried out by Vincent Pistrutto. The construction of anilines using ammonium carbamate as a nucleophile was studied initially, as our lab has had great success using this compound as an ammonia source.^{42,155} Using 4-fluoroanisole as a model substrate **Catalyst G**, we investigated the selectivity of the transformation when two potential nucleofuges were present in the substrate. As shown in entry 1 of **Table 4-5**, when TFE was used as the reaction solvent, very little desired product was formed. This is likely due to ammonium carbamate's solubility in TFE, which results in rapid release of ammonia and hinders product formation. Considering how to resolve this

issue, a mixture of TFE and DCE was employed as the solvent system for the transformation, as ammonium carbamate is only sparingly soluble in DCE. The reduced solubility would hopefully allow for a controlled release of ammonia and an increase in the amount of desired product formed. As entries 2-5 of **Table 4-5** show, decreasing the amount of TFE used in the solvent mixture dramatically improved the amount of desired product that was formed. Additionally, we were pleased to observe complete selectivity for C-F bond functionalization.

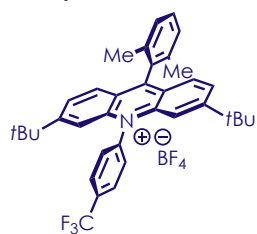
Table 4-5. Reaction Optimization for Defluorination with Ammonium Carbamate



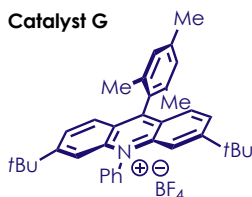
Entry	Deviations from above conditions	Yield ^a
1	None	<5%
2	TFE:DCE (2:1)	29%
3	TFE:DCE (1:1)	48%
4	TFE:DCE (1:2)	64%
5	TFE:DCE (1:3)	74%
6	1 equiv. ammonium carbamate; TFE:DCE (1:3)	18%
7	2 equiv. ammonium carbamate; TFE:DCE (1:3)	50%
8	3 equiv. ammonium carbamate; TFE:DCE (1:3)	54%
9	5 equiv. ammonium carbamate; TFE:DCE (1:3)	72%
10	0.03 equiv Catalyst G; TFE:DCE (1:3)	57%
11	0.05 equiv Catalyst B; TFE:DCE (1:3)	72%
12	0.05 equiv Catalyst H; TFE:DCE (1:3)	48%
13	0.05 equiv Catalyst I; TFE:DCE (1:3)	55%
14	0.05 equiv Catalyst J; TFE:DCE (1:3)	43%

^aYield determined by ¹H NMR using HMDSO as an internal standard

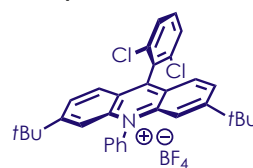
Catalyst B



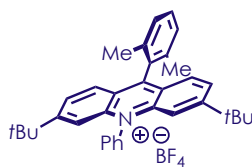
Catalyst G



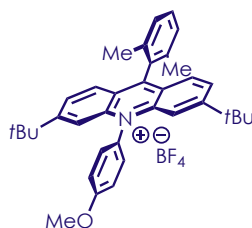
Catalyst H



Catalyst I



Catalyst J



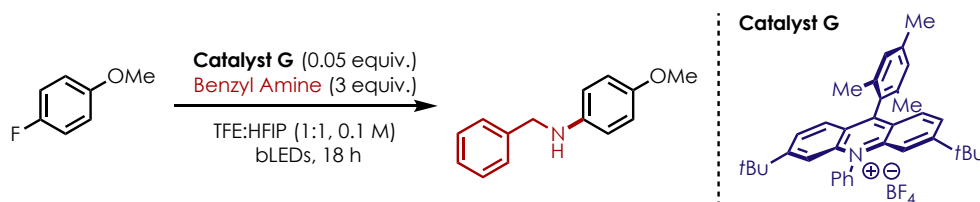
The origin of the selectivity will be discussed in greater detail later in section 4.2.5.

Decreasing the amount of ammonium carbamate used in the reaction (**Table 4-5**, entries 6-9) had deleterious effects the yield of desired product, as did reducing the amount of **Catalyst G** (**Table 4-5**, entry 10). Interested in probing the effects of various acridinium salts on the outcome of the transformation, a range of catalysts were investigated. The use of **Catalyst B** resulted in comparable amounts of desired product formation (**Table 4-5**, entry 11), while **Catalysts H, I, and J** all had deleterious effects on the reaction yield. While **Catalysts B and G** resulted in similar yields of the desired product, **Catalyst B** was ultimately chosen as the optimal catalyst for this transformation, and this will be discussed later.

Concurrently, conditions for the defluoroamination of 4-fluoroanisole using a primary amine nucleophile, benzyl amine, were explored. Using conditions similar to the ones explored above, the desired defluorinated product was observed in moderate yields. However, as shown in entry 2 of **Table 4-6**, reducing the amount of benzyl amine used in the reaction had deleterious effects on the amount of desired product that was formed. As solvent identity proved to be relatively important for the defluorination transformation, several solvent systems were explored (**Table 4-6**, entries 3-5), and both TFE and DCE were competent solvents for this transformation. We elected to pursue the use of TFE as a solvent to maintain continuity between the transformations studied. Another catalyst identity was shown to be an important component that had profound impacts on the outcome of the reaction, we surveyed a variety of acridinium salts that had proven successful in previously discussed studies. **Catalyst B** (**Table 4-6**, entry 6) facilitated the desired transformation in excellent yields, and this may be due to the length of the excited state lifetime of the catalyst.

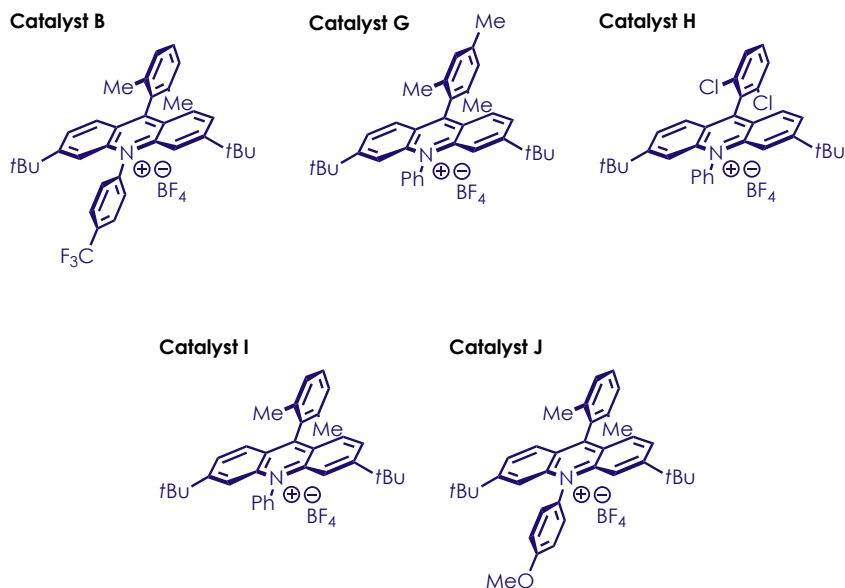
As such, **Catalyst B** was chosen as the optimal catalyst for the defluoroamination of electron-rich fluoroarenes.

Table 4-6. Reaction Optimization for Defluorination with Benzyl Amine



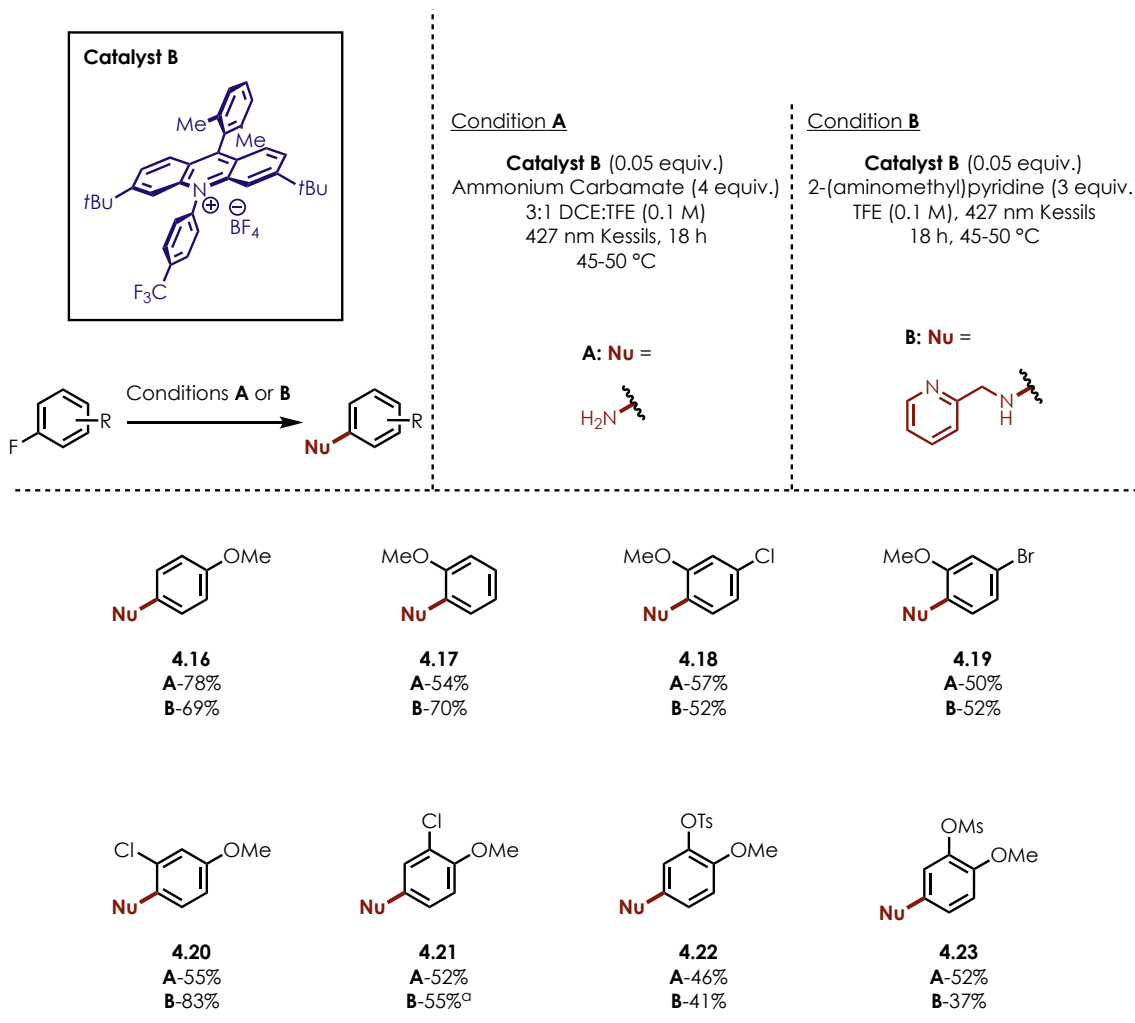
Entry	Deviations from above conditions	Yield ^a
1	None	41%
2	2 equiv. benzyl amine	25%
3	TFE	60%
4	HFIP	11%
5	DCE	59%
6	Catalyst B ; TFE	88% (79%) ^b
7	Catalyst H ; TFE	41%
8	Catalyst I ; TFE	67%
9	Catalyst J ; TFE	45%

^aYield determined by ¹H NMR using HMDSO as an internal standard. ^b Isolated yield.



Satisfied with the yields of defluoroaminated products, we set out to evaluate a substrate scope using both ammonium carbamate and benzyl amine as nucleophiles.

Scheme 4-15. Fluoroanisole Derivatives Compatible with Defluoroamination



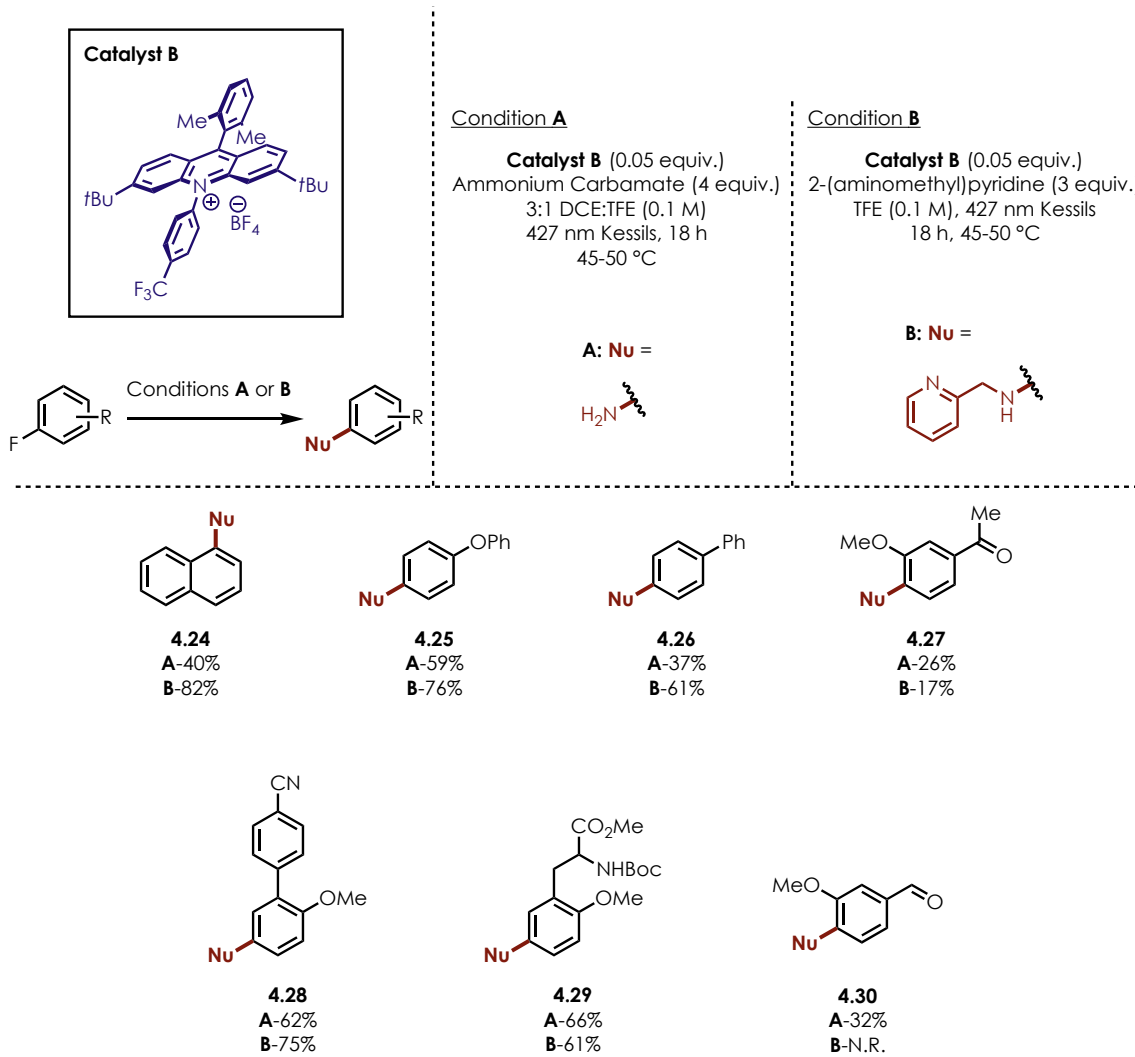
Yields reported are isolated yields (n = 2) on 0.300 mmol scale unless otherwise noted. ^a11% C-O product observed.

Due to purification challenges, 2-picolylamine was employed as a nucleophile, which rendered isolation of the desired products much easier. We were pleased to find that fluoroanisole regioisomers (**4.16-4.17**) were competent substrates in this transformation with both desired products formed in moderate to good yields (**Scheme 4-15**). Halogenated fluoroanisole derivatives were also tolerated in the reaction with no C-X bond functionalization occurring. Yields for these products were moderate with both nucleophiles,

except for **4.20B**, which was formed in excellent yields. As noted, compound **4.21B** was the sole substrate for which a small amount of C-O functionalization occurred, and the reason for this reactivity will be discussed later. Additionally, fluoroanisole derivatives with pseudohalide substituents were also competent substrates in the reaction with **4.22** and **4.23** formed in moderate yields. The presence of halide and pseudohalide substituents and lack of C-X functionalization is exciting, as these groups serve as functional handles for further structural modifications at a later stage.

In addition to fluoroanisole derivatives, a variety of fluoroarenes with extended conjugation and sensitive functional groups were tolerated in the reaction (**Scheme 4-16**).

Scheme 4-16. Scope of Fluoroarenes Compatible with Defluoroamination

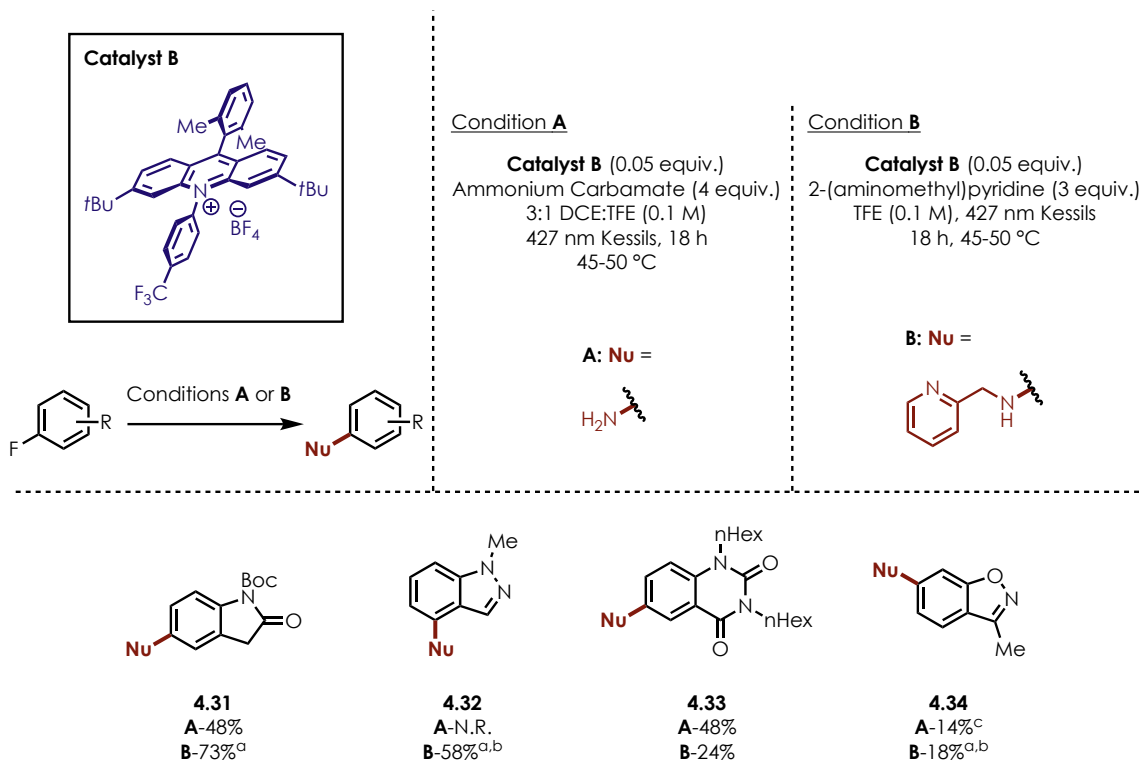


Yields reported are isolated yields (n = 2) on 0.300 mmol scale unless otherwise noted.

Yields ranged from poor to good for compounds **4.24-4.26**. An acetophenone derivative was also tolerated in the reaction conditions, but the yields were quite poor for both nucleophiles. Substrates with relevance towards liquid crystals (**4.28**) and biological applications (**4.29**) were competent substrates in the transformation, and the desired products were formed in good yields with both nucleophiles. Compound **4.30** was incompatible with 2-picolylamine

as a nucleophile, but formation of the aniline product (**4.30A**) was observed, albeit in poor yields.

Scheme 4-17. Heterofluoroarene Scope Compatible with Defluoroamination Conditions



Yields reported are isolated yields ($n = 2$) on 0.300 mmol scale unless otherwise noted. ^a3.0 equiv. benzyl amine used as the nucleophile. ^bIsolated yield ($n = 1$) on a 0.150 mmol scale. ^cYield determined by ¹H NMR using HMDSO as an internal standard.

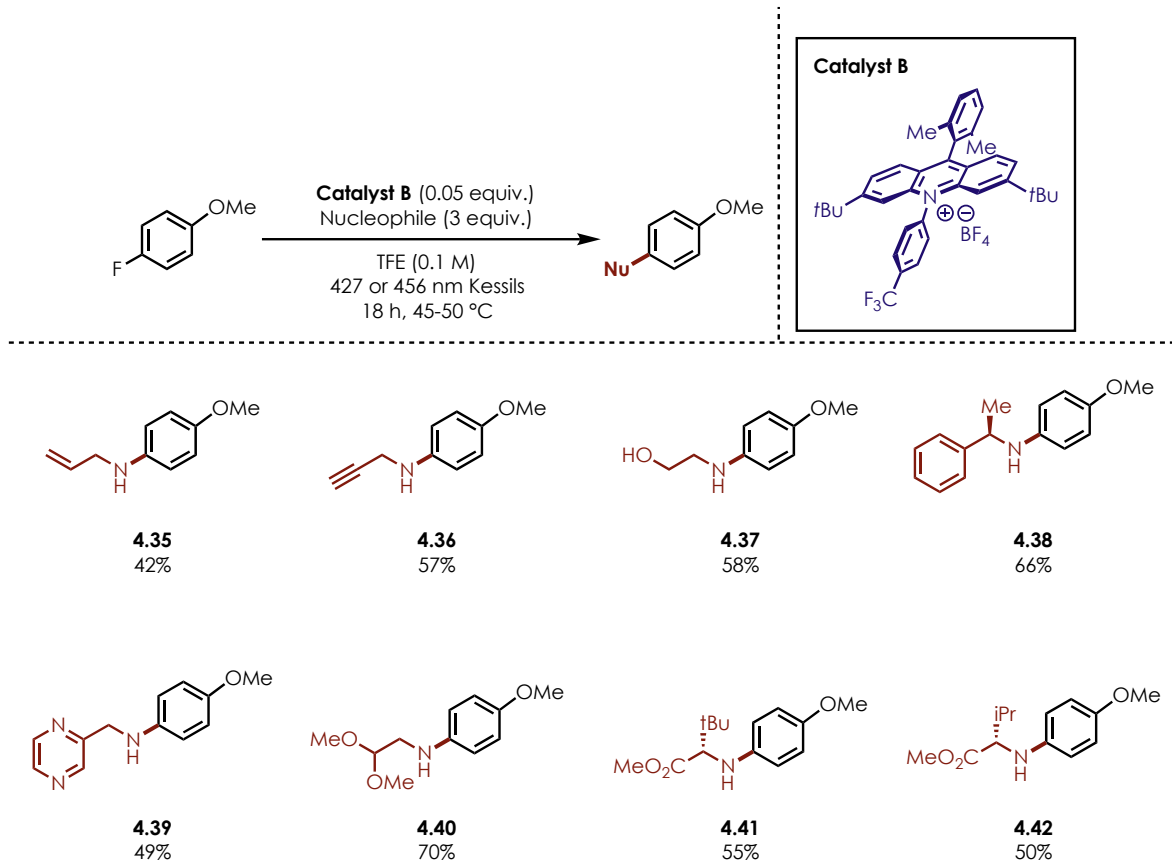
Fluorinated heterocycles were also evaluated as substrates for this defluoroamination transformation (**Scheme 4-17**). Due to the industrial importance of heterocycles, we were particularly interested in utilizing compounds like this in our methodology. Compound **4.31** was a competent substrate for this transformation with **4.31B** formed in good yields. **4.32** and **4.33** were successful substrates, although yields were diminished for all desired products, and no desired product was obtained in the case of **4.32A**. We were particularly excited by the success of **4.34**, as this compound maps on to the structures of a family of antipsychotics,

including risperidone and iloperidone, which suggests that this method may be useful in the preparation of new derivatives.¹⁶³

The use of primary amine nucleophiles results in some limitations in regard to substrate compatibility. As discussed earlier, aldehydes are not tolerated in substrates, and neither is benzylic functionality. Due to the increased acidity of benzylic protons upon arene oxidation, deprotonation can occur instead of nucleophilic addition.¹⁶⁴ Additionally, it is worth noting that the products of the defluorination transformation are likely able to be oxidized by the excited state catalyst, and so product inhibition may be the cause of some of the diminished yields that were obtained.

In addition to exploring a scope of fluoro(hetero)arenes, we were also interested in identifying a small scope of primary amines that were able to act as nucleophiles in this transformation (**Scheme 4-18**).

Scheme 4-18. Amine Nucleophile Scope for Defluoroamination Reaction



Yields are isolated yields (n = 2) on 0.300 mmol scale unless otherwise noted.

Primary amines with various functionality were capable nucleophiles in this transformation (**4.35-4.37** and **4.39-4.40**), and the desired products were formed in moderate yields.

Impressively, **4.37** was formed as the sole product of the reaction; no evidence of the alcohol acting as a nucleophile was observed. No racemization of enantiomerically pure compounds **4.38** and **4.41-4.42** was observed during the defluoroamination reaction, which is particularly noteworthy. The desired products were formed as single enantiomers in moderate yields.

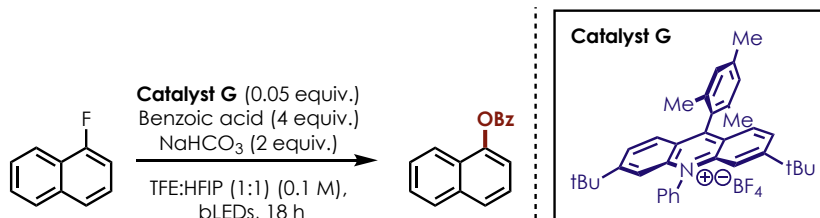
4.2.4 Defluorination of Electron-Rich Fluoroarenes Using Carboxylic Acids as Nucleophiles

As nitrogenous nucleophiles were used so successfully in the previously discussed defluoroamination reaction, we were interested in whether a similar defluoroxygenation method could be developed. As carboxylic acid nucleophiles were not compatible with the xanthylium catalysts, we felt that a more appropriate system for their use would involve the use of an acridinium salt, which are less sensitive to the pH of reaction conditions. A model substrate, 1-fluoronaphthalene, was chosen for initial defluoroxygenation investigations, as it is oxidizable by acridinium salts. By using our standard acridinium catalyst, **Catalyst G**, we were able to observe formation of the desired product in a 34% yield (**Table 4-7**, entry 1). However, the ^1H NMR spectrum of the crude reaction mixture revealed the presence of returned starting material, as well as other unidentifiable peaks.

Table 4-7. Identification of Optimal Base for Defluorination with Benzoic Acid

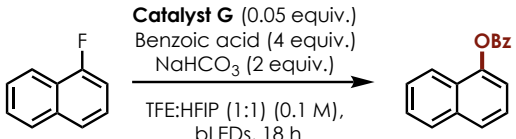
Entry	Deviations from above conditions	Yield ^a
1	None	34%
2	2,6-lutidine	22%
3	3,5-lutidine	<10%
4	2,4,6-collidine	14%
5	KH_2PO_4	<10%
6	K_2HPO_4	<10%
7	K_3PO_4	<10%

^aYield determined by ^1H NMR using HMDSO as an internal standard



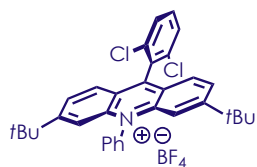
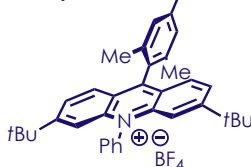
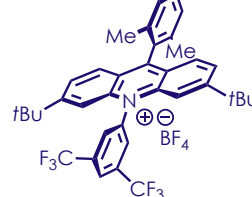
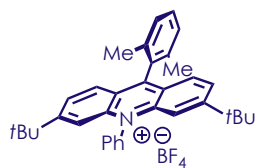
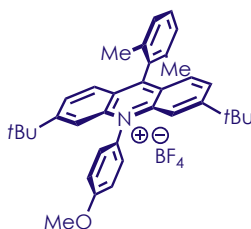
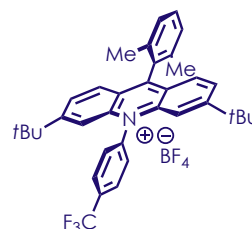
Encouraged by this success, we sought to improve the yield of desired product by investigating whether a different base would more efficiently deprotonate the nucleophile. However, as shown in entries 2-7, only deleterious effects were observed upon screening alternate bases. Thinking that perhaps the deprotonation of the nucleophile was not preventing formation of the desired product, we chose to investigate the acridinium catalyst used in the reaction (**Table 4-8**). We chose a variety of acridinium salts with potent oxidizing abilities and varying excited state lifetimes to investigate. As shown in entries 3, 4, and 7, several catalysts gave comparable or improved results when compared with our parent acridinium species. However, we were interested in improving the transformation further, and due to the complicated ^1H NMR spectra, we chose to modify our model substrate to make analysis more facile.

Table 4-8. Identification of Optimal Catalyst for Defluorooxygenation



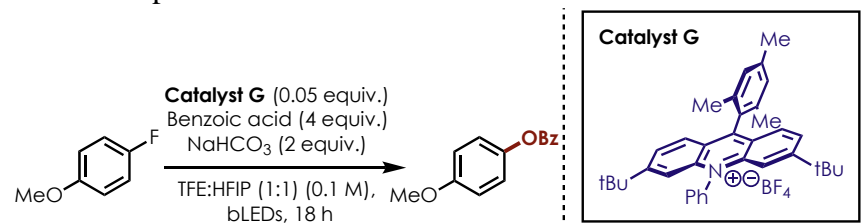
Entry	Deviations from above conditions	Yield ^a
1	None	34%
2	Catalyst H	16%
3	Catalyst K	41%
4	Catalyst L	44%
5	Catalyst I	29%
6	Catalyst J	26%
7	Catalyst B	31%

^aYields determined by ¹H NMR using HMDSO as an internal standard.

Catalyst H**Catalyst K****Catalyst L****Catalyst I****Catalyst J****Catalyst B**

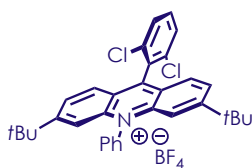
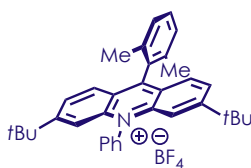
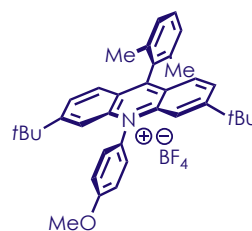
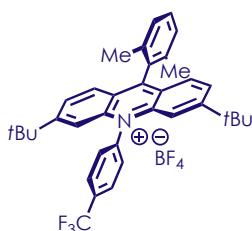
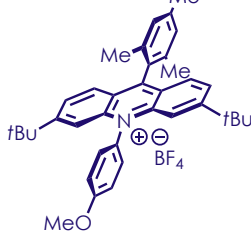
We opted to explore the use of 4-fluoroanisole as a model substrate, as analysis of crude reaction mixtures by ¹H NMR was anticipated to be more straightforward. We began by exploring the effect of different acridinium catalysts in the system, as data from **Table 4-9** indicated that catalyst identity could significantly impact the yield of the reaction. Entry 1 in **Table 4-9** shows that simply using 4-fluoroanisole as the substrate with previously identified conditions resulted in very little product formation. However, upon using **Catalyst B** in the

reaction (**Table 4-9**, entry 5), 46% of the desired product could be obtained. The increase in the yield of desired product upon switching to **Catalyst B** may be attributed to its longer excited state lifetime or to its highly potent oxidizing ability. We next chose to investigate the effects of using fluorinated alcoholic solvents independently and were pleased to observe the formation of the desired product in a 66% yield when TFE was used as the solvent (**Table 4-9**, entry 7).

Table 4-9. Reaction Optimization with 4-Fluoroanisole as the Model Substrate

Entry	Deviations from above conditions	Yield ^a
1	None	<10%
2	Catalyst H	<10%
3	Catalyst I	15%
4	Catalyst J	16%
5	Catalyst B	46%
6	Catalyst M	26%
7	TFE (0.1 M)	66%
8	HFIP (0.1 M)	<10%

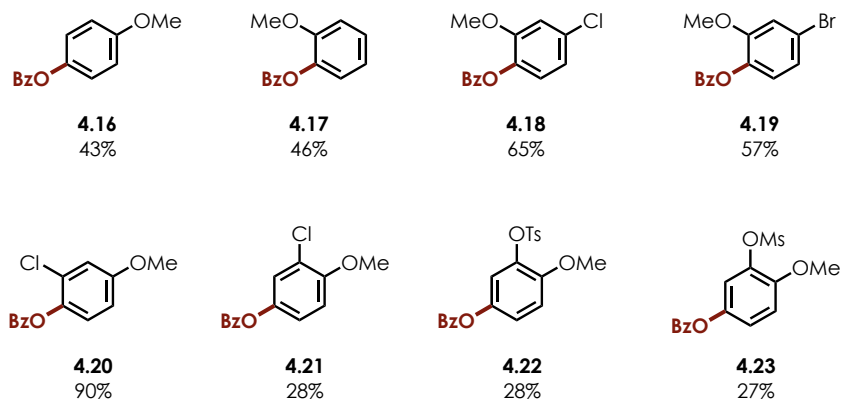
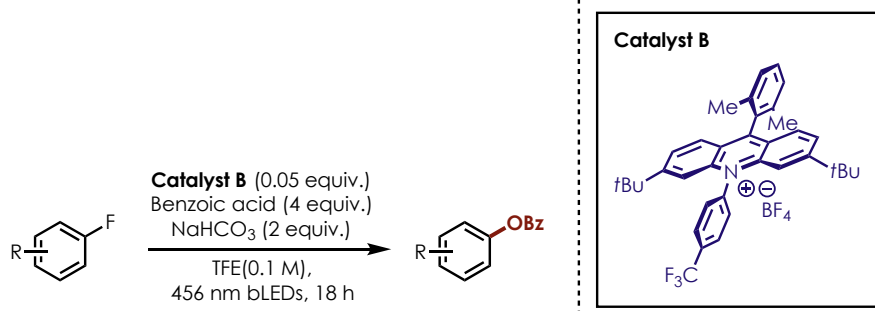
^aYields determined by ¹H NMR using HMDSO as an internal standard.

Catalyst H**Catalyst I****Catalyst J****Catalyst B****Catalyst M**

Satisfied with the conditions, we next began to explore a substrate scope in order to determine how general these defluoroxygenation conditions were. As shown in **Scheme 4-19**, fluoroanisole regioisomers were competent substrates in the reaction with modest yields of the desired products, **4.16C** and **4.17C**, formed. Fluoroanisole derivatives with halogen substituents were well tolerated in the reaction, with yields ranging from poor to excellent (**4.18C-4.21C**). Additionally, fluoroanisole derivatives with pseudohalide substituents were

also competent substrates in the reaction; although, the yields of defluorooxygenated products, **4.22C** and **4.23C** were quite poor. Overall, the reaction conditions seemed to be reasonably general when fluoroanisole derivatives were employed as reaction substrates.

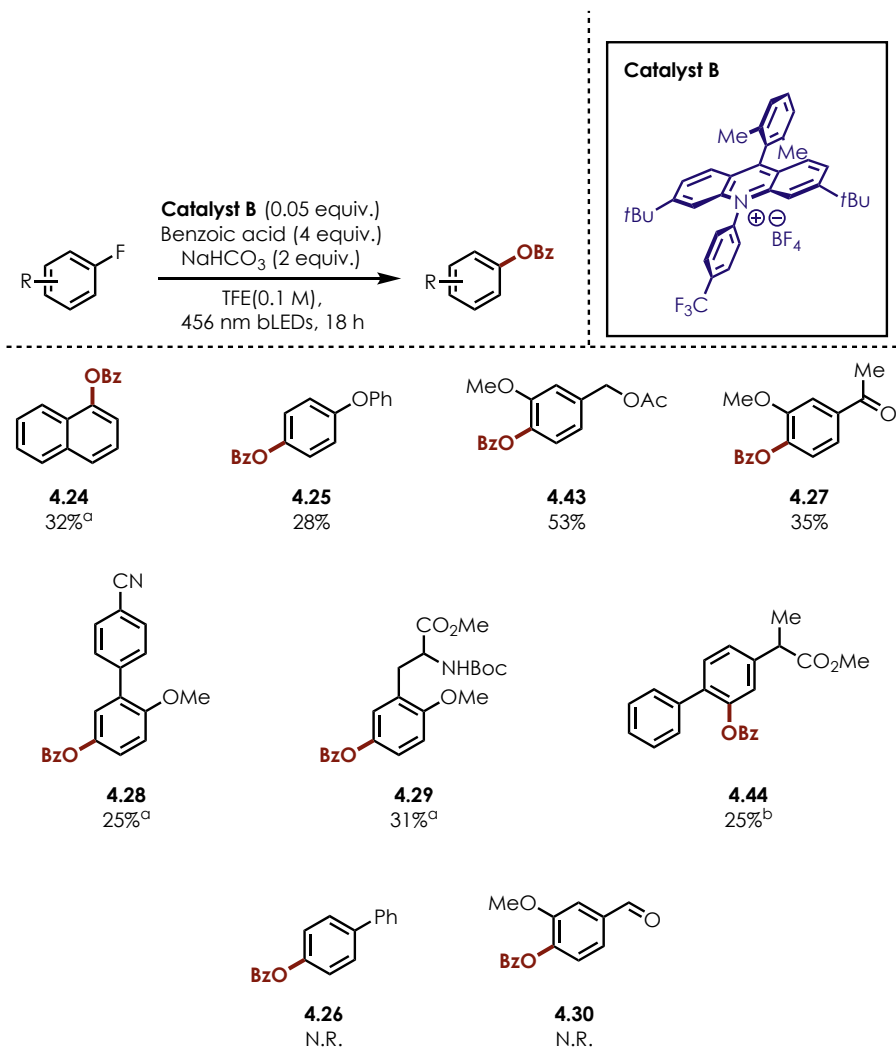
Scheme 4-19. Fluoroanisole Derivatives Compatible with Defluorooxygenation



Reactions run on 0.3 mmol scale unless otherwise noted.
Yields are isolated yields ($n = 2$).

We next chose to investigate fluoroarenes with more sensitive functional groups and fluoroarenes without strongly donating substituents, such as methoxy groups. As shown in **Scheme 4-20**, we had limited success with these substrates. Compounds **4.24C**, **4.28C**, **4.29C**, and **4.44C** all required higher loadings of **Catalyst B** to achieve yields over 20%. Despite this, the reaction conditions were tolerant of many sensitive functional groups, such as benzylic alcohols (**4.43C**), ketones (**4.27C**), and esters (**4.29C** and **4.44C**). Additionally, several of these substrates have applications in the realms of liquid crystals (**4.28C**) and biology (**4.29C**), which illustrates this method's utility as a means to rapidly derivatize molecules with important properties. We were particularly excited to observe the formation of compound **4.44C**, as it is a derivative of the pharmaceutical, flurbiprofen methyl ester. Several substrates, **4.26** and **4.30**, were completely unreactive and only unreacted starting material was observed. Although a biphenyl derivative, **4.44C**, was compatible with reaction conditions, biphenyl (**4.26**) was not a competent substrate in the defluorooxygenation reaction. This may be due to **4.26** being less electron-rich than **4.44**. **4.30** was also not compatible with reaction conditions, which is not unsurprising as most other nucleophiles did not display reactivity with this substrate either. In general, benzoic acid is considerably less reactive towards fluoroarenes than amine nucleophiles. This may be due to unproductive SET events occurring between the excited state acridinium catalyst and benzoate anion, as ET between the two species is favorable.

Scheme 4-20. Scope of Fluoroarenes Compatible with Defluoroxygenation Conditions

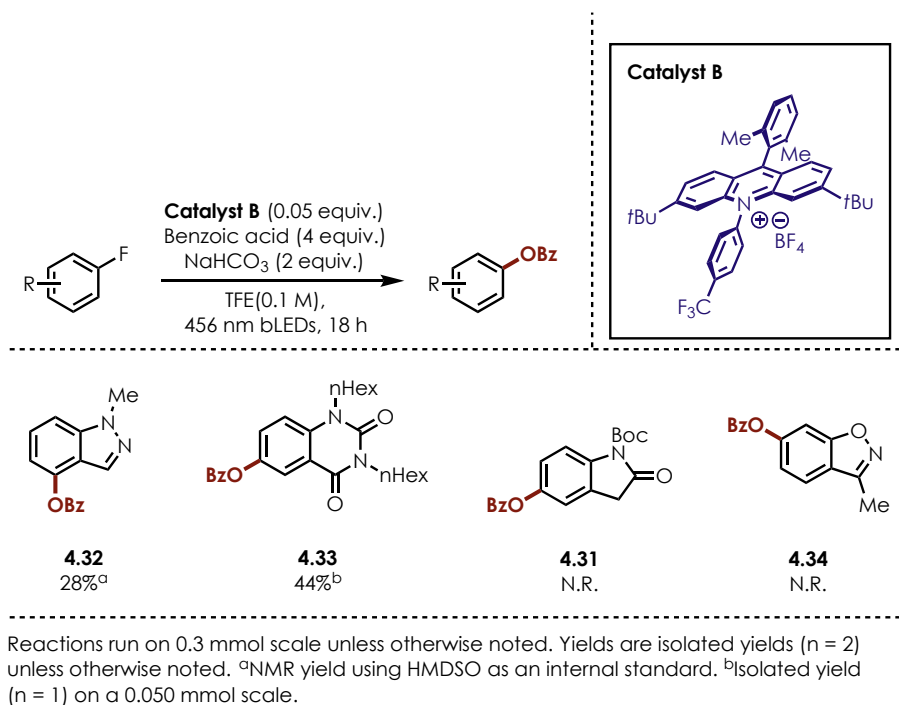


Reactions run on 0.3 mmol scale unless otherwise noted. Yields are isolated yields (n = 2).
^a0.1 equiv. **Catalyst B** used. ^b0.075 equiv. **Catalyst B** used.

The last class of substrates to be evaluated was fluoroheteroarenes, as heteroarenes are important scaffolds in both the pharmaceutical and agrochemical industries (**Scheme 4-21**). In an effort to showcase the utility of our nucleophilic defluorination method, we evaluated a variety of fluoroheteroarenes – many of which possessed relevance to the pharmaceutical or agrochemical industries. Unfortunately, limited success was had with

fluoroheteroarenes using benzoic acid as nucleophile. Compounds **4.32** and **4.33** were compatible with the reaction conditions and the desired products, **4.32C** and **4.33C**, were formed in moderate yields. However, use of **4.31** and **4.34** resulted in returned starting material, despite reactivity being observed with other nucleophiles.

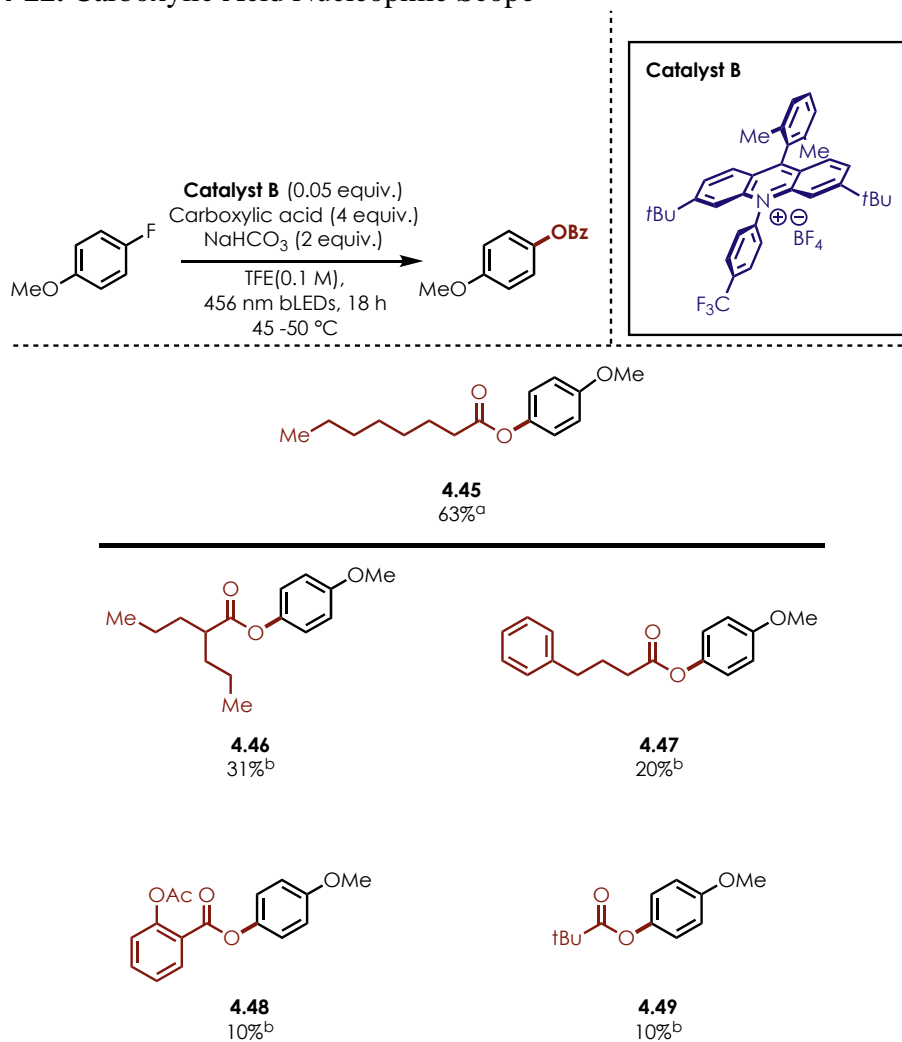
Scheme 4-21. Heterofluoroarenes Compatible with Defluorooxygenation



We were also interested in determining the scope of carboxylic acids that could be used as nucleophiles in this transformation (**Scheme 4-22**). A variety of alkyl and aryl carboxylic acids were investigated as nucleophiles, but we were met with limited success. Only octanoic acid proved to be an effective nucleophile with the desired product formed in a 63% yield (**4.45**). We studied pharmaceutically relevant carboxylic acids, such as aspirin (**4.48**) and valproic acid (**4.46**), as nucleophiles, but yields were quite poor. We were concerned that unproductive SET between the excited state acridinium catalyst and the

carboxylic acid, as well as decarboxylation, may be responsible for the low yields of desired product. Due to time constraints, no further optimization was carried out, and only **4.45** was reported as a successful example of defluorooxygenation using an alkyl carboxylic acid.

Scheme 4-22. Carboxylic Acid Nucleophile Scope



Reactions run on 0.3 mmol scale unless otherwise noted. Yields are isolated yields (n = 2) unless otherwise noted. ^aIsolated yield (n = 1) on a 0.150 mmol scale. ^bNMR yield using HMDSO as an internal standard.

Although detailed mechanistic studies have not been carried out for these nucleophilic defluorination transformations, we propose that these reactions proceed in an analogous manner to our previously disclosed CRA-S_NAr reactions.^{155,156}

4.2.5 Computational Studies

As discussed earlier, our lab has previously shown that nitrogenous heterocycles and cyanide nucleophiles are capable of undergoing *ipso* substitution at the position occupied by a methoxy-substituent on electron-rich arenes.^{155,156} As we hoped to identify conditions for the selective nucleophilic defluorination of electron-rich fluoroarenes, we were concerned about controlling the chemoselectivity to prevent substitution at sites bearing groups other than fluoride. We began by studying the addition of nitrogenous nucleophiles to arenes containing both fluoro- and methoxy-substituents in order to understand the product distribution, as none of the substrates reported previously contained both groups. We were surprised to discover that, in all but one case, the only products observed were the defluorinated products. There was one substrate that yielded a small amount of C-O substituted product, which will be discussed later.

Curious as to why such excellent chemoselectivity was observed, we turned to computations to explain this phenomenon. Based on previously published precedent from our group⁴³, we elected to use NPA to study the ground state fluoroarenes and their cation radical counterparts. Computational work was carried out by Vincent Pistritto, and experimental details are included in Appendix C, along with data for each substrate. Computations revealed that the site with the greatest degree of positive charge for both the ground state fluoroarenes and cation radicals could be found at the site bearing the fluoro-substituent

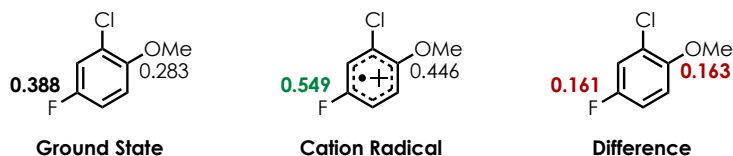
(**Figure 4-4**). The decreased electron density that is found at the position bearing the fluorine allows for efficient, chemoselective nucleophilic substitution with a variety of nucleophiles.

Figure 4-4. NPA Values for Ground State and Cation Radical of 4-Fluoroanisole



This work marks a divergence from the previously reported computational methods disclosed by our group.^{43,156,165} In the earlier work, the site of functionalization could be predicted by identifying the site with the largest change in NPA values upon oxidation. We hypothesize that this divergence is due to the superior nucleofugality of fluoride when compared to methoxy-substituents, as well as the less sterically encumbered environment at the site occupied by fluorine. As discussed previously, excellent chemoselectivity was observed in the scope of the transformation with only one exception where the C-O substitution product was observed in small quantities. **Figure 4-5** displays the computational data for **4.21B**, and it can be seen that the difference in NPA values is nearly identical, which may be responsible for the poor chemoselectivity.

Figure 4-5. NPA Values for 2-Chloro-4-Fluoroanisole



4.3 Conclusions

In conclusion, we were able to develop a highly selective method for the nucleophilic defluorination of electron-neutral and electron-rich (hetero)arenes. A variety of nucleophiles were competent in the transformation, including several with pharmaceutical relevance. We also utilized ground and excited state NPA values obtained from a computational study to explain the excellent chemoselectivity that was observed in this transformation. We believe this work provides a mild alternative to existing methods and could be of interest to the industrial communities for the rapid derivatization of important molecules.

4.4 Future Work

Moving forward, the method described in 4.2.2 could be elaborated to prepare a wider variety of 3,4-dihydrocoumarin derivatives. Additionally, other oxygen-containing nucleophiles could be identified that are compatible with both xanthylium and acridinium salts to expand the utility of this transformation with both electron-neutral and electron-rich fluoroarenes.

4.5 Acknowledgements

I gratefully acknowledge all of the work that Vincent Pistritto contributed to this project. His work on the defluoroamination chemistry and computational studies make up a large part of this study, and I appreciate all of his efforts.

APPENDIX A: EXPERIMENTAL DATA FOR CHAPTER 2

A.1 General Experimental Information

General Reagent Information

Commercially available reagents were purchased from Sigma Aldrich, TCI Corporation, Combi-Blocks, Matrix Scientific, Oakwood Chemical, and Fisher Scientific and were used without further purification. Fluorinated solvent (TFE) was purchased from Oakwood Chemical and was used as received unless otherwise noted.

General Analytical Information

Proton, carbon, and fluorine nuclear magnetic resonance spectra (^1H NMR and ^{13}C NMR) were obtained using a Bruker AVANCE III Nanobay 400 (^1H NMR at 400 MHz, ^{13}C NMR at 100 MHz) and Bruker AVANCE III 600 (^1H NMR at 600 MHz, ^{13}C NMR at 151 MHz) spectrometers. Unless otherwise noted, ^1H NMR and ^{13}C NMR spectra are referenced to Chloroform-d (^1H NMR: 7.26 ppm and ^{13}C NMR: 77.16 ppm). All spectra are reported as parts per million. ^1H , ^{13}C , and ^{19}F NMR data are reported as follows: chemical shift (ppm), multiplicity (s = singlet, d = doublet, t = triplet, q = quartet, quint = quintet, dd = doublet of doublets, td = triplet of doublets, ddd = doublet of doublet of doublets, m = multiplet, app = apparent), coupling constants (Hz), and integration.

Flash chromatography was performed using SiliaFlash P60 silica gel (40-63 μm) that was purchased from Silicycle.

Yield refers to the ^1H NMR yield as determined by the addition of HMDSO as an internal standard unless otherwise noted.

General Photoreactor Configuration

Reactions were irradiated using two Par38 Royal Blue Aquarium LED lamps (Model #6851) ($\lambda = 440\text{--}460$ nm) while stirring on stir plates purchased from IKA (various models). The reactions were placed approximately 3 cm away from the LEDs, and an external cooling fan was used to ensure that temperatures remained as close to 25–30 °C as possible. Reactions were optimized with four vials sharing irradiation from two LED lamps, and scaled up reactions for isolation were run with two vials sharing irradiation from two LED lamps.

General Reaction Procedure

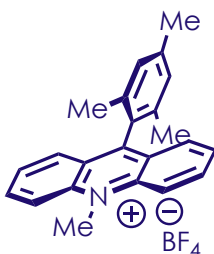
As conditions vary for each nucleophile employed, please see section A.3 for more detailed information on reaction setup.

A flame-dried 2-dram borosilicate vial (purchased from Fisher Scientific, catalogue # 03-339-22D), equipped with a stir bar, was charged with 3,6-Di-tert-butyl-9-mesityl-10-phenylacridin-10-ium tetrafluoroborate (0.05 eq., 0.05 mmol) and 2,5,6-triisopropylthiophenol (0.10 mmol, 0.20 eq.). For solid/non-volatile substrates, the substrate (0.10 mmol) was then added. Solvent was then added, and vials were capped tightly with a Teflon lined phenolic resin septum cap (purchased through VWR international, Microliter Product # 15-0060K). The reaction mixture was the sparged by bubbling with nitrogen or argon for 5 minutes. Liquid/volatile substrates/reagents were then added through the septum with a microliter syringe. Prior to irradiation, vials were sealed with Teflon tape and electrical tape to ensure maximal oxygen exclusion. The reaction vial was then placed into the LED setup and irradiated for 18 hours unless otherwise noted. Following irradiation, the reaction mixture was diluted with dichloromethane and filtered through a plug of silica. The silica plug was washed with ethyl acetate, and the sample was concentrated down. Samples

were then dissolved in ~1.0 mL of CDCl₃ and transferred to an NMR tube. Then 10 μL of HMDSO was added to the sample with a microliter syringe. Reaction yields were determined by ¹H NMR on a 0.10 mmol scale unless otherwise noted. Select compounds were isolated *via* column chromatography and conditions are reported individually.

A.2 Synthesis of Photoredox Catalysts and Substrates

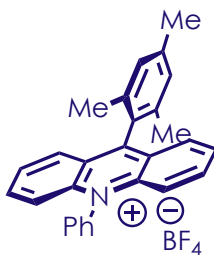
Catalyst A



9-mesityl-10-methylacridin-10-ium tetrafluoroborate (Catalyst A)

The title compound was synthesized according to literature procedures. Spectral data matches that reported in the literature.³⁵

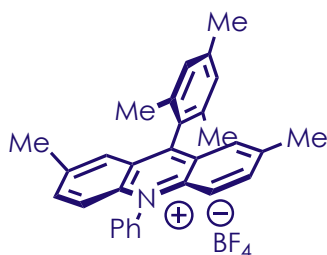
Catalyst B



9-mesityl-10-phenylacridin-10-ium tetrafluoroborate (Catalyst B)

The title compound was synthesized according to literature procedures. Spectral data matches that reported in the literature.³⁹

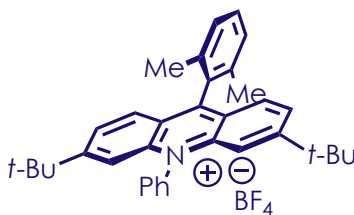
Catalyst C



9-mesityl-2,7-dimethyl-10-phenylacridin-10-ium tetrafluoroborate (Catalyst C)

The title compound was synthesized according to literature procedures. Spectral data matches that reported in the literature.³⁹

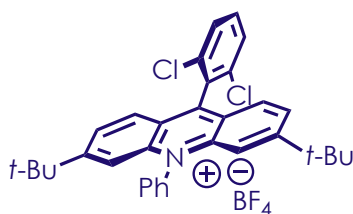
Catalyst D



**3,6-di-tert-butyl-9-(2,6-dimethylphenyl)-10-phenylacridin-10-ium tetrafluoroborate
(Catalyst D)**

The title compound was synthesized according to literature procedures. Spectral data matches that reported in the literature.³³

Catalyst E

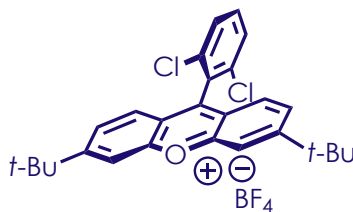


3,6-di-*tert*-butyl-9-(2,6-dichlorophenyl)-10-phenylacridin-10-ium tetrafluoroborate

(Catalyst E)

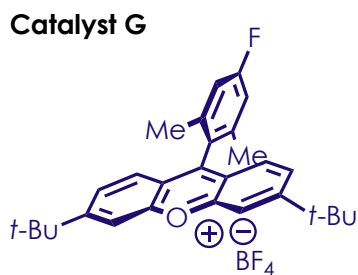
The title compound was synthesized according to literature procedures. Spectral data matches that reported in the literature.³³

Catalyst F



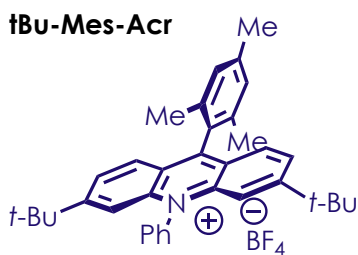
3,6-di-*tert*-butyl-9-(2,6-dichlorophenyl)xanthylium tetrafluoroborate (Catalyst F)

The title compound was synthesized according to literature procedures. Spectral data matches that reported in the literature.³³



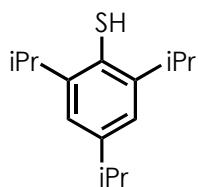
3,6-di-*tert*-butyl-9-(4-fluoro-2,6-dimethylphenyl)xanthylium tetrafluoroborate (Catalyst G)

The title compound was synthesized according to literature procedures. Spectral data matches that reported in the literature.³³



3,6-di-*tert*-butyl-9-mesityl-10-phenylacridin-10-ium tetrafluoroborate (tBu-Mes-Acr)

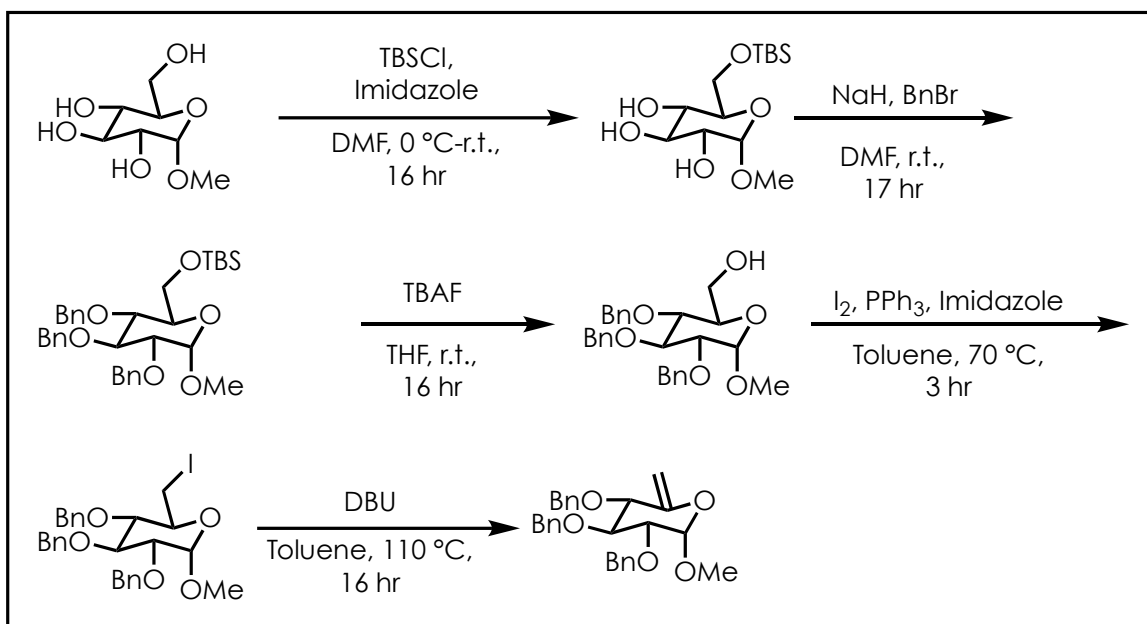
The title compound was synthesized according to literature procedures. Spectral data matches that reported in the literature.³³

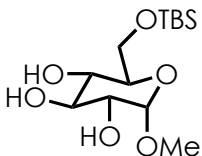


2,4,6-triisopropylbenzenethiol (TRIP-SH)

The title compound was synthesized according to literature procedures. Spectral data matches that reported in the literature.¹⁶⁶

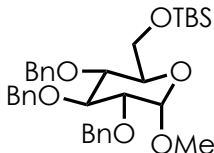
Scheme A-1. Synthesis of 2.29





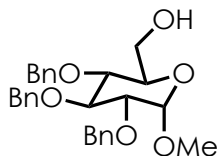
**(2*R*,3*S*,4*S*,5*R*,6*S*)-2-(((*tert*-butyldimethylsilyl)oxy)methyl)-6-methoxytetrahydro-2*H*-
pyran-3,4,5-triol (2.25)**

The title compound was prepared according to literature procedure. The product was isolated as a white solid in a 72% yield. Spectral data matches that reported in the literature.¹⁶⁷



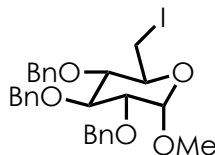
***tert*-butyldimethyl(((2*R*,3*R*,4*S*,5*R*,6*S*)-3,4,5-tris(benzyloxy)-6-methoxytetrahydro-2*H*-
pyran-2-yl)methoxy)silane (2.26)**

The title compound was prepared according to literature procedure. The product was isolated as a pale yellow oil in a 75% yield. Spectral data matches that reported in the literature.¹⁶⁷



**((2*R*,3*R*,4*S*,5*R*,6*S*)-3,4,5-tris(benzyloxy)-6-methoxytetrahydro-2*H*-pyran-2-yl)methanol
(2.27)**

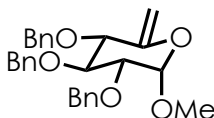
The title compound was prepared according to literature procedure. The product was isolated as a pale orange oil in a quantitative (>99%) yield. Spectral data matches that reported in the literature.¹⁶⁷



(2*S*,3*S*,4*S*,5*R*,6*S*)-3,4,5-tris(benzyloxy)-2-(iodomethyl)-6-methoxytetrahydro-2*H*-pyran

(2.28)

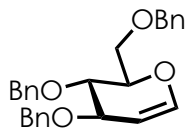
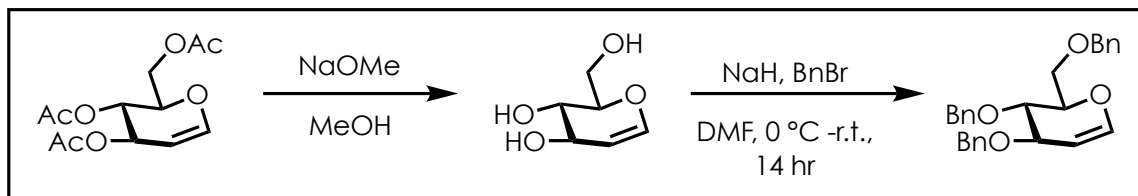
The title compound was prepared according to literature procedure. The product was isolated as an orange oil in an 84% yield. Spectral data matches that reported in the literature.¹⁶⁷



(2*S*,3*R*,4*S*,5*S*)-3,4,5-tris(benzyloxy)-2-methoxy-6-methylenetetrahydro-2*H*-pyran (2.29)

The title compound was prepared by charging a flame dried round bottom flask and stir bar with **2.28** and 20.0 mL of toluene. The reaction was cooled to 0 °C with an ice bath, and the DBU was added slowly over a period of 10 minutes. The reaction was allowed to slowly warm to r.t., and then it was heated to 110 °C and stirred for 16 hours. The reaction was cooled to r.t. and diluted with EtOAc. The mixture was washed with H₂O and brine, and the combined organic layers were dried with Na₂SO₄. The crude reaction mixture was purified *via* column chromatography (10% EtOAc/Hexanes – 20% EtOAc/Hexanes) and isolated as a colorless oil in a 35% yield. Spectral data matched that reported in the literature.¹⁶⁸

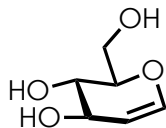
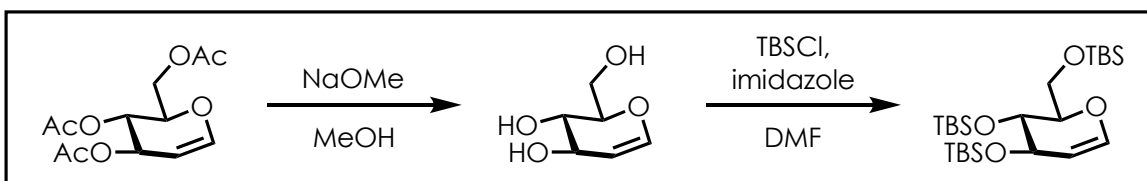
Scheme A-2. Synthesis of 2.30



(2*R*,3*S*)-3,4-bis(benzyloxy)-2-((benzyloxy)methyl)-3,4-dihydro-2*H*-pyran (2.30)

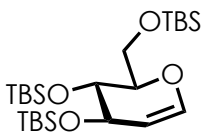
The title compound was prepared according to literature procedure. The product was isolated as a sticky, white solid in a 91% yield. Spectral data matches that reported in the literature.¹⁶⁹

Scheme A-3. Synthesis of 2.32



(2*R*,3*S*)-2-(hydroxymethyl)-3,4-dihydro-2*H*-pyran-3,4-diol (2.31)

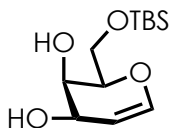
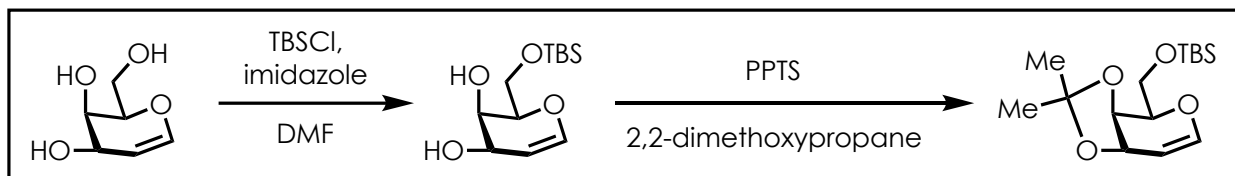
The title compound was prepared according to a literature procedure.¹⁷⁰ The crude product (colorless, sticky oil) was not analyzed or purified and was directly carried forward to the next step.



(((2*R*,3*R*)-2-(((*tert*-butyldimethylsilyl)oxy)methyl)-3,4-dihydro-2*H*-pyran-3,4-diyl)bis(oxy))bis(*tert*-butyldimethylsilane) (2.32)

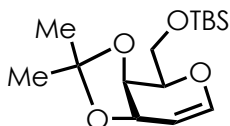
The title compound was prepared according to a literature procedure. The crude product was purified by column chromatography (100% hexanes – 10% ethyl acetate/hexanes) and isolated as a white solid. Spectral data matches that reported in the literature.¹⁷⁰

Scheme A-4. Synthesis of 2.34



(2*R*,3*R*)-2-(((*tert*-butyldimethylsilyl)oxy)methyl)-3,4-dihydro-2*H*-pyran-3,4-diol (2.33)

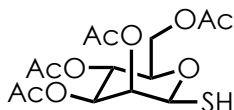
The title compound was synthesized according to literature procedures. The crude material was purified *via* column chromatography (50% ethyl acetate/hexanes; TLC plates stained with CAM). The title compound was isolated as a clear oil in a 70% yield. Spectral data matches that reported in the literature.¹⁷¹



***tert*-butyl(((3a*R*,4*R*)-2,2-dimethyl-3a,7a-dihydro-4*H*-[1,3]dioxolo[4,5-*c*]pyran-4-yl)methoxy)dimethylsilane (2.34)**

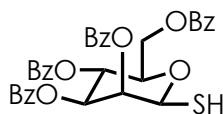
A 250-mL round bottom flask and stir bar were flame dried and cooled to room temperature under an atmosphere of N₂. The (2*R*,3*R*)-2-(((*tert*-butyldimethylsilyl)oxy)methyl)-3,4-dihydro-2*H*-pyran-3,4-diol (1.08 g, 4.15 mmol, 1.0 equiv.) was added to the flask, and the system was placed under vacuum to ensure that the material was dry. The flask was refilled with nitrogen, and the 2,2-dimethoxypropane (20.0 mL) was added *via* syringe. PPTS (0.104 g, 0.415 mmol, 0.10 equiv.) was added to the flask, and the mixture was heated with 50 °C with stirring. After one hour of stirring, an additional 10.0 mL of 2,2-dimethoxypropane was added to the reaction *via* syringe. The process was repeated after another hour of stirring (10.0 mL). The reaction was stirred for an additional 4 hours and then cooled to room temperature. Na₂CO₃ was added until the reaction mixture was cloudy. The heterogeneous mixture was stirred for 30 minutes, and then the reaction was filtered. The filtrate was concentrated down to afford a pale tan oil. The crude reaction mixture was purified *via* column chromatography (20% ethyl acetate/hexanes; TLC plates stained with CAM). Upon

complete removal of solvent, the desired product was isolated as a pale white solid in a yield of 52%. Spectral data matches that reported in the literature.¹⁷²



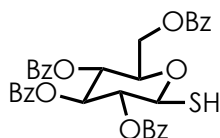
**(2*R*,3*R*,4*S*,5*S*,6*S*)-2-(acetoxymethyl)-6-mercaptotetrahydro-2*H*-pyran-3,4,5-triyl
triacetate (2.14)**

The title compound was obtained from a colleague's samples. The literature indicates that it can be synthesized by following the procedure in one of the cited references.¹⁷³



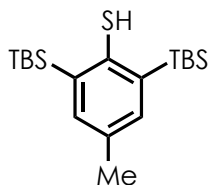
**(2*R*,3*R*,4*S*,5*S*,6*S*)-2-((benzyloxy)methyl)-6-mercaptotetrahydro-2*H*-pyran-3,4,5-triyl
tribenzoate (2.15)**

The title compound was obtained from a colleague's samples. The literature indicates that it can be synthesized by following the procedure in one of the cited references.¹⁷⁴



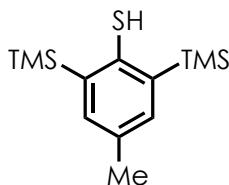
**(2*R*,3*R*,4*S*,5*R*,6*S*)-2-((benzyloxy)methyl)-6-mercaptotetrahydro-2*H*-pyran-3,4,5-triyl
tribenzoate (2.16)**

The title compound was obtained from a colleague's samples. The literature indicates that it can be synthesized by following the procedure in one of the cited references.¹⁷⁵



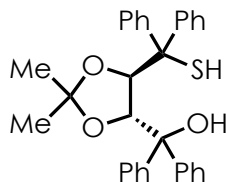
2,6-bis(*tert*-butyldimethylsilyl)-4-methylbenzenethiol (2.10)

The title compound was obtained from a colleague's samples. Procedure will be included upon return to lab as it is located in a colleague's notebook.



4-methyl-2,6-bis(trimethylsilyl)benzenethiol (2.11)

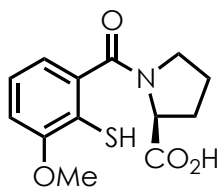
The title compound was obtained from a colleague's samples. Procedure will be included upon return to lab as it is located in a colleague's notebook.



((4*R*,5*R*)-5-(mercaptodiphenylmethyl)-2,2-dimethyl-1,3-dioxolan-4-yl)diphenylmethanol

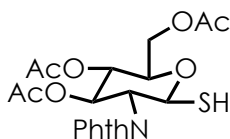
(2.12)

The title compound was obtained from a colleague's samples. The literature indicates that it can be synthesized by following the procedure in one of the cited references.¹⁷⁶



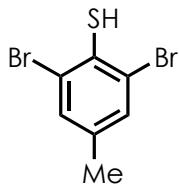
(2-mercapto-3-methoxybenzoyl)-L-proline (2.13)

The title compound was obtained from a colleague's samples. Procedure will be added upon return to lab as the procedure is located in a colleague's notebook.



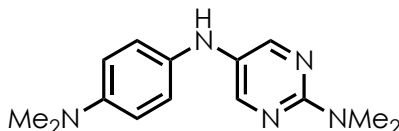
(2R,3S,4R,5R,6S)-2-(acetoxymethyl)-5-(1,3-dioxoisindolin-2-yl)-6-mercaptotetrahydro-2H-pyran-3,4-diyl diacetate (2.20)

The title compound was obtained from a colleague's samples. The literature indicates that it can be synthesized by following the procedure in one of the cited references.¹⁷⁷



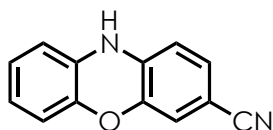
2,6-dibromo-4-methylbenzenethiol (2.18)

The title compound was obtained from a colleague's samples. Procedure will be added upon return to the lab as it is located in a colleague's notebook.



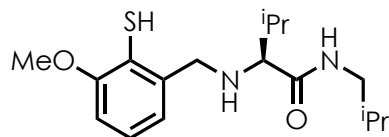
***N*₅-(4-(dimethylamino)phenyl)-*N*₂,*N*₂-dimethylpyrimidine-2,5-diamine (2.19)**

The title compound was obtained from a colleague's samples. The literature indicates that it can be synthesized by following the procedure in one of the cited references.¹¹⁰



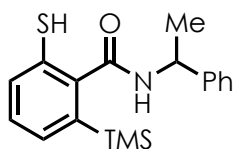
10*H*-phenoxazine-3-carbonitrile (2.22)

The title compound was obtained from a colleague's samples. The literature indicates that it can be synthesized by following the procedure in one of the cited references.¹⁷⁸



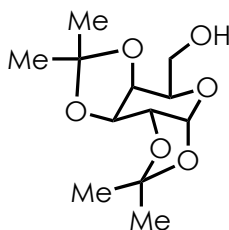
(S)-N-isobutyl-2-((2-mercapto-3-methoxybenzyl)amino)-3-methylbutanamide (2.17)

The title compound was obtained from a colleague's samples. Procedure will be added upon return to lab as it is located in a colleague's notebook.



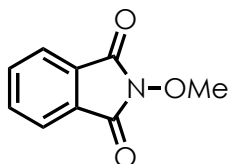
2-mercapto-N-(1-phenylethyl)-6-(trimethylsilyl)benzamide (2.21)

The title compound was obtained from a colleague's samples. Procedure will be added upon return to lab as it is located in a colleague's notebook.



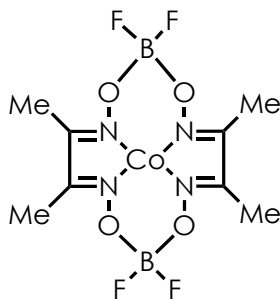
((3aR,5R,5aS,8aS)-2,2,7,7-tetramethyltetrahydro-5H-bis([1,3]dioxolo)[4,5-b:4',5'-d]pyran-5-yl)methanol (2.35)

The title compound was prepared according to a literature procedure. The spectral data matches that reported in the literature.¹⁷⁹ The title compound was isolated as a sticky, colorless oil in an 80% yield.



2-methoxyisoindoline-1,3-dione (2.23)

The title compound was prepared according to a literature procedure. The spectral data matches that reported in the literature.¹⁸⁰ The title compound was isolated as a crystalline, white solid in an 54% yield.



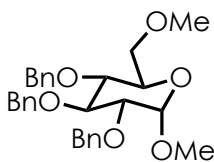
bis(dimethylglyoximatodifluoroboryl)cobalt(II) (2.24)

The title compound was obtained from a colleague's samples. The literature indicates that it can be synthesized by following the procedure in one of the cited references.¹⁸¹

A.3 General Procedure for Hydrofunctionalization of *Exo*- and *Endo*-Glycals and Characterization of Products

Exo-Glycal Hydroalkoxylation:

A two-dram vial and stir bar were flame dried and cooled to room temperature. The vial was charged with solid reagents: **tBu-Mes-Acr** (2.9 mg, 0.005 mmol, 0.05 equiv.), glycal substrate (45.0 mg, 0.10 mmol, 1.0 equiv.), and TRIP-SH (4.4 mg, 0.01 mmol, 0.20 equiv.). The *o*-xylene (0.20 mL) was then added *via* syringe, and the reaction was sparged with nitrogen for five minutes. The 2,4,6-collidine (3.3 μ L, 0.025 mmol, 0.25 equiv.) and alcohol nucleophile were then added to the vial through the septum cap with a microliter syringe. The vial cap was sealed with both Teflon and electrical tape before stirring and irradiation began. The reaction was stirred and irradiated with 455 nm bLEDs for 18 hours. Upon completion, the reaction mixture was diluted with DCM and filtered through a plug of silica. The silica plug was washed with EtOAc (2 x 5 mL), and the crude material was concentrated down. The crude product was either analyzed by ^1H NMR to obtain a yield or purified by column chromatography.

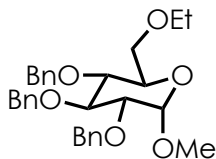


(2*S*,3*R*,4*S*,5*R*,6*R*)-3,4,5-tris(benzyloxy)-2-methoxy-6-(methoxymethyl)tetrahydro-2*H*-pyran (**2.36**)

The title compound was prepared from **2.29** (45.0 mg, 0.10 mmol, 1.0 equiv.) and MeOH (61.0 μ L, 1.50 mmol, 15.0 equiv.). The title compound was isolated by column

chromatography (100% Hexanes – 35% EtOAc/Hexanes) as a yellow oil in an 87% yield.

Spectral data matches that reported in the literature.¹⁸²

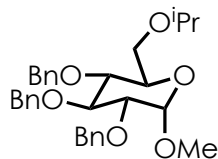


**(2*R*,3*R*,4*S*,5*R*,6*S*)-3,4,5-tris(benzyloxy)-2-(ethoxymethyl)-6-methoxytetrahydro-2*H*-
pyran (2.37)**

The title compound was prepared from **2.29** (45.0 mg, 0.10 mmol, 1.0 equiv.) and EtOH (88.0 μ L, 1.50 mmol, 15.0 equiv.). The title compound was isolated by column chromatography (100% Hexanes – 35% EtOAc/Hexanes) as a yellow oil in an 70% yield (37.0 mg).

¹H NMR (400 MHz, CDCl₃) δ 7.34 (dq, $J = 21.8, 6.9, 6.2$ Hz, 15H), 5.01 (d, $J = 10.8$ Hz, 1H), 4.91 (d, $J = 10.9$ Hz, 1H), 4.87 – 4.81 (m, 2H), 4.68 (d, $J = 12.2$ Hz, 1H), 4.64 – 4.62 (m, 2H), 4.01 (t, $J = 9.2$ Hz, 1H), 3.76 – 3.72 (m, 1H), 3.69 – 3.53 (m, 5H), 3.49 – 3.43 (m, 1H), 3.40 (s, 3H), 1.22 (t, $J = 6.9$ Hz, 3H).

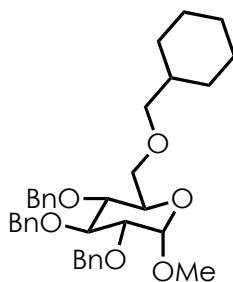
¹³C NMR (151 MHz, CDCl₃) δ 138.80, 138.39, 138.12, 128.36, 128.33, 128.30, 128.09, 127.88, 127.86, 127.81, 127.77, 127.62, 127.47, 98.17, 82.07, 79.75, 77.55, 77.16, 76.95, 76.74, 75.65, 74.95, 73.32, 69.91, 68.76, 66.77, 55.06, 15.04.



(2R,3R,4S,5R,6S)-3,4,5-tris(benzyloxy)-2-(isopropoxymethyl)-6-methoxytetrahydro-2H-pyran (2.38)

The title compound was prepared from **2.29** (45.0 mg, 0.10 mmol, 1.0 equiv.) and iPrOH (115.0 μ L, 1.50 mmol, 15.0 equiv.). The title compound was isolated by column chromatography (100% Hexanes – 30% EtOAc/Hexanes) as a yellow oil in an 70% yield (35.4 mg).

¹H NMR (400 MHz, CDCl₃) δ 7.54 – 7.30 (m, 15H), 5.01 (d, J = 10.8 Hz, 1H), 4.93 (d, J = 10.9 Hz, 1H), 4.89 – 4.79 (m, 2H), 4.69 (d, J = 12.2 Hz, 1H), 4.67 – 4.61 (m, 2H), 4.02 (t, J = 9.1 Hz, 1H), 3.78 – 3.62 (m, 5H), 3.61 – 3.51 (m, 2H), 3.40 (s, 3H), 1.19 (d, J = 6.1 Hz, 6H).

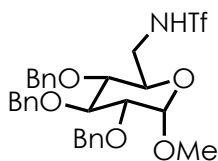


(2R,3R,4S,5R,6S)-3,4,5-tris(benzyloxy)-2-((cyclohexylmethoxy)methyl)-6-methoxytetrahydro-2H-pyran (2.39)

The title compound was prepared from **2.29** (0.18 mL, 0.10 mmol, 1.0 equiv.) and cyclohexylmethanol (22.0 mg, 1.5 mmol mmol, 15.0 equiv.). The title compound was formed in a 60% ¹H NMR yield using HMDSO as an internal standard.

¹H NMR (400 MHz, CDCl₃) δ 7.42 – 7.29 (m, 15H), 4.99 (d, *J* = 10.8 Hz, 1H), 4.95 – 4.77 (m, 7H), 4.76 – 4.59 (m, 5H), 3.99 (td, *J* = 9.2, 6.4 Hz, 2H), 3.35 (dd, *J* = 9.1, 5.7 Hz, 1H), 3.16 (dd, *J* = 9.1, 7.4 Hz, 1H).

NOTE: Due to the presence of large amounts of excess cyclohexylmethanol, not all peaks could be identified.



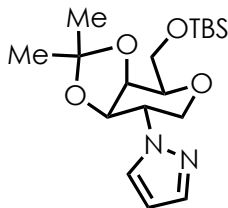
1,1,1-trifluoro-*N*-(((2*R*,3*R*,4*S*,5*R*,6*S*)-3,4,5-tris(benzyloxy)-6-methoxytetrahydro-2*H*-pyran-2-yl)methyl)methanesulfonamide (2.40)

The title compound was prepared from **2.29** (45.0 mg, 0.10 mmol, 1.0 equiv.) and NH₂Tf (22.0 mg, 0.15 mmol, 1.50 equiv.). **NOTE: The NH₂Tf was added prior to sparging with N₂ as it is a solid.** The title compound was formed in a 26% ¹H NMR yield using HMDSO as an internal standard. Spectral data matches that reported in the literature.¹⁸³

Endo-Glycal Hydroamination with Pyrazole:

A 2-dram vial and stir bar were flame dried and cooled to room temperature. The solid reagents: **tBu-Mes-Acr** (5.7 mg, 0.01 mmol, 0.05 equiv.), glycal substrate (**2.34**) (60.0 mg, 0.20 mmol, 1.0 equiv.), pyrazole (41.0 mg, 0.60 mmol, 3.0 equiv.), NaHCO₃ (4.2 mg, 0.05

mmol, 0.25 equiv.), and TRIP-SH (9.5 mg, 0.04 mmol, 0.20 equiv.). **NOTE: NaHCO₃ was used in this trial as comparable results could be obtained with its use, and it allowed for the addition of all reagents prior to sparging.** The MeCN (0.20 mL) was then added to the vial *via* syringe. The vial was sealed with a septum cap and sparged with N₂ for five minutes. The vial was sealed with both Teflon and electrical tape before stirring and irradiation began. The reaction was stirred and irradiated with 455 nm bLEDs for 20 hours. Upon completion, the reaction mixture was diluted with DCM and filtered through a plug of silica. The silica plug was washed with EtOAc (2 x 5 mL), and the crude material was concentrated down. The crude product was purified by column chromatography (20% EtOAc/Hexanes; TLC plates stained with CAM), and the two regioisomers were isolated as a pale tan solid (47.0 mg, 64% yield). **NOTE: Although separation of regioisomers was achieved, isolated yield is reported as the combined overall yield of all products isolated.**

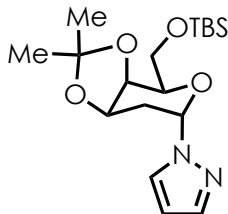


1-((3aR,4R,7S,7aR)-4-(((*tert*-butyldimethylsilyloxy)methyl)-2,2-dimethyltetrahydro-4H-[1,3]dioxolo[4,5-*c*]pyran-7-yl)-1H-pyrazole (2.41A)

The title compound was prepared according to the procedure reported above. ¹H NMR data is included below.

¹H NMR (400 MHz, CDCl₃) δ 7.55 (d, *J* = 1.9 Hz, 1H), 7.47 (d, *J* = 2.3 Hz, 1H), 6.26 (t, *J* = 2.1 Hz, 1H), 4.57 (dd, *J* = 8.5, 5.2 Hz, 1H), 4.32 (dd, *J* = 5.4, 1.7 Hz, 1H), 4.26 (ddd, *J* =

11.4, 8.5, 5.1 Hz, 1H), 4.10 (dd, $J = 11.6, 5.0$ Hz, 1H), 3.92 – 3.79 (m, 3H), 3.76 (t, $J = 11.4$ Hz, 1H), 1.59 (s, 3H), 1.35 (s, 3H), 0.91 (s, 9H), 0.09 (s, 6H).



1-((3aR,4R,6S,7aR)-4-(((tert-butyl)dimethylsilyloxy)methyl)-2,2-dimethyltetrahydro-4H-[1,3]dioxolo[4,5-c]pyran-6-yl)-1H-pyrazole (2.41B)

The title compound was prepared according to the procedure reported above. ^1H NMR data is included below.

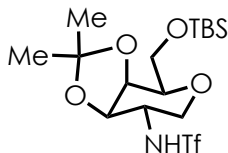
^1H NMR (400 MHz, CDCl_3) δ 7.61 (d, $J = 2.4$ Hz, 1H), 7.54 (d, $J = 1.8$ Hz, 1H), 6.27 (d, $J = 2.1$ Hz, 1H), 5.90 (dd, $J = 9.2, 5.5$ Hz, 1H), 4.72 (dt, $J = 7.2, 3.4$ Hz, 1H), 4.31 (m, 1H), 3.94 (td, $J = 6.4, 1.7$ Hz, 1H), 3.86 (dtd, $J = 10.8, 7.1, 4.8$ Hz, 1H), 3.80 – 3.67 (m, 1H), 2.69 (ddd, $J = 15.1, 9.2, 3.2$ Hz, 1H), 2.43 (ddd, $J = 15.1, 5.6, 3.6$ Hz, 1H), 1.52 (s, 3H), 1.35 (s, 3H), 0.84 (s, 9H), 0.09 (s, 6H).

NOTE: The formation of a negligible amount of a minor diastereomer of 2.41B was observed as well, but an adequate ^1H NMR spectrum could not be obtained.

Endo-Glycol Hydroamination with Triflamide:

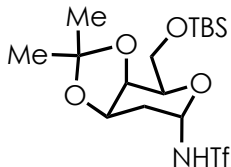
A 2-dram vial and stir bar were flame dried and cooled to room temperature. The solid reagents: **tBu-Mes-Acr** (2.9 mg, 0.005 mmol, 0.05 equiv.), glycol substrate (**2.34**) (30.0 mg, 0.10 mmol, 1.0 equiv.), NH_2Tf (45.0 mg, 0.30 mmol, 3.0 equiv.) and TRIP-SH (4.7 mg, 0.01

mmol, 0.20 equiv.). The DCM (0.20 mL) was then added to the vial *via* syringe. The vial was sealed with a septum cap and sparged with N₂ for five minutes. The 2,4,6-collidine (25.0 μL, 0.025 mmol, 0.25 equiv.) was added through the septum cap with a microliter syringe. The vial was sealed with both Teflon and electrical tape before stirring and irradiation began. The reaction was stirred and irradiated with 455 nm bLEDs for 20 hours. Upon completion, the reaction mixture was diluted with DCM and filtered through a plug of silica. The silica plug was washed with EtOAc (2 x 5 mL), and the crude material was concentrated down. The yield of product was determined by ¹H NMR of the crude reaction mixture using dimethyl dimethyl terephthalate as an internal standard: (42% yield **2.42A**); (13% yield, **2.42B** (two diastereomers)).



***N*-((3*aR*,4*R*,7*S*,7*aR*)-4-(((*tert*-butyldimethylsilyl)oxy)methyl)-2,2-dimethyltetrahydro-4*H*-[1,3]dioxolo[4,5-*c*]pyran-7-yl)-1,1,1-trifluoromethanesulfonamide (2.42A)**

¹H NMR (400 MHz, CDCl₃) δ 5.23 (d, *J* = 8.0 Hz, 1H), 4.28 – 4.24 (m, 1H), 4.11 – 4.04 (m, 1H), 3.90 (dd, *J* = 8.4, 5.1 Hz, 1H), 3.81 (d, *J* = 2.4 Hz, 1H), 3.72 – 3.66 (m, 1H), 3.14 (t, *J* = 11.2 Hz, 1H), 1.52 (s, 3H), 1.36 (s, 3H), 0.89 (s, 9H), 0.07 (s, 6H).



***N*-((3a*R*,4*R*,6*S*,7a*R*)-4-(((*tert*-butyldimethylsilyl)oxy)methyl)-2,2-dimethyltetrahydro-4*H*-[1,3]dioxolo[4,5-*c*]pyran-6-yl)-1,1,1-trifluoromethanesulfonamide (2.42B)**

Major diastereomer:

¹H NMR (400 MHz, CDCl₃) δ 6.59 (d, *J* = 9.7 Hz, 1H), 5.23 (ddd, *J* = 9.3, 5.3, 2.8 Hz, 1H), 4.57 – 4.53 (m, 1H), 4.28 – 4.24 (m, 1H), 3.75 – 3.65 (m, 1H), 3.57 (ddd, *J* = 7.4, 5.8, 1.9 Hz, 1H), 2.19 – 2.06 (m, 2H), 1.53 (s, 3H), 1.34 (s, 3H), 0.89 (s, 9H), 0.07 (s, 6H).

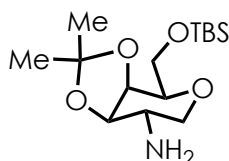
Minor diastereomer:

¹H NMR (400 MHz, CDCl₃) δ 5.73 (d, *J* = 9.4 Hz, 1H), 5.36 (td, *J* = 9.9, 5.0 Hz, 1H), 4.57–4.53 (m 1H), 4.28 – 4.24 (m, 1H), 3.75 – 3.65 (m, 1H), 2.35 (ddd, *J* = 14.9, 5.1, 2.9 Hz, 1H), 1.75 (ddd, *J* = 15.0, 10.3, 3.1 Hz, 1H), 1.46 (s, 3H), 1.32 (s, 3H), 0.89 (s, 9H), 0.07 (s, 6H).

Endo-Glycal Hydroamination with Ammonium Carbamate:

A 2-dram vial and stir bar were flame dried and cooled to room temperature. The solid reagents: **tBu-Mes-Acr** (2.9 mg, 0.005 mmol, 0.05 equiv.), glycal substrate (**2.34**) (30.0 mg, 0.10 mmol, 1.0 equiv.), ammonium carbamate (23.0 mg, 0.30 mmol, 3.0 equiv.) and TRIP-SH (4.7 mg, 0.01 mmol, 0.20 equiv.). The DCE:TFE (4:1) (0.20 mL) was then added to the vial *via* syringe. The vial was sealed with a septum cap and sparged with N₂ for five minutes. The 2,4,6-collidine (25.0 μL, 0.025 mmol, 0.25 equiv.) was added through the septum cap

with a microliter syringe. The vial was sealed with both Teflon and electrical tape before stirring and irradiation began. The reaction was stirred and irradiated with 455 nm bLEDs for 20 hours. Upon completion, the reaction mixture was diluted with DCM and filtered through a plug of silica. The silica plug was washed with EtOAc (2 x 5 mL), and the crude material was concentrated down. The crude product was either analyzed by ^1H NMR to obtain a yield or purified by column chromatography.

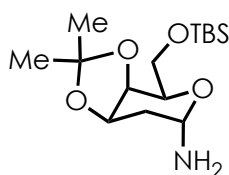


(3aR,4R,7S,7aR)-4-(((*tert*-butyldimethylsilyl)oxy)methyl)-2,2-dimethyltetrahydro-4H-[1,3]dioxolo[4,5-*c*]pyran-7-amine (2.43A)

^1H NMR (400 MHz, CDCl_3) δ 3.55 – 3.48 (m, 1H), 3.12 (dd, $J = 11.6, 10.3$ Hz, 1H)

NOTE: Due to poor separation, compounds 2.43A and 2.43B could not be purified.

NMR signals that could be clearly identified are reported. Remaining signals are part of complex mixtures.



(3aR,4R,6S,7aR)-4-(((*tert*-butyldimethylsilyl)oxy)methyl)-2,2-dimethyltetrahydro-4H-[1,3]dioxolo[4,5-*c*]pyran-6-amine (2.43B)

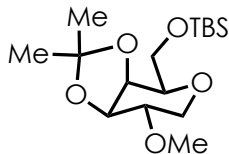
¹H NMR (400 MHz, CDCl₃) δ 5.02 (t, *J* = 6.0 Hz, 1H), 4.49 (dt, *J* = 7.6, 3.9 Hz, 1H), 4.23 (dd, *J* = 5.6, 2.1 Hz, 1H), 2.31 (ddd, *J* = 15.2, 5.6, 4.1 Hz, 1H), 1.75 (ddd, *J* = 15.2, 6.6, 3.6 Hz, 1H)

NOTE: Due to poor separation, compounds 2.43A and 2.43B could not be purified.

NMR signals that could be clearly identified are reported. Remaining signals are part of complex mixtures.

Endo-Glycal Hydroalkoxylation with Methanol:

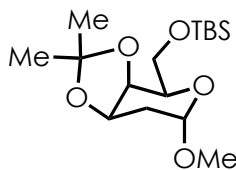
A 2-dram vial and stir bar were flame dried and cooled to room temperature. The solid reagents: **tBu-Mes-Acr** (2.9 mg, 0.005 mmol, 0.05 equiv.), glycal substrate (**2.34**) (30.0 mg, 0.10 mmol, 1.0 equiv.), and TRIP-SH (4.7 mg, 0.01 mmol, 0.20 equiv.). The DCE (0.20 mL) was then added to the vial *via* syringe. The vial was sealed with a septum cap and sparged with N₂ for five minutes. The 2,4,6-collidine (50.0 μL, 0.05 mmol, 0.50 equiv.) and MeOH (41.0 μL, 1.0 mmol, 10.0 equiv.) were added through the septum cap with a microliter syringe. The vial was sealed with both Teflon and electrical tape before stirring and irradiation began. The reaction was stirred and irradiated with 455 nm bLEDs for 20 hours. Upon completion, the reaction mixture was diluted with DCM and filtered through a plug of silica. The silica plug was washed with EtOAc (2 x 5 mL), and the crude material was concentrated down. The crude product was either analyzed by ¹H NMR to obtain a yield or purified by column chromatography.



***tert*-butyl(((3*a*S,4*R*,7*a*R)-7-methoxy-2,2-dimethyltetrahydro-4*H*-[1,3]dioxolo[4,5-
c]pyran-4-yl)methoxy)dimethylsilane (2.44A)**

The title compound was prepared according to the above procedure. The title compound was formed as an inseparable mixture with **2.44B** and was formed in a 44% ¹H NMR yield using dimethyl terephthalate as an internal standard.

¹H NMR (400 MHz, CDCl₃) δ 4.17 – 4.13 (m, 1H), 4.04 – 4.00 (m, 2H), 3.84 – 3.72 (m, 2H), 3.51 – 3.45 (m, 1H), 3.4 (s, 3H), 3.08 (dd, *J* = 11.5, 10.0 Hz, 1H), 1.46 (s, 3H), 1.31 (s, 3H), 0.88 (s, 9H), 0.06 (s, 6H).



***tert*-butyl(((3*a*R,4*R*,7*a*R)-6-methoxy-2,2-dimethyltetrahydro-4*H*-[1,3]dioxolo[4,5-
c]pyran-4-yl)methoxy)dimethylsilane (2.44B)**

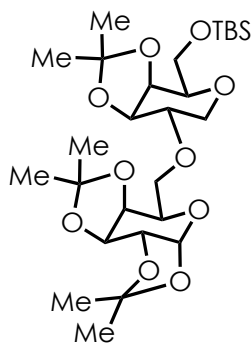
The title compound was prepared according to the above procedure. The title compound was formed as an inseparable mixture with **2.44A** and was formed in a 44% ¹H NMR yield using dimethyl terephthalate as an internal standard.

¹H NMR (400 MHz, CDCl₃) δ 4.44 (ddd, *J* = 7.0, 5.2, 4.2 Hz, 1H), 4.22 (dd, *J* = 5.7, 2.1 Hz, 1H), 3.84 – 3.72 (m, 3H), 3.67 (ddd, *J* = 7.2, 5.9, 2.1 Hz, 1H), 3.47 (s, 3H), 2.15 (dt, *J* = 14.8,

5.2 Hz, 1H), 1.72 (ddd, $J = 14.8, 5.9, 4.2$ Hz, 1H), 1.52 (s, 3H), 1.34 (s, 3H), 0.89 (s, 9H), 0.07 (s, 6H).

Endo-Glycal Glycosylation with 2.35:

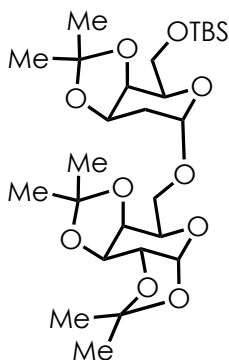
A 2-dram vial and stir bar were flame dried and cooled to room temperature. The solid reagents: **tBu-Mes-Acr** (2.9 mg, 0.005 mmol, 0.05 equiv.), glycal substrate (**2.34**) (30.0 mg, 0.10 mmol, 1.0 equiv.), TRIP-SH (4.7 mg, 0.01 mmol, 0.20 equiv.), and glycoside nucleophile (**2.35**) (52.0 mg, 0.20 mmol, 2.0 equiv.). The MeCN (0.20 mL) was then added to the vial *via* syringe. The vial was sealed with a septum cap and sparged with N₂ for five minutes. The NaHCO₃ (8.4 mg, 0.10 mmol, 1.0 equiv.) was added through the septum cap with a microliter syringe. The vial was sealed with both Teflon and electrical tape before stirring and irradiation began. The reaction was stirred and irradiated with 455 nm bLEDs for 20 hours. Upon completion, the reaction mixture was diluted with DCM and filtered through a plug of silica. The silica plug was washed with EtOAc (2 x 5 mL), and the crude material was concentrated down. The crude product was either analyzed by ¹H NMR to obtain a yield or purified by column chromatography.



tert-butyl(((3*aS*,4*R*,7*S*,7*aR*)-2,2-dimethyl-7-(((3*aR*,5*R*,5*aS*,8*aS*)-2,2,7,7-tetramethyltetrahydro-5*H*-bis([1,3]dioxolo)[4,5-*b*:4',5'-*d*]pyran-5-yl)methoxy)tetrahydro-4*H*-[1,3]dioxolo[4,5-*c*]pyran-4-yl)methoxy)dimethylsilane
(2.45A)

¹H NMR (400 MHz, CDCl₃) δ 3.10 (m, 1H)

NOTE: Spectrum was complicated and majority of peaks were part of complex multiplet.



tert-butyl(((3*aR*,4*R*,6*S*,7*aR*)-2,2-dimethyl-6-(((3*aR*,5*R*,5*aS*,8*aS*)-2,2,7,7-tetramethyltetrahydro-5*H*-bis([1,3]dioxolo)[4,5-*b*:4',5'-*d*]pyran-5-yl)methoxy)tetrahydro-4*H*-[1,3]dioxolo[4,5-*c*]pyran-4-yl)methoxy)dimethylsilane
(2.45B)

¹H NMR (400 MHz, CDCl₃) δ 5.50 (dd, *J* = 5.1, 1.8 Hz, 1H), 4.95 (t, *J* = 5.5 Hz, 1H), 2.13 (dt, *J* = 14.8, 5.0 Hz, 1H), 1.76 (ddd, *J* = 10.3, 8.2, 4.2 Hz, 1H).

NOTE: Spectrum was complicated and majority of peaks were part of complex multiplet.

APPENDIX B: EXPERIMENTAL DATA FOR CHAPTER 3

B.1 General Experimental Information

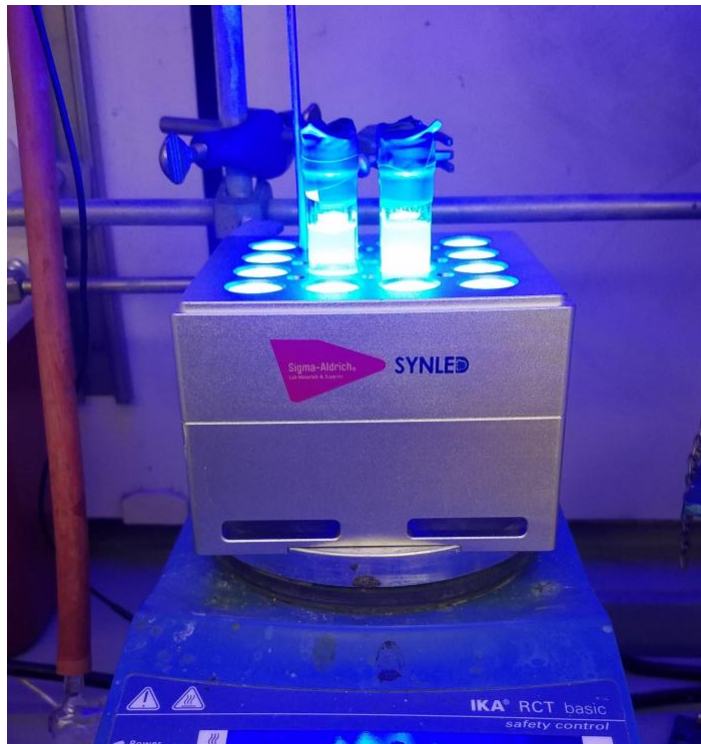
General Reagent Information: Commercially available reagents were purchased from Sigma-Aldrich, Fischer Scientific or TCI Corporation and were used without further purification. Styrenes containing radical inhibitors were filtered through a small pad of silica gel to remove any inhibitors. Styrenes which appeared impure upon purchase/preparation were also purified by passing them through a short pad of silica. Solvents were used as received unless otherwise noted. TMS-azide was used as received and stored in a refrigerator.

WARNING: TMS-azide is an acutely toxic reagent and should be treated with extreme care. When scaling up reactions, ensure that all waste is kept basic to prevent the formation of hydrazoic acid at any point during work-up. Please familiarize yourself with the handling of this hazardous reagent before attempting any of the reactions disclosed within.

General Analytical Information: Proton and carbon (^1H and ^{13}C) magnetic resonance spectra were collected on a Bruker AVANCE III 600 CryoProbe (^1H NMR at 600 MHz and ^{13}C NMR at 151 MHz) spectrometer or Bruker AVANCE III 500 (^1H NMR at 500 MHz and ^{13}C NMR at 126 MHz) spectrometer. Unless otherwise noted, spectra are referenced to Chloroform- d (^1H NMR at 7.26 ppm and ^{13}C at 77.16 ppm) and reported as parts per million. ^1H NMR data are reported as follows: chemical shift, multiplicity (s = singlet, d = doublet, t = triplet, dd = doublet of doublets, ddd = doublet of doublets of doublets, ddddd =

doublet of doublets of doublets of doublets of doublets, dt = doublet of triplets, ddt = doublet of doublets of triplets, td = triplet of doublets, tt = triplet of triplets, m = multiplet, q = quartet), coupling constants (Hz), and integration. High Resolution Mass Spectra (HRMS) were obtained *via* direct infusion using a Thermo LTQ FT mass spectrometer with positive mode electrospray ionization or APCI. Low resolution mass spectra were obtained using an Agilent Technologies 5977E MSD GC/MS unit with electron impact (EI) ionization. Flash chromatography was performed using SiliaFlash P60 silica gel (40-63 μm) purchased from Silicycle.

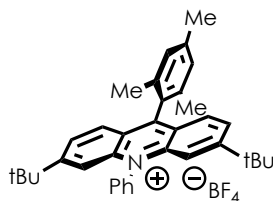
General Photoreactor Configuration: All photochemical reactions were conducted using a SynLED Parallel Photoreactor, available for purchase from Sigma-Aldrich (item number: **Z742680**). The unit has bottom-lit LEDs (465-470 nm) with 130-140 lm intensity and a built-in cooling fan. The measured temperature range was 35 - 40°C. The reactor was fit to an IKA magnetic stirrer with round plate (item number: Z645052). Small stir bars are sometimes required for efficient stirring when using 2 dram vials.



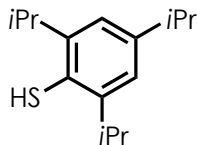
General Procedure for Photochemical Reactions: A flame-dried 2-dram borosilicate vial (purchased from Fisher Scientific, catalogue # 03-339-22D), equipped with a stir bar, was charged with 3,6-Di-tert-butyl-9-mesityl-10-phenylacridin-10-ium tetrafluoroborate (0.01 eq., 0.01 mmol) and 2,5,6-triisopropylthiophenol (0.10 mmol, 0.20 eq.). For solid/non-volatile substrates, the substrate (0.50 mmol) was then added. 2,2,2-trifluoroethanol (5.0 mL) was added and vials were capped tightly with a Teflon lined phenolic resin septum cap (purchased through VWR international, Microliter Product # 15-0060K). The reaction mixture was sparged by bubbling with nitrogen or argon for 5 minutes.

Trimethylsilylazide (0.625 mmol, 1.25 eq.) was then added *via* microliter syringe. Prior to irradiation, vials were sealed with Teflon tape and electrical tape to ensure maximal oxygen exclusion. The reaction vial was then placed into the reactor and irradiated for 18 hours unless otherwise noted. Following irradiation, the reaction mixture was concentrated under reduced pressure and the desired products were isolated *via* flash column chromatography (see substrate/product details for solvent information). Unless otherwise noted, all reaction yields are reported as the average of two separate trials (including chromatography).

B.2 Catalyst and Substrate Synthesis



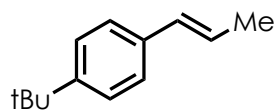
3,6-Di-tert-butyl-9-mesityl-10-phenylacridin-10-ium tetrafluoroborate (tBu-Acr-BF₄) was prepared according to published procedure. Spectral data matched that reported in the literature.¹⁸⁴



2,4,6-triisopropylbenzenethiol (TRIP-SH) was prepared according to the procedure of Knowles and coworkers. Spectral data matched that reported in the literature.¹⁸⁵

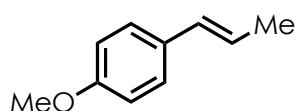
General procedure for preparation of beta-methylstyrene derived substrates:

In a flame-dried round bottom flask under an atmosphere of nitrogen, ethyltriphenylphosphonium iodide (1.1 eq.) was stirred with THF (0.5 M) and cooled to 0 °C using an ice/water bath. Potassium *tert*-butoxide (1.1 eq.) was added portionwise across several minutes, resulting in the formation of a vibrant orange suspension. This suspension was stirred at 0 °C for one hour. Following this, the corresponding benzaldehyde derivative (1.0 eq.) was added, either by syringe for liquid aldehydes or portionwise for solid aldehydes. As the aldehyde was added, the bright orange color gradually faded, accompanied by the formation of a white precipitate. To simplify purification, the addition of aldehyde should be halted upon the complete disappearance of color. The reaction mixture was stirred and allowed to warm to RT overnight (12-18 hours). After ensuring that the reaction had reached completion by TLC, the reaction mixture was concentrated under reduced pressure to remove THF. Following this, the resulting crude mixture was loaded onto silica gel. The desired product was isolated *via* flash column chromatography (typically using hexane as the eluent). In some cases, distillation is also an effective purification method for more volatile substrates. Styrenes are typically isolated as a mixture of (E)- and (Z)- isomers. This isomeric mixture can be used in the hydroazidation reaction with no effect on yield or reaction efficiency.



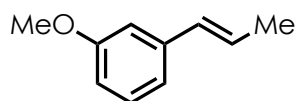
1-(*tert*-butyl)-4-(prop-1-en-1-yl)benzene (3.33)

The alkene was prepared according to the general procedure. Spectral data matches those previously reported.¹⁸⁶



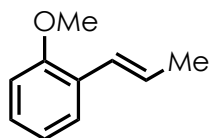
1-methoxy-4-(prop-1-en-1-yl)benzene (3.34)

The alkene was purchased commercially and used with no additional purification.



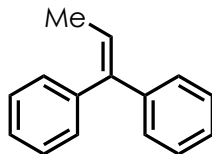
1-methoxy-3-(prop-1-en-1-yl)benzene (3.35)

The alkene was prepared according to the general procedure. Spectral data matched that reported in the literature.¹⁸⁷



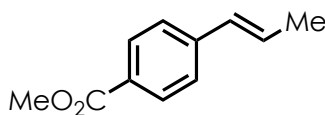
1-methoxy-2-(prop-1-en-1-yl)benzene (3.36)

The alkene was prepared according to the general procedure. Spectral data matched that reported in the literature.¹⁸⁸



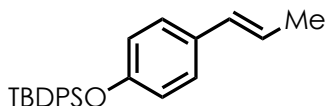
prop-1-ene-1,1-diyl dibenzene (3.37)

The alkene was prepared according to a modified general procedure. Instead of potassium *tert*-butoxide, *n*-butyllithium (1.6 M in hexanes) was used in the deprotonation step, per literature precedent. Spectral data matched that reported in the literature.¹⁸⁹



methyl-4-(prop-1-en-1-yl)benzoate (3.38)

The alkene was purchased commercially and used without further purification.



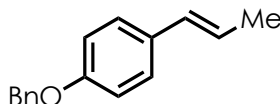
***tert*-butyldiphenyl(4-(prop-1-en-1-yl)phenoxy)silane (3.39)**

The alkene was prepared from the corresponding aldehyde according to the general procedure. The desired product was isolated as a pale yellow semi-solid following purification by flash column chromatography (60% yield, 1.24 g). NMR data is given for mixture of alkene isomers.

¹H NMR (600 MHz, Chloroform-*d*) δ 7.79 – 7.67 (m, 5H), 7.57 – 7.49 (m, 1H), 7.48 – 7.33 (m, 9H), 7.26 – 7.17 (m, 2H), 7.13 – 6.99 (m, 2H), 6.71 (ddt, *J* = 27.1, 8.6, 2.3 Hz, 2H), 6.36 – 6.20 (m, 1H), 6.10 – 5.46 (m, 1H), 1.91 – 1.79 (m, 3H), 1.14 – 1.08 (m, 9H).

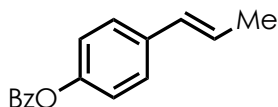
^{13}C NMR (151 MHz, Chloroform-*d*) δ 154.68, 154.21, 135.82, 135.64, 134.93, 133.06, 130.00, 129.90, 129.44, 127.89, 127.39, 126.74, 125.13, 119.80, 119.45, 27.42, 26.64, 19.68, 19.60

HRMS (APCI, positive mode): calculated: 373.1982, found: 373.1983 (M+H)



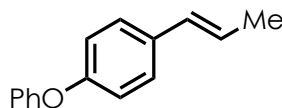
1-(benzyloxy)-4-(prop-1-en-1-yl)benzene (3.40)

The alkene was prepared in two steps starting from 4-hydroxybenzaldehyde. 4-hydroxybenzaldehyde (2.00 g, 16.4 mmol), potassium carbonate (2.94 g, 21.3 mmol), benzyl bromide (3.08 g, 18.0 mmol) were stirred together in DMF (10 mL) and the mixture was heated at 60 °C for one hour. At this time, the mixture was cooled to RT and poured onto water. The resulting mixture was extracted with diethyl ether. The ethereal extracts were washed with brine, dried with magnesium sulfate, and concentrated under reduced pressure to yield the crude product as an oil (60% yield, 2.07 g). This material was used in the next step without further purification. The aldehyde was converted to the alkene product according to the general procedure. The desired product was isolated as a clear oil following purification by column chromatography (66% yield, 1.44 g). Spectral data matched that reported in the literature.¹⁹⁰



4-(prop-1-en-1-yl)phenyl benzoate (3.41)

The alkene was prepared in two steps starting from 4-hydroxybenzaldehyde. 4-hydroxybenzaldehyde (1.50 g, 12.0 mmol), triethylamine (2.5 mL, 18 mmol) and dichloromethane (35 mL) were stirred together in a flame-dried RBF and cooled to 0 °C using an ice/water bath. Benzoyl chloride (2.1 mL, 18 mmol) was added dropwise and the reaction mixture was stirred and warmed to RT overnight. The next day, the reaction mixture was quenched with sodium bicarbonate and extracted with dichloromethane (3 x 30 mL). The combined organic washings were washed with brine, dried with sodium sulfate, and concentrated under reduced pressure to yield the desired product as a yellow oil (quant.). The crude material was used in the next step according to the general procedure to prepare the alkene. The final product was isolated as a clear oil (62% yield, 1.31 g). Spectral data matched that reported in the literature.¹⁹¹



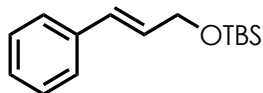
1-phenoxy-4-(prop-1-en-1-yl)benzene (3.42)

The alkene was prepared according to the general procedure using the corresponding, known aldehyde. The desired product was isolated as a pale yellow oil following flash column chromatography as a 2.7:1 ratio of Z/E alkene isomers. NMR data is given for mixture of alkene isomers.

¹H NMR (600 MHz, Chloroform-d) δ 7.40 – 7.27 (m, 4H), 7.11 (t, J = 7.7 Hz, 1H), 7.07 – 6.98 (m, 2H), 6.98 – 6.93 (m, 2H), 6.40 (t, J = 14.6 Hz, 1H), 6.17 (dq, J = 19.4, 6.6 Hz, 1H), 5.77 (dq, J = 11.6, 7.2 Hz, 1H), 1.92 (d, J = 7.1 Hz, 1.5H), 1.89 (d, J = 6.8 Hz, 1.5H).

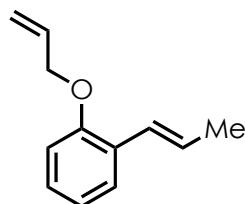
^{13}C NMR (151 MHz, Chloroform- d) δ 157.50, 157.35, 156.07, 155.75, 133.44, 132.91, 130.32, 130.26, 129.86, 129.83, 129.18, 127.19, 126.26, 124.99, 123.34, 123.22, 119.17, 118.97, 118.80, 118.65, 18.63, 14.78.

HRMS (APCI, positive mode): calculated: 211.1174, found: 211.1117 (M+H)



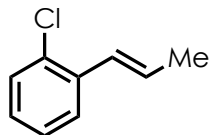
***tert*-butyl(cinnamyloxy)dimethylsilane (3.43)**

The substrate was prepared with a previously reported method.¹⁹² Spectral data matched that reported in the literature.¹⁹²



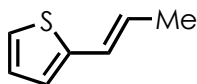
1-(allyloxy)-2-(prop-1-en-1-yl)benzene (3.44)

The corresponding aldehyde starting material was prepared from salicylaldehyde according to a previously reported procedure.¹⁹³ The alkene was prepared according to the general procedure. The desired product was isolated as a pale yellow oil following purification by flash column chromatography (100% hexane) (813 mg, 76% yield). Spectral data matched those previously reported.¹⁹⁴



1-chloro-2-(prop-1-en-1-yl)benzene (3.45)

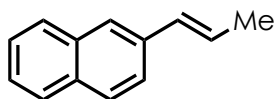
The alkene was prepared according to the general procedure. Spectral data matched that reported in the literature.¹⁹⁵



2-(prop-1-en-1-yl)thiophene (3.46)

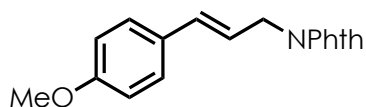
The alkene was prepared according to the general procedure. Spectral data (¹H NMR) matched that reported in the literature.¹⁹⁶

¹³C NMR (151 MHz, Chloroform-*d*) δ 175.70, 136.39, 131.02, 128.52, 128.05, 63.84, 28.13.



2-(prop-1-en-1-yl)naphthalene (3.47)

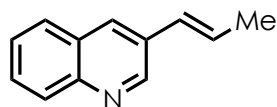
The alkene was prepared according to the general procedure. Spectral data matched that reported in the literature.¹⁹⁷



(*E*)-2-(3-(4-methoxyphenyl)allyl)isoindoline-1,3-dione (3.48)

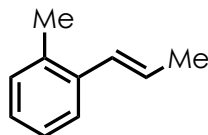
Substrate was prepared according to a previously published procedure. Spectral data matched that reported in the literature.¹⁹⁴

HRMS (APCI, positive mode): calculated: 294.1125, found: 294.1126 (M+H)



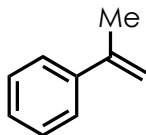
(E)-3-(prop-1-en-1-yl)quinoline (3.49)

The alkene was prepared according to the general procedure. Spectral data matched that reported in the literature.¹⁹⁸



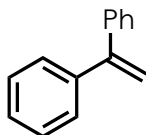
(E)-1-methyl-2-(prop-1-en-1-yl)benzene (3.50)

The alkene was prepared according to the general procedure. Spectral data matched that reported in the literature.¹⁸⁸



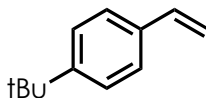
prop-1-en-2-ylbenzene (3.51)

The alkene was purchased commercially and used without further purification.



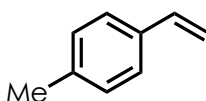
ethene-1,1-diyl dibenzene (3.52)

The alkene was purchased commercially and used without further purification.



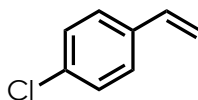
1-*tert*-butyl-4-vinylbenzene (3.53)

The alkene was purchased commercially and used without further purification.



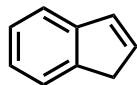
1-methyl-4-vinylbenzene (3.54)

The alkene was purchased commercially and used without further purification.



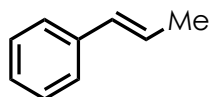
1-chloro-4-vinylbenzene (3.55)

The alkene was purchased commercially and used without further purification.



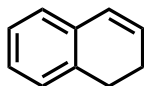
1H-indene (3.56)

The alkene was purchased commercially and used without further purification.



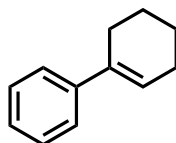
(E)-prop-1-en-1-ylbenzene (3.57)

The alkene was purchased commercially and used without further purification.



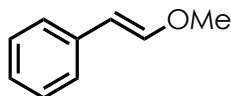
1,2-dihydronaphthalene (3.58)

The alkene was purchased commercially and used without further purification.



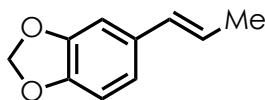
2,3,4,5-tetrahydro-1,1'-biphenyl (3.59)

The alkene was purchased commercially and used without further purification.



(E)-(2-methoxyvinyl)benzene (3.60)

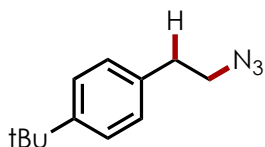
The alkene was purchased commercially and used without further purification.



(E)-5-(prop-1-en-1-yl)benzo[d][1,3]dioxole (3.61)

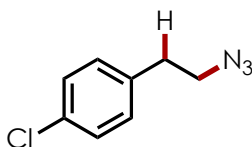
The alkene was purchased commercially and used without further purification.

B.3 Characterization of Hydroazidation Products



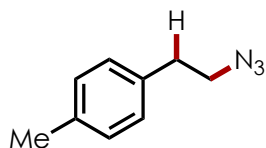
1-(2-azidoethyl)-4-(tert-butyl)benzene (3.1)

Following irradiation, the crude reaction mixture was concentrated under reduced pressure. HMDSO was added as an internal standard and the resulting mixture was dissolved in deuterated chloroform and analyzed by NMR. Integration relative to the internal standard showed the product was formed in 43% yield (n=2).



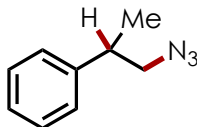
1-(2-azidoethyl)-4-chlorobenzene (3.2)

Following irradiation, the crude reaction mixture was concentrated under reduced pressure. HMDSO was added as an internal standard and the resulting mixture was dissolved in deuterated chloroform and analyzed by NMR. Spectral data matched those previously reported. (22% yield, n = 2).¹⁹⁹



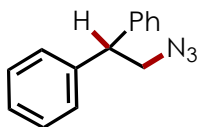
1-(2-azidoethyl)-4-methylbenzene (3.3)

Following irradiation, the crude reaction mixture was concentrated under reduced pressure. HMDSO was added as an internal standard and the resulting mixture was dissolved in deuterated chloroform and analyzed by NMR. Spectral data matched those previously reported. (22% yield, n =2).¹⁹⁹



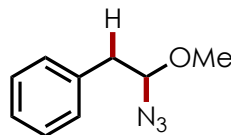
(1-azidopropan-2-yl)benzene (3.4)

Following irradiation, the crude reaction mixture was concentrated under reduced pressure. HMDSO was added as an internal standard and the resulting mixture was dissolved in deuterated chloroform and analyzed by NMR. Spectral data matched those previously reported. (49% yield, n =2).²⁰⁰



(2-azidoethane-1,1-diyl)dibenzene (3.5)

Following irradiation, the crude reaction mixture was concentrated under reduced pressure. HMDSO was added as an internal standard and the resulting mixture was dissolved in deuterated chloroform and analyzed by NMR. Spectral data matched those previously reported (24% yield, n =2).²⁰¹



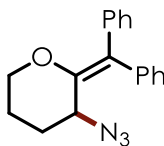
(2-azido-2-methoxyethyl)benzene (3.6)

The desired product was isolated as a pale yellow oil following purification by flash column chromatography (100% hexane \rightarrow 5% EtOAc/hexane gradient). The product was isolated in a 58% yield ($n = 2$).

^1H NMR (400 MHz, Chloroform-*d*) δ 7.45 – 6.98 (m, 5H), 4.49 (t, $J = 6.0$ Hz, 1H), 3.47 (s, 3H), 3.07 (dd, $J = 14.0, 6.2$ Hz, 1H), 2.99 (dd, $J = 14.0, 5.8$ Hz, 1H).

^{13}C NMR (151 MHz, Chloroform-*d*) δ 135.79, 129.65, 128.65, 127.11, 94.67, 56.96, 41.25.

MS (EI): calculated: 177.090, found: 177.00 (M^+)



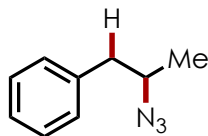
3-azido-2-(diphenylmethylene)tetrahydro-2H-pyran (3.7)

The desired product was isolated following purification by flash column chromatography (79% yield, $n = 2$).

^1H NMR (600 MHz, Chloroform-*d*) δ 7.36 (dd, $J = 8.1, 6.7$ Hz, 2H), 7.32 – 7.25 (m, 5H), 7.25 – 7.17 (m, 3H), 4.31 (t, $J = 3.2$ Hz, 1H), 4.27 (ddt, $J = 11.0, 4.5, 1.9$ Hz, 1H), 3.80 (ddd, $J = 12.4, 11.0, 2.8$ Hz, 1H), 2.29 – 2.17 (m, 1H), 1.97 – 1.90 (m, 1H), 1.88 – 1.80 (m, 1H), 1.63 – 1.51 (m, 1H).

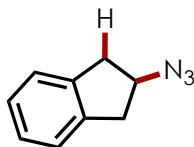
^{13}C NMR (151 MHz, Chloroform-*d*) δ 146.89, 139.35, 138.66, 130.67, 129.86, 128.61, 127.91, 127.49, 127.37, 126.99, 70.09, 56.02, 28.66, 20.37.

HRMS (APCI, positive mode): calculated: 264.1310, found: 264.1382 (M+H, -N₂)



(2-azidopropyl)benzene (3.9)

Following irradiation, the crude reaction mixture was concentrated under reduced pressure to yield a yellow oil. HMDSO was added as an internal standard and the resulting mixture was dissolved in CDCl₃ and analyzed by ¹H NMR to determine yield (98% yield, n=2). Spectral data matched those previously reported.²⁰²



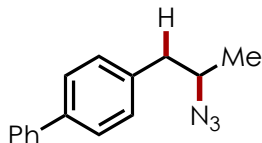
2-azido-2,3-dihydro-1H-indene (3.10)

Following irradiation, the crude reaction mixture was concentrated under reduced pressure and dry loaded onto silica gel. The desired product was isolated as a pale yellow oil following column chromatography (100% hexane -> 1% EtOAc/hex, 52% yield, n=3). Spectral data matched those previously reported.²⁰³

¹H NMR (500 MHz, Chloroform-*d*) δ 7.29 (dd, $J = 5.3, 3.5$ Hz, 2H), 7.26 – 7.17 (m, 2H), 4.40 (dt, $J = 11.1, 6.7, 4.4$ Hz, 1H), 3.28 (dd, $J = 16.2, 6.7$ Hz, 2H), 3.06 (dd, $J = 16.2, 4.4$ Hz, 2H).

¹³C NMR (126 MHz, Chloroform-*d*) δ 140.23, 127.10, 124.77, 61.86, 39.09.

MS (EI): calculated: 159.08, found: 159.10



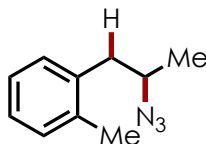
4-(2-azidopropyl)-1,1'-biphenyl (3.11)

Following irradiation, the crude reaction mixture was concentrated under reduced pressure and dry loaded onto silica gel. The desired product was isolated as a pale yellow oil following column chromatography (100% hexane \rightarrow 1% EtOAc/hex, 97% yield, $n=2$). Spectral data matches those previously reported.

^1H NMR (600 MHz, Chloroform-*d*) δ 7.63 (dd, $J = 26.1, 7.7$ Hz, 4H), 7.49 (t, $J = 7.6$ Hz, 2H), 7.39 (t, $J = 7.4$ Hz, 1H), 7.32 (d, $J = 7.8$ Hz, 2H), 3.77 (h, $J = 6.6$ Hz, 1H), 2.92 (dd, $J = 13.7, 7.3$ Hz, 1H), 2.82 (dd, $J = 13.7, 6.4$ Hz, 1H), **1.35 (d, $J = 6.5$ Hz, 3H).**

^{13}C NMR (151 MHz, Chloroform-*d*) δ 140.90, 139.73, 136.91, 129.79, 128.84, 127.29, 127.10, 59.04, 42.24, 19.22.

HRMS (APCI, positive mode): calculated 210.1277, found: 210.1278 (M+H, $-\text{N}_2$)



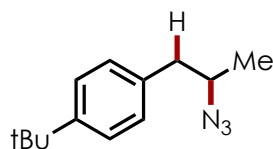
1-(2-azidopropyl)-2-methylbenzene (3.12)

The desired product was isolated as a clear oil following purification by flash chromatography (100% hexane, 76% yield, $n=2$).

^1H NMR (500 MHz, Chloroform-*d*) δ 7.26 – 7.12 (app s., 4H), 3.72 (m, 1H), 2.92 (dd, $J = 13.7, 7.4$ Hz, 1H), 2.77 (dd, $J = 13.7, 6.6$ Hz, 1H), 2.38 (s, 3Hu), **1.33 (d, $J = 6.5$ Hz, 3H).**

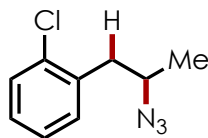
¹³C NMR (126 MHz, Chloroform-*d*) δ 136.40, 136.19, 130.53, 130.20, 126.95, 126.11, 58.36, 39.87, 19.65, 19.42.

HRMS (APCI, positive mode): calculated: 193.1447, found: 193.1423 (M+NH₄)



1-(2-azidopropyl)-4-(tert-butyl)benzene (3.13)

Following irradiation, the crude reaction mixture was concentrated under reduced pressure and dry loaded onto silica gel. The desired product was isolated as a pale yellow oil following column chromatography (100% hexane \rightarrow 1% EtOAc/hex, 51% yield, n=2). Spectral data matched those previously reported.²⁰²



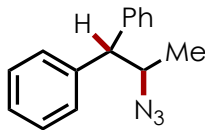
1-(2-azidopropyl)-2-chlorobenzene (3.14)

Following irradiation, the crude reaction mixture was concentrated under reduced pressure and dry loaded onto silica gel. The desired product was isolated as a pale yellow oil following column chromatography (100% hexane \rightarrow 3% EtOAc/hex, 64% yield, n=2).

¹H NMR (600 MHz, Chloroform-*d*) δ 7.40 (dd, $J = 7.2, 1.9$ Hz, 1H), 7.28 (dd, $J = 7.1, 2.3$ Hz, 1H), 7.25 – 7.19 (m, 2H), 3.85 (h, $J = 6.7$ Hz, 1H), 3.00 – 2.84 (m, 2H), 1.33 (d, $J = 6.5$ Hz, 3H).

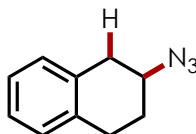
¹³C NMR (151 MHz, Chloroform-*d*) δ 135.70, 134.32, 131.85, 129.74, 128.42, 126.95, 57.57, 40.40, 19.43.

MS (EI): calculated: 195.056, found: 195.05 (M⁺)



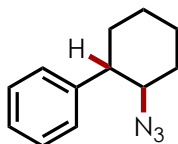
(2-azidopropane-1,1-diyl)dibenzene (3.15)

Following irradiation, the crude reaction mixture was concentrated under reduced pressure and dry loaded onto silica gel. The desired product was isolated as a clear oil following column chromatography (100% hexane -> 1% EtOAc/hex, 66% yield, n=2). Spectral data matched those previously reported.²⁰⁴



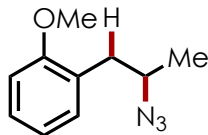
2-azido-1,2,3,4-tetrahydronaphthalene (3.16)

Following irradiation, the crude reaction mixture was concentrated under reduced pressure and dry loaded onto silica gel. The desired product was isolated as a clear oil following column chromatography (100% hexane -> 1% EtOAc/hex, 81% yield, n=2). Spectral data matched those previously reported.²⁰⁵



(2-azidocyclohexyl)benzene (3.17)

Following irradiation, the crude reaction mixture was concentrated under reduced pressure and dry loaded onto silica gel. The desired product was isolated as a clear oil following column chromatography (100% hexane -> 1% EtOAc/Hexanes, 44% yield, n=2) as a single diastereomer. Spectral data matched those previously reported.²⁰⁶



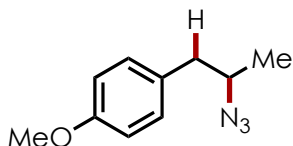
1-(2-azidopropyl)-2-methoxybenzene (3.18)

Following irradiation, the crude reaction mixture was concentrated under reduced pressure and dry loaded onto silica gel. The desired product was isolated as a clear oil following column chromatography (100% hexanes – 5% EtOAc/Hexanes, 75% yield, $n = 2$).

^1H NMR (600 MHz, Chloroform-*d*) δ 7.24 (td, $J = 7.8, 1.7$ Hz, 1H), 7.14 (dd, $J = 7.4, 1.7$ Hz, 1H), 6.91 (td, $J = 7.4, 1.1$ Hz, 1H), 6.86 (dd, $J = 8.1, 1.0$ Hz, 1H), 3.83 (s, 3H), 3.81 – 3.72 (m, 1H), 2.85 (dd, $J = 13.3, 7.3$ Hz, 1H), 2.76 (dd, $J = 13.4, 6.6$ Hz, 1H), 1.24 (d, $J = 6.5$ Hz, 3H).

^{13}C NMR (151 MHz, Chloroform-*d*) δ 157.66, 131.32, 128.23, 126.35, 120.55, 110.38, 57.73, 55.35, 37.51, 19.48

MS (EI): calculated: 191.106, found: 191.10 (M^+)



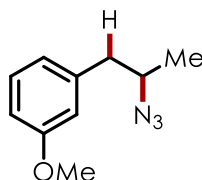
1-(2-azidopropyl)-4-methoxybenzene (3.19)

Following irradiation, the crude reaction mixture was concentrated under reduced pressure and dry loaded onto silica gel. The desired product was isolated as a clear oil following column chromatography (100% hexanes – 5% EtOAc/Hexanes, 90% yield, $n = 2$).

¹H NMR (500 MHz, Chloroform-*d*) δ 7.12 (d, $J = 8.6$ Hz, 2H), 6.85 (d, $J = 8.6$ Hz, 2H), 3.80 (s, 3H), 3.64 (h, $J = 6.6$ Hz, 1H), 2.77 (dd, $J = 13.8, 7.3$ Hz, 1H), 2.67 (dd, $J = 13.8, 6.4$ Hz, 1H), 1.25 (d, $J = 6.5$ Hz, 3H).

¹³C NMR (151 MHz, Chloroform-*d*) δ 158.52, 130.39, 129.92, 114.01, 59.36, 55.39, 41.80, 19.18

MS (EI): calculated: 191.106, found: 191.10 (M⁺)



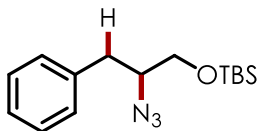
1-(2-azidopropyl)-3-methoxybenzene (3.20)

Following irradiation, the crude reaction mixture was concentrated under reduced pressure and dry loaded onto silica gel. The desired product was isolated as a clear oil following column chromatography (100% hexanes – 5% EtOAc/Hexanes, 80% yield, $n = 2$).

¹H NMR (500 MHz, Chloroform-*d*) δ 7.23 (t, $J = 7.9$ Hz, 1H), 6.89 – 6.68 (m, 3H), 3.81 (s, 3H), 3.68 (p, $J = 6.6$ Hz, 1H), 2.82 (dd, $J = 13.6, 7.3$ Hz, 1H), 2.70 (dd, $J = 13.6, 6.5$ Hz, 1H), 1.27 (d, $J = 6.5$ Hz, 3H).

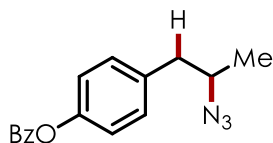
¹³C NMR (126 MHz, Chloroform-*d*) δ 159.77, 139.47, 129.62, 121.76, 115.22, 112.04, 59.07, 55.32, 42.72, 19.31

MS (EI): calculated: 191.106, found: 191.05 (M⁺)



(2-azido-3-phenylpropoxy)(tert-butyl)dimethylsilane (3.21)

Following irradiation, the crude reaction mixture was concentrated under reduced pressure. HMDSO was added as an internal standard and the sample was dissolved in deuterated chloroform and analyzed by NMR. Integration relative to the internal standard showed that the product was formed in 39% yield ($n = 2$).



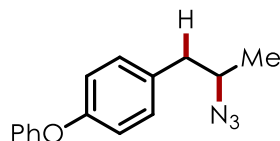
4-(2-azidopropyl)phenyl benzoate (3.22)

Following irradiation, the crude reaction mixture was concentrated under reduced pressure and dry loaded onto silica gel. The desired product was isolated as a clear oil following purification by column chromatography (5 % EtOAc/Hexanes to 30 % EtOAc/Hexanes, 62% yield, $n = 2$).

^1H NMR (600 MHz, Chloroform-*d*) δ 8.20 (dd, $J = 8.3, 1.4$ Hz, 2H), 7.68 – 7.60 (m, 1H), 7.58 – 7.44 (m, 2H), 7.32 – 7.24 (m, 2H), 7.17 (d, $J = 8.4$ Hz, 2H), 3.71 (h, $J = 6.6$ Hz, 1H), 2.86 (dd, $J = 13.7, 7.3$ Hz, 1H), 2.75 (dd, $J = 13.7, 6.4$ Hz, 1H), 1.29 (d, $J = 6.5$ Hz, 3H).

^{13}C NMR (151 MHz, Chloroform-*d*) δ 165.19, 149.76, 135.39, 133.60, 130.33, 130.17, 129.56, 128.58, 121.72, 58.96, 41.97, 19.12.

HRMS (APCI, positive mode): calculated: 254.1175, found: 254.1175 ($\text{M}+\text{H}, -\text{N}_2$)



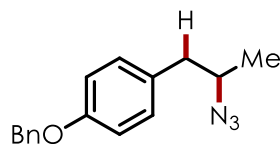
1-(2-azidopropyl)-4-phenoxybenzene (3.23)

The desired product was isolated as a clear oil following purification by column chromatography (100% hexane -> 1 % EtOAc/Hexane, 91% yield, n=2)

¹H NMR (600 MHz, Chloroform-*d*) δ 7.38 – 7.30 (m, 2H), 7.16 (d, *J* = 8.5 Hz, 2H), 7.13 – 7.06 (m, 1H), 7.01 (dd, *J* = 8.7, 1.1 Hz, 2H), 6.96 (d, *J* = 8.5 Hz, 2H), 3.77 – 3.47 (m, 1H), 2.80 (dd, *J* = 13.8, 7.4 Hz, 1H), 2.72 (dd, *J* = 13.8, 6.3 Hz, 1H), 1.28 (d, *J* = 6.5 Hz, 3H).

¹³C NMR (151 MHz, Chloroform-*d*) δ 157.31, 156.03, 132.62, 130.57, 129.72, 123.18, 118.96, 118.78, 59.14, 41.87, 19.16.

HRMS (APCI, positive mode): calculated: 226.1226, found: 226.1227 (M+H, -N₂)



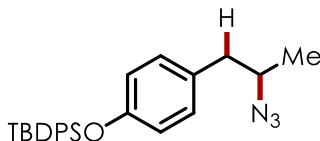
1-(2-azidopropyl)-4-(benzyloxy)benzene (3.24)

The desired product was isolated as clear oil and purified using column chromatography (1 % EtOAc/hexane, Yield: 91 %, n =2).

¹H NMR (500 MHz, Chloroform-*d*) δ 7.44 (d, *J* = 6.9 Hz, 2H), 7.39 (t, *J* = 7.4 Hz, 2H), 7.33 (t, *J* = 7.2 Hz, 1H), 7.12 (d, *J* = 8.6 Hz, 2H), 6.93 (d, *J* = 8.6 Hz, 2H), 5.05 (s, 2H), 3.64 (h, *J* = 6.7 Hz, 1H), 2.77 (dd, *J* = 13.8, 7.3 Hz, 1H), 2.67 (dd, *J* = 13.8, 6.4 Hz, 1H), 1.25 (d, *J* = 6.5 Hz, 3H).

¹³C NMR (151 MHz, Chloroform-*d*) δ 157.69, 137.07, 130.29, 130.12, 128.59, 127.95, 127.49, 114.87, 70.06, 59.20, 41.71, 19.05.

HRMS (APCI, positive mode): calculated: 240.1383, found: 240.1383 (M+H, -N₂)



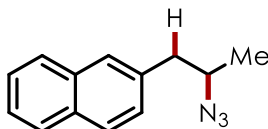
(4-(2-azidopropyl)phenoxy)(tert-butyl)diphenylsilane (3.25)

The desired product was isolated as clear oil following purification by column chromatography (100 % pentane to 100 % hexane, 76% yield, n=2)

¹H NMR (500 MHz, Chloroform-*d*) δ 7.71 (dd, $J = 6.8, 1.3$ Hz, 4H), 7.47 – 7.38 (m, 2H), 7.36 (d, $J = 8.0$ Hz, 4H), 6.91 (d, $J = 8.5$ Hz, 2H), 6.70 (d, $J = 8.5$ Hz, 2H), 3.57 (h, $J = 6.6$ Hz, 1H), 2.69 (dd, $J = 13.8, 7.2$ Hz, 1H), 2.58 (dd, $J = 13.8, 6.5$ Hz, 1H), 1.18 (d, $J = 6.5$ Hz, 3H), 1.09 (s, 9H).

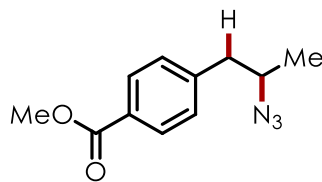
¹³C NMR (151 MHz, Chloroform-*d*) δ 154.40, 135.53, 132.99, 130.17, 130.01, 129.84, 127.73, 119.69, 59.21, 41.80, 26.53, 19.47, 19.04

HRMS (APCI, positive mode): calculated: 388.2018, found: 388.2090 (M+H, -N₂)



2-(2-azidopropyl)naphthalene (3.26)

The desired product was isolated as a clear oil following purification by column chromatography (100% hexane -> 2% EtOAc/hexane, 67% yield, n=2). Spectral data matched those previously reported.²⁰⁷



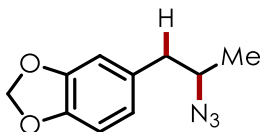
methyl 4-(2-azidopropyl)benzoate (3.27)

The desired product was isolated as clear oil and purified using column chromatography (100 % hexane, 70% yield, n=2)

¹H NMR (600 MHz, Chloroform-*d*) δ 7.99 (d, *J* = 8.2 Hz, 2H), 7.28 (d, *J* = 8.1 Hz, 2H), 3.91 (s, 3H), 3.72 (h, *J* = 6.5 Hz, 1H), 2.87 (dd, *J* = 13.7, 7.5 Hz, 1H), 2.79 (dd, *J* = 13.7, 6.2 Hz, 1H), 1.28 (d, *J* = 6.5 Hz, 3H).

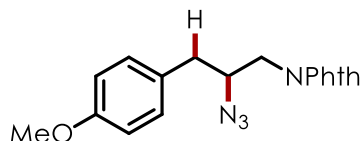
¹³C NMR (151 MHz, Chloroform-*d*) δ 166.94, 143.11, 129.82, 129.35, 128.74, 58.65, 52.08, 42.54, 19.21.

HRMS (APCI, positive mode): calculated: 192.1019, found: 192.1019(M+H, -N₂)



5-(2-azidopropyl)benzo[d][1,3]dioxole (3.28)

The desired product was isolated as a pale yellow oil following purification by column chromatography (100% hexane -> 3% EtOAc/hex, 92% yield, n =2). Spectral data matched those previously reported.²⁰⁸



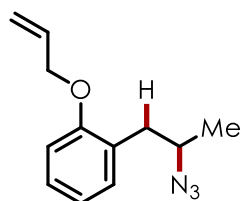
2-(2-azido-3-(4-methoxyphenyl)propyl)isoindoline-1,3-dione (3.29)

The desired product was isolated as a clear oil following purification by flash chromatography (100% hexane \rightarrow 1% EtOAc/hexane gradient, 87% yield, $n = 2$).

^1H NMR (500 MHz, Chloroform-*d*) δ 7.83 (dd, $J = 5.4, 3.0$ Hz, 1H), 7.70 (dd, $J = 5.4, 3.0$ Hz, 1H), 7.16 (d, $J = 8.6$ Hz, 1H), 6.83 (d, $J = 8.6$ Hz, 1H), 3.99 (tt, $J = 8.6, 5.1$ Hz, 1H), 3.82 (dd, $J = 14.0, 8.9$ Hz, 1H), 3.75 (s, 2H), 3.70 (dd, $J = 14.0, 4.6$ Hz, 1H), 2.88 (dd, $J = 14.2, 5.5$ Hz, 1H), 2.81 (dd, $J = 14.2, 8.4$ Hz, 1H).

^{13}C NMR (126 MHz, Chloroform-*d*) δ 168.08, 158.60, 134.17, 131.78, 130.16, 128.44, 123.44, 114.08, 61.52, 55.19, 41.20, 38.01.

HRMS (APCI, positive mode): calculated: 337.1295, found: 337.1295 (M+H)



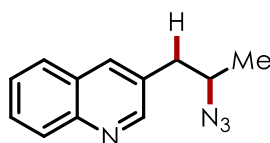
1-(allyloxy)-2-(2-azidopropyl)benzene (3.30)

The desired product was isolated as a clear oil following purification by flash chromatography (100% hexane \rightarrow 1% EtOAc/hexane gradient, 71% yield, $n = 2$).

^1H NMR (600 MHz, Chloroform-*d*) δ 7.30 – 7.24 (m, 1H), 7.21 (dd, $J = 7.4, 1.7$ Hz, 1H), 6.96 (td, $J = 7.4, 1.1$ Hz, 1H), 6.89 (dd, $J = 8.2, 1.0$ Hz, 1H), 6.11 (ddd, $J = 17.3, 10.3, 5.0$ Hz, 1H), 5.46 (dd, $J = 17.3, 1.7$ Hz, 1H), 5.33 (dd, $J = 10.3, 1.5$ Hz, 1H), 4.68 – 4.46 (m, 2H), 3.85 (h, $J = 6.7$ Hz, 1H), 2.95 (dd, $J = 13.3, 7.3$ Hz, 1H), 2.85 (dd, $J = 13.3, 6.7$ Hz, 1H), 1.29 (d, $J = 6.6$ Hz, 3H).

^{13}C NMR (151 MHz, Chloroform-*d*) δ 156.62, 133.42, 131.39, 128.12, 126.59, 120.73, 117.08, 111.63, 68.67, 57.75, 37.57, 19.42.

HRMS (APCI, positive mode): calculated: 190.1226, found: 190.1226 (M+H, -N₂)



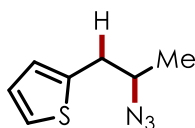
3-(2-azidopropyl)quinoline (3.31)

The desired product was isolated as a clear oil following purification by column chromatography (3% EtOAc/hexane to 30% EtOAc/hexane, 55% yield, *n* = 2).

^1H NMR (600 MHz, Chloroform-*d*) δ 8.79 (d, *J* = 2.2 Hz, 1H), 8.10 (d, *J* = 8.4 Hz, 1H), 8.04 – 7.95 (m, 1H), 7.82 – 7.76 (m, 1H), 7.70 (ddd, *J* = 8.4, 6.9, 1.5 Hz, 1H), 7.55 (ddd, *J* = 8.1, 6.9, 1.2 Hz, 1H), 3.85 – 3.78 (m, 1H), 2.98 (dd, *J* = 14.1, 7.4 Hz, 1H), 2.94 (dd, *J* = 14.0, 6.0 Hz, 1H), 1.35 (d, *J* = 6.5 Hz, 3H).

^{13}C NMR (151 MHz, Chloroform-*d*) δ 151.91, 147.16, 135.82, 130.48, 129.18, 127.93, 126.83, 58.57, 39.79, 19.15.

HRMS (APCI, positive mode): calculated: 185.1073, found: 185.1074 (M+H, -N₂)



2-(2-azidopropyl)thiophene (3.32)

Following irradiation, the reaction mixture was concentrated under reduced pressure to yield a red oil. This oil was dissolved in deuterated chloroform and HMDSO was added as an

internal standard. Yield was then determined *via* NMR spectroscopy (average (n=2) = 65% yield).

¹H NMR (600 MHz, Chloroform-*d*) δ 7.21 (dd, $J = 5.1, 1.2$ Hz, 1H), 6.98 (dd, $J = 5.1, 3.4$ Hz, 1H), 6.91 – 6.88 (m, 1H), 3.74 (h, $J = 6.6$ Hz, 1H), 3.03 (dd, $J = 14.7, 7.1$ Hz, 1H), 2.98 (dd, $J = 14.7, 6.1$ Hz, 1H), 1.32 (d, $J = 6.5$ Hz, 3H).

¹³C NMR (151 MHz, Chloroform-*d*) δ 139.72, 126.99, 126.33, 124.48, 59.03, 36.67, 19.09.

MS (EI): calculated: 167.051, found: 167.05 (M⁺)

APPENDIX C: EXPERIMENTAL DATA FOR CHAPTER 4

C.1 General Experimental Information

General Reagent Information

Commercially available reagents were purchased from Sigma Aldrich, TCI Corporation, Combi-Blocks, Matrix Scientific, Oakwood Chemical, and Fisher Scientific and were used without further purification. Fluorinated solvents (TFE and HFIP) were purchased from Oakwood Chemical and were used as received unless otherwise noted.

General Analytical Information

Proton, carbon, and fluorine nuclear magnetic resonance spectra (^1H NMR, ^{13}C NMR, and ^{19}F NMR) were obtained using a Bruker AVANCE III Nanobay 400 (^1H NMR at 400 MHz, ^{13}C NMR at 100 MHz, ^{19}F at 376 MHz), Bruker AVANCE NEO 400 (^1H NMR at 400 MHz, ^{13}C NMR at 100 MHz, ^{19}F at 376 MHz), or Bruker AVANCE III 600 (^1H NMR at 600 MHz, ^{13}C NMR at 151 MHz, ^{19}F at 565 MHz) spectrometers. Unless otherwise noted, ^1H NMR and ^{13}C NMR spectra are referenced to Chloroform- d (^1H NMR: 7.26 ppm and ^{13}C NMR: 77.16 ppm), and ^{19}F NMR are referenced to fluorobenzene (-112.96 ppm).²⁰⁹ All spectra are reported as parts per million. ^1H , ^{13}C , and ^{19}F NMR data are reported as follows: chemical shift (ppm), multiplicity (s = singlet, d = doublet, t = triplet, q = quartet, quint = quintet, dd = doublet of doublets, td = triplet of doublets, ddd = double of doublet of doublets, m = multiplet, app = apparent), coupling constants (Hz), and integration.

Low resolution mass spectrometry data was obtained using an Agilent Technologies 5977E MSD GC/MS unit with electron impact (EI) ionization.

Flash chromatography was performed using SiliaFlash P60 silica gel (40-63 μm) that was purchased from Silicycle.

Yield refers to the isolated yield of analytically pure material unless otherwise noted. All defluorinated products were isolated multiple times and reported yields are averages of two trials unless otherwise noted.

General Photoreactor Configuration

Reactions were irradiated using one Kessil lamp (427 nm or 456 nm) while stirring on stir plates purchased from IKA (various models). A foil barrier was erected to prevent dual irradiation (see photo below). The reactions were placed approximately 3 cm away from the LEDs, and an external cooling fan was used to ensure that temperatures above 50 °C were not reached (ranged from 45-50°C on average).



C.2 Electrochemical and Photophysical Methods

Electrochemistry Methods

Cyclic voltammetry was performed using a Pine Instruments WaveNow potentiostat with a standard three electrode setup: working (glassy carbon), reference (Ag/AgCl in 3 M NaCl), and counter (platinum wire). All measurements were taken at a substrate concentration of 5.0 mM in degassed MeCN with 0.1 M tetrabutylammonium hexafluorophosphate as a supporting electrolyte. Experiments were conducted at a scan rate of 100 mV/s. The glassy carbon working electrode was polished between scans. Voltammograms have been corrected by subtracting the background current of the electrolyte from that of the substrate. Ground

state reduction potentials [$E_{1/2}(C/C\cdot)$ for completely reversible waves, $E_{p/2}$ for irreversible waves] were identified as half of the absolute maximum current during the reduction event. The values obtained were referenced to Saturated Calomel Electrode (SCE) by subtracting 0.030 V from the potential measured against Ag/AgCl.

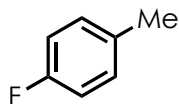
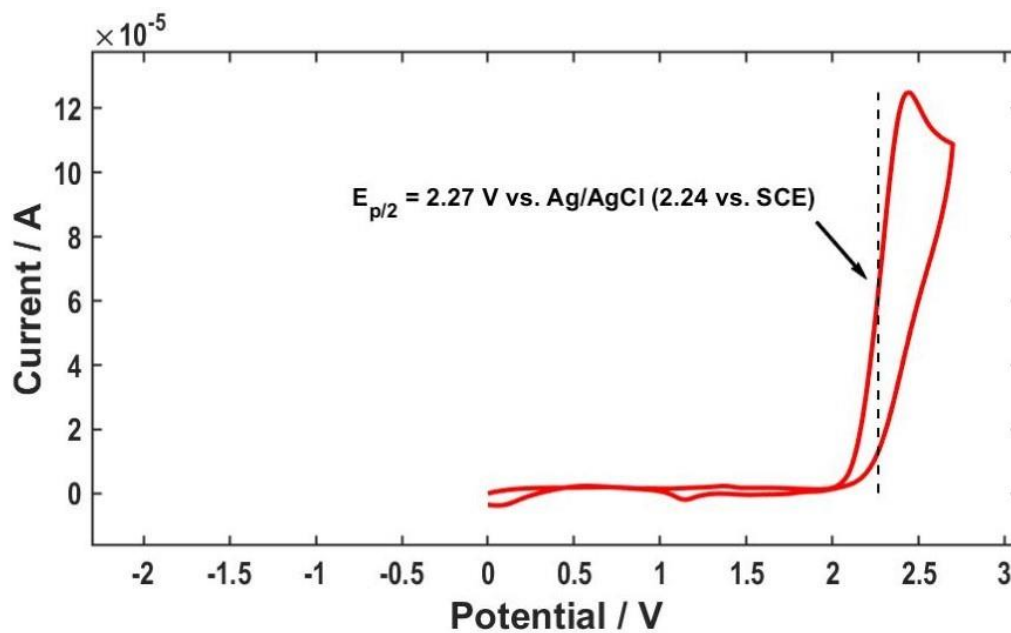


Figure C-1. CV of 4-Fluorotoluene



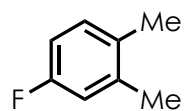
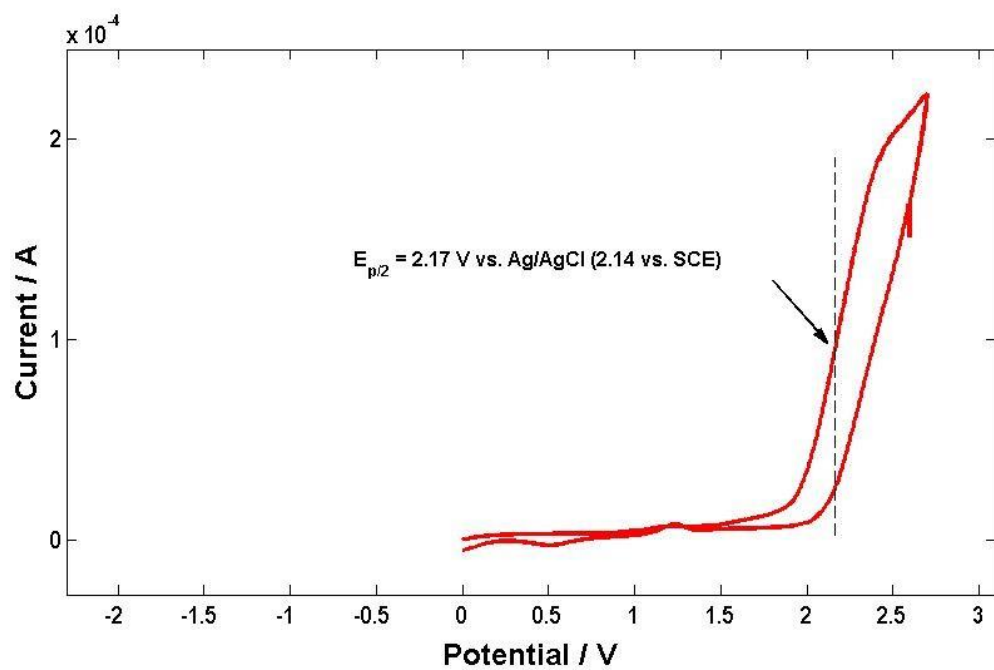


Figure C-2. CV of 3,4-Dimethyl-fluorobenzene



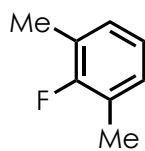
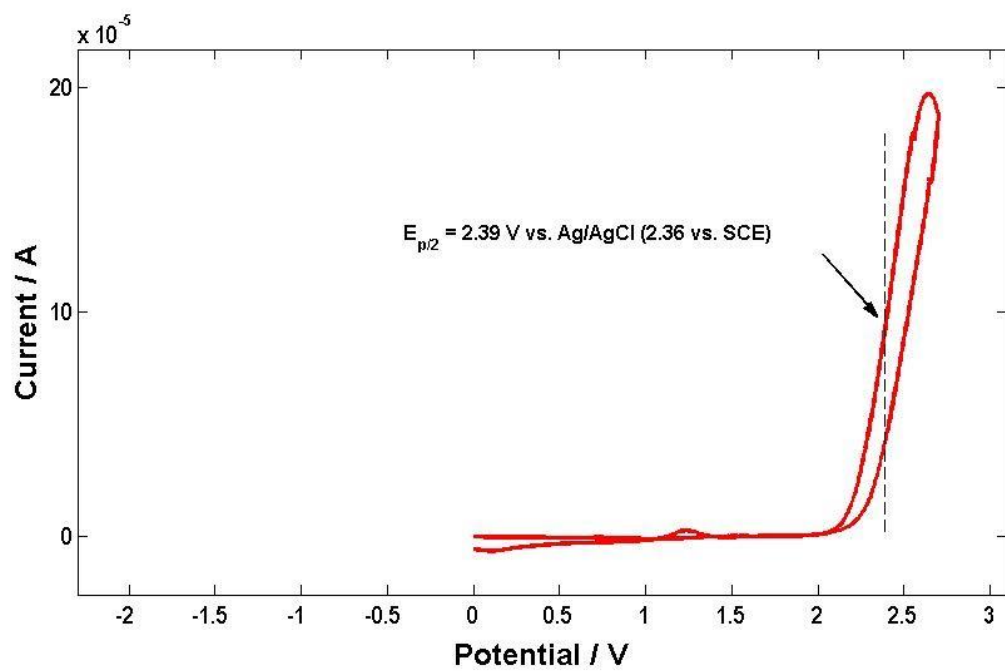


Figure C-3. CV of 2,6-Dimethyl-fluorobenzene



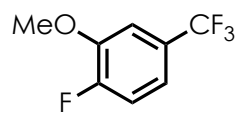
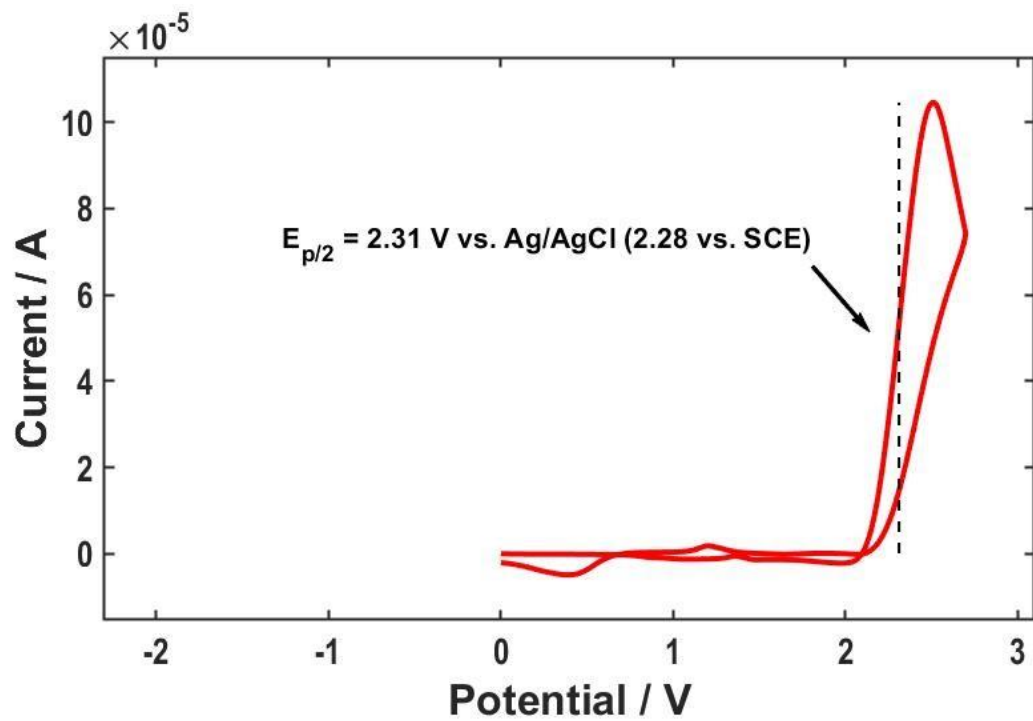


Figure C-4. CV of 2-Fluoro-5-trifluoromethylanisole



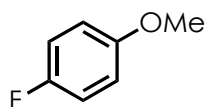
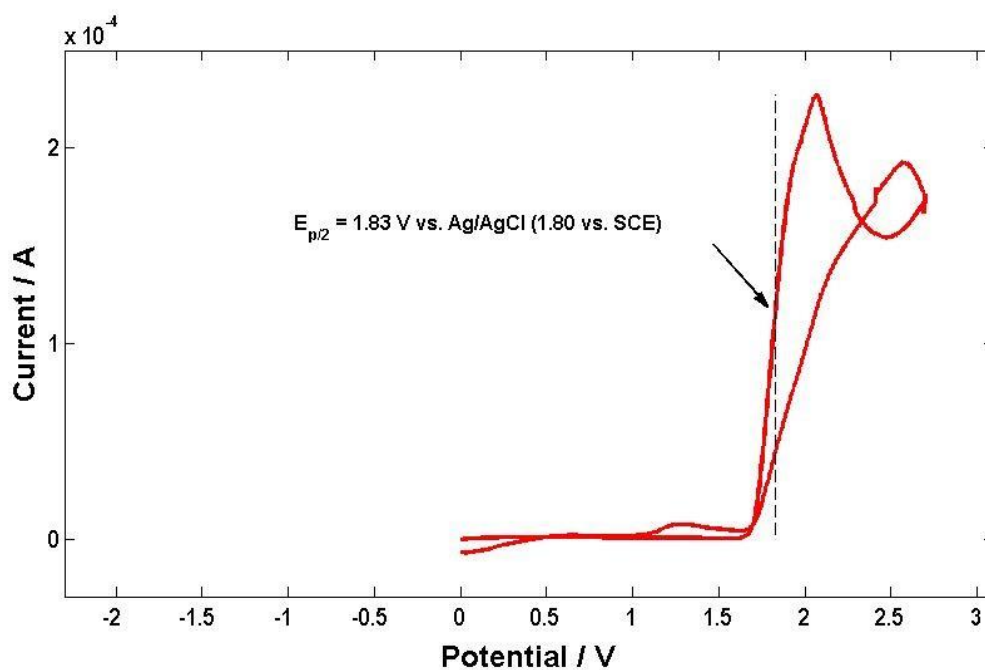


Figure C-5. CV of 4-Fluoroanisole



Photophysical Methods and Measurements

Samples for photophysical measurements were prepared using spectrophotometric grade 1,2-dichloroethane (DCE). Solutions of xanthylium salts were prepared at a concentration of 16 μM , transferred to a 4 mL quartz cell, and sealed with a PTFE-lined screw cap. Absorbance spectra were recorded on a Varian Cary 50 Bio UV-Visible spectrophotometer. The solvent absorbance background was subtracted from the reported spectra. Steady state emission spectra were recorded on a Varian Cary Eclipse fluorescence spectrophotometer.

Excited state reduction potentials [$E_{1/2\text{red}}(\text{C}^*/\text{C}^-)$] were calculated by adding the ground-state reduction potential [$E_{1/2}(\text{C}/\text{C}^-)$], obtained *via* cyclic voltammetry, with the excited state energy ($E_{0,0}$). The excited state energy is the energy corresponding to the wavelength at which the normalized absorption and emission spectra intersect.

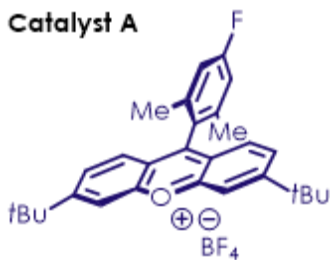


Figure C-6. Absorption and Emission Spectra for **Catalyst A**

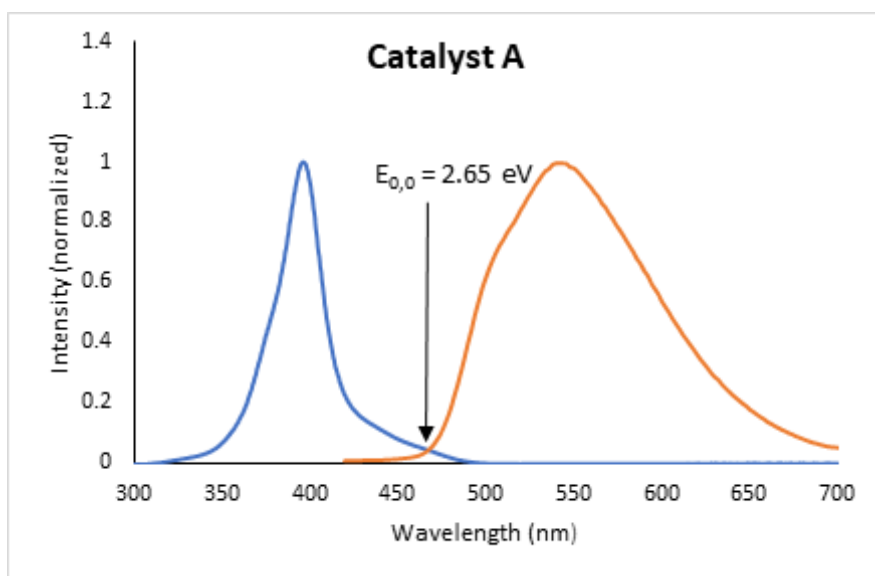
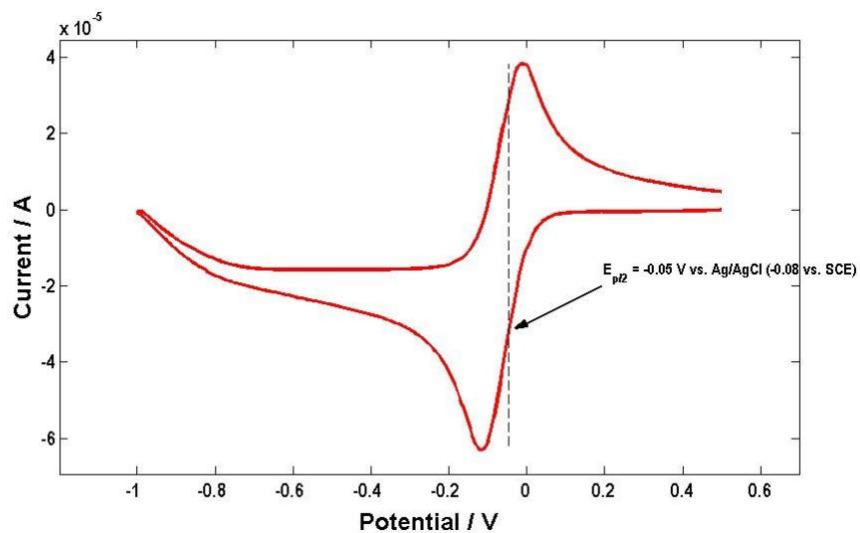


Figure C-7. CV of Catalyst A



$$E_{0,0} = 2.65 \text{ eV}$$

$$E_{1/2}(C/C^-) = -0.08 \text{ V vs. SCE}$$

$$E_{1/2\text{red}}(C^*/C^-) = 2.65 + (-0.08) = + 2.57 \text{ V vs. SCE}$$

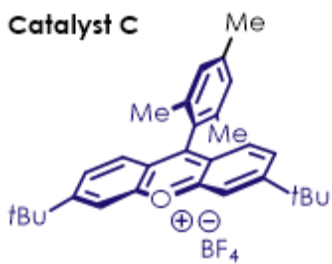


Figure C-8. Absorption and Emission Spectra for **Catalyst C**

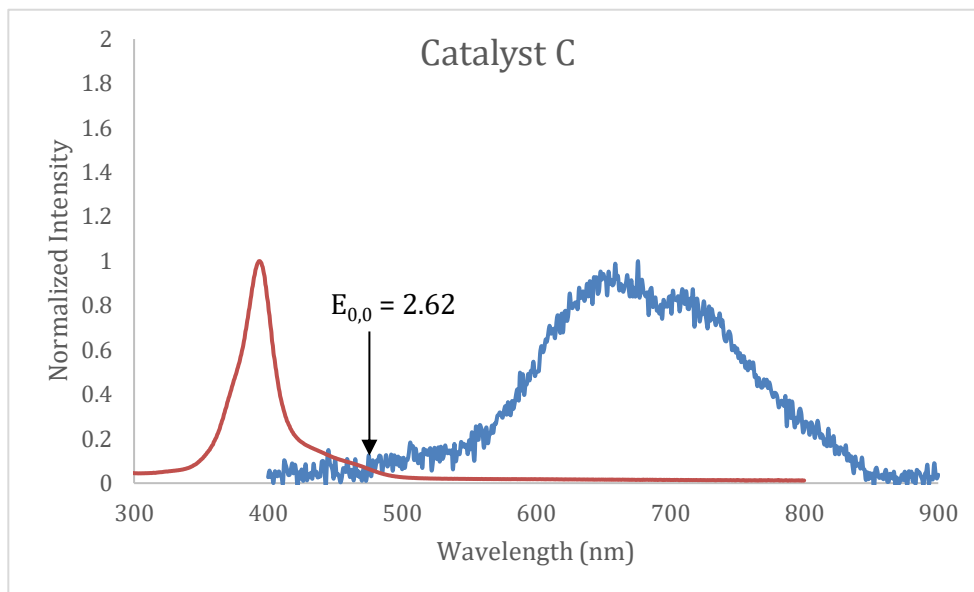
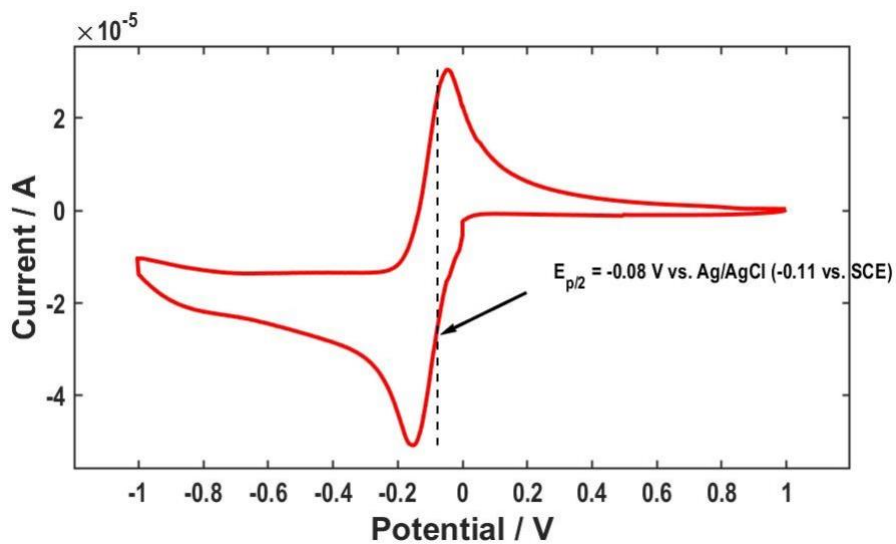


Figure C-9. CV of **Catalyst C**



$$E_{0,0} = 2.62 \text{ eV}$$

$$E_{1/2}(C/C^-) = -0.11 \text{ V vs. SCE}$$

$$E_{1/2\text{red}}(C^*/C^-) = 2.62 + (-0.11) = + 2.51 \text{ V vs. SCE}$$

Note: Due to the noise present in the fluorescence spectrum, the intersection between the two curves was estimated to reside at 474 nm. This noisy signal is presumably due to intramolecular charge transfer in the excited state. Current efforts in the lab are on-going to further study the photophysics of xanthylium salt catalysts.



Figure C-10. Absorption and Emission Spectra for **Catalyst D**

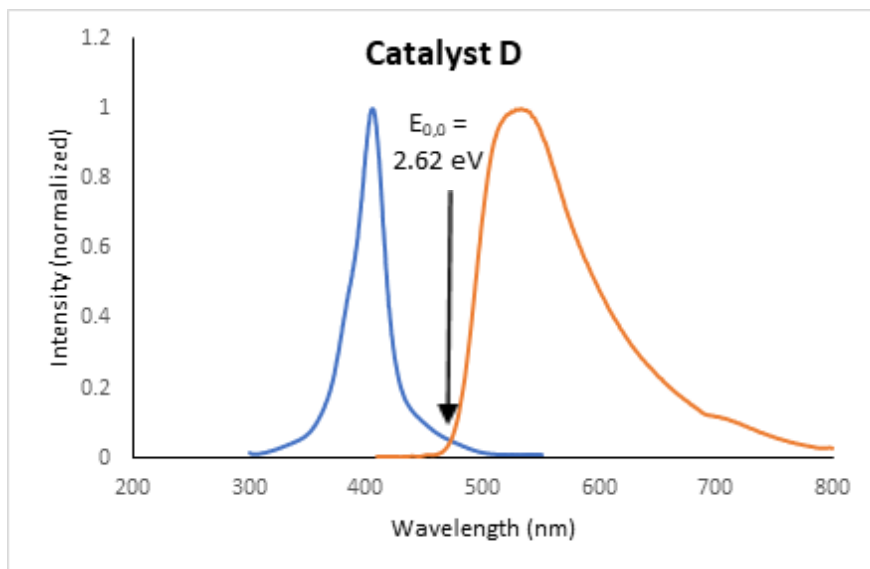
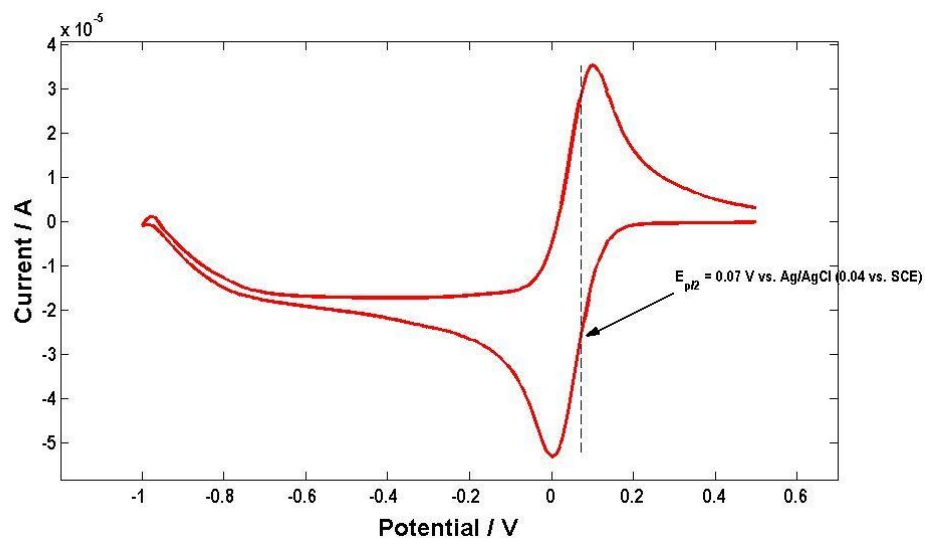


Figure C-11. CV of Catalyst D



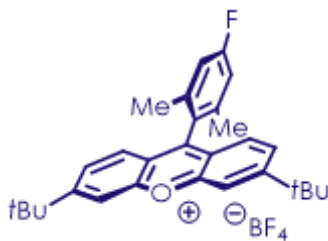
$$E_{0,0} = 2.62 \text{ eV}$$

$$E_{1/2}(\text{C}/\text{C}\cdot) = 0.04 \text{ V vs. SCE}$$

$$E_{1/2\text{red}}(\text{C}^*/\text{C}\cdot) = 2.62 + (0.04) = + 2.66 \text{ V vs. SCE}$$

C.3 Synthesis and Characterization of Catalysts and Substrates

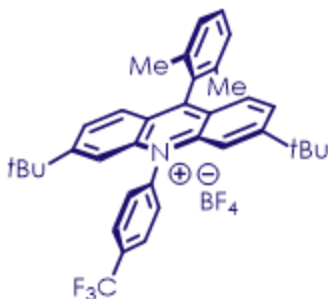
Photoredox Catalyst Synthesis and Characterization



3,6-di-*tert*-butyl-9-(4-fluoro-2,6-dimethylphenyl)xanthylium tetrafluoroborate (Catalyst

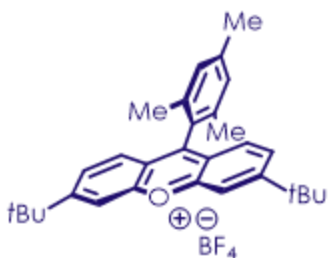
A)

The title compound was prepared according to literature procedure. Spectral data align with literature values.³³



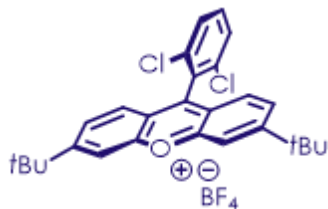
**3,6-di-*tert*-butyl-9-(2,6-dimethylphenyl)-10-(4-(trifluoromethyl)phenyl)acridin-10-ium
tetrafluoroborate (Catalyst B)**

The title compound was prepared according to literature procedures. Spectral data align with literature values.³³



3,6-di-*tert*-butyl-9-mesitylxanthylum tetrafluoroborate (Catalyst C)

The title compound was prepared according to literature procedures. Spectral data align with literature values.³³



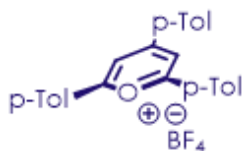
3,6-di-tert-butyl-9-(2,6-dichlorophenyl)xanthylium tetrafluoroborate (Catalyst D)

The title compound was prepared according to literature procedures. Spectral data align with literature values.³³



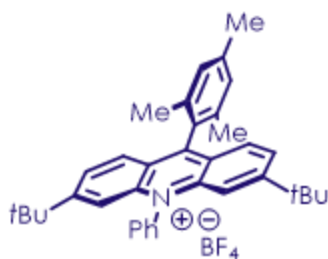
3,6-di-tert-butyl-9-(2,4,6-trimethylpyrimidin-5-yl)xanthylium tetrafluoroborate (Catalyst E)

The title compound was prepared according to literature procedures. Spectral data align with literature values.³³



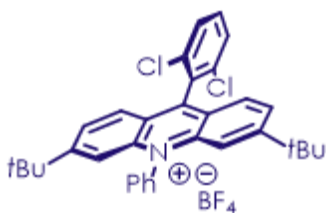
2,4,6-tri-p-tolylpyrylium tetrafluoroborate (Catalyst F)

The title compound was prepared according to literature procedures. Spectral data align with literature values.²¹⁰



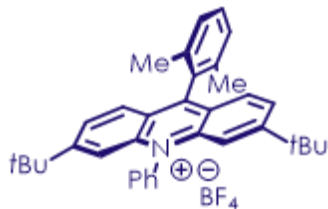
3,6-di-*tert*-butyl-9-mesityl-10-phenylacridin-10-ium tetrafluoroborate (Catalyst G)

The title compound was prepared according to literature procedures. Spectral data align with literature values.³³



3,6-di-*tert*-butyl-9-(2,6-dichlorophenyl)-10-phenylacridin-10-ium tetrafluoroborate (Catalyst H)

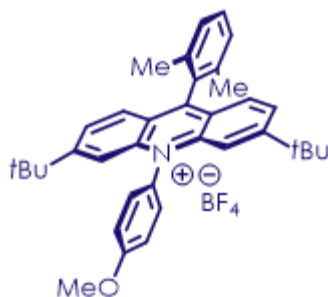
The title compound was prepared according to literature procedures. Spectral data align with literature values.³³



3,6-di-*tert*-butyl-9-(2,6-dimethylphenyl)-10-phenylacridin-10-ium

tetrafluoroborate (Catalyst I)

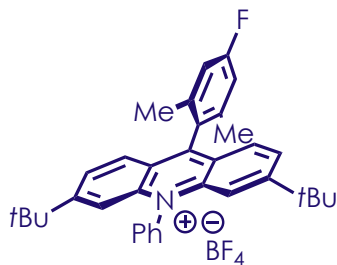
The title compound was prepared according to literature procedures. Spectral data align with literature values.³³



3,6-di-*tert*-butyl-9-(2,6-dimethylphenyl)-10-(4-methoxyphenyl)acridin-10-ium

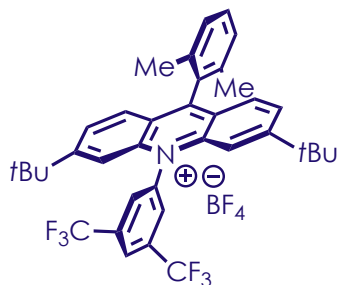
tetrafluoroborate (Catalyst J)

The title compound was prepared according to literature procedures. Spectral data align with literature values.³³



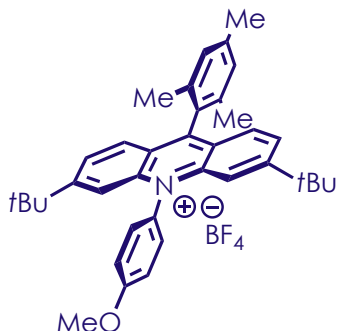
**3,6-di-*tert*-butyl-9-(4-fluoro-2,6-dimethylphenyl)-10-phenylacridin-10-ium
tetrafluoroborate (Catalyst K)**

The title compound was prepared according to literature procedures. Spectral data align with literature values.³³



**10-(3,5-bis(trifluoromethyl)phenyl)-3,6-di-*tert*-butyl-9-(2,6-dimethylphenyl)acridin-10-ium
tetrafluoroborate (Catalyst L)**

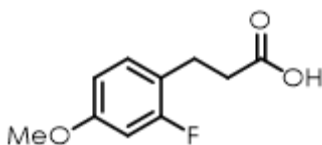
The title compound was prepared according to literature procedures. Spectral data align with literature values.³³



3,6-di-*tert*-butyl-9-mesityl-10-(4-methoxyphenyl)acridin-10-ium tetrafluoroborate
(Catalyst M)

The title compound was prepared according to literature procedures. Spectral data align with literature values.³³

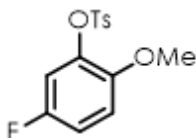
Substrate Synthesis and Characterization



3-(2-fluoro-4-methoxyphenyl)propanoic acid (4.50)

The title compound was prepared from 2-fluoro-4-methoxybenzaldehyde by adaptation of an existing literature protocol.²¹¹ Spectral data (¹H and ¹³C NMR spectra, mass spectrometry data) align with literature values.²¹²

¹⁹F NMR (565 MHz, CDCl₃) δ -116.2 (dd, J = 11.8, 9.1 Hz).

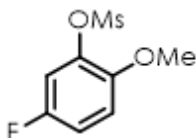


5-fluoro-2-methoxyphenyl 4-methylbenzenesulfonate (4.51)

The title compound was prepared from 5-fluoro-2-methoxyphenol by adaptation of an existing literature protocol.²¹³

¹H NMR (600 MHz, CDCl₃) δ 7.76 (d, J = 8.4 Hz, 1H), 7.31 (d, J = 8.3 Hz, 2H), 6.92 (td, J = 8.1, 3.3 Hz, 2H), 6.82 – 6.74 (m, 1H), 3.55 (s, 1H), 2.45 (s, 2H).

¹³C NMR (151 MHz, CDCl₃) δ 155.9 (d, J = 241.2 Hz), 148.5 (d, J = 3.0 Hz), 145.5, 138.3 (d, J = 10.9 Hz), 132.9, 129.6, 128.7, 114.2 (d, J = 22.6 Hz), 113.1 (d, J = 8.9 Hz), 112.1 (d, J = 25.9 Hz), 56.1, 21.8.



5-fluoro-2-methoxyphenyl methanesulfonate (4.52)

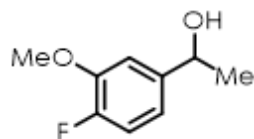
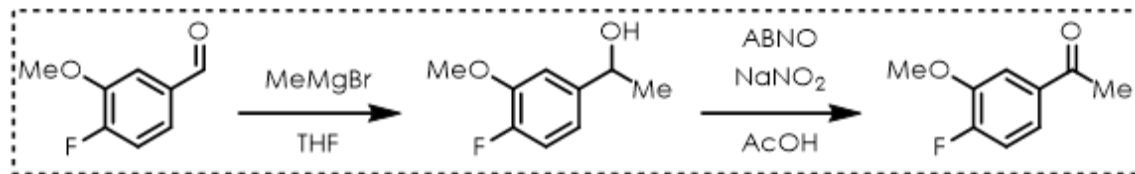
The title compound was prepared from 5-fluoro-2-methoxyphenol by adaptation of an existing literature protocol.²¹⁴

¹H NMR (600 MHz, CDCl₃) δ 7.07 (dd, J = 8.2, 3.0 Hz, 1H), 6.99 (tdd, J = 7.7, 3.5, 1.0 Hz, 1H), 6.94 (dd, J = 9.1, 5.0 Hz, 1H), 3.86 (s, 3H), 3.19 (s, 3H).

¹³C NMR (151 MHz, CDCl₃) δ 156.1 (d, J = 242.2 Hz), 148.1 (d, J = 3.3 Hz), 138.2 (d, J = 10.7 Hz), 114.6 (d, J = 22.6 Hz), 113.4 (d, J = 9.0 Hz), 112.7 (d, J = 26.0 Hz), 56.6, 38.5.

LRMS (EI): Calculated for C₈H₉FO₄S [M]⁺ : 220.02, found: 220.00.

Scheme C-1. Synthesis of 4.54



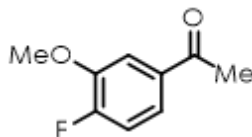
1-(4-fluoro-3-methoxyphenyl)ethan-1-ol (4.53)

To a flame dried 50 mL round bottom flask equipped with stirbar was added 4-fluoro-3-methoxybenzaldehyde (771 mg, 5.00 mmol, 1 equiv.) and dry THF (7 mL). The solution was cooled to 0°C for 5 minutes, after which time methylmagnesium bromide (2.86 M, 2.10 mL, 6.00 mmol, 1.2 equiv.) was added dropwise under N₂. The flask slowly warmed to room temperature and stirred for 8 hours. The reaction was quenched with 1 M HCl and diluted with EtOAc. The aqueous layer was extracted with EtOAc (3 x 25 mL). The combined organic layers were washed with brine (1 x 25 mL) and dried over sodium sulfate. The crude product was purified by filtering over a pad of silica gel (30% EtOAc in Hex). The title compound was isolated as a light-yellow oil (736 mg, 87%).

¹H NMR (600 MHz, CDCl₃) δ 7.05 – 6.99 (m, 2H), 6.86 (ddd, J = 8.3, 4.3, 2.1 Hz, 1H), 4.87 (q, J = 6.5 Hz, 1H), 3.90 (s, 3H), 1.76 (s, 1H), 1.48 (d, J = 6.5 Hz, 3H).

¹³C NMR (151 MHz, CDCl₃) δ 151.8 (d, J = 245.1 Hz), 147.8 (d, J = 10.7 Hz), 142.4 (d, J = 3.6 Hz), 117.7 (d, J = 6.9 Hz), 115.9 (d, J = 18.5 Hz), 110.7 (d, J = 2.1 Hz), 70.2, 56.4, 25.5.

¹⁹F NMR (376 MHz, CDCl₃) δ -137.12 (ddd, J = 11.8, 8.1, 4.3 Hz).



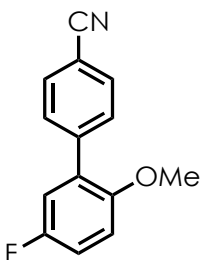
1-(4-fluoro-3-methoxyphenyl)ethan-1-one (4.54)

The title compound was prepared from 1-(4-fluoro-3-methoxyphenyl)ethan-1-ol by adaptation of an existing literature protocol.²¹⁵

¹H NMR (600 MHz, CDCl₃) δ 7.61 (dd, J = 8.3, 2.1 Hz, 1H), 7.52 (ddd, J = 8.3, 4.3, 2.1 Hz, 1H), 7.13 (dd, J = 10.6, 8.3 Hz, 1H), 3.94 (s, 3H), 2.59 (s, 3H).

¹³C NMR (151 MHz, CDCl₃) δ 196.7, 155.8 (d, J = 255.2 Hz), 148.1 (d, J = 11.0 Hz), 134.0 (d, J = 3.6 Hz), 122.6 (d, J = 8.0 Hz), 116.0 (d, J = 19.2 Hz), 112.7 (d, J = 3.3 Hz), 56.4, 26.6.

¹⁹F NMR (376 MHz, CDCl₃) δ -126.92 (ddd, J = 11.6, 8.2, 4.1 Hz).



5'-fluoro-2'-methoxy-[1,1'-biphenyl]-4-carbonitrile (4.55)

To a flame dried 100 mL round bottom flask equipped with stirbar was added (5-fluoro-2-methoxyphenyl)boronic acid (892 mg, 5.25 mmol, 1.05 equiv.), 4-bromobenzonitrile (910 mg, 5.0 mmol, 1 equiv.), and potassium carbonate (2.07 g, 15.0 mmol, 3 equiv.). The flask was brought into the glovebox where Pd(PPh₃)₄ (289 mg, 0.25 mmol, 0.05 equiv.) was added. Outside the glovebox, water (11 mL) and DME (32 mL) were added *via* syringe. The

reaction was stirred and heated at 80°C overnight. After this time, the reaction was quenched with 3 M HCl and diluted with EtOAc. The aqueous layer was extracted with EtOAc (3 x 50 mL). The combined organic layers were washed with saturated aqueous sodium bicarbonate (1 x 50 mL), brine (1 x 50 mL), and dried over sodium sulfate. The crude product was purified by column chromatography using gradient elution (10 – 20% EtOAc in Hex). The title compound was isolated as a white solid (880 mg, 77%).

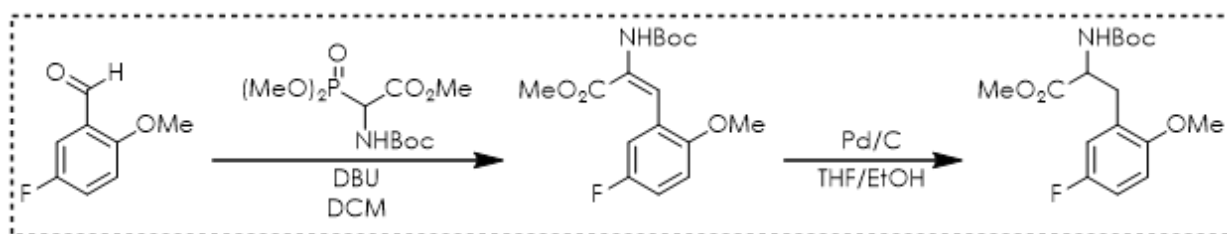
¹H NMR (600 MHz, CDCl₃) δ 7.70 (d, J = 8.4 Hz, 2H), 7.62 (d, J = 8.4 Hz, 2H), 7.07 (ddd, J = 8.9, 7.8, 3.1 Hz, 1H), 7.03 (dd, J = 8.8, 3.1 Hz, 1H), 6.93 (dd, J = 9.0, 4.4 Hz, 1H), 3.80 (s, 3H).

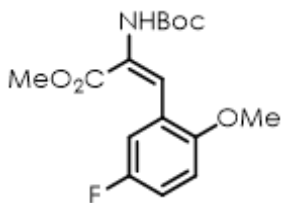
¹³C NMR (151 MHz, CDCl₃) δ 157.2 (d, J = 239.7 Hz), 152.6 (d, J = 2.3 Hz), 142.3, 132.0, 130.3, 129.8 (d, J = 7.5 Hz), 119.1, 117.3 (d, J = 23.7 Hz), 115.9 (d, J = 22.6 Hz), 112.6 (d, J = 8.2 Hz), 111.1, 56.3.

¹⁹F NMR (376 MHz, CDCl₃) δ -123.29 (td, J = 8.2, 4.4 Hz).

LRMS (EI): Calculated for C₁₄H₁₀FNO [M]⁺: 227.07, found: 227.10.

Scheme C-2. Synthesis of **4.57**





methyl (E)-2-((tert-butoxycarbonyl)amino)-3-(5-fluoro-2-methoxyphenyl)acrylate (4.56)

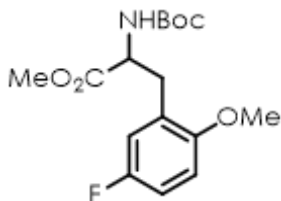
To a flame dried 25 mL round bottom flask equipped with stirbar was added methyl 2-((tert-butoxycarbonyl)amino)-2-(dimethoxyphosphoryl)acetate (1.74 g, 5.84 mmol, 1.2 equiv.), DBU (741 mg, 0.73 mL, 4.87 mmol, 1 equiv.), and DCM (4 mL). This was stirred for 15 minutes under an atmosphere of N₂. Separately, a solution of 5-fluoro-2-methoxybenzaldehyde (750 mg, 4.87 mmol, 1 equiv.) in DCM (4 mL) was prepared. The aldehyde solution was added to the stirred round bottom flask and allowed to react overnight. The reaction was diluted with water and transferred to a separatory funnel. The aqueous was separated and extracted with DCM (3 x 25 mL). The combined organic layers were washed with saturated aqueous ammonium chloride solution (1 x 25 mL), dried over sodium sulfate, and concentrated in vacuo. The crude product was purified by flash column chromatography using gradient elution (10 – 20% EtOAc in Hex). The title compound was isolated as a white solid (971 mg, 61%).

¹H NMR (600 MHz, CDCl₃) δ 7.40 – 7.30 (m, 1H), 7.28 – 7.24 (m, 1H), 6.98 (ddd, *J* = 8.9, 7.7, 3.1 Hz, 1H), 6.83 (dd, *J* = 9.1, 4.5 Hz, 1H), 6.44 (s, 1H), 3.85 (s, 3H), 3.85 (s, 3H), 1.39 (s, 8H).

¹³C NMR (151 MHz, CDCl₃) δ 166.0, 156.6 (d, *J* = 238.2 Hz), 153.4, 152.3, 124.4 (d, *J* = 8.2 Hz), 122.3, 116.5, 116.3, 115.7 (d, *J* = 24.0 Hz), 111.9 (d, *J* = 8.3 Hz), 81.0, 56.3, 52.7,

28.1.

^{19}F NMR (376 MHz, CDCl_3) δ -123.79 (s).



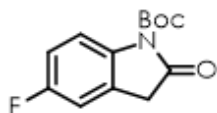
methyl 2-((tert-butoxycarbonyl)amino)-3-(5-fluoro-2-methoxyphenyl)propanoate (4.57)

To a 100 mL round bottom flask with stirbar was added methyl (E)-2-((tert-butoxycarbonyl)amino)-3-(5-fluoro-2-methoxyphenyl)acrylate (936.4 mg, 2.88 mmol, 1 equiv.), 10% palladium on carbon (31 mg, .29 mmol, 0.10 equiv.), THF (20 mL), and EtOH (10 mL). The flask was evacuated and backfilled with a H_2 balloon (3x). The flask was stirred overnight. After this time, the reaction mixture was filtered over a plug of celite, eluted with EtOAc, and concentrated in vacuo. The title compound was isolated as a white solid (927 mg, 98%).

^1H NMR (600 MHz, CDCl_3) δ 6.89 (td, J = 8.5, 3.1 Hz, 1H), 6.81 (dd, J = 8.7, 3.1 Hz, 1H), 6.76 (dd, J = 8.9, 4.4 Hz, 1H), 5.18 (d, J = 8.2 Hz, 1H), 4.51 (td, J = 7.9, 5.5 Hz, 1H), 3.79 (s, 3H), 3.70 (s, 3H), 3.08 (dd, J = 13.6, 5.5 Hz, 1H), 2.98 (dd, J = 13.6, 7.8 Hz, 1H), 1.37 (s, 9H).

^{13}C NMR (151 MHz, CDCl_3) δ 172.7, 156.8 (d, J = 238.7 Hz), 155.3, 153.9, 126.4 (d, J = 7.5 Hz), 118.0 (d, J = 23.1 Hz), 114.2 (d, J = 22.6 Hz), 111.2 (d, J = 8.3 Hz), 79.8, 56.0, 53.8, 52.3, 33.0, 28.3.

^{19}F NMR (565 MHz, CDCl_3) δ -124.09 (q, J = 7.9 Hz).



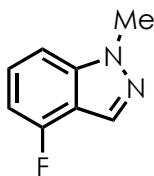
tert-butyl 5-fluoro-2-oxoindoline-1-carboxylate (**4.58**)

The title compound was prepared from 5-fluoroindolin-2-one by adaptation of an existing literature protocol.²¹⁶

¹H NMR (600 MHz, CDCl₃) δ 7.75 (dd, $J = 8.9, 4.6$ Hz, 1H), 6.96 (ddt, $J = 10.5, 4.9, 2.6$ Hz, 2H), 3.62 (s, 2H), 1.62 (s, 9H).

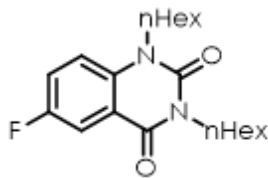
¹³C NMR (151 MHz, CDCl₃) δ 172.7, 159.8 (d, $J = 243.2$ Hz), 149.2, 137.1 (d, $J = 2.6$ Hz), 125.0 (d, $J = 8.8$ Hz), 116.4 (d, $J = 8.0$ Hz), 114.7 (d, $J = 22.7$ Hz), 111.9 (d, $J = 24.4$ Hz), 84.7, 36.8 (d, $J = 2.0$ Hz), 28.2.

¹⁹F NMR (376 MHz, CDCl₃) δ -118.24 (td, $J = 8.3, 4.5$ Hz).



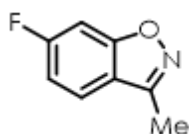
4-fluoro-1-methyl-1*H*-indazole (**4.59**)

The title compound was prepared from 4-fluoro-1*H*-indazole according to an existing literature procedure.²¹⁷ Spectral data align with literature values.²¹⁷



6-fluoro-1,3-dihexylquinazoline-2,4(1H,3H)-dione (**4.60**)

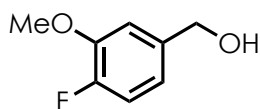
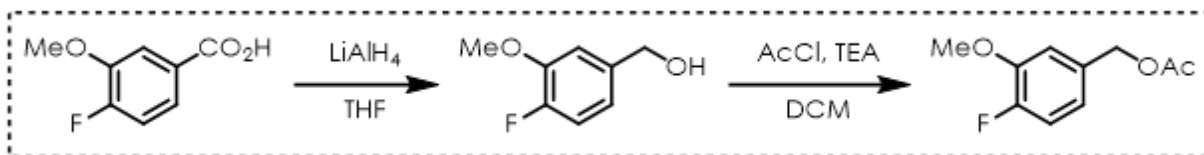
The title compound was prepared in three steps from 2-amino-5-fluorobenzoic acid according to an existing literature protocol.⁴⁵ Spectra data align with literature values.⁴⁵



6-fluoro-3-methylbenzo[*d*]isoxazole (**4.61**)

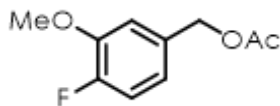
The title compound was prepared in two steps from 1-(4-fluoro-2-hydroxyphenyl)ethan-1-one (commercially available) according to an existing literature procedure.²¹⁸ Spectral data align with literature values.²¹⁸

Scheme C-3. Synthesis of 4.63



(4-fluoro-3-methoxyphenyl)methanol (**4.62**)

The title compound was prepared from 4-fluoro-3-methoxybenzoic acid by adaptation of an existing literature protocol.²¹⁹ Spectral data align with literature values.²²⁰



4-fluoro-3-methoxybenzyl acetate (4.63)

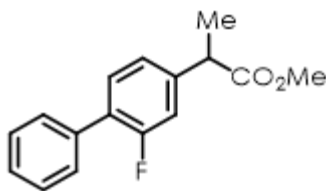
To a dry round bottomed flask equipped with a stirbar was added: (4-fluoro-3-methoxyphenyl)methanol (312 mg, 2.00 mmol, 1 equiv.) dissolved in DCM (12 mL). The flask was cooled to 0°C. Then, triethylamine (0.42 mL, 3.00 mmol, 1.5 equiv.) and acetyl chloride (0.17 mL, 2.4 mmol, 1.2 equiv.) were added sequentially. The mixture was stirred at room temperature overnight. After this time, the reaction was quenched with 1 M HCl. The aqueous layer was separated and extracted with DCM (3 x 15 mL). The combined organic layers were washed with saturated aqueous sodium bicarbonate (1 x 15 mL) and brine (1 x 15 mL). The organic layer was dried over sodium sulfate and concentrated in vacuo. The crude product was purified by filtration over a silica plug, with 15% EtOAc in Hex. The title compound was isolated as a clear, colorless oil (343 mg, 87%).

¹H NMR (600 MHz, CDCl₃) δ 7.05 (dd, J = 11.2, 8.4 Hz, 1H), 6.97 (dd, J = 8.1, 2.3 Hz, 1H), 6.92 – 6.85 (m, 1H), 5.04 (s, 2H), 3.90 (s, 3H), 2.10 (s, 3H).

¹³C NMR (151 MHz, CDCl₃) δ 171.0, 152.4 (d, J = 246.6 Hz), 147.8 (d, J = 11.2 Hz), 132.4, 121.1 (d, J = 7.4 Hz), 116.1 (d, J = 18.6 Hz), 113.7, 66.1, 56.4, 21.2.

¹⁹F NMR (376 MHz, CDCl₃) δ -135.47 (ddd, J = 11.7, 7.8, 4.2 Hz).

LRMS (EI): Calculated for C₁₀H₁₁FO₃ [M]⁺: 198.07, found: 198.10.



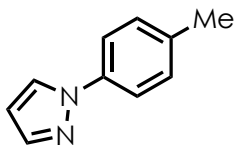
methyl 2-(2-fluoro-[1,1'-biphenyl]-4-yl)propanoate (4.64)

To a flame dried 50 mL round bottom flask equipped with stirbar was added potassium carbonate (2.89 g, 20.9 mmol, 5.1 eq.), flurbiprofen (1.00 g, 4.09 mmol, 1.0 eq.), and DMF (8.0 mL). The reaction was cooled to 0 °C and methyl iodide (0.80 mL, 12.7 mmol, 3.1 eq.) was added slowly over a period of five minutes. The reaction was allowed to slowly warm to room temperature and stir overnight. The reaction was quenched with a saturated aqueous solution of sodium bicarbonate (10 mL). The organic layer was extracted using ethyl acetate (3 x 15 mL) and washed with brine (1 x 15 mL) and an aqueous LiCl solution (2 x 15 mL). The combined organic layers were dried with sodium sulfate and concentrated down. The title compound was purified *via* column chromatography (5% ethyl acetate/hexanes) and was isolated as a clear oil (1.05 g, 99%). Spectral data align with literature values.²²¹

C.4 Experimental Procedures and Characterization of Reaction Products

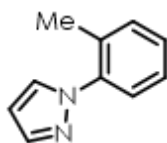
Procedure and Data for Use of Azoles as Nucleophiles:

To a 2 dram vial equipped with a stirbar was added: **Catalyst A** (11.3 mg, 0.0225 mmol, 0.075 equiv.), azole (0.900 mmol, 3 equiv.), and HFIP (3 mL). The vial was sealed with a septum cap and sparged with N₂ for 5 minutes. Then, fluoroarene (0.300 mmol, 1 equiv.) was added *via* microsyringe. The cap was lined with Teflon tape and electrical tape and then irradiated for 18 h using 427 nm Kessil lamps. After irradiation, the solvent was removed in vacuo and purification was carried out as specified for each compound.



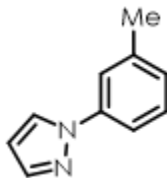
1-(p-tolyl)-1H-pyrazole (4.1)

Prepared from 4-fluorotoluene (33.0 mg, 0.300 mmol, 1 equiv.) and 1H-pyrazole (61.3 mg, 0.900 mmol, 3 equiv.). Purified by flash column chromatography using gradient elution (2.5 – 10% EtOAc in Hex). The title compound was isolated as a yellow liquid in an average yield of 67%. Spectral data align with literature values.²²²



1-(o-tolyl)-1H-pyrazole (4.2)

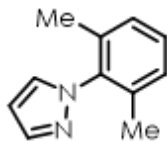
Prepared from 2-fluorotoluene (33.0 mg, 0.300 mmol, 1 equiv.) and 1H-pyrazole (61.3 mg, 0.900 mmol, 3 equiv.). Purified by flash column chromatography using gradient elution (2.5 – 10% EtOAc in Hex). The title compound was isolated as a pale yellow oil in an average yield of 69%. Spectral data align with literature values.²²³



1-(m-tolyl)-1H-pyrazole (4.3)

Prepared from 3-fluorotoluene (33.0 mg, 0.300 mmol, 1 equiv.) and 1H-pyrazole (61.3 mg, 0.900 mmol, 3 equiv.). Purified by flash column chromatography using isocratic elution

(5% EtOAc in Hex). The title compound was isolated as a light-yellow oil in an average yield of 23%. Spectral data align with literature values.²²⁴



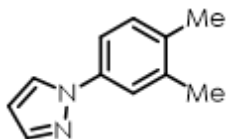
1-(2,6-dimethylphenyl)-1H-pyrazole (4.4)

Prepared from 2-fluoro-1,3-dimethylbenzene (37.2 mg, 0.300 mmol, 1 equiv.) and 1H-pyrazole (61.3 mg, 0.900 mmol, 3 equiv.). Purified by flash column chromatography using gradient elution (5 – 10% EtOAc in Hex). The title compound was isolated as light yellow oil in an average yield of 60%.

¹H NMR (600 MHz, CDCl₃) δ 7.74 (d, $J = 1.9$ Hz, 1H), 7.46 (dd, $J = 2.3, 0.7$ Hz, 1H), 7.26 – 7.23 (m, 1H), 7.13 (d, $J = 7.6$ Hz, 2H), 6.46 (t, $J = 2.1$ Hz, 1H), 2.00 (s, 6H).

¹³C NMR (151 MHz, CDCl₃) δ 140.1, 139.3, 136.4, 130.9, 129.1, 128.2, 106.0, 17.4.

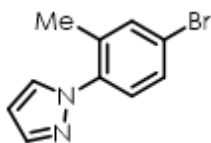
LRMS (EI): Calculated for C₁₁H₁₂N₂ [M]⁺: 172.10, found: 172.20.



1-(3,4-dimethylphenyl)-1H-pyrazole (4.5)

Prepared from 4-fluoro-1,2-dimethylbenzene (37.2 mg, 0.300 mmol, 1 equiv.) and 1H-pyrazole (61.3 mg, 0.900 mmol, 3 equiv.). Purified by flash column chromatography using

isocratic elution (5% EtOAc in Hex). The title compound was isolated as a yellow oil in an average yield of 23%. Spectral data align with literature values.²²⁵



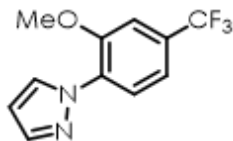
1-(4-bromo-2-methylphenyl)-1H-pyrazole (4.6)

Prepared from 4-bromo-1-fluoro-2-methylbenzene (56.7 mg, 0.300 mmol, 1 equiv.) and 1H-pyrazole (61.3 mg, 0.900 mmol, 3 equiv.). Purified by flash column chromatography using isocratic elution (5% EtOAc in Hex). The title compound was isolated as a light-yellow oil in an average yield of 43%.

¹H NMR (600 MHz, CDCl₃) δ 8.17 (d, $J = 2.6$ Hz, 1H), 7.94 (dd, $J = 8.3, 1.1$ Hz, 1H), 7.73 (d, $J = 1.8$ Hz, 1H), 7.34 (ddd, $J = 8.3, 1.9, 0.9$ Hz, 1H), 7.30 – 7.19 (m, 1H), 6.45 (dd, $J = 2.5, 1.8$ Hz, 1H), 3.96 (s, 3H).

¹³C NMR (151 MHz, CDCl₃) δ 150.78, 140.86, 132.42, 131.82, 129.57 (q, $J = 32.8$ Hz), 124.98, 123.91 (q, $J = 272.2$ Hz), 118.41 (q, $J = 4.0$ Hz), 109.49 (q, $J = 3.8$ Hz), 107.04, 56.37.

LRMS (EI): Calculated for C₁₀H₉BrN₂ [M]⁺: 235.99, found: 236.00.



1-(2-methoxy-4-(trifluoromethyl)phenyl)-1H-pyrazole (4.7)

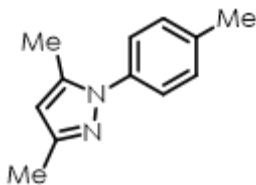
Prepared from 1-fluoro-2-methoxy-4-(trifluoromethyl)benzene (58.2 mg, 0.300 mmol, 1 equiv.) and 1H-pyrazole (61.3 mg, 0.900 mmol, 3 equiv.). Purified by flash column chromatography using isocratic elution (5% EtOAc in Hex). The title compound was isolated as a yellow oil in an average yield of 44%.

¹H NMR (600 MHz, CDCl₃) δ 8.17 (d, J = 2.6 Hz, 1H), 7.94 (dd, J = 8.3, 1.1 Hz, 1H), 7.73 (d, J = 1.8 Hz, 1H), 7.34 (ddd, J = 8.3, 1.9, 0.9 Hz, 1H), 7.30 – 7.19 (m, 1H), 6.45 (dd, J = 2.5, 1.8 Hz, 1H), 3.96 (s, 3H).

¹³C NMR (151 MHz, CDCl₃) δ 150.8, 140.9, 132.4, 131.8, 129.6 (q, J = 32.8 Hz), 125.0, 123.9 (q, J = 272.2 Hz), 118.4 (q, J = 4.0 Hz), 109.5 (q, J = 3.8 Hz), 107.0, 56.4.

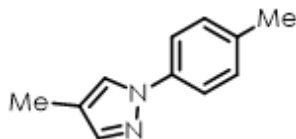
¹⁹F NMR (376 MHz, CDCl₃) δ -62.24 (s).

LRMS (EI): Calculated for C₁₁H₉F₃N₂O [M]⁺: 242.07, found: 242.10.



3,5-dimethyl-1-(*p*-tolyl)-1H-pyrazole (4.8)

Prepared from 4-fluorotoluene (33.0 mg, 0.300 mmol, 1 equiv.) and 3,5-dimethyl-1H-pyrazole (144 mg, 1.5 mmol, 5 equiv.). Purified by flash column chromatography using isocratic elution (10% EtOAc in Hex). The title compound was isolated as an off-white solid in an average yield of 29%. Spectral data align with literature values.²²⁶



4-methyl-1-(*p*-tolyl)-1*H*-pyrazole (4.9)

Prepared from 4-fluorotoluene (33.0 mg, 0.300 mmol, 1 equiv.) and 4-methyl-1*H*-pyrazole (123 mg, 1.50 mmol, 5 equiv.). Purified by flash column chromatography using isocratic elution (10% EtOAc in Hex). The title compound was isolated as a yellow oil in an average yield of 63%.

¹H NMR (400 MHz, CDCl₃) δ 7.66 (m, 1H), 7.53 (m, 3H), 7.25 – 7.19 (m, 2H), 2.37 (s, 3H), 2.15 (s, 3H).

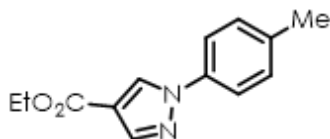
¹³C NMR (101 MHz, CDCl₃) δ 141.5, 138.1, 135.8, 123.0, 125.4, 118.8, 118.0, 21.0, 9.1.

LRMS (EI): Calculated for C₁₁H₁₂N₂ [M]⁺: 172.10, found: 172.10.



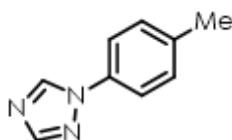
3-methyl-1-(*p*-tolyl)-1*H*-pyrazole (4.10)

Prepared from 4-fluorotoluene (33.0 mg, 0.300 mmol, 1 equiv.) and 3-methyl-1*H*-pyrazole (123 mg, 1.50 mmol, 5 equiv.). Purified by flash column chromatography using gradient elution (10 – 20% EtOAc in Hex). The title compound was isolated as a yellow oil in an average yield of 50%. Spectral data align with literature values.²²⁷



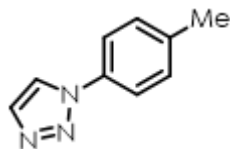
ethyl 1-(*p*-tolyl)-1*H*-pyrazole-4-carboxylate (4.11)

Prepared from 4-fluorotoluene (17.0 mg, 0.150 mmol, 1 equiv.), **Catalyst A** (5.6 mg, 0.011 mmol, 0.075 equiv.), and ethyl 1*H*-pyrazole-4-carboxylate (105 mg, 0.750 mmol, 5 equiv.). Purified by flash column chromatography using isocratic elution (20% EtOAc in Hex). The title compound was isolated as an off-white solid in a yield of 56% (*n* = 1). Spectral data align with literature values.²²⁸



1-(*p*-tolyl)-1*H*-1,2,4-triazole (4.12)

Prepared from 4-fluorotoluene (33.0 mg, 0.300 mmol, 1 equiv.) and 1*H*-1,2,4-triazole (104 mg, 1.5 mmol, 5 equiv.). Purified by flash column chromatography using isocratic elution (20% EtOAc in Hex). The title compound was isolated as a tan solid in an average yield of 36%. Spectral data align with literature values.²²⁹



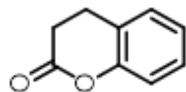
1-(*p*-tolyl)-1*H*-1,2,3-triazole (4.13)

Prepared from 4-fluorotoluene (33.0 mg, 0.300 mmol, 1 equiv.) and 1*H*-1,2,3-triazole (104 mg, 1.5 mmol, 5 equiv.). Purified by flash column chromatography using gradient elution (0

– 40% EtOAc in Hex). The title compound was isolated as an off-white solid in an average yield of 82%. Spectral data align with literature values.²³⁰

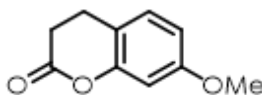
Procedure and Data for Use of Acids as Intramolecular Nucleophiles:

A two-dram vial was equipped with a stir bar, and the solid reagents were added: **Catalyst A** (11.3 mg, 0.0225 mmol, 0.075 equiv.), sodium bicarbonate (25.2 mg, 0.300 mmol, 1 equiv.), and substrate (0.300 mmol). TFE (1.5 mL) and HFIP (1.5 mL) were added *via* syringe, and the system was sparged with N₂ for five minutes. The vial was sealed with electrical tape and stirred while irradiated with 465 nm blue Kessil LEDs for 18 hours. The reaction mixture was concentrated and purified by column chromatography.



chroman-2-one (4.14)

Prepared from 3-(2-fluorophenyl)propanoic acid (50.0 mg, 0.300 mmol, 1 equiv.). The reaction was purified by column chromatography (20% ethyl acetate/hexanes), and the title compound was isolated as a pale yellow oil in an average yield of 54%. Spectral data align with literature values.²³¹



7-methoxychroman-2-one (4.15)

Prepared from 3-(2-fluoro-4-methoxyphenyl)propionic acid (59.0 mg, 0.300 mmol, 1 equiv.). The reaction was purified by column chromatography (20% ethyl acetate/hexanes),

and the title compound was isolated as a clear oil in an average yield of 33%. Spectral data align with literature values.²³²

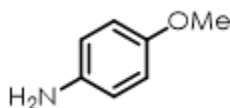
General Procedure for Use of Ammonium Carbamate as a Nucleophile:

For liquid starting materials:

To a 2 dram vial equipped with a stirbar was added: **Catalyst B** (9.4 mg, 0.015 mmol, 0.05 equiv.), ammonium carbamate (93.7 mg, 1.20 mmol, 4 equiv.), DCE (2.25 mL), and TFE (0.75 mL). The vial was sealed with a septum cap and sparged with N₂ for 5 minutes. Then, fluoroarene (0.300 mmol, 1 equiv.) was added *via* microsyringe. The cap was lined with Teflon tape and electrical tape and then irradiated for 18 h using 427 nm Kessil lamps. After irradiation, the solvent was removed in vacuo and purification was carried out as specified for each compound.

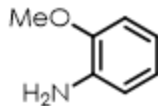
For solid starting materials:

Procedure was carried out as above, with fluoroarene added to the vial prior to sparging with N₂.



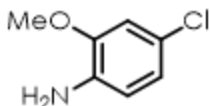
4-methoxyaniline (4.16A)

Prepared from 4-fluoroanisole (37.8 mg, 34.0 μ L, 0.300 mmol, 1 equiv.). Purified by flash column chromatography using isocratic elution (30% EtOAc in Hex). The title compound was isolated as a red-brown solid in an average yield of 78%. Spectral data align with literature values.²³³



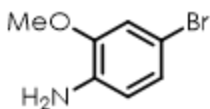
2-methoxyaniline (4.17A)

Prepared from 2-fluoroanisole (37.8 mg, 33.7 μ L, 0.300 mmol, 1 equiv.). Purified by flash column chromatography using gradient elution (10 – 20% EtOAc in Hex). The title compound was isolated as an orange-yellow oil in an average yield of 54%. Spectral data align with literature values.²³⁴



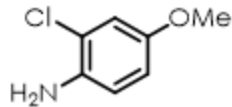
4-chloro-2-methoxyaniline (4.18A)

Prepared from 4-chloro-1-fluoro-2-methoxybenzene (48.2 mg, 0.300 mmol, 1 equiv.). Purified by flash column chromatography using gradient elution (10 – 20% EtOAc in Hex). The title compound was isolated as a red-brown solid in an average yield of 57%. Spectral data align with literature values.



4-bromo-2-methoxyaniline (4.19A)

Prepared from 4-bromo-1-fluoro-2-methoxybenzene (61.5 mg, 0.300 mmol, 1 equiv.). Purified by flash column chromatography using gradient elution (10 – 20% EtOAc in Hex). The title compound was isolated as a red oil in an average yield of 50%. Spectral data align with literature values.²³⁵

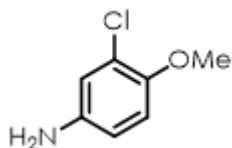


2-chloro-4-methoxyaniline (4.20A)

Prepared from 2-chloro-1-fluoro-4-methoxybenzene (48.2 mg, 0.300 mmol, 1 equiv.).

Purified by flash column chromatography using gradient elution (10 – 20% EtOAc in Hex).

The title compound was isolated as a red-orange oil in an average yield of 55%. Spectral data align with literature values.²³⁶

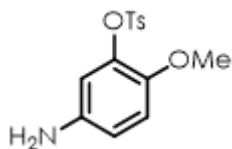


3-chloro-4-methoxyaniline (4.21A)

Prepared from 2-chloro-4-fluoro-1-methoxybenzene (48.2 mg, 0.300 mmol, 1 equiv.).

Purified by flash column chromatography using gradient elution (10 – 30% EtOAc in Hex).

The title compound was isolated as a red-orange oil in an average yield of 52%. Spectral data align with literature values.²³⁷



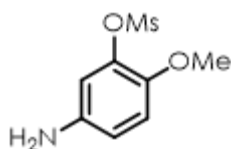
5-amino-2-methoxyphenyl 4-methylbenzenesulfonate (4.22A)

Prepared from 5-fluoro-2-methoxyphenyl 4-methylbenzenesulfonate (88.9 mg, 0.300 mmol, 1 equiv.). Purified by flash column chromatography using gradient elution (25 –

50% EtOAc in Hex). The title compound was isolated as a peach colored solid in an average yield of 46%.

¹H NMR (600 MHz, CDCl₃) δ 7.76 (d, J = 8.3 Hz, 2H), 7.29 (d, J = 7.8 Hz, 2H), 6.65 (d, J = 8.7 Hz, 1H), 6.63 (d, J = 2.8 Hz, 1H), 6.55 (dd, J = 8.7, 2.8 Hz, 1H), 3.52 (br s, 1H), 3.45 (s, 3H), 2.43 (s, 3H).

¹³C NMR (151 MHz, CDCl₃) δ 145.1, 145.0, 139.6, 138.9, 133.2, 129.4, 128.8, 114.8, 114.3, 112.1, 56.3, 21.8.

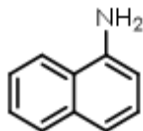


5-amino-2-methoxyphenyl methanesulfonate (4.23A)

Prepared from 5-fluoro-2-methoxyphenyl methanesulfonate (66.1 mg, 0.300 mmol, 1 equiv.). Purified by flash column chromatography using gradient elution (30 – 60% EtOAc in Hex). The title compound was isolated as a tan colored solid in an average yield of 52%.

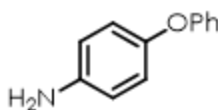
¹H NMR (600 MHz, CDCl₃) δ 6.83 (d, J = 8.7 Hz, 1H), 6.69 (d, J = 1.6 Hz, 1H), 6.59 (dd, J = 8.7, 2.8 Hz, 1H), 3.81 (s, 3H), 3.54 (s, 2H), 3.16 (s, 3H).

¹³C NMR (151 MHz, CDCl₃) δ 144.1, 140.9, 139.0, 114.7, 114.6, 112.1, 56.9, 38.2.



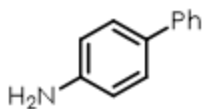
naphthalen-1-amine (4.24A)

Prepared from 1-fluoronaphthalene (43.8 mg, 0.300 mmol, 1 equiv.). Purified by flash column chromatography using gradient elution (10 – 20% EtOAc in Hex). The title compound was isolated as an orange-brown oil in an average yield of 40%. Spectral data align with literature values.²³⁸



4-phenoxyaniline (4.25A)

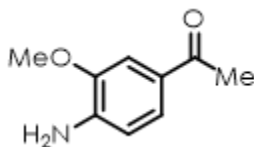
Prepared from 1-fluoro-4-phenoxybenzene (56.5 mg, 48.9 μ L, 0.300 mmol, 1 equiv.). Purified by flash column chromatography using gradient elution (20 – 30% EtOAc in Hex). The title compound was isolated as a brown solid in an average yield of 59%. Spectral data align with literature values.²³⁹



[1,1'-biphenyl]-4-amine (4.26A)

Prepared from 4-fluoro-1,1'-biphenyl (51.7 mg, 0.300 mmol, 1 equiv.). Purified by flash column chromatography using isocratic elution (20% EtOAc in Hex). The title compound

was isolated as a tan colored solid in an average yield of 37%. Spectral data align with literature values.²⁴⁰



1-(4-amino-3-methoxyphenyl)ethan-1-one (4.27A)

Prepared from 1-(4-fluoro-3-methoxyphenyl)ethan-1-one (50.5 mg, 0.300 mmol, 1 equiv.).

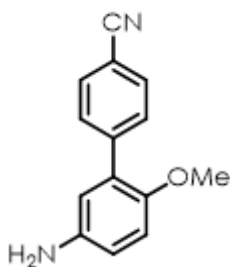
Purified by flash column chromatography using gradient elution (30 – 40% EtOAc in Hex).

The title compound was isolated as a yellow-orange solid in an average yield of 26%.

¹H NMR (600 MHz, CDCl₃) δ 7.48 – 7.42 (m, 2H), 6.65 (d, J = 8.6 Hz, 1H), 4.32 (s, 2H), 3.90 (s, 3H), 2.52 (s, 3H).

¹³C NMR (151 MHz, CDCl₃) δ 196.8, 146.6, 141.8, 127.9, 124.3, 112.6, 109.3, 55.7, 26.2.

LRMS (EI): Calculated for C₉H₁₁NO₂ [M]⁺: 165.08, found: 165.10.



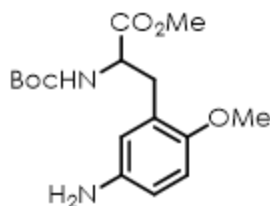
5'-amino-2'-methoxy-[1,1'-biphenyl]-4-carbonitrile (4.28A)

Prepared from 5'-fluoro-2'-methoxy-[1,1'-biphenyl]-4-carbonitrile (68.2 mg, 0.300 mmol, 1 equiv.). Purified by flash column chromatography using gradient elution (30 – 40% EtOAc in

Hex). The title compound was isolated as a light brown solid in an average yield of 62%.

¹H NMR (600 MHz, CDCl₃) δ 7.67 (d, J = 8.6 Hz, 2H), 7.62 (d, J = 8.5 Hz, 2H), 6.84 (d, J = 8.6 Hz, 1H), 6.72 (dd, J = 8.6, 2.9 Hz, 1H), 6.67 (d, J = 2.9 Hz, 1H), 3.73 (s, 3H), 3.53 (s, 2H).

¹³C NMR (151 MHz, CDCl₃) δ 149.7, 143.6, 140.4, 131.9, 130.3, 129.5, 119.4, 117.9, 116.4, 113.3, 110.5, 56.4.

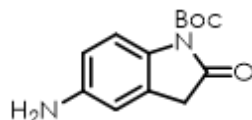


methyl 3-(5-amino-2-methoxyphenyl)-2-((tert-butoxycarbonyl)amino)propanoate (4.29A)

Prepared from methyl 2-((tert-butoxycarbonyl)amino)-3-(5-fluoro-2-methoxyphenyl)propanoate (98.2 mg, 0.300 mmol, 1 equiv.). Purified by flash column chromatography using gradient elution (50 – 75% EtOAc in Hex). The title compound was isolated as a brown oil in an average yield of 66%.

¹H NMR (600 MHz, CDCl₃) δ 6.67 (d, J = 8.6 Hz, 1H), 6.55 (dd, J = 8.6, 2.8 Hz, 1H), 6.48 (d, J = 2.7 Hz, 1H), 5.34 (d, J = 7.6 Hz, 1H), 4.41 (q, J = 7.1 Hz, 1H), 3.73 (s, 3H), 3.68 (s, 3H), 3.45 (s, 2H), 3.01 – 2.81 (m, 2H), 1.37 (s, 9H).

¹³C NMR (151 MHz, CDCl₃) δ 173.0, 155.4, 150.9, 139.8, 125.6, 118.7, 114.9, 111.7, 79.6, 55.8, 54.4, 52.2, 32.6, 28.3.



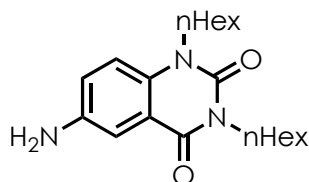
tert-butyl 5-amino-2-oxoindoline-1-carboxylate (4.30A)

Prepared from tert-butyl 5-fluoro-2-oxoindoline-1-carboxylate (75.4 mg, 0.300 mmol, 1 equiv.). Purified by flash column chromatography using gradient elution (30 – 50% EtOAc in Hex). The title compound was isolated as a yellow-brown solid in an average yield of 48%.

¹H NMR (600 MHz, CDCl₃) δ 7.54 (dd, J = 9.4, 1.9 Hz, 1H), 6.60 (dd, J = 6.5, 2.7 Hz, 2H), 3.63 (s, 2H), 3.56 (s, 2H), 1.62 (s, 9H).

(Minor rotamer peaks observed: 6.96 (ddt, J = 8.4, 5.5, 2.4 Hz), 6.91 (d, J = 8.8 Hz), 3.51 (s), 1.50 (s).)

¹³C NMR (151 MHz, CDCl₃) δ 173.57, 149.34, 143.38, 124.52, 116.08, 114.32, 111.45, 84.13, 36.96, 28.44, 28.22. (Note: data shown for major rotamer only)



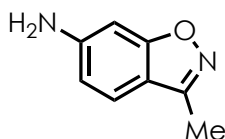
6-amino-1,3-dihexylquinazoline-2,4(1H,3H)-dione (4.32A)

Prepared from 6-fluoro-1,3-dihexylquinazoline-2,4(1H,3H)-dione (104.5 mg, 0.300 mmol, 1 equiv.). Purified by flash column chromatography using gradient elution (20 – 30% EtOAc in Hex). The title compound was isolated as an off-white solid in an average yield of 48%.

¹H NMR (600 MHz, CDCl₃) δ 7.50 (d, J = 2.8 Hz, 1H), 7.03 (dd, J = 8.8, 2.8 Hz, 1H), 7.00 (d, J = 8.8 Hz, 1H), 4.05 (td, J = 8.0, 2.8 Hz, 4H), 3.75 (s, 2H), 1.73 – 1.59 (m, 4H), 1.42 –

1.29 (m, 12H), 0.88 (dt, $J = 11.2, 7.1$ Hz, 6H).

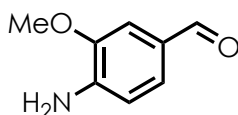
^{13}C NMR (101 MHz, CDCl_3) δ 161.86, 150.48, 141.81, 132.55, 123.04, 116.74, 114.85, 113.18, 43.82, 42.08, 31.67, 31.62, 27.95, 27.50, 26.82, 26.63, 22.71, 14.21, 14.16.



3-methylbenzo[d]isoxazol-6-amine (4.33A)

Prepared from 6-fluoro-3-methylbenzo[d]isoxazole (12.0 mg, 0.08 mmol, 1 equiv.), **Catalyst B** (2.5 mg, 0.004 mmol, 0.05 equiv.), ammonium carbamate (93.7 mg, 0.32 mmol, 4 equiv.), DCE (0.6 mL), and TFE (0.2 mL) to give the title compound in a 14% ^1H NMR yield using HMDSO as an internal standard. The crude ^1H NMR data is given below.

^1H NMR (400 MHz, CDCl_3) δ 6.89 (dd, $J = 8.8, 5.7$ Hz, 1H), 6.73 (dd, $J = 9.9, 2.8$ Hz, 1H), 6.57 (ddd, $J = 8.7, 7.6, 2.8$ Hz, 1H), 2.26 (s, 3H).



4-amino-3-methoxybenzaldehyde (4.34A)

Prepared from 4-fluoro-3-methoxybenzaldehyde (46.2 mg, 0.300 mmol, 1 equiv.). Purified by flash column chromatography using gradient elution (20 – 30% EtOAc in Hex). The title compound was isolated as a yellow-orange solid in an average yield of 32%.

^1H NMR (600 MHz, CDCl_3) δ 9.71 (s, 1H), 7.31 (d, $J = 7.9$ Hz, 2H), 6.72 (d, $J = 7.8$ Hz, 1H), 4.47 (s, 2H), 3.90 (s, 3H).

^{13}C NMR (151 MHz, CDCl_3) δ 190.8, 146.9, 143.3, 128.1, 127.6, 112.8, 108.3, 55.7.

LRMS (EI): Calculated for $\text{C}_8\text{H}_9\text{NO}_2$ $[\text{M}]^+$: 151.06, found: 151.05.

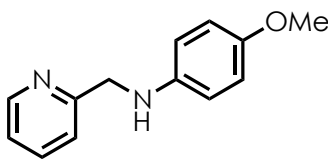
Procedure and Data for Use of Primary Benzylic Amines as Nucleophiles:

For liquid starting materials:

To a 2-dram vial equipped with a stirbar was added: **Catalyst B** (9.4 mg, 0.015 mmol, 0.05 equiv.), pyridin-2-ylmethanamine (97.3 mg, 92.8 μL , 0.900 mmol, 3 equiv.), and TFE (3 mL). The vial was sealed with a septum cap and sparged with N_2 for 5 minutes. Then, fluoroarene (0.300 mmol, 1 equiv.) was added *via* microsyringe. The cap was lined with Teflon tape and electrical tape and then irradiated for 18 h using 427 nm Kessil lamps. After irradiation, the solvent was removed in vacuo and purification was carried out as specified for each compound.

For solid starting materials:

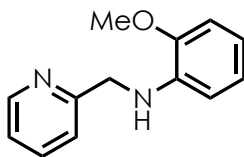
Procedure was carried out as above, but fluoroarene was added to the flask prior to sparging with N_2 .



4-methoxy-N-(pyridin-2-ylmethyl)aniline (4.16B)

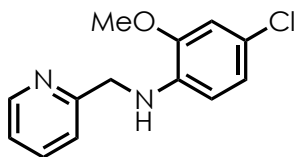
Prepared from 4-fluoroanisole (37.8 mg, 0.300 mmol, 1 equiv.). Purified by flash column chromatography using gradient elution (20 – 30% Acetone in Hex). The title compound was

isolated as an orange-brown solid in an average yield of 69%. Spectral data align with literature values.²⁴¹



2-methoxy-N-(pyridin-2-ylmethyl)aniline (4.17B)

Prepared from 2-fluoroanisole (37.8 mg, 0.300 mmol, 1 equiv.). Purified by flash column chromatography using gradient elution (20 – 40% EtOAc in Hex). The title compound was isolated as a light-yellow oil in an average yield of 70%. Spectral data align with literature values.²⁴²

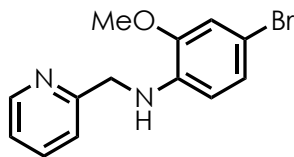


4-chloro-2-methoxy-N-(pyridin-2-ylmethyl)aniline (4.18B)

Prepared from 4-chloro-1-fluoro-2-methoxybenzene (48.2 mg, 0.300 mmol, 1 equiv.). Purified by flash column chromatography using gradient elution (25 – 40% EtOAc in Hex). The title compound was isolated as a yellow oil in an average yield of 52%.

¹H NMR (600 MHz, CDCl₃) δ 8.59 (ddd, $J = 4.9, 1.8, 0.9$ Hz, 1H), 7.63 (td, $J = 7.7, 1.8$ Hz, 1H), 7.31 (d, $J = 7.8$ Hz, 1H), 7.17 (ddd, $J = 7.4, 4.9, 1.1$ Hz, 1H), 6.79 – 6.69 (m, 2H), 6.42 (d, $J = 8.3$ Hz, 1H), 5.16 (s, 1H), 4.46 (s, 2H), 3.87 (s, 3H).

^{13}C NMR (151 MHz, CDCl_3) δ 158.57, 149.38, 147.48, 136.84, 136.54, 122.25, 121.49, 121.40, 120.77, 110.49, 110.21, 55.78, 49.22.

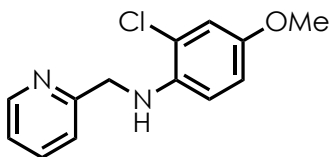


4-bromo-2-methoxy-N-(pyridin-2-ylmethyl)aniline (4.19B)

Prepared from 4-bromo-1-fluoro-2-methoxybenzene (61.5 mg, 0.300 mmol, 1 equiv.). Purified by flash column chromatography using gradient elution (20 – 40% EtOAc in Hex). The title compound was isolated as a yellow oil in an average yield of 52%.

^1H NMR (600 MHz, CDCl_3) δ 8.62 – 8.56 (m, 1H), 7.64 (t, $J = 7.7$ Hz, 1H), 7.32 (d, $J = 7.8$ Hz, 1H), 7.19 (dd, $J = 7.6, 4.9$ Hz, 1H), 6.91 (dd, $J = 8.4, 2.1$ Hz, 1H), 6.87 (d, $J = 2.1$ Hz, 1H), 6.38 (d, $J = 8.4$ Hz, 1H), 4.47 (s, 2H), 3.87 (s, 3H).

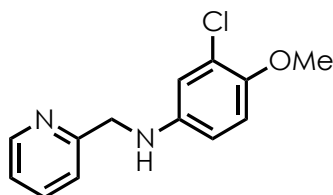
^{13}C NMR (151 MHz, CDCl_3) δ 158.47, 149.20, 147.67, 137.07, 136.95, 123.82, 122.34, 121.58, 112.87, 111.07, 108.30, 55.83, 49.03.



2-chloro-4-methoxy-N-(pyridin-2-ylmethyl)aniline (4.20B)

Prepared from 2-chloro-1-fluoro-4-methoxybenzene (48.2 mg, 38.1 μL , 0.300 mmol, 1 equiv.). Purified by flash column chromatography using gradient elution (25 – 30% EtOAc in

Hex). The title compound was isolated as a light-yellow oil in an average yield of 83%. Spectral data align with literature values.²⁴³



3-chloro-4-methoxy-N-(pyridin-2-ylmethyl)aniline (4.21B)

Prepared from 2-chloro-4-fluoro-1-methoxybenzene (48.2 mg, 0.300 mmol, 1 equiv.).

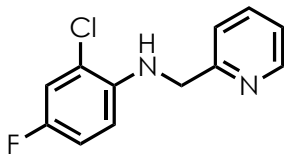
Purified by flash column chromatography using gradient elution (30 – 60% EtOAc in Hex).

The title compound was isolated as a pale yellow oil in an average yield of 55%.

¹H NMR (600 MHz, CDCl₃) δ 8.57 (d, *J* = 4.9 Hz, 1H), 7.64 (td, *J* = 7.7, 1.8 Hz, 1H), 7.30 (d, *J* = 7.8 Hz, 1H), 7.21 – 7.14 (m, 1H), 6.79 (d, *J* = 8.8 Hz, 1H), 6.73 (d, *J* = 2.8 Hz, 1H), 6.53 (dd, *J* = 8.8, 2.8 Hz, 1H), 4.38 (s, 2H), 3.80 (s, 3H).

¹³C NMR (151 MHz, CDCl₃) δ 158.15, 149.33, 147.57, 142.96, 136.81, 123.52, 122.34, 121.80, 115.28, 114.37, 112.30, 57.12, 49.86.

Substitution was also observed at the C-O position. The product was isolated as a yellow oil in an average yield of 11%. The corresponding characterization data are included below.

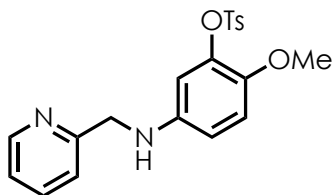


2-chloro-4-fluoro-N-(pyridin-2-ylmethyl)aniline (4.21B-Oxygen)

¹H NMR (600 MHz, CDCl₃) δ 8.66 – 8.54 (m, 1H), 7.65 (td, J = 7.7, 1.8 Hz, 1H), 7.31 (d, J = 7.8 Hz, 1H), 7.24 – 7.16 (m, 1H), 7.07 (dd, J = 8.2, 2.9 Hz, 1H), 6.84 (ddd, J = 8.9, 8.1, 2.9 Hz, 1H), 6.54 (dd, J = 9.0, 5.0 Hz, 1H), 5.22 (s, 1H), 4.49 (d, J = 4.0 Hz, 2H).

¹³C NMR (151 MHz, CDCl₃) δ 157.93, 154.65 (d, J = 237.7 Hz), 149.53, 140.57 (d, J = 2.5 Hz), 136.90, 122.44, 121.45, 119.29 (d, J = 10.4 Hz), 116.62 (d, J = 25.7 Hz), 114.45 (d, J = 21.6 Hz), 111.76 (d, J = 8.1 Hz), 49.55.

¹⁹F NMR (376 MHz, CDCl₃) δ -126.91 (td, J = 7.8, 4.8 Hz).



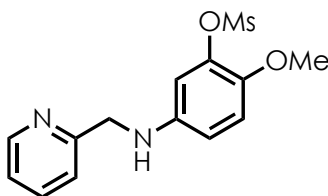
2-methoxy-5-((pyridin-2-ylmethyl)amino)phenyl 4-methylbenzenesulfonate (4.22B)

Prepared from 5-fluoro-2-methoxyphenyl 4-methylbenzenesulfonate (88.9 mg, 0.300 mmol, 1 equiv.). Purified by flash column chromatography using gradient elution (20 – 40% Acetone in Hex). The title compound was isolated as a brown solid in an average yield of 41%.

¹H NMR (600 MHz, CDCl₃) δ 8.58 (d, J = 4.5 Hz, 1H), 7.75 – 7.72 (m, 2H), 7.72 – 7.65 (m, 2H), 7.33 (d, J = 7.6 Hz, 1H), 7.28 – 7.25 (m, 3H), 7.23 (d, J = 5.4 Hz, 1H), 6.68 (d, J = 8.7 Hz, 1H), 6.58 (s, 1H), 6.54 – 6.46 (m, 1H), 4.36 (d, J = 1.9 Hz, 1H), 3.44 (s, 2H), 2.43 (s,

3H).

^{13}C NMR (151 MHz, CDCl_3) δ 157.80, 148.84, 144.88, 143.83, 142.27, 139.15, 137.16, 133.20, 129.27, 128.65, 122.41, 122.05, 114.48, 112.18, 109.36, 56.34, 49.51, 21.72.



2-methoxy-5-((pyridin-2-ylmethyl)amino)phenyl methanesulfonate (4.23B)

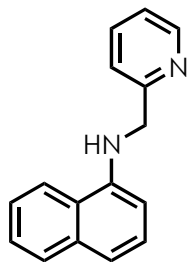
Prepared from 5-fluoro-2-methoxyphenyl methanesulfonate (66.1 mg, 0.300 mmol, 1 equiv.).

Purified by flash column chromatography using gradient elution (50 – 80% EtOAc in Hex.

The title compound was isolated as a light yellow solid in an average yield of 37%.

^1H NMR (600 MHz, CDCl_3) δ 8.57 (d, J = 4.5 Hz, 1H), 7.69 – 7.63 (m, 1H), 7.32 (d, J = 7.9 Hz, 1H), 7.20 (dd, J = 7.5, 4.9 Hz, 1H), 6.85 (d, J = 8.9 Hz, 1H), 6.67 (d, J = 2.8 Hz, 1H), 6.55 (dd, J = 8.9, 2.9 Hz, 1H), 4.47 (s, 1H), 4.39 (s, 2H), 3.79 (s, 3H), 3.15 (s, 3H).

^{13}C NMR (151 MHz, CDCl_3) δ 157.82, 149.11, 143.36, 142.87, 139.29, 137.02, 122.43, 121.97, 114.92, 112.33, 109.81, 56.92, 49.61, 38.16.

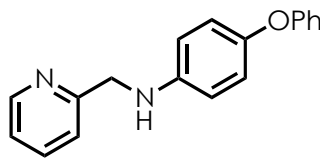


***N*-(pyridin-2-ylmethyl)naphthalen-1-amine (4.24B)**

Prepared from 1-fluoronaphthalene (43.8 mg, 0.300 mmol, 1 equiv.). Purified by flash column chromatography using gradient elution (20 – 40% EtOAc in Hex). The title compound was isolated as a yellow oil in an average yield of 82%.

¹H NMR (600 MHz, CDCl₃) δ 8.64 (d, *J* = 3.3 Hz, 1H), 8.03 – 7.98 (m, 1H), 7.83 – 7.79 (m, 1H), 7.70 – 7.64 (m, 1H), 7.51 – 7.46 (m, 2H), 7.39 (d, *J* = 7.4 Hz, 1H), 7.33 (td, *J* = 7.8, 1.5 Hz, 1H), 7.27 – 7.25 (m, 1H), 7.24 – 7.21 (m, 1H), 6.58 (d, *J* = 7.5 Hz, 1H), 4.64 (s, 2H).

¹³C NMR (151 MHz, CDCl₃) δ 158.05, 149.17, 143.15, 136.97, 134.42, 128.73, 126.71, 125.93, 124.91, 123.66, 122.39, 121.93, 120.38, 117.65, 104.78, 49.21.

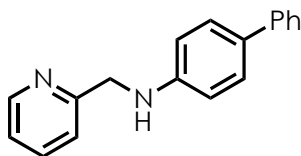


4-phenoxy-*N*-(pyridin-2-ylmethyl)aniline (4.25B)

Prepared from 1-fluoro-4-phenoxybenzene (56.5 mg, 48.9 μ L, 0.300 mmol, 1 equiv.). Purified by flash column chromatography using gradient elution (30% Hex – 50% EtOAc in Hex). The title compound was isolated as a yellow oil in an average yield of 76%.

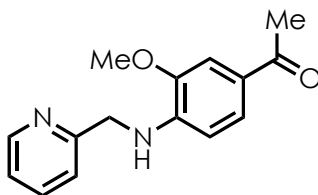
¹H NMR (600 MHz, CDCl₃) δ 8.61 – 8.59 (m, 1H), 7.71 – 7.66 (m, 1H), 7.37 (d, *J* = 7.8 Hz, 1H), 7.27 (dd, *J* = 7.8, 6.4 Hz, 2H), 7.22 (dd, *J* = 7.5, 4.9 Hz, 1H), 7.04 – 6.98 (m, 1H), 6.95 – 6.89 (m, 4H), 6.67 (d, *J* = 8.8 Hz, 2H), 4.47 (s, 2H), 4.18 (br s, 1H).

¹³C NMR (151 MHz, CDCl₃) δ 159.1, 158.4, 149.0, 148.0, 144.6, 137.2, 129.6, 122.4, 122.1, 122.0, 121.3, 117.3, 114.2, 49.8.



***N*-(pyridin-2-ylmethyl)-[1,1'-biphenyl]-4-amine (4.26B)**

Prepared from 4-fluoro-1,1'-biphenyl (51.7 mg, 0.300 mmol, 1 equiv.). Purified by flash column chromatography using gradient elution (30 – 50% EtOAc in Hex). The title compound was isolated as a light yellow solid in an average yield of 61%. Spectral data align with literature values.²⁴³

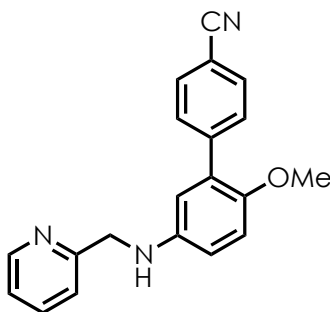


1-(3-methoxy-4-((pyridin-2-ylmethyl)amino)phenyl)ethan-1-one (4.27B)

Prepared from 1-(4-fluoro-3-methoxyphenyl)ethan-1-one (50.5 mg, 0.300 mmol, 1 equiv.). Purified by flash column chromatography using gradient elution (30 – 50% EtOAc in Hex). The title compound was isolated as an off white solid in an average yield of 17%.

¹H NMR (600 MHz, CDCl₃) δ 8.64 – 8.58 (m, 1H), 7.66 (td, J = 7.7, 1.8 Hz, 1H), 7.49 (dd, J = 8.2, 1.8 Hz, 1H), 7.45 (d, J = 1.9 Hz, 1H), 7.30 (d, J = 7.8 Hz, 1H), 7.23 – 7.18 (m, 1H), 6.48 (d, J = 8.2 Hz, 1H), 5.82 (s, 1H), 4.61 – 4.51 (m, 2H), 3.95 (s, 3H), 2.51 (s, 3H).

¹³C NMR (151 MHz, CDCl₃) δ 196.7, 157.7, 149.5, 146.5, 142.5, 136.9, 126.4, 125.0, 122.5, 121.5, 108.0, 107.9, 55.8, 48.5, 26.1.

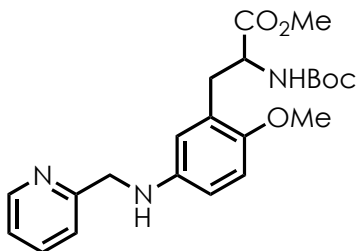


2'-methoxy-5'-((pyridin-2-ylmethyl)amino)-[1,1'-biphenyl]-4-carbonitrile (4.28B)

Prepared from 5'-fluoro-2'-methoxy-[1,1'-biphenyl]-4-carbonitrile (68.2 mg, 0.300 mmol, 1 equiv.). Purified by flash column chromatography using gradient elution (40 – 70% EtOAc in Hex). The title compound was isolated as a yellow solid in an average yield of 74%.

¹H NMR (600 MHz, CDCl₃) δ 8.58 (d, J = 4.5 Hz, 1H), 7.68 – 7.62 (m, 3H), 7.60 (d, J = 8.2 Hz, 2H), 7.34 (d, J = 7.8 Hz, 1H), 7.21 – 7.16 (m, 1H), 6.87 (d, J = 8.7 Hz, 1H), 6.69 (dd, J = 8.7, 3.0 Hz, 1H), 6.66 (d, J = 2.9 Hz, 1H), 4.44 (s, 2H), 4.27 (s, 1H), 3.71 (s, 3H).

¹³C NMR (151 MHz, CDCl₃) δ 158.4, 149.3, 149.0, 143.8, 142.5, 136.8, 131.8, 130.3, 129.6, 122.3, 121.8, 119.3, 115.9, 114.1, 113.5, 110.4, 56.4, 50.1.

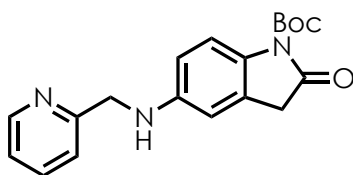


methyl 2-((tert-butoxycarbonyl)amino)-3-(2-methoxy-5-((pyridin-2-ylmethyl)amino)phenyl)propanoate (4.29B)

Prepared from methyl 2-((tert-butoxycarbonyl)amino)-3-(5-fluoro-2-methoxyphenyl)propanoate (98.2 mg, 0.300 mmol, 1 equiv.). Purified by flash column chromatography using isocratic elution (75% EtOAc in Hex). The title compound was isolated as a yellow oil in an average yield of 61%.

¹H NMR (600 MHz, CDCl₃) δ 8.55 (d, J = 4.9 Hz, 1H), 7.63 (t, J = 7.7 Hz, 1H), 7.32 (d, J = 7.9 Hz, 1H), 7.17 (dd, J = 7.5, 5.1 Hz, 1H), 6.70 (d, J = 8.6 Hz, 1H), 6.51 (d, J = 8.6 Hz, 1H), 6.48 (d, J = 2.9 Hz, 1H), 5.38 (d, J = 7.5 Hz, 1H), 4.42 (q, J = 7.1 Hz, 1H), 4.38 (s, 2H), 4.15 (s, 1H), 3.72 (s, 3H), 3.67 (s, 3H), 3.01 – 2.86 (m, 2H), 1.37 (s, 9H).

¹³C NMR (151 MHz, CDCl₃) δ 173.03, 158.59, 155.46, 150.29, 149.05, 142.00, 136.92, 125.63, 122.24, 121.83, 116.79, 112.47, 111.84, 79.57, 55.86, 54.51, 52.14, 50.00, 32.78, 28.36.



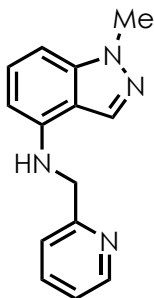
tert-butyl 5-(benzylamino)-2-oxoindoline-1-carboxylate (4.30B)

Prepared from tert-butyl 5-fluoro-2-oxoindoline-1-carboxylate (75.4 mg, 0.300 mmol, 1 equiv.) and phenylmethanamine (75.6 mg, 77.1 μL, 0.900 mmol, 3 equiv.) in place

of pyridin-2-ylmethanamine due to difficulties associated with purification. Purified by flash column chromatography using gradient elution (20 – 30% EtOAc in Hex). The title compound was isolated as an off-white solid in an average yield of 73%.

¹H NMR (600 MHz, CDCl₃) δ 7.31 (tt, J = 6.7, 1.2 Hz, 2H), 7.29 – 7.27 (m, 1H), 7.24 – 7.19 (m, 2H), 7.00 – 6.92 (m, 1H), 6.84 (dd, J = 8.9, 3.0 Hz, 1H), 6.39 (s, 1H), 4.38 (d, J = 5.7 Hz, 2H), 3.48 (s, 2H), 1.50 (s, 9H).

¹³C NMR (101 MHz, CDCl₃) δ 171.18, 160.46, 158.04, 154.37, 137.51, 133.46 (app d, J = 2.9 Hz), 129.34, 128.87, 127.78, 125.86, 116.62 (app d, J = 22.9 Hz), 114.80 (app d, J = 21.8 Hz), 80.50, 43.95, 40.68, 28.46.



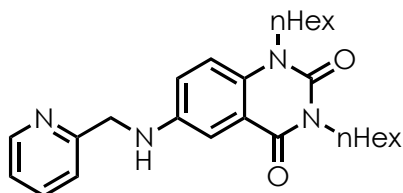
***N*-benzyl-1-methyl-1H-indazol-4-amine (4.31B)**

Prepared from 4-fluoro-1-methyl-1H-indazole (22.5 mg, 0.150 mmol, 1 equiv.), **Catalyst B** (4.7 mg, 0.008 mmol, 0.05 equiv.), phenylmethanamine (48.2 mg, 49.2 μL, 0.450 mmol, 3 equiv.), and TFE (1.5 mL). Purified by flash column chromatography using gradient elution (20 – 30% EtOAc in Hex). The title compound was isolated as a yellow solid in a yield of 58% (n = 1).

¹H NMR (600 MHz, CDCl₃) δ 7.91 (s, 1H), 7.46 – 7.40 (m, 2H), 7.39 – 7.35 (m, 2H), 7.33 – 7.29 (m, 1H), 7.22 (dd, J = 8.4, 7.5 Hz, 1H), 6.75 (d, J = 8.4 Hz, 1H), 6.23 (d, J = 7.5 Hz,

1H), 4.57 (s, 1H), 4.50 (s, 2H), 4.02 (s, 3H).

¹³C NMR

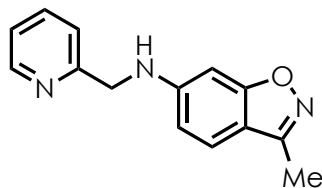


1,3-dihexyl-6-((pyridin-2-ylmethyl)amino)quinazoline-2,4(1H,3H)-dione (4.32B)

Prepared from 6-fluoro-1,3-dihexylquinazoline-2,4(1H,3H)-dione (104.5 mg, 0.300 mmol, 1 equiv.). Purified by flash column chromatography using gradient elution (30 – 50% EtOAc in Hex). The title compound was isolated as a yellow oil in an average yield of 24%.

¹H NMR (600 MHz, CDCl₃) δ 8.61 – 8.56 (m, 1H), 7.70 – 7.63 (m, 1H), 7.44 (d, J = 2.8 Hz, 1H), 7.33 (d, J = 7.8 Hz, 1H), 7.21 (dd, J = 7.6, 4.8 Hz, 1H), 7.06 (dd, J = 8.9, 2.8 Hz, 1H), 7.02 (d, J = 9.0 Hz, 1H), 5.02 (s, 1H), 4.49 (s, 2H), 4.05 (q, J = 8.3 Hz, 4H), 1.74 – 1.61 (m, 4H), 1.43 – 1.28 (m, 12H), 0.88 (dt, J = 9.2, 7.1 Hz, 6H).

¹³C NMR (101 MHz, CDCl₃) δ 162.06, 157.47, 150.46, 149.27, 143.69, 136.97, 131.85, 122.52, 122.08, 122.06, 116.74, 114.89, 109.64, 49.23, 43.79, 42.06, 31.67, 31.62, 27.95, 27.56, 26.83, 26.63, 22.73, 22.71, 14.21, 14.16.



***N*-benzyl-3-methylbenzo[d]isoxazol-6-amine (4.33B)**

Prepared from 6-fluoro-3-methylbenzo[d]isoxazole (22.7 mg, 0.150 mmol, 1 equiv.), **Catalyst B** (4.7 mg, 0.008 mmol, 0.05 equiv.), phenylmethanamine (48.2 mg, 49.2 μ L, 0.450 mmol, 3 equiv.), and TFE (1.5 mL). Purified by flash column chromatography using isocratic elution (30% EtOAc in Hex). The title compound was isolated as a yellow solid in a yield of 18% ($n = 1$).

$^1\text{H NMR}$ (600 MHz, CDCl_3) δ 7.42 – 7.36 (m, 3H), 7.36 – 7.29 (m, 3H), 7.26 (s, 1H), 6.43 (ddd, $J = 9.4, 8.3, 1.2$ Hz, 1H), 4.80 (s, 2H), 2.49 (s, 3H).

$^{13}\text{C NMR}$ (101 MHz, CDCl_3) δ 173.42, 169.52, 161.50, 135.60, 129.32, 128.28, 127.96, 127.84, 127.64, 113.62, 103.47, 50.52, 15.06.

Procedure and Data for Use of Benzoic Acid as a Nucleophile:

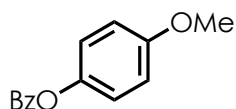
For liquid starting materials:

A two-dram vial was equipped with a stir bar, and the solid reagents were added: **Catalyst B** (9.4 mg, 0.015 mmol, 0.05 equiv.), benzoic acid (150.0 mg, 1.20 mmol, 4 equiv.), sodium bicarbonate (50.0 mg, 0.600 mmol, 2 equiv.), and solvent (3.0 mL TFE). The vial was sealed with a septum cap and sparged with N_2 for 5 minutes. Then, fluoroarene (0.300 mmol, 1 equiv.) was added *via* microsyringe. The cap was lined with Teflon tape and electrical tape and then irradiated for 18 h using 465 nm Kessil lamps. The reaction mixture was diluted with DCM, transferred to a separatory funnel, and washed with saturated aqueous sodium bicarbonate solution (2 x 25 mL), water (1 x 25 mL), and brine (1 x 25 mL). The combined

organic layers were dried with Na₂SO₄ and concentrated under vacuum. The crude reaction material was purified as specified for each compound.

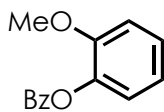
For solid starting materials:

Procedure was carried out as above, but fluoroarene was added to the flask prior to sparging with N₂.



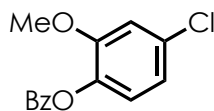
4-methoxyphenyl benzoate (4.16C)

Prepared from 4-fluoroanisole (56.0 μL, 0.500 mmol, 1 equiv.). The reaction was purified by filtering the crude reaction material through a plug of silica, eluting with DCM. The organic layer was washed with saturated aqueous sodium bicarbonate, water, and brine. The organic layer was dried using Na₂SO₄ and concentrated. The title compound was isolated as a pale yellow oil in an average yield of 43%. Spectral data aligns with literature values.²⁴⁴



2-methoxyphenyl benzoate (4.17C)

Prepared from 2-fluoroanisole (56.0 μL, 0.500 mmol, 1 equiv.). Purified by flash column chromatography using isocratic elution (20% EtOAc in Hex). The title compound was isolated as an off-white oil in an average yield of 46%. Spectral data aligns with literature values.²⁴⁵



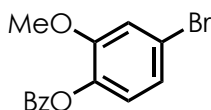
4-chloro-2-methoxyphenyl benzoate (4.18C)

Prepared from 2-fluoro-5-chloroanisole (48.0 mg, 0.300 mmol, 1 equiv.). Purified *via* the aqueous workup described above without chromatography. The title compound was isolated as a pale-yellow oil in an average yield of 65%.

¹H NMR (400 MHz, CDCl₃) δ 8.30 – 8.11 (m, 2H), 7.71 – 7.56 (m, 1H), 7.51 (dd, $J = 8.4$, 7.1 Hz, 2H), 7.08 (d, $J = 8.2$ Hz, 1H), 7.03 – 6.89 (m, 2H), 3.81 (s, 3H).

¹³C NMR (101 MHz, CDCl₃) δ 164.7, 152.0, 138.7, 133.8, 132.1, 130.4, 129.2, 128.7, 123.9, 120.8, 113.3, 56.2.

LRMS (EI): Calculated for C₁₄H₁₁ClO₃ [M]⁺: 262.04, found: 262.00.

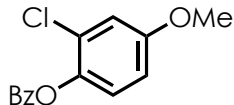


4-bromo-2-methoxyphenyl benzoate (4.19C)

Prepared from 2-fluoro-5-bromoanisole (62.0 mg, 0.300 mmol, 1 equiv.). Purified *via* the aqueous workup described above without chromatography. The title compound was isolated as a pale-yellow oil in an average yield of 57%.

¹H NMR (400 MHz, CDCl₃) δ 8.27 – 8.13 (m, 2H), 7.75 – 7.59 (m, 1H), 7.51 (t, $J = 7.7$ Hz, 2H), 7.13 (d, $J = 6.9$ Hz, 2H), 7.03 (d, $J = 9.0$ Hz, 1H), 3.81 (s, 3H).

¹³C NMR (101 MHz, CDCl₃) δ 164.6, 152.1, 139.2, 133.8, 130.4, 129.1, 128.7, 124.3, 123.8, 119.6, 116.1, 56.3.



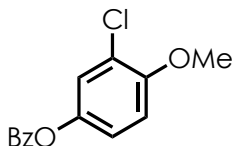
2-chloro-4-methoxyphenyl benzoate (4.20C)

Prepared from 3-chloro-4-fluoroanisole (48.0 mg, 0.300 mmol, 1 equiv.). Purified *via* the aqueous workup described above without chromatography. The title compound was isolated as a pale-yellow solid in an average yield of 90%.

¹H NMR (400 MHz, CDCl₃) δ 8.31 – 8.17 (m, 2H), 7.72 – 7.57 (m, 1H), 7.53 (dd, *J* = 8.4, 7.1 Hz, 2H), 7.18 (d, *J* = 8.9 Hz, 1H), 7.03 (d, *J* = 2.9 Hz, 1H), 6.86 (dd, *J* = 8.9, 2.9 Hz, 1H), 3.82 (s, 3H).

¹³C NMR (101 MHz, CDCl₃) δ 164.8, 158.0, 140.9, 133.9, 130.5, 129.2, 128.8, 127.5, 124.2, 115.5, 113.6, 56.0.

LRMS (EI): Calculated for C₁₄H₁₁ClO₃: 262.04, found: 262.00.



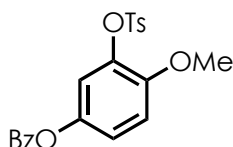
3-chloro-4-methoxyphenyl benzoate (4.21C)

Prepared from 2-chloro-4-fluoroanisole (80.0 mg, 0.500 mmol, 1 equiv.). Purified by flash column chromatography using isocratic elution (20% EtOAc in Hex). The title compound was isolated as an off-white solid in an average yield of 28%.

¹H NMR (400 MHz, CDCl₃) δ 8.18 (dd, *J* = 8.3, 1.4 Hz, 2H), 7.69 – 7.59 (m, 1H), 7.52 (t, *J* = 7.8 Hz, 2H), 7.29 (d, *J* = 2.8 Hz, 1H), 7.11 (dd, *J* = 8.9, 2.8 Hz, 1H), 6.97 (d, *J* = 9.0 Hz, 1H), 3.93 (s, 3H).

¹³C NMR (101 MHz, CDCl₃) δ 165.4, 153.2, 144.3, 133.9, 130.3, 129.4, 128.8, 124.0, 122.9, 120.9, 112.3, 56.7.

LRMS (EI): Calculated for C₁₄H₁₁ClO₃: 262.04, found: 262.00.

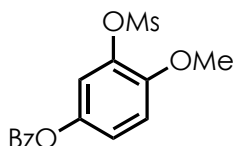


4-methoxy-3-(tosyloxy)phenyl benzoate (4.22C)

Prepared from 5-fluoro-2-methoxyphenyl 4-methylbenzenesulfonate (89.0 mg, 0.300 mmol, 1 equiv.). Purified by flash column chromatography using isocratic elution (20% Acetone in Hex). The title compound was isolated as a white solid in an average yield of 28%.

¹H NMR (400 MHz, CDCl₃) δ 8.17 (d, *J* = 7.8 Hz, 2H), 7.79 (d, *J* = 8.0 Hz, 2H), 7.65 (t, *J* = 7.4 Hz, 1H), 7.52 (t, *J* = 7.6 Hz, 2H), 7.31 (d, *J* = 8.0 Hz, 2H), 7.10 (d, *J* = 8.8 Hz, 2H), 6.86 (d, *J* = 8.5 Hz, 1H), 3.59 (s, 3H), 2.44 (s, 3H).

¹³C NMR (101 MHz, CDCl₃) δ 165.1, 149.9, 145.3, 143.7, 138.3, 133.9, 133.1, 130.3, 129.5, 128.8, 128.7, 121.1, 118.3, 112.8, 56.1, 21.8.



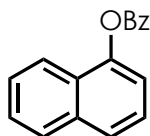
4-methoxy-3-((methylsulfonyl)oxy)phenyl benzoate (4.23C)

Prepared from 5-fluoro-2-methoxyphenyl methanesulfonate (66.0 mg, 0.300 mmol, 1 equiv.).

Purified by flash column chromatography using isocratic elution (20% Acetone in Hex). The title compound was isolated as a white solid in an average yield of 27%.

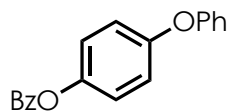
$^1\text{H NMR}$ (400 MHz, CDCl_3) δ 8.21 – 8.14 (m, 2H), 7.67 – 7.60 (m, 1H), 7.52 (dd, $J = 8.5$, 7.0 Hz, 2H), 7.19 (dd, $J = 9.0$, 2.8 Hz, 1H), 7.05 (d, $J = 9.0$ Hz, 1H), 3.92 (s, 3H), 3.21 (s, 3H).

$^{13}\text{C NMR}$ (101 MHz, CDCl_3) δ 165.1, 149.6, 144.1, 138.2, 133.9, 130.3, 129.2, 128.8, 121.4, 118.7, 113.1, 56.6, 38.5.



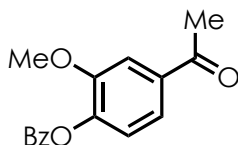
naphthalen-1-yl benzoate (4.24C)

Prepared from 1-fluoronaphthalene (39.0 μL , 0.300 mmol, 1 equiv.) and **Catalyst B** (18.8 mg, 0.030 mmol, 0.1 equiv.). Purified by flash column chromatography using isocratic elution (10% Acetone in Hex). The title compound was isolated as an off-white solid in an average yield of 32%. Spectral data aligns with literature values.²⁴⁶



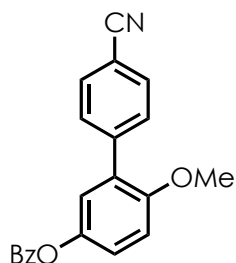
4-phenoxyphenyl benzoate (4.25C)

Prepared from 1-fluoro-4-phenoxybenzene (49.0 μ L, 0.300 mmol, 1 equiv.). Purified by flash column chromatography using isocratic elution (10% Acetone in Hex). The title compound was isolated as an off-white solid in an average yield of 24%. Spectral data aligns with literature values.²⁴⁷



4-acetyl-2-methoxyphenyl benzoate (4.27C)

Prepared from 1-(4-fluoro-3-methoxyphenyl)ethan-1-one (50.0 mg, 0.300 mmol, 1 equiv.). Purified by flash column chromatography using isocratic elution (20% Acetone in Hex). The title compound was isolated as a white solid in an average yield of 35%. Spectral data align with literature values.²⁴⁸

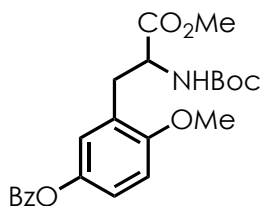


4'-cyano-6-methoxy-[1,1'-biphenyl]-3-yl benzoate (4.28C)

Prepared from 5'-fluoro-2'-methoxy-[1,1'-biphenyl]-4-carbonitrile (68.0 mg, 0.300 mmol, 1 equiv.) and **Catalyst B** (18.8 mg, 0.030 mmol, 0.1 equiv.). Purified by flash column chromatography (20% Acetone in Hex). The title compound was isolated as an off-white solid in an average yield of 25%.

¹H NMR (400 MHz, CDCl₃) δ 8.27 – 8.16 (m, 2H), 7.67 (m, 5H), 7.52 (t, $J = 7.6$ Hz, 2H), 7.25 – 7.14 (m, 2H), 7.04 (d, $J = 8.9$ Hz, 1H), 3.85 (s, 3H).

¹³C NMR (101 MHz, CDCl₃) δ 165.7, 154.2, 144.6, 142.5, 133.9, 132.0, 130.4, 130.3, 129.5, 129.4, 128.8, 123.9, 122.7, 119.2, 112.2, 110.9, 56.1.



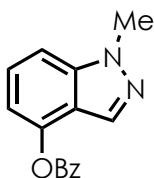
3-(2-((*tert*-butoxycarbonyl)amino)-3-methoxy-3-oxopropyl)-4-methoxyphenyl benzoate (4.29C)

Prepared from methyl 2-((*tert*-butoxycarbonyl)amino)-3-(5-fluoro-2-methoxyphenyl)propanoate (98.0 mg, 0.300 mmol, 1 equiv.) and **Catalyst B** (18.8 mg, 0.030

mmol, 0.1 equiv.). Purified *via* column chromatography (20% Acetone in Hex). The title compound was isolated as a clear oil in an average yield of 31%.

¹H NMR (400 MHz, CDCl₃) δ 8.2 – 8.1 (m, 2H), 7.7 – 7.6 (m, 1H), 7.5 (t, *J* = 7.8 Hz, 2H), 7.1 (dd, *J* = 8.8, 2.9 Hz, 1H), 7.0 (d, *J* = 2.9 Hz, 1H), 6.9 (d, *J* = 8.9 Hz, 1H), 5.2 (d, *J* = 8.0 Hz, 1H), 4.6 – 4.4 (m, 1H), 3.8 (s, 3H), 3.7 (s, 3H), 3.1 (dt, *J* = 13.7, 7.1 Hz, 1H), 1.4 (s, 9H).

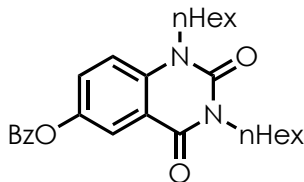
¹³C NMR (101 MHz, CDCl₃) δ 172.8, 165.5, 155.5, 155.3, 144.2, 133.7, 130.2, 129.6, 128.7, 126.0, 124.4, 121.2, 111.0, 79.8, 77.2, 55.9, 53.9, 52.3, 33.0, 28.4.



1-methyl-1*H*-indazol-4-yl benzoate (4.32C)

Prepared from 4-fluoro-1-methyl-1*H*-indazole (23.0 mg 0.150 mmol, 1 equiv.). The reported yield of 28% was obtained by ¹H NMR using HMDSO as an internal standard. The crude ¹H NMR data is given below.

¹H NMR (400 MHz, CDCl₃) δ 8.30 (dd, *J* = 7.8, 1.4 Hz, 2H), 7.99 (d, *J* = 0.9 Hz, 1H), 7.71 – 7.66 (m, 1H), 7.56 (t, *J* = 7.7 Hz, 2H), 7.45 – 7.42 (m, 1H), 7.34 – 7.30 (m, 1H), 7.08 (d, *J* = 7.5 Hz, 1H), 4.13 (s, 3H).

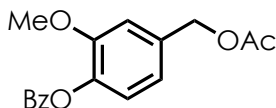


1,3-dihexanoyl-2,4-dioxo-1,2,3,4-tetrahydroquinazolin-6-yl benzoate (4.33C)

Prepared from 6-fluoro-1,3-dihexanoylquinazoline-2,4(1*H*,3*H*)-dione (17.5 mg, 0.050 mmol, 1 equiv.). The reaction was purified *via* column chromatography (10% acetone/hexanes), and the title compound was isolated as a clear oil in a 44% yield (*n* = 1).

¹H NMR (400 MHz, CDCl₃) δ 8.26 – 8.16 (m, 2H), 8.05 (d, *J* = 2.8 Hz, 1H), 7.72 – 7.63 (m, 1H), 7.59 – 7.49 (m, 3H), 7.23 (d, *J* = 9.1 Hz, 1H), 4.15 – 4.02 (m, 4H), 1.77 – 1.62 (m, 4H), 1.40 – 1.28 (m, 12H), 0.89 (dt, *J* = 10.0, 6.9 Hz, 6H).

¹³C NMR (101 MHz, CDCl₃) δ 165.33, 161.12, 150.66, 146.05, 137.75, 134.08, 130.40, 129.05, 128.83, 121.69, 116.84, 114.97, 77.16, 44.18, 42.25, 31.66, 31.60, 27.87, 27.40, 26.79, 26.61, 22.72, 14.21.



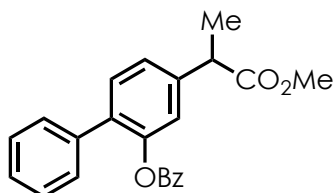
4-(acetoxymethyl)-2-methoxyphenyl benzoate (4.43C)

Prepared from 4-fluoro-3-methoxybenzyl acetate (59.0 mg, 0.300 mmol, 1 equiv.). Purified by flash column chromatography using isocratic elution (20% EtOAc in Hex). The title compound was isolated as an off-white solid in an average yield of 53%.

¹H NMR (400 MHz, CDCl₃) δ 8.24 – 8.16 (m, 2H), 7.64 (t, *J* = 7.4 Hz, 1H), 7.51 (t, *J* = 7.7 Hz, 2H), 7.14 (d, *J* = 7.9 Hz, 1H), 7.03 – 6.93 (m, 2H), 5.11 (s, 2H), 3.83 (s, 3H), 2.13 (s,

3H).

^{13}C NMR (101 MHz, CDCl_3) δ 171.0, 164.8, 151.5, 140.1, 135.0, 133.7, 130.5, 129.5, 128.5, 123.1, 121.0, 112.8, 66.2, 56.1, 21.2.



4-(1-methoxy-1-oxopropan-2-yl)-[1,1'-biphenyl]-2-yl benzoate (4.44C)

Prepared from flurbiprofen methyl ester (77.0 mg, 0.300 mmol, 1 equiv.) and **Catalyst B** (14.1 mg, 0.023 mmol, 0.075 equiv.). Purified *via* column chromatography using isocratic elution (10% Acetone in Hex). The title compound was isolated as a clear oil in an average yield of 25%.

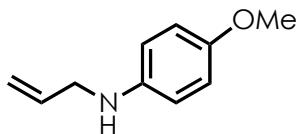
^1H NMR (400 MHz, CDCl_3) δ 8.1 – 8.0 (m, 2H), 7.6 – 7.5 (m, 1H), 7.4 (ddd, $J = 10.6, 7.2, 2.2$ Hz, 5H), 7.4 – 7.3 (m, 3H), 7.3 – 7.2 (m, 2H), 3.8 (q, $J = 7.2$ Hz, 1H), 3.7 (s, 3H), 1.6 (d, $J = 7.2$ Hz, 3H).

^{13}C NMR (101 MHz, CDCl_3) δ 174.8, 165.1, 148.1, 141.1, 137.3, 133.9, 133.6, 131.2, 130.2, 129.4, 129.0, 128.6, 128.4, 127.5, 125.7, 122.4, 77.2, 52.4, 45.1, 18.6.

Procedure and Data for Use of Other Primary Amines as Nucleophiles:

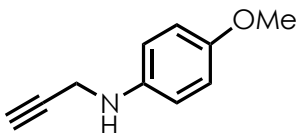
To a 2-dram vial equipped with a stirbar was added: **Catalyst B** (9.4 mg, 0.015 mmol, 0.05 equiv.), amine (0.900 mmol, 3 equiv.), and TFE (3 mL). The vial was sealed with a septum cap and sparged with N_2 for 5 minutes. Then, 4-fluoroanisole (37.8 mg, 34.0 μL , 0.300 mmol, 1.0 eq) was added *via* microsyringe. The cap was lined with Teflon tape and electrical

tape and then irradiated for 18 h using 427 nm Kessil lamps. After irradiation, the solvent was removed in vacuo and purification was carried out as specified for each compound.



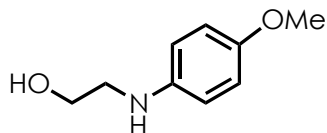
N-allyl-4-methoxyaniline (4.35)

Prepared using prop-2-en-1-amine (51.4 mg, 67.4 μ L, 0.900 mmol, 3 equiv.). Purified *via* column chromatography using isocratic elution (10% EtOAc in Hex). The title compound was isolated as a light-yellow oil in an average yield of 42%. Spectral data align with literature values.²⁴⁹



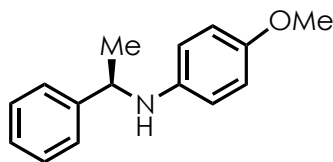
4-methoxy-N-(prop-2-yn-1-yl)aniline (4.36)

Prepared using prop-2-yn-1-amine (49.6 mg, 58.0 μ L, 0.900 mmol, 3 equiv.). Purified *via* column chromatography using isocratic elution (10% EtOAc in Hex). The title compound was isolated as a yellow oil in an average yield of 57%. Spectral data align with literature values.²⁵⁰



2-((4-methoxyphenyl)amino)ethan-1-ol (4.37)

Prepared using 2-aminoethan-1-ol (55.0 mg, 54.3 μ L, 0.900 mmol, 3 equiv.). Purified *via* column chromatography using gradient elution (60 – 75% EtOAc in Hex). The title compound was isolated as a yellow oil in an average yield of 58%. Spectral data align with literature values.²⁵¹



(R)-4-methoxy-N-(1-phenylethyl)aniline (4.38)

Prepared using (R)-1-phenylethan-1-amine (109 mg, 120. μ L, 0.900 mmol, 3 equiv.). Purified *via* column chromatography using gradient elution (2.5 – 10% EtOAc in Hex). The title compound was isolated as a pale yellow oil in an average yield of 66% as a single enantiomer. Spectral data align with literature values.²⁵²

The enantiopurity of the product was determined using an Agilent 1200 series HPLC with detection at 210, 230, 250 and 254 nm using a Chiralpak IC column using a flow rate of 1 mL per minute. The solvent system used for HPLC resolution of enantiomers was hexanes (A1) and isopropanol (B2). Using a method of 99.5A1: 0.5B2 for 30 minutes, the racemic

standard (prepared according to a literature procedure²⁵³) made through the present methodology was observed at 13.947 min and 14.871 min of equal area. **4.38** was observed as one peak under identical HPLC conditions at 13.970 min. No racemization of this product was observed.

Figure C-12. Racemic HPLC Trace for Standard of **4.38**

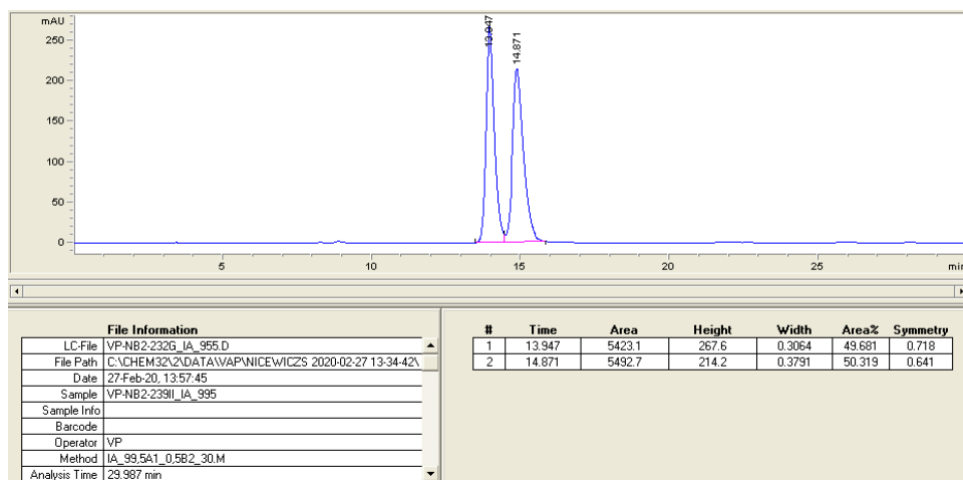
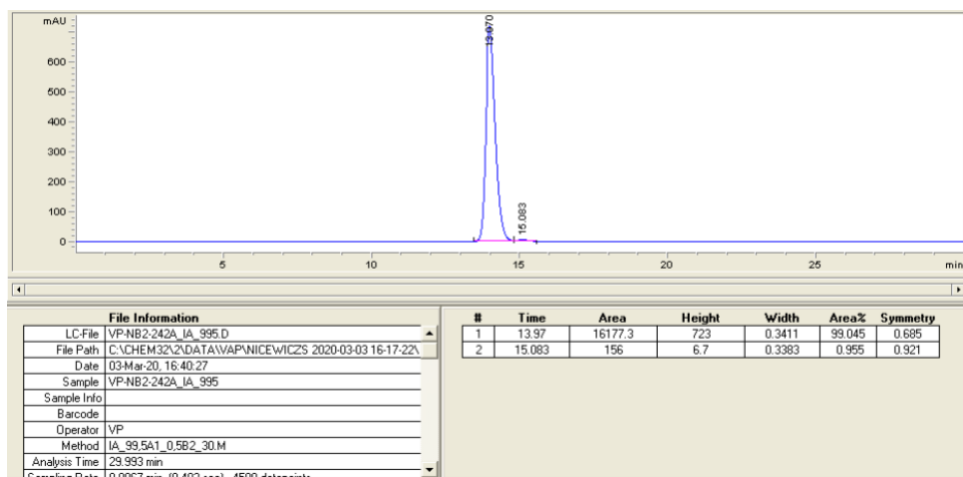
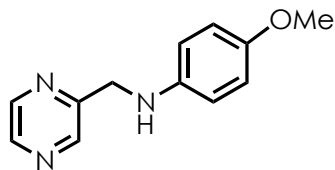


Figure C-13. HPLC Trace of Enantiopure **4.38**



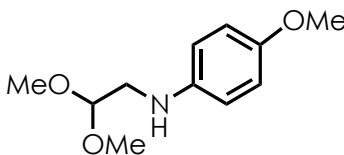


4-methoxy-N-(pyrazin-2-ylmethyl)aniline (4.39)

Prepared using pyrazin-2-ylmethanamine (98.2 mg, 0.900 mmol, 3 equiv.). Purified *via* column chromatography using gradient elution (60 – 80% EtOAc in Hex). The title compound was isolated as a yellow solid in an average yield of 49%.

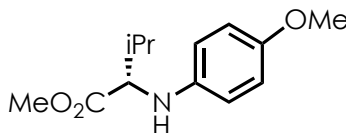
¹H NMR (600 MHz, CDCl₃) δ 8.67 – 8.61 (m, 1H), 8.54 (s, 1H), 8.48 (d, *J* = 2.5 Hz, 1H), 6.78 (d, *J* = 8.9 Hz, 2H), 6.64 (d, *J* = 8.9 Hz, 2H), 4.47 (s, 2H), 3.74 (s, 3H).

¹³C NMR (151 MHz, CDCl₃) δ 154.57, 152.69, 144.07, 143.40, 141.66, 115.06, 114.61, 55.88, 48.33.



N-(2,2-dimethoxyethyl)-4-methoxyaniline (4.40)

Prepared using 2,2-dimethoxyethan-1-amine (94.6 mg, 0.900 mmol, 3 equiv.). Purified *via* column chromatography using gradient elution (10 – 20% EtOAc in Hex). The title compound was isolated as a yellow oil in an average yield of 70%. Spectral data align with literature values.²⁵⁴

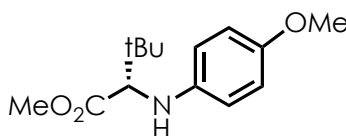


methyl (4-methoxyphenyl)-L-valinate (**4.41**)

Prepared from methyl L-valinate (118 mg, 0.900 mmol, 3 equiv.). Purified *via* column chromatography using isocratic elution (10 % EtOAc in Hex). The title compound was isolated as a light-yellow oil in an average yield of 50%.

¹H NMR (600 MHz, CDCl₃) δ 6.76 (d, *J* = 9.0 Hz, 2H), 6.61 (d, *J* = 8.9 Hz, 2H), 3.91 (s, 1H), 3.76 (d, *J* = 6.0 Hz, 1H), 3.73 (s, 3H), 3.69 (s, 3H), 2.13 – 2.02 (m, *J* = 6.8 Hz, 1H), 1.04 (d, *J* = 6.9 Hz, 3H), 1.01 (d, *J* = 6.8 Hz, 3H).

¹³C NMR (151 MHz, CDCl₃) δ 174.67, 152.82, 141.53, 115.36, 114.98, 63.92, 55.84, 51.93, 31.70, 19.30, 18.85.



methyl (S)-2-((4-methoxyphenyl)amino)-3,3-dimethylbutanoate (**4.42**)

Prepared from methyl (S)-2-amino-3,3-dimethylbutanoate (131 mg, 0.900 mmol, 3 equiv.). Purified *via* column chromatography using gradient elution (5 – 10 % EtOAc in Hex). The title compound was isolated as a light-yellow oil in an average yield of 55%.

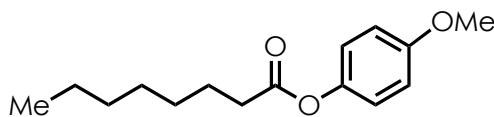
¹H NMR (600 MHz, CDCl₃) δ 6.76 (d, *J* = 5.9 Hz, 2H), 6.63 (d, *J* = 6.0 Hz, 2H), 3.73 (s, 3H), 3.68 (s, 1H), 3.66 (s, 3H), 1.05 (s, 9H).

¹³C NMR (151 MHz, CDCl₃) δ 174.42, 152.90, 141.83, 115.65, 114.96, 67.11, 55.83, 51.60,

34.42, 26.88.

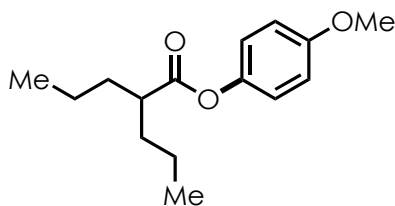
Procedure and Data for Use of Octanoic Acid as a Nucleophile:

A two-dram vial was equipped with a stir bar, and the solid reagents were added: **Catalyst B** (7.1 mg, 0.011 mmol, 0.075 equiv.) and sodium bicarbonate (25.0 mg, 0.300 mmol, 2.0 equiv.). The TFE (3.0 mL) was then added *via* syringe, and the system was sparged with N₂ for five minutes. The 4-fluoroanisole (19.0 mg, 0.150 mmol, 1.0 equiv.) and octanoic acid (87.0 mg, 0.600 mmol, 4.0 equiv.) were then added *via* microsyringe, and the vial was sealed with electrical tape. The reactions were stirred while irradiated with 465 nm blue Kessil LEDs for 18 hours. The reaction mixture was diluted with DCM (20 mL), transferred to a separatory funnel, and washed with saturated aqueous sodium bicarbonate solution (2 x 25 mL), water (1 x 25 mL), and brine (1 x 25 mL). The combined organic layers were dried with Na₂SO₄ and concentrated under vacuum. The crude reaction material was purified by filtering through a plug of silica and eluting with DCM and EtOAc.



4-methoxyphenyl octanoate (4.45)

The title compound was isolated as a pale-yellow oil in a 63% yield by aqueous workup and filtration through a silica plug ($n = 1$). Spectral data align with literature values.²⁵⁵



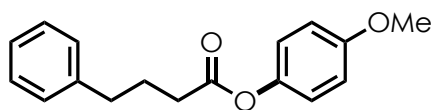
4-methoxyphenyl 2-propylpentanoate (4.46)

The title compound was prepared from 4-fluoroanisole (19.0 mg, 0.150 mmol, 1.0 equiv.).

The reported yield of 31% ($n = 1$) was obtained by ^1H NMR using HMDSO as an internal standard. The crude ^1H NMR data is given below.

^1H NMR (400 MHz, CDCl_3) δ 6.96 (d, $J = 9.0$ Hz, 2H), 6.87 (d, $J = 9.1$ Hz, 2H), 3.78 (s, 3H), 2.65 – 2.53 (m, 1H).

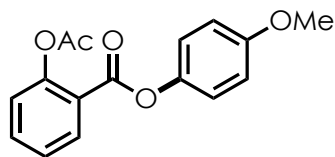
NOTE: Due to the presence of excess nucleophile in the crude reaction mixture, not all peaks in the alkyl chains were visible.



4-methoxyphenyl 4-phenylbutanoate (4.47)

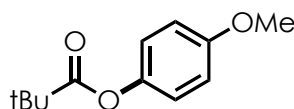
The title compound was prepared from 4-fluoroanisole (19.0 mg, 0.150 mmol, 1.0 equiv.).

The reported yield of 20% ($n = 1$) was obtained by ^1H NMR using HMDSO as an internal standard. The crude ^1H NMR data matches that reported in the literature.²⁵⁶



4-methoxyphenyl 2-acetoxybenzoate (4.48)

The title compound was prepared from 4-fluoroanisole (19.0 mg, 0.150 mmol, 1.0 equiv.). The reported yield of 10% (n = 1) was obtained by ^1H NMR using HMDSO as an internal standard. The crude ^1H NMR data matches that reported in the literature.²⁵⁷



4-methoxyphenyl pivalate (4.49)

The title compound was prepared from 4-fluoroanisole (19.0 mg, 0.150 mmol, 1.0 equiv.). The reported yield of 10% (n = 1) was obtained by ^1H NMR using HMDSO as an internal standard. The crude ^1H NMR data matches that reported in the literature.²⁵⁸

Electron Density Computational Data for Ground State Arenes and Radical Cation Counterparts

The following figures detail the results of the calculations designed to probe the electron density for the ground state arene substrates and their radical cation counterparts. For clarity, only the values for the carbons bearing substituents are shown. Values shown in bolded black indicate the position with the most electron density in the ground state arenes. Values shown in green indicate the position with the most electron density when it is the position bearing

the fluorine, and values shown in red indicate the position with the most electron density when it is the position bearing an oxygen-containing substituent.

DFT calculations were carried out using Gaussian 09 at the B3LYP level of theory with the 6-31+G(d,p) basis set. Geometry optimizations were carried out, with frequency calculations were performed on the minimized geometry. Optimized structures were verified to be located at a local minimum by ensuring no imaginary frequencies existed in the optimized geometry. Solvation was modeled in dichloromethane using the Conductor-like Polarizable Continuum Model (CPCM) formalism for the Self Consistent Reaction Field (SCRF).

Figure C-14. Ground State and Excited State NPA Values for Substrates

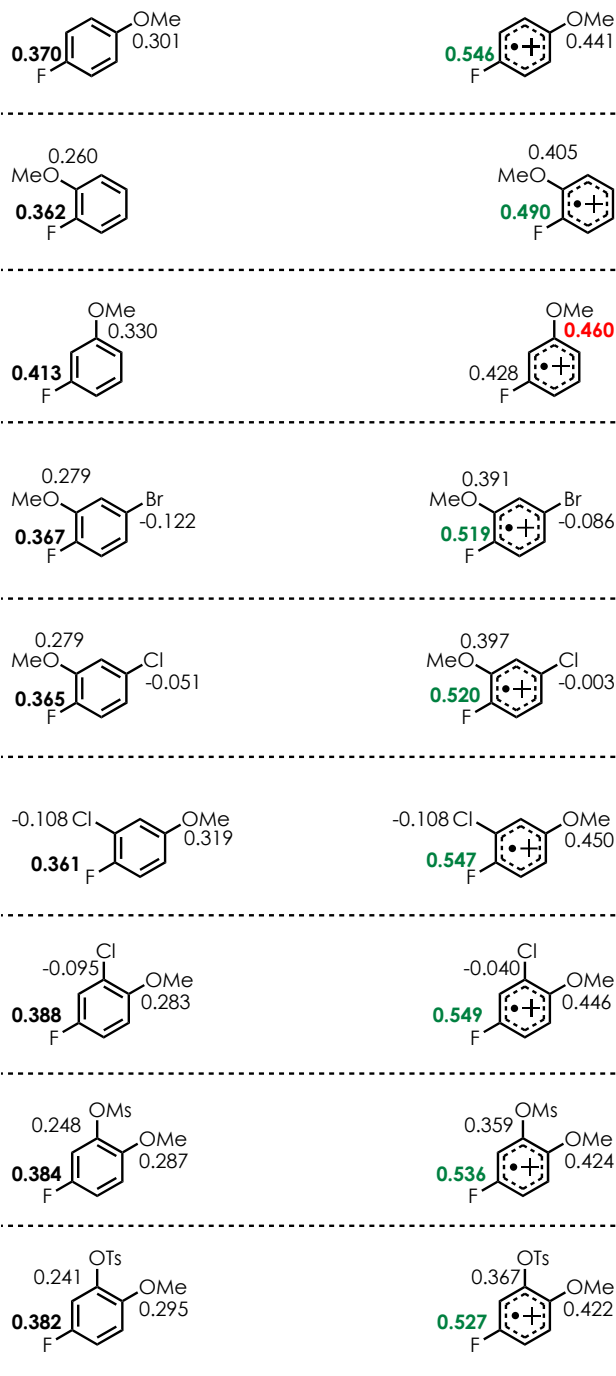
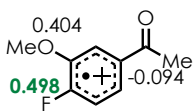
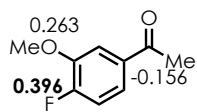
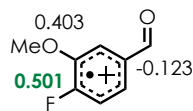
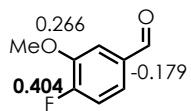
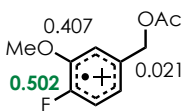
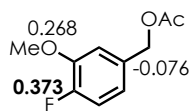
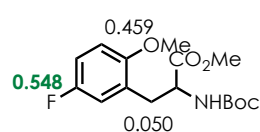
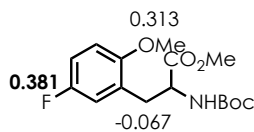
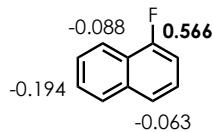
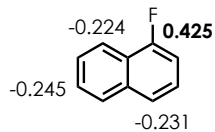
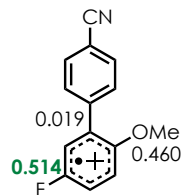
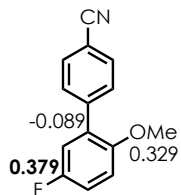
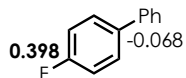
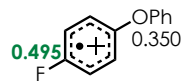
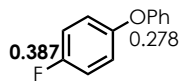


Figure C-15. Additional NPA Data for Substrates



REFERENCES

- (1) Yan, M.; Kawamata, Y.; Baran, P. S. Synthetic Organic Electrochemical Methods Since 2000: On the Verge of a Renaissance. *Chem. Rev.* **2017**, *117* (21), 13230–13319.
- (2) Plutschack, M. B.; Pieber, B.; Gilmore, K.; Seeberger, P. H. The Hitchhiker's Guide to Flow Chemistry. *Chem. Rev.* **2017**, *117* (18), 11796–11893.
- (3) Romero, N. A.; Nicewicz, D. A. Organic Photoredox Catalysis. *Chem. Rev.* **2016**, *116* (17), 10075–10166.
- (4) Prier, C. K.; Rankic, D. A.; MacMillan, D. W. C. Visible Light Photoredox Catalysis with Transition Metal Complexes: Applications in Organic Synthesis. *Chem. Rev.* **2013**, *113* (7), 5322–5363.
- (5) Narayanam, J. M. R.; Stephenson, C. R. J. Visible Light Photoredox Catalysis: Applications in Organic Synthesis. *Chem. Soc. Rev.* **2011**, *40* (1), 102–113.
- (6) Skubi, K. L.; Blum, T. R.; Yoon, T. P. Dual Catalysis Strategies in Photochemical Synthesis. *Chem. Rev.* **2016**, *116* (17), 10035–10074.
- (7) Juris, A.; Balzani, V.; Barigelletti, F.; Campagna, S.; Belser, P.; von Zelewsky, A. Ru(II) Polypyridine Complexes: Photophysics, Photochemistry, Electrochemistry, and Chemiluminescence. *Coord. Chem. Rev.* **1988**, *84*, 85–277.
- (8) Flamigni, L.; Barbieri, A.; Sabatini, C.; Ventura, B.; Barigelletti, F. Photochemistry and Photophysics of Coordination Compounds: Iridium. In *Photochemistry and Photophysics of Coordination Compounds II*; Balzani, V., Campagna, S., Eds.; Topics in Current Chemistry; Springer: Berlin, Heidelberg, 2007; pp 143–203.
- (9) Mattay, J. Photoinduced Electron Transfer in Organic Synthesis. *Synthesis* **1989**, *1989* (4), 233–252.
- (10) Roth, H. G.; Romero, N. A.; Nicewicz, D. A. Experimental and Calculated Electrochemical Potentials of Common Organic Molecules for Applications to Single-Electron Redox Chemistry. *Synlett* **2016**, *27* (05), 714–723.
- (11) Fukuzumi, S.; Kotani, H.; Ohkubo, K.; Ogo, S.; Tkachenko, N. V.; Lemmetyinen, H. Electron-Transfer State of 9-Mesityl-10-Methylacridinium Ion with a Much Longer Lifetime and Higher Energy Than That of the Natural Photosynthetic Reaction Center. *J. Am. Chem. Soc.* **2004**, *126* (6), 1600–1601.
- (12) Fukuzumi, S.; Kotani, H.; Ohkubo, K. Response: Why Had Long-Lived Electron-Transfer States of Donor-Substituted 10-Methylacridinium Ions Been Overlooked?

Formation of the Dimer Radical Cations Detected in the near-IR Region. *Physical Chem. Chem. Phys.* **2008**, *10* (33), 5159–5162.

- (13) Hoshino, M.; Uekusa, H.; Tomita, A.; Koshihara, S.; Sato, T.; Nozawa, S.; Adachi, S.; Ohkubo, K.; Kotani, H.; Fukuzumi, S. Determination of the Structural Features of a Long-Lived Electron-Transfer State of 9-Mesityl-10-Methylacridinium Ion. *J. Am. Chem. Soc.* **2012**, *134* (10), 4569–4572.
- (14) Verhoeven, J. W.; Ramesdonk, H. J. van; Zhang, H.; Groeneveld, M. M.; Benniston, A. C.; Harriman, A. Long-Lived Charge-Transfer States in 9-Aryl-Acridinium Ions; a Critical Reinvestigation. *International journal of photoenergy* **2005**, *7* (2), 103–108.
- (15) Benniston, A. C.; Harriman, A.; Li, P.; Rostron, J. P.; Verhoeven, J. W. Illumination of the 9-Mesityl-10-Methylacridinium Ion Does Not Give a Long-Lived Photoredox State. *Chemical Communications* **2005**, No. 21, 2701–2703.
- (16) Benniston, A. C.; Harriman, A.; Verhoeven, J. W. Comment: Electron-Transfer Reactions in the 9-Mesityl-10-Methylacridinium Ion: Impurities, Triplet States and Infinitely Long-Lived Charge-Shift States? *Phys. Chem. Chem. Phys.* **2008**, *10* (33), 5156–5156.
- (17) Benniston, A. C.; Harriman, A.; Li, P.; Rostron, J. P.; van Ramesdonk, H. J.; Groeneveld, M. M.; Zhang, H.; Verhoeven, J. W. Charge Shift and Triplet State Formation in the 9-Mesityl-10-Methylacridinium Cation. *J. Am. Chem. Soc.* **2005**, *127* (46), 16054–16064.
- (18) Ohkubo, K.; Mizushima, K.; Iwata, R.; Fukuzumi, S. Selective Photocatalytic Aerobic Bromination with Hydrogen Bromide via an Electron-Transfer State of 9-Mesityl-10-Methylacridinium Ion. *Chem. Sci.* **2011**, *2* (4), 715–722.
- (19) Ohkubo, K.; Nanjo, T.; Fukuzumi, S. Photocatalytic Oxygenation of Olefins with Oxygen: Isolation of 1,2-Dioxetane and the Photocatalytic O–O Bond Cleavage. *Catalysis Today* **2006**, *117* (1), 356–361.
- (20) Ohkubo, K.; Iwata, R.; Yanagimoto, T.; Fukuzumi, S. Enhanced Photoinduced Oligomerization of Fullerene via Radical Coupling between Fullerene Radical Cation and Radical Anion Using 9-Mesityl-10-Methylacridinium Ion. *Chem. Commun.* **2007**, No. 30, 3139.
- (21) Ohkubo, K.; Mizushima, K.; Fukuzumi, S. Oxygenation and Chlorination of Aromatic Hydrocarbons with Hydrochloric Acid Photosensitized by 9-Mesityl-10-Methylacridinium under Visible Light Irradiation. *Research on Chemical Intermediates* **2013**, *39* (1), 205–220.

- (22) Hering, T.; Slanina, T.; Hancock, A.; Wille, U.; König, B. Visible Light Photooxidation of Nitrate: The Dawn of a Nocturnal Radical. *Chem. Commun.* **2015**, *51* (30), 6568–6571.
- (23) Xu, H.-J.; Zhu, F.-F.; Shen, Y.-Y.; Wan, X.; Feng, Y.-S. Baeyer–Villiger Oxidation of Cyclobutanones with 10-Methylacridinium as an Efficient Organocatalyst. *Tetrahedron* **2012**, *68* (22), 4145–4151.
- (24) Ramirez, N. P.; Bosque, I.; Gonzalez-Gomez, J. C. Photocatalytic Dehydrogenative Lactonization of 2-Arylbenzoic Acids. *Org. Lett.* **2015**, *17* (18), 4550–4553.
- (25) Wu, X.; Meng, C.; Yuan, X.; Jia, X.; Qian, X.; Ye, J. Transition-Metal-Free Visible-Light Photoredox Catalysis at Room-Temperature for Decarboxylative Fluorination of Aliphatic Carboxylic Acids by Organic Dyes. *Chem. Commun.* **2015**, *51* (59), 11864–11867.
- (26) Xuan, J.; Xia, X.-D.; Zeng, T.-T.; Feng, Z.-J.; Chen, J.-R.; Lu, L.-Q.; Xiao, W.-J. Visible-Light-Induced Formal [3+2] Cycloaddition for Pyrrole Synthesis under Metal-Free Conditions. *Angew. Chem. Int. Ed.* **2014**, *53* (22), 5653–5656.
- (27) Griffin, J. D.; Cavanaugh, C. L.; Nicewicz, D. A. Reversing the Regioselectivity of Halofunctionalization Reactions through Cooperative Photoredox and Copper Catalysis. *Angew. Chem. Int. Ed.* **2017**, *56* (8), 2097–2100.
- (28) Huang, L.; Ji, T.; Rueping, M. Remote Nickel-Catalyzed Cross-Coupling Arylation via Proton-Coupled Electron Transfer-Enabled C–C Bond Cleavage. *J. Am. Chem. Soc.* **2020**, *142*, 3532–3539.
- (29) Kalsi, D.; Dutta, S.; Barsu, N.; Rueping, M.; Sundararaju, B. Room-Temperature C–H Bond Functionalization by Merging Cobalt and Photoredox Catalysis. *ACS Catal.* **2018**, *8* (9), 8115–8120.
- (30) Fuse, H.; Mitsunuma, H.; Kanai, M. Catalytic Acceptorless Dehydrogenation of Aliphatic Alcohols. *J. Am. Chem. Soc.* **2020**, *142*, 4493–4499.
- (31) Dempsey, J. L.; Brunschwig, B. S.; Winkler, J. R.; Gray, H. B. Hydrogen Evolution Catalyzed by Cobaloximes. *Acc. Chem. Res.* **2009**, *42* (12), 1995–2004.
- (32) Xiang, M.; Meng, Q.-Y.; Li, J.-X.; Zheng, Y.-W.; Ye, C.; Li, Z.-J.; Chen, B.; Tung, C.-H.; Wu, L.-Z. Activation of C-H Bonds through Oxidant-Free Photoredox Catalysis: Cross-Coupling Hydrogen-Evolution Transformation of Isochromans and β -Keto Esters. *Chem. Eur. J.* **2015**, *21* (50), 18080–18084.
- (33) White, A. R.; Wang, L.; Nicewicz, D. A. Synthesis and Characterization of Acridinium Dyes for Photoredox Catalysis. *Synlett* **2019**, *30* (07), 827–832.

- (34) Margrey, K. A.; Nicewicz, D. A. A General Approach to Catalytic Alkene Anti-Markovnikov Hydrofunctionalization Reactions via Acridinium Photoredox Catalysis. *Acc. Chem. Res.* **2016**, *49* (9), 1997–2006.
- (35) Hamilton, D. S.; Nicewicz, D. A. Direct Catalytic Anti-Markovnikov Hydroetherification of Alkenols. *J. Am. Chem. Soc.* **2012**, *134* (45), 18577–18580.
- (36) Perkowski, A. J.; Nicewicz, D. A. Direct Catalytic Anti-Markovnikov Addition of Carboxylic Acids to Alkenes. *J. Am. Chem. Soc.* **2013**, *135* (28), 10334–10337.
- (37) Nguyen, T. M.; Nicewicz, D. A. Anti-Markovnikov Hydroamination of Alkenes Catalyzed by an Organic Photoredox System. *J. Am. Chem. Soc.* **2013**, *135* (26), 9588–9591.
- (38) Nguyen, T. M.; Manohar, N.; Nicewicz, D. A. Anti-Markovnikov Hydroamination of Alkenes Catalyzed by a Two-Component Organic Photoredox System: Direct Access to Phenethylamine Derivatives. *Angew. Chem. Int. Ed.* **2014**, *53* (24), 6198–6201.
- (39) Wilger, D. J.; Grandjean, J.-M. M.; Lammert, T. R.; Nicewicz, D. A. The Direct Anti-Markovnikov Addition of Mineral Acids to Styrenes. *Nat Chem* **2014**, *6* (8), 720–726.
- (40) Wilger, D. J.; Gesmundo, N. J.; Nicewicz, D. A. Catalytic Hydrotrifluoromethylation of Styrenes and Unactivated Aliphatic Alkenes via an Organic Photoredox System. *Chem. Sci.* **2013**, *4* (8), 3160–3165.
- (41) Romero, N. A.; Nicewicz, D. A. Mechanistic Insight into the Photoredox Catalysis of Anti-Markovnikov Alkene Hydrofunctionalization Reactions. *J. Am. Chem. Soc.* **2014**, *136* (49), 17024–17035.
- (42) Romero, N. A.; Margrey, K. A.; Tay, N. E.; Nicewicz, D. A. Site-Selective Arene C-H Amination via Photoredox Catalysis. *Science* **2015**, *349* (6254), 1326–1330.
- (43) Margrey, K. A.; McManus, J. B.; Bonazzi, S.; Zecri, F.; Nicewicz, D. A. Predictive Model for Site-Selective Aryl and Heteroaryl C–H Functionalization via Organic Photoredox Catalysis. *J. Am. Chem. Soc.* **2017**, *139* (32), 11288–11299.
- (44) McManus, J. B.; Nicewicz, D. A. Direct C-H Cyanation of Arenes via Organic Photoredox Catalysis. *J. Am. Chem. Soc.* **2017**, *139* (8), 2880–2883.
- (45) Chen, W.; Huang, Z.; Tay, N. E. S.; Giglio, B.; Wang, M.; Wang, H.; Wu, Z.; Nicewicz, D. A.; Li, Z. Direct Arene C–H Fluorination with 18F⁻ via Organic Photoredox Catalysis. *Science* **2019**, *364* (6446), 1170–1174.

- (46) Holmberg-Douglas, N.; Onuska, N. P. R.; Nicewicz, D. A. Regioselective Arene C–H Alkylation Enabled by Organic Photoredox Catalysis. *Angew. Chem. Int. Ed.* **2020**, *59* (19), 7425–7429.
- (47) Weymouth-Wilson, A. C. The Role of Carbohydrates in Biologically Active Natural Products. *Natural Product Reports* **1997**, *14* (2), 99.
- (48) Mirabella, S.; Cardona, F.; Goti, A. From Glycals to Aminosugars: A Challenging Test for New Stereoselective Aminohydroxylation and Related Methodologies. *Organic & Biomolecular Chemistry* **2016**, *14* (23), 5186–5204.
- (49) Schauer, R. Chemistry, Metabolism, and Biological Functions of Sialic Acids. In *Advances in Carbohydrate Chemistry and Biochemistry*; Tipson, R. S., Horton, D., Eds.; Academic Press, 1982; Vol. 40, pp 131–234.
- (50) Hakomori, S. Tumor-Associated Carbohydrate Antigens. *Annual Review of Immunology* **1984**, *2* (1), 103–126.
- (51) Shibuya, M.; Tomizawa, M.; Sasano, Y.; Iwabuchi, Y. An Expedient Entry to 9-Azabicyclo[3.3.1]Nonane *N*-Oxyl (ABNO): Another Highly Active Organocatalyst for Oxidation of Alcohols. *J. Org. Chem.* **2009**, *74* (12), 4619–4622.
- (52) Dungan, K. M. 1,5-Anhydroglucitol (GlycoMark™) as a Marker of Short-Term Glycemic Control and Glycemic Excursions. *Expert Review of Molecular Diagnostics* **2008**, *8* (1), 9–19.
- (53) Kühn, A.; Yu, S.; Giffhorn, F. Catabolism of 1,5-Anhydro-d-Fructose in *Sinorhizobium Morelense* S-30.7.5: Discovery, Characterization, and Overexpression of a New 1,5-Anhydro-d-Fructose Reductase and Its Application in Sugar Analysis and Rare Sugar Synthesis. *Applied and Environmental Microbiology* **2006**, *72* (2), 1248–1257.
- (54) Ernst, B.; Magnani, J. L. From Carbohydrate Leads to Glycomimetic Drugs. *Nat Rev Drug Discov* **2009**, *8* (8), 661–677.
- (55) Nicolaou, K. C.; Mitchell, H. J. Adventures in Carbohydrate Chemistry: New Synthetic Technologies, Chemical Synthesis, Molecular Design, and Chemical Biology. *Angew. Chem. Int. Ed.* **2001**, *40* (9), 1576–1624.
- (56) Taillefumier, C.; Chapleur, Y. Synthesis and Uses of Exo-Glycals. *Chem. Rev.* **2004**, *104* (1), 263–292.
- (57) Kine, H. H. Versatility of Glycals in Synthetic Organic Chemistry: Coupling Reactions, Diversity Oriented Synthesis and Natural Product Synthesis. *Org. Biomol. Chem.* **2019**, *17* (17), 4153–4182.

- (58) Lahiri, R.; Dharuman, S.; Vankar, Y. D. Functionalization of Glycals Leading to 2-Deoxy-O-glycosides, Aminosugars, Nitrosugars and Glycosidase Inhibitors: Our Experience. *CHIMIA Int. Journal for Chem.*, **2012**, *66*, 905-912.
- (59) Haworth, W. N.; Lake, W. H. G.; Peat, S. 59. The Configuration of Glucosamine (Chitosamine). *Journal of the Chemical Society (Resumed)* **1939**, 271.
- (60) Rosenthal, A.; Catsoulacos, P. Aminodideoxy Sugars. Methyl 3-Acetamido-2,3-Dideoxy- α -D - *Arabino* -Hexopyranoside and Methyl 2-Acetamido-2,3-Dideoxy- α -D - *Ribo* -Hexopyranoside. *Can. J. Chem.* **1969**, *47* (15), 2747–2750.
- (61) Veit, A.; Giese, B. Synthesis of Mannosamine via Cobaloximes. *Synlett* **1990**, *1990* (3), 166–166.
- (62) Lemieux, R. U.; Ratcliffe, R. M. The Azidonitration of Tri-O-Acetyl-D-Galactal. *Can. J. Chem.* **1979**, *57* (10), 1244–1251.
- (63) Paulsen, H.; Lorentzen, J. P.; Kutschker, W. Erprobte synthese von 2-azido-2-desoxy-d-mannose und 2-azido-2-desoxy-d-mannuronsäure als baustein zum aufbau von bakterien-polysaccharid-sequenzen. *Carbohyd. Res.* **1985**, *136*, 153–176.
- (64) Lafont, D.; Descotes, G. Synthèse de phosphoramidates de 2-désoxy-2-iodoglycosyles. *Carbohyd. Res.* **1987**, *166* (2), 195–209.
- (65) Lafont, D.; Descotes, G. Nouvelle voie d'accès aux 1,2-trans-2-amino-2-désoxyglycopyranosides par l'intermédiaire des phosphoramidates de 1,2-trans-2-désoxy-2-iodoglycopyranosyles. *Carbohyd. Res.* **1988**, *175* (1), 35–48.
- (66) Griffith, D. A.; Danishefsky, S. J. Sulfonamidoglycosylation of Glycals. A Route to Oligosaccharides with 2-Aminohexose Subunits. *J. Am. Chem. Soc.* **1990**, *112* (15), 5811–5819.
- (67) McDonald, F. E.; Danishefsky, S. J. A Stereoselective Route from Glycals to Asparagine-Linked N-Protected Glycopeptides. *J. Org. Chem.* **1992**, *57* (26), 7001–7002.
- (68) Kumar, V.; Ramesh, N. G. Iodine Catalyzed One-Pot Diamination of Glycals with Chloramine-T: A New Approach to 2-Amino- β -Glycosylamines for Applications in N-Glycopeptide Synthesis. *Chem. Commun.* **2006**, No. 47, 4952–4954.
- (69) Du Bois, J.; Tomooka, C. S.; Hong, J.; Carreira, E. M. Novel, Stereoselective Synthesis of 2-Amino Saccharides. *J. Am. Chem. Soc.* **1997**, *119* (13), 3179–3180.
- (70) Du Bois, J.; Hong, J.; Carreira, E. M.; Day, M. W. Nitrogen Transfer from a Nitridomanganese(V) Complex: Amination of Silyl Enol Ethers. *J. Am. Chem. Soc.* **1996**, *118* (4), 915–916.

- (71) Guthikonda, K.; Wehn, P. M.; Caliendo, B. J.; Du Bois, J. Rh-Catalyzed Alkene Oxidation: A Highly Efficient and Selective Process for Preparing N-Alkoxysulfonyl Aziridines. *Tetrahedron* **2006**, *62* (49), 11331–11342.
- (72) Hoang, K. M.; Lees, N. R.; Herzon, S. B. Programmable Synthesis of 2-Deoxyglycosides. *J. Am. Chem. Soc.* **2019**, *141* (20), 8098–8103.
- (73) Palo-Nieto, C.; Sau, A.; Galan, M. C. Gold(I)-Catalyzed Direct Stereoselective Synthesis of Deoxyglycosides from Glycals. *J. Am. Chem. Soc.* **2017**, *139* (40), 14041–14044.
- (74) Sau, A.; Palo-Nieto, C.; Galan, M. C. Substrate-Controlled Direct α -Stereoselective Synthesis of Deoxyglycosides from Glycals Using B(C₆F₅)₃ as Catalyst. *J. Org. Chem.* **2019**, *84* (5), 2415–2424.
- (75) Nicolaou, K. C.; Dolle, R. E.; Chucholowski, A.; Randall, J. L. Reactions of Glycosyl Fluorides. Synthesis of C-Glycosides. *J. Chem. Soc., Chem. Commun.* **1984**, No. 17, 1153–1154.
- (76) Guo, Z.-W.; Hui, Y.-Z. A New Strategy for the Stereoselective Syntheses of C-Glycosyl Compounds of β -Pentapyranoses. *Synth. Commun.* **1996**, *26* (11), 2067–2073.
- (77) Hunter, R.; Bartels, B.; Michael, J. P. Reduction of Activated Ketals with Borane-Dimethyl Sulphide. *Tet. Lett.* **1991**, *32* (8), 1095–1098.
- (78) Carpintero, M.; Nieto, I.; Fernández-Mayoralas, A. Stereospecific Synthesis of α - and β -C-Glycosides from Glycosyl Sulfoxides: Scope and Limitations. *J. Org. Chem.* **2001**, *66* (5), 1768–1774.
- (79) Jaramillo, C.; Corrales, G.; Fernández-Mayoralas, A. Glycosyl Phenyl Sulfoxides as a Source of Glycosyl Carbanions: Stereoselective Synthesis of C-Fucosides. *Tet. Lett.* **1998**, *39* (42), 7783–7786.
- (80) Seo, Y.; Gagné, M. R. Positional Selectivity in the Hydrosilylative Partial Deoxygenation of Disaccharides by Boron Catalysts. *ACS Catal.* **2018**, *8* (1), 81–85.
- (81) Seo, Y.; Lowe, J. M.; Gagné, M. R. Controlling Sugar Deoxygenation Products from Biomass by Choice of Fluoroarylborane Catalyst. *ACS Catal.* **2019**, *9* (8), 6648–6652.
- (82) Tamburrini, A.; Colombo, C.; Bernardi, A. Design and Synthesis of Glycomimetics: Recent Advances. *Medicinal Research Reviews* **2020**, *40* (2), 495–531.
- (83) Yang, Y.; Yu, B. Recent Advances in the Chemical Synthesis of C-Glycosides. *Chem. Rev.* **2017**, *117* (19), 12281–12356.

- (84) Zhu, F.; Rourke, M. J.; Yang, T.; Rodriguez, J.; Walczak, M. A. Highly Stereospecific Cross-Coupling Reactions of Anomeric Stannanes for the Synthesis of C-Aryl Glycosides. *J. Am. Chem. Soc.* **2016**, *138* (37), 12049–12052.
- (85) Zhu, F.; Rodriguez, J.; O'Neill, S.; Walczak, M. A. Acyl Glycosides through Stereospecific Glycosyl Cross-Coupling: Rapid Access to C(Sp³)-Linked Glycomimetics. *ACS Cent. Sci.* **2018**, *4* (12), 1652–1662.
- (86) Bouvet, V. R.; Ben, R. N. A Short and Economical Synthesis of Orthogonally Protected C-Linked 2-Deoxy-2-Acetamido- α -D-Galactopyranose Derivatives. *J. Org. Chem.* **2006**, *71* (9), 3619–3622.
- (87) Kancharla, P. K.; Navuluri, C.; Crich, D. Dissecting the Influence of Oxazolidinones and Cyclic Carbonates in Sialic Acid Chemistry. *Angew. Chem. Int. Ed.* **2012**, *51* (44), 11105–11109.
- (88) Vidal, S.; Bruyère, I.; Malleron, A.; Augé, C.; Praly, J.-P. Non-Isosteric C-Glycosyl Analogues of Natural Nucleotide Diphosphate Sugars as Glycosyltransferase Inhibitors. *Bioorganic & Medicinal Chemistry* **2006**, *14* (21), 7293–7301.
- (89) Chen, G.-R.; Praly, J.-P. Free-Radical and Ionic Routes towards Hydrolytically Stable and Bioactive C-Glycosyl Compounds. *Comptes Rendus Chimie* **2008**, *11* (1), 19–28.
- (90) Readman, S. K.; Marsden, S. P.; Hodgson, A. Nickel-Catalysed Synthesis of C-Glycosides and Deoxysugars from Glycosyl Bromides. *Synlett* **2000**, *2000* (11), 1628–1630.
- (91) Libnow, S.; Hein, M.; Langer, P. The First N-Glycosylated Indoxyls and Their Application to the Synthesis of Indirubin- *N* -Glycosides (Purple Sugars). *Synlett* **2009**, *2009* (02), 221–224.
- (92) Colombo, C.; Bernardi, A. Synthesis of α -N-Linked Glycopeptides. *Eur. J. Org. Chem.* **2011**, *2011* (20–21), 3911–3919.
- (93) Cumpstey, I.; Agrawal, S.; Borbas, K. E.; Martín-Matute, B. Iridium-Catalysed Condensation of Alcohols and Amines as a Method for Aminosugar Synthesis. *Chem. Commun.* **2011**, *47* (27), 7827–7829.
- (94) AL-Shuaeeb, R. A. A.; Montoir, D.; Alami, M.; Messaoudi, S. Synthesis of (1 \rightarrow 2)-S-Linked Saccharides and S-Linked Glycoconjugates via a Palladium-G3-XantPhos Precatalyst Catalysis. *J. Org. Chem.* **2017**, *82* (13), 6720–6728.
- (95) Belz, T.; Williams, S. J. A Building Block Approach to the Synthesis of a Family of S-Linked α -1,6-Oligomannosides. *Carbohydr. Res.* **2016**, *429*, 38–47.

- (96) Dondoni, A.; Marra, A. Recent Applications of Thiol–Ene Coupling as a Click Process for Glycoconjugation. *Chem. Soc. Rev.* **2012**, *41* (2), 573–586.
- (97) József, J.; Juhász, L.; Somsák, L. Thio-Click Reaction of 2-Deoxy- *Exo* -Glycals towards New Glycomimetics: Stereoselective Synthesis of *C* -2-Deoxy- *D* -Glycopyranosyl Compounds. *New Journal of Chemistry* **2019**, *43* (15), 5670–5686.
- (98) Frédéric, C. J.-M.; Cornil, J.; Vandamme, M.; Dumitrescu, L.; Tikad, A.; Robiette, R.; Vincent, S. P. Highly (*Z*)-Diastereoselective Synthesis of Trifluoromethylated *Exo* -Glycals via Photoredox and Copper Catalysis. *Org. Lett.* **2018**, *20* (21), 6769–6773.
- (99) Zhao, G.; Wang, T. Stereoselective Synthesis of 2-Deoxyglycosides from Glycals by Visible-Light-Induced Photoacid Catalysis. *Angew. Chem. Int. Ed.* **2018**, *57* (21), 6120–6124.
- (100) Li, J.; Zhao, G.; Wang, T. Organic-Photoacid-Catalyzed Glycosylation. *Synlett* **2020**, *31*, 823-828.
- (101) Margrey, K. A.; Nicewicz, D. A. A General Approach to Catalytic Alkene Anti-Markovnikov Hydrofunctionalization Reactions via Acridinium Photoredox Catalysis. *Acc. Chem. Res.* **2016**, *49* (9), 1997–2006.
- (102) Tolbert, L. M.; Solntsev, K. M. Excited-State Proton Transfer: From Constrained Systems to “Super” Photoacids to Superfast Proton Transfer. *Acc. Chem. Res.* **2002**, *35* (1), 19–27.
- (103) Badir, S. O.; Dumoulin, A.; Matsui, J. K.; Molander, G. A. Synthesis of Reversed *C*-Acyl Glycosides through Ni/Photoredox Dual Catalysis. *Angew. Chem. Int. Ed.* **2018**, *57* (22), 6610–6613.
- (104) Machida, S.; Mukai, S.; Kono, R.; Funato, M.; Saito, H.; Uchiyama, T. Synthesis and Comparative Structure–Activity Study of Carbohydrate-Based Phenolic Compounds as α -Glucosidase Inhibitors and Antioxidants. *Molecules* **2019**, *24* (23).
- (105) Verheggen, I.; Van Aerschot, A.; Toppet, S.; Snoeck, R.; Janssen, G.; Balzarini, J.; De Clercq, E.; Herdewijn, P. Synthesis and Antiherpes Virus Activity of 1,5-Anhydrohexitol Nucleosides. *J. Med. Chem.* **1993**, *36* (14), 2033–2040.
- (106) Saliba, R. C.; Pohl, N. L. Designing Sugar Mimetics: Non-Natural Pyranosides as Innovative Chemical Tools. *Current Opinion in Chemical Biology* **2016**, *34*, 127–134.
- (107) Rico, M.; Santoro, J. Complete Analysis of the ¹H NMR Spectra of Acetylated Glycals—a Conformational Study. *Organic Magnetic Resonance* **1976**, *8* (1), 49–55.

- (108) Liberek, B.; Tuwalska, D.; Konitz, A.; Sikorski, A. X-Ray Diffraction and High-Resolution NMR Spectroscopy of Methyl 3,4-Di-O-Acetyl-1,5-Anhydro-2-Deoxy-d-Arabino-Hex-1-Enopyranuronate. *Carbohydr. Res.* **2007**, *342* (9), 1280–1284.
- (109) Farmer, L. A.; Haidasz, E. A.; Griesser, M.; Pratt, D. A. Phenoxazine: A Privileged Scaffold for Radical-Trapping Antioxidants. *J. Org. Chem.* **2017**, *82* (19), 10523–10536.
- (110) Hanthorn, J. J.; Valgimigli, L.; Pratt, D. A. Incorporation of Ring Nitrogens into Diphenylamine Antioxidants: Striking a Balance between Reactivity and Stability. *J. Am. Chem. Soc.* **2012**, *134* (20), 8306–8309.
- (111) Wentrup, C. Carbenes and Nitrenes: Recent Developments in Fundamental Chemistry. *Angew. Chem. Int. Ed.* **2018**, *57* (36), 11508–11521.
- (112) Ray, K.; Heims, F.; Pfaff, F. F. Terminal Oxo and Imido Transition-Metal Complexes of Groups 9–11. *Eur. J. Inorg. Chem.* **2013**, *2013* (22-23), 3784–3807.
- (113) Halland, N.; Braunton, A.; Bachmann, S.; Marigo, M.; Jørgensen, K. A. Direct Organocatalytic Asymmetric α -Chlorination of Aldehydes. *J. Am. Chem. Soc.* **2004**, *126* (15), 4790–4791.
- (114) Hughes, D. L. The Mitsunobu Reaction. In *Organic Reactions*; American Cancer Society, 2004; pp 335–656.
- (115) Boyer, J. H.; Canter, F. C. Alkyl and Aryl Azides. *Chem. Rev.* **1954**, *54* (1), 1–57.
- (116) Swamy, K. C. K.; Kumar, N. N. B.; Balaraman, E.; Kumar, K. V. P. P. Mitsunobu and Related Reactions: Advances and Applications. *Chem. Rev.* **2009**, *109* (6), 2551–2651.
- (117) Jiang, B.; Yang, C.-G.; Wang, J. Enantioselective Synthesis of Marine Indole Alkaloid Hamacanthin B. *J. Org. Chem.* **2002**, *67* (4), 1396–1398.
- (118) Waser, J.; Nambu, H.; Carreira, E. M. Cobalt-Catalyzed Hydroazidation of Olefins: Convenient Access to Alkyl Azides. *J. Am. Chem. Soc.* **2005**, *127* (23), 8294–8295.
- (119) Hassner, A.; Fibiger, R.; Andisik, D. Synthetic Methods. 19. Lewis Acid Catalyzed Conversion of Alkenes and Alcohols to Azides. *J. Org. Chem.* **1984**, *49* (22), 4237–4244.
- (120) Breton, G. W.; Daus, K. A.; Kropp, P. J. Surface-Mediated Reactions. 2. Addition of Hydrazoic Acid to Alkenes. *J. Org. Chem.* **1992**, *57* (24), 6646–6649.

- (121) Kapat, A.; König, A.; Montermini, F.; Renaud, P. A Radical Procedure for the Anti-Markovnikov Hydroazidation of Alkenes. *J. Am. Chem. Soc.* **2011**, *133* (35), 13890–13893.
- (122) Lonca, G. H.; Ong, D. Y.; Tran, T. M. H.; Tejo, C.; Chiba, S.; Gagosz, F. Anti-Markovnikov Hydrofunctionalization of Alkenes: Use of a Benzyl Group as a Traceless Redox-Active Hydrogen Donor. *Angew. Chem. Int. Ed.* **2017**, *56* (38), 11440–11444.
- (123) Fu, N.; Sauer, G. S.; Saha, A.; Loo, A.; Lin, S. Metal-Catalyzed Electrochemical Diazidation of Alkenes. *Science* **2017**, *357* (6351), 575–579.
- (124) Siu, J. C.; Sauer, G. S.; Saha, A.; Macey, R. L.; Fu, N.; Chauviré, T.; Lancaster, K. M.; Lin, S. Electrochemical Azidooxygenation of Alkenes Mediated by a TEMPO–N₃ Charge-Transfer Complex. *J. Am. Chem. Soc.* **2018**, *140* (39), 12511–12520.
- (125) Wang, J.-J.; Yu, W. Anti-Markovnikov Hydroazidation of Alkenes by Visible-Light Photoredox Catalysis. *Chem. Eur. J.* **2019**, *25* (14), 3510–3514.
- (126) Li, H.; Shen, S.-J.; Zhu, C.-L.; Xu, H. Direct Intermolecular Anti-Markovnikov Hydroazidation of Unactivated Olefins. *J. Am. Chem. Soc.* **2019**, *141* (23), 9415–9421.
- (127) Shulgin, A.; Shulgin, A. *PIHKAL: A Chemical Love Story*; Transform Press, 1991.
- (128) Workentin, M. S.; Schepp, N. P.; Johnston, L. J.; Wayner, D. D. M. Solvation Control of Chemoselectivity in Reactions of Radical Cations. *J. Am. Chem. Soc.* **1994**, *116* (3), 1141–1142.
- (129) Schepp, N. P.; Johnston, L. J. Reactivity of Radical Cations. Effect of Radical Cation and Alkene Structure on the Absolute Rate Constants of Radical Cation Mediated Cycloaddition Reactions¹. *J. Am. Chem. Soc.* **1996**, *118* (12), 2872–2881.
- (130) Johnston, L. J.; Schepp, N. P. Reactivities of Radical Cations: Characterization of Styrene Radical Cations and Measurements of Their Reactivity toward Nucleophiles. *J. Am. Chem. Soc.* **1993**, *115* (15), 6564–6571.
- (131) Johnston, L. J.; Schepp, N. P. Laser Flash Photolysis Studies of the Reactivity of Styrene Radical Cations. *Pure Appl. Chem.* **1995**, *67* (1), 71–78.
- (132) Perkowski, A. J.; You, W.; Nicewicz, D. A. Visible Light Photoinitiated Metal-Free Living Cationic Polymerization of 4-Methoxystyrene. *J. Am. Chem. Soc.* **2015**, *137* (24), 7580–7583.

- (133) Onuska, N. P. R.; Schutzbach-Horton, M. E.; Collazo, J. L. R.; Nicewicz, D. A. Anti-Markovnikov Hydroazidation of Activated Olefins via Organic Photoredox Catalysis. *Synlett* **2019**.
- (134) Roughley, S. D.; Jordan, A. M. The Medicinal Chemist's Toolbox: An Analysis of Reactions Used in the Pursuit of Drug Candidates. *J. Med. Chem.* **2011**, *54* (10), 3451–3479.
- (135) Blakemore, D. C.; Castro, L.; Churcher, I.; Rees, D. C.; Thomas, A. W.; Wilson, D. M.; Wood, A. Organic Synthesis Provides Opportunities to Transform Drug Discovery. *Nature Chemistry; London* **2018**, *10* (4), 383–394.
- (136) Bunnett, J. F.; Zahler, R. E. Aromatic Nucleophilic Substitution Reactions. *Chem. Rev.* **1951**, *49* (2), 273–412.
- (137) Kwan, E. E.; Zeng, Y.; Besser, H. A.; Jacobsen, E. N. Concerted Nucleophilic Aromatic Substitutions. *Nature Chemistry; London* **2018**, *10* (9), 917–923.
- (138) Neumann, C. N.; Hooker, J. M.; Ritter, T. Concerted Nucleophilic Aromatic Substitution with 19 F⁻ and 18 F⁻. *Nature* **2016**, *534* (7607), 369–373.
- (139) Rohrbach, S.; Smith, A. J.; Pang, J. H.; Poole, D. L.; Tuttle, T.; Chiba, S.; Murphy, J. A. Concerted Nucleophilic Aromatic Substitution Reactions. *Angew. Chem. Int. Ed.* **2019**, *58* (46), 16368–16388.
- (140) Neumann, C. N.; Ritter, T. Facile C–F Bond Formation through a Concerted Nucleophilic Aromatic Substitution Mediated by the PhenoFluor Reagent. *Acc. Chem. Res.* **2017**, *50* (11), 2822–2833.
- (141) Roberts, J. D.; Simmons, H. E.; Carlsmith, L. A.; Vaughan, C. W. REARRANGEMENT IN THE REACTION OF CHLOROBENZENE-1-C14 WITH POTASSIUM AMIDE1. *J. Am. Chem. Soc.* **1953**, *75* (13), 3290–3291.
- (142) Heaney, H. The Benzyne and Related Intermediates. *Chem. Rev.* **1962**, *62* (2), 81–97.
- (143) Wenk, H. H.; Winkler, M.; Sander, W. One Century of Aryne Chemistry. *Angew. Chem. Int. Ed.* **2003**, *42* (5), 502–528.
- (144) Fine Nathel, N. F.; Morrill, L. A.; Mayr, H.; Garg, N. K. Quantification of the Electrophilicity of Benzyne and Related Intermediates. *J. Am. Chem. Soc.* **2016**, *138* (33), 10402–10405.
- (145) Medina, J. M.; Mackey, J. L.; Garg, N. K.; Houk, K. N. The Role of Aryne Distortions, Steric Effects, and Charges in Regioselectivities of Aryne Reactions. *J. Am. Chem. Soc.* **2014**, *136* (44), 15798–15805.

- (146) Terrier, F. The S_NAr Reactions: Mechanistic Aspects. In *Modern Nucleophilic Aromatic Substitution*; John Wiley & Sons, Ltd, 2013; pp 1–94.
- (147) Huisgen, R.; Sauer, J. Nucleophile Aromatische Substitutionen, IV. Umsetzungen Der Halogen-Benzole Und -Toluole Mit Lithium-Piperidid in Äther. *Chem. Ber.* **1958**, *91* (7), 1453–1460.
- (148) Cogolli, P.; Maiolo, F.; Testaferri, L.; Tingoli, M.; Tiecco, M. Nucleophilic Aromatic Substitution Reactions of Unactivated Aryl Halides with Thiolate Ions in Hexamethylphosphoramide. *J. Org. Chem.* **1979**, *44* (15), 2642–2646.
- (149) Rodriguez, J. R.; Agejas, J.; Bueno, A. B. Practical Synthesis of Aromatic Ethers by S_NAr of Fluorobenzenes with Alkoxides. *Tet. Lett.* **2006**, *47* (32), 5661–5663.
- (150) Hong, F.-E.; Lo, S.-C.; Liou, M.-W.; Chou, L.-F.; Lin, C.-C. Nucleophilic Substitution Reactions of (H6-Fluorotoluene)Cr(CO)₃ and (H6-Fluoroanisole)Cr(CO)₃ toward Phenylacetylide, Fluorenyl, Indolinyll and Carbazolinyll Lithium: Crystal Structures of Tricarbonyl[H6-(1,2-Diphenylethynyl)Benzene]Chromium and Tricarbonyl[H6-(1,4-Fluorenyl)Toluene]Chromium. *J. Organomet. Chem.* **1996**, *516* (1), 123–131.
- (151) Gilday, J. P.; Widdowson, D. A. Fluorine Directed Lithiation in Tricarbonylarenechromium(0) Complexes: The Regiospecific Synthesis of Polysubstituted Arenes. *Tet. Lett.* **1986**, *27* (45), 5525–5528.
- (152) Diness, F.; Fairlie, D. P. Catalyst-Free N-Arylation Using Unactivated Fluorobenzenes. *Angew. Chem. Int. Ed.* **2012**, *51* (32), 8012–8016.
- (153) Borch Jacobsen, C.; Meldal, M.; Diness, F. Mechanism and Scope of Base-Controlled Catalyst-Free N-Arylation of Amines with Unactivated Fluorobenzenes. *Chem. Eur. J.* **2017**, *23* (4), 846–851.
- (154) Huang, H.; Lambert, T. H. Electrophotocatalytic S_NAr Reactions of Unactivated Aryl Fluorides at Ambient Temperature and Without Base. *Angew. Chem. Int. Ed.* **2020**, *59* (2), 658–662.
- (155) Tay, N. E. S.; Nicewicz, D. A. Cation Radical Accelerated Nucleophilic Aromatic Substitution via Organic Photoredox Catalysis. *J. Am. Chem. Soc.* **2017**, *139* (45), 16100–16104.
- (156) Holmberg-Douglas, N.; Nicewicz, D. A. Arene Cyanation via Cation-Radical Accelerated-Nucleophilic Aromatic Substitution. *Org. Lett.* **2019**, *21* (17), 7114–7118.

- (157) Colomer, I.; Chamberlain, A. E. R.; Haughey, M. B.; Donohoe, T. J. Hexafluoroisopropanol as a Highly Versatile Solvent. *Nat Rev Chem* **2017**, *1* (11), 1–12.
- (158) Shida, N.; Imada, Y.; Nagahara, S.; Okada, Y.; Chiba, K. Interplay of Arene Radical Cations with Anions and Fluorinated Alcohols in Hole Catalysis. *Commun Chem* **2019**, *2* (1), 1–8.
- (159) Casavant, M. J. Fomepizole in the Treatment of Poisoning. *Pediatrics* **2001**, *107* (1), 170–170.
- (160) Bretschneider, T.; Koehler, A.; Fischer, R.; Fueslein, M.; Jeschke, P.; Kluth, J.; Muehlthau, F. A.; Voerste, A.; Malsam, O.; Goergens, U.; Sato, Y. Novel Heterocyclic Compounds as Pesticides. US2012095023 (A1).
- (161) Lançois, D. F. A.; Guillemont, J. É. G.; Raboisson, P. J.-M. B.; Roymans, D. A. E.; Rogovoy, B.; Bichko, V.; Lardeau, D. Y. R.; Michaut, A. B. Rsv Antiviral Pyrazolo- and Triazolo-Pyrimidine Compounds. WO2016174079 (A1).
- (162) Naim, M. J.; Alam, O.; Nawaz, F.; Alam, Md. J.; Alam, P. Current Status of Pyrazole and Its Biological Activities. *J Pharm Bioallied Sci* **2016**, *8* (1), 2–17.
- (163) Caccia, S.; Pasina, L.; Nobili, A. New Atypical Antipsychotics for Schizophrenia: Iloperidone. *Drug Des Devel Ther* **2010**, *4*, 33–48.
- (164) Schmittel, M.; Burghart, A. Understanding Reactivity Patterns of Radical Cations. *Angew. Chem. Int. Ed.* **1997**, *36* (23), 2550–2589.
- (165) McManus, J. B.; Onuska, N. P. R.; Nicewicz, D. A. Generation and Alkylation of α -Carbamyl Radicals via Organic Photoredox Catalysis. *J. Am. Chem. Soc.* **2018**, *140* (29), 9056–9060.
- (166) Choi, G. J.; Knowles, R. R. Catalytic Alkene Carboaminations Enabled by Oxidative Proton-Coupled Electron Transfer. *J. Am. Chem. Soc.* **2015**, *137* (29), 9226–9229.
- (167) Lee, J. C.; Francis, S.; Dutta, D.; Gupta, V.; Yang, Y.; Zhu, J.-Y.; Tash, J. S.; Schönbrunn, E.; Georg, G. I. Synthesis and Evaluation of Eight- and Four-Membered Iminosugar Analogues as Inhibitors of Testicular Ceramide-Specific Glucosyltransferase, Testicular β -Glucosidase 2, and Other Glycosidases. *J. Org. Chem.* **2012**, *77* (7), 3082–3098.
- (168) Tardieu, D.; Desnoyers, M.; Laye, C.; Hazelard, D.; Kern, N.; Compain, P. Stereoselective Synthesis of C,C-Glycosides from Exo-Glycals Enabled by Iron-Mediated Hydrogen Atom Transfer. *Org. Lett.* **2019**, *21* (18), 7262–7267.

- (169) Campbell, A S.; Lohman, G.; Plante, O. J. Synthetic Oligosaccharides for Moraxella Vaccine. WO2011137181 (A1).
- (170) Xiong, D.; Zhang, L.; Ye, X. Oxidant-Controlled Heck-Type C-Glycosylation of Glycals with Arylboronic Acids: Stereoselective Synthesis of Aryl 2-Deoxy-C-glycosides. *Org. Lett.*, **2009**, *11*, 1709-1712.
- (171) Kim, Y.; Oh, K.; Song, H.; Lee, D.-S.; Park, S. B. Synthesis and Biological Evaluation of α -Galactosylceramide Analogues with Heteroaromatic Rings and Varying Positions of a Phenyl Group in the Sphingosine Backbone. *J. Med. Chem.* **2013**, *56* (17), 7100–7109.
- (172) Czernecki, S.; Ayadi, E.; Randriamandimby, D. Seleno Glycosides. 2. Synthesis of Phenyl 2-(N-Acetylamino)- and 2-Azido-2-Deoxy-1-Seleno-.Alpha.-D-Glycopyranosides via Azido-Phenylselenylation of Diversely Protected Glycals. *J. Org. Chem.* **1994**, *59* (26), 8256–8260.
- (173) Shu, P.; Zeng, J.; Tao, J.; Zhao, Y.; Yao, G.; Wan, Q. Selective S-Deacetylation Inspired by Native Chemical Ligation: Practical Syntheses of Glycosyl Thiols and Drug Mercapto-Analogues. *Green Chem.* **2015**, *17* (4), 2545–2551.
- (174) Doyle, L. M.; O’Sullivan, S.; Di Salvo, C.; McKinney, M.; McArdle, P.; Murphy, P. V. Stereoselective Epimerizations of Glycosyl Thiols. *Org. Lett.* **2017**, *19* (21), 5802–5805.
- (175) Bruneau, A.; Roche, M.; Hamze, A.; Brion, J.-D.; Alami, M.; Messaoudi, S. Stereoretentive Palladium-Catalyzed Arylation, Alkenylation, and Alkynylation of 1-Thiosugars and Thiols Using Aminobiphenyl Palladacycle Precatalyst at Room Temperature. *Chem. Eur. J.* **2015**, *21* (23), 8375–8379.
- (176) Pichota, A.; Gramlich, V.; Beck, A. K.; Seebach, D. Preparation and Characterization of New C2- and C1-Symmetric Nitrogen, Oxygen, Phosphorous, and Sulfur Derivatives and Analogs of TADDOL. Part I. *Helvetica Chimica Acta* **2012**, *95* (8), 1239–1272.
- (177) Jana, M.; Misra, A. K. Stereoselective Synthesis of β -Glycosyl Thiols and Their Synthetic Applications. *J. Org. Chem.* **2013**, *78* (6), 2680–2686.
- (178) Moritomo, A.; Yamada, H.; Watanabe, T.; Itahana, H.; Akuzawa, S.; Okada, M.; Ohta, M. Synthesis and Structure–Activity Relationships of New Carbonyl Guanidine Derivatives as Novel Dual 5-HT_{2B} and 5-HT₇ Receptor Antagonists. *Bioorganic & Medicinal Chemistry* **2013**, *21* (24), 7841–7852.
- (179) Braga, F. G.; Coimbra, E. S.; de Oliveira Matos, M.; Lino Carmo, A. M.; Cancio, M. D.; da Silva, A. D. Synthesis and Biological Evaluation of Some 6-Substituted Purines. *Eur. J. Med. Chem.* **2007**, *42* (4), 530–537.

- (180) Kim, J. N.; Kim, K. M.; Ryu, E. K. Improved Synthesis of N-Alkoxyphthalimides. *Synth. Commun.* **1992**, *22* (10), 1427–1432.
- (181) Bakac, A.; Espenson, J. H. Unimolecular and Bimolecular Homolytic Reactions of Organochromium and Organocobalt Complexes. Kinetics and Equilibria. *J. Am. Chem. Soc.* **1984**, *106* (18), 5197–5202.
- (182) Matwiejuk, M.; Thiem, J. New Method for Regioselective Glycosylation Employing Saccharide Oxyanions. *Eur. J. Org. Chem.* **2011**, *2011* (29), 5860–5878.
- (183) Akhtar, T.; Cumpstey, I. Investigations into the Synthesis of Amine-Linked Neodisaccharides. *Tet. Lett.*, **2007**, *48*, 8673–8677.
- (184) McManus, J. B.; Nicewicz, D. A. Direct C–H Cyanation of Arenes via Organic Photoredox Catalysis. *J. Am. Chem. Soc.* **2017**, *139* (8), 2880–2883.
- (185) Zhu, Q.; Graff, D. E.; Knowles, R. R. Intermolecular Anti-Markovnikov Hydroamination of Unactivated Alkenes with Sulfonamides Enabled by Proton-Coupled Electron Transfer. *J. Am. Chem. Soc.* **2018**, *140* (2), 741–747.
- (186) Michigami, K.; Mita, T.; Sato, Y. Cobalt-Catalyzed Allylic C(Sp³)–H Carboxylation with CO₂. *J. Am. Chem. Soc.* **2017**, *139* (17), 6094–6097.
- (187) Lu, X.-L.; Shannon, M.; Peng, X.-S.; Wong, H. N. C. Stereospecific Iron-Catalyzed Carbon(Sp²)–Carbon(Sp³) Cross-Coupling with Alkylolithium and Alkenyl Iodides. *Org. Lett.* **2019**, *21* (8), 2546–2549.
- (188) Nakayama, K.; Maeta, N.; Horiguchi, G.; Kamiya, H.; Okada, Y. Radical Cation Diels–Alder Reactions by TiO₂ Photocatalysis. *Org. Lett.* **2019**, *21* (7), 2246–2250.
- (189) Brown, M.; Kumar, R.; Rehbein, J.; Wirth, T. Enantioselective Oxidative Rearrangements with Chiral Hypervalent Iodine Reagents. *Chem. Eur. J.* **2016**, *22* (12), 4030–4035.
- (190) Shin, J. H.; Seong, E. Y.; Mun, H. J.; Jang, Y. J.; Kang, E. J. Electronically Mismatched Cycloaddition Reactions via First-Row Transition Metal, Iron(III)–Polypyridyl Complex. *Org. Lett.* **2018**, *20* (18), 5872–5876.
- (191) Díaz-Álvarez, A. E.; Crochet, P.; Cadierno, V. A General Route for the Stereoselective Synthesis of (E)-(1-Propenyl)Phenyl Esters by Catalytic CC Bond Isomerization. *Tetrahedron* **2012**, *68* (12), 2611–2620.
- (192) Yu, J.; Ko, S. Y. The Synthesis of (R,S)-Reboxetine Employing a Tandem Cyclic Sulfate Rearrangement—Opening Process. *Tetrahedron: Asymmetry* **2012**, *23* (9), 650–654.

- (193) Miege, F.; Meyer, C.; Cossy, J. Rhodium-Catalyzed Cycloisomerization Involving Cyclopropenes: Efficient Stereoselective Synthesis of Medium-Sized Heterocyclic Scaffolds. *Angew. Chem. Int. Ed.* **2011**, *50* (26), 5932–5937.
- (194) Chen, C.; Jin, S.; Zhang, Z.; Wei, B.; Wang, H.; Zhang, K.; Lv, H.; Dong, X.-Q.; Zhang, X. Rhodium/Yanphos-Catalyzed Asymmetric Interrupted Intramolecular Hydroaminomethylation of Trans-1,2-Disubstituted Alkenes. *J. Am. Chem. Soc.* **2016**, *138* (29), 9017–9020.
- (195) Kabalka, G. W.; Tejedor, D.; Li, N.-S.; Malladi, R. R.; Trotman, S. A Tandem Aldol-Grob Reaction of Ketones with Aromatic Aldehydes. *Tetrahedron* **1998**, *54* (51), 15525–15532.
- (196) Lara, M.; Mutti, F. G.; Glueck, S. M.; Kroutil, W. Biocatalytic Cleavage of Alkenes with O₂ and *Trametes Hirsuta* G FCC 047. *Eur. J. Org. Chem.* **2008**, *2008* (21), 3668–3672.
- (197) Srimani, D.; Leitus, G.; Ben-David, Y.; Milstein, D. Direct Catalytic Olefination of Alcohols with Sulfones. *Angew. Chem. Int. Ed.* **2014**, *53* (41), 11092–11095.
- (198) Berthiol, F.; Doucet, H.; Santelli, M. Heck Reaction of Aryl Bromides with Pent-4-En-2-ol, 2-Phenylpent-4-en-2-ol, or Hept-6-en-3-ol Catalysed by a Palladium-Tetraphosphine Complex. *Synthesis* **2005**, *2005* (20), 3589–3602.
- (199) Suzuki, T.; Ota, Y.; Ri, M.; Bando, M.; Gotoh, A.; Itoh, Y.; Tsumoto, H.; Tatum, P. R.; Mizukami, T.; Nakagawa, H.; Iida, S.; Ueda, R.; Shirahige, K.; Miyata, N. Rapid Discovery of Highly Potent and Selective Inhibitors of Histone Deacetylase 8 Using Click Chemistry to Generate Candidate Libraries. *J. Med. Chem.* **2012**, *55* (22), 9562–9575.
- (200) Peng, B.; Thorsell, A.-G.; Karlberg, T.; Schüler, H.; Yao, S. Q. Small Molecule Microarray Based Discovery of PARP14 Inhibitors. *Angew. Chem. Int. Ed.* **2017**, *56* (1), 248–253.
- (201) Amegadzie, A. K.; Gardinier, K. M.; Hembre, E. J.; Hipskind, P. A.; Jungheim, L. N.; Muehl, B. S.; Savin, K. A.; Thrasher, K. J.; Boyd, S. A. Tachykinin Receptor Antagonists. WO2005000821 (A1).
- (202) Zhu, Y.; Li, X.; Wang, X.; Huang, X.; Shen, T.; Zhang, Y.; Sun, X.; Zou, M.; Song, S.; Jiao, N. Silver-Catalyzed Decarboxylative Azidation of Aliphatic Carboxylic Acids. *Org. Lett.* **2015**, *17* (19), 4702–4705.
- (203) Bowers, N. I.; Boyd, D. R.; Sharma, N. D.; Goodrich, P. A.; Grocock, M. R.; Blacker, A. J.; Goode, P.; Dalton, H. Stereoselective Benzylic Hydroxylation of 2-Substituted Indanes Using Toluene Dioxygenase as Biocatalyst. *J. Chem. Soc., Perkin Trans. 1* **1999**, No. 11, 1453–1462.

- (204) Barluenga, J.; Tomás-Gamasa, M.; Valdés, C. Reductive Azidation of Carbonyl Compounds via Tosylhydrazone Intermediates Using Sodium Azide. *Angew. Chem. Int. Ed.* **2012**, *51* (24), 5950–5952.
- (205) Barlow, J. W.; Walsh, J. J. Synthesis and Evaluation of Dimeric 1,2,3,4-Tetrahydro-Naphthalenylamine and Indan-1-Ylamine Derivatives with Mast Cell-Stabilising and Anti-Allergic Activity. *Eur. J. Med. Chem.* **2010**, *45* (1), 25–37.
- (206) Kapat, A.; König, A.; Montermini, F.; Renaud, P. A Radical Procedure for the Anti-Markovnikov Hydroazidation of Alkenes. *J. Am. Chem. Soc.* **2011**, *133* (35), 13890–13893.
- (207) Nyfeler, E.; Renaud, P. Decarboxylative Radical Azidation Using MPDOC and MMDOC Esters. *Org. Lett.* **2008**, *10* (5), 985–988.
- (208) Waser, J.; Nambu, H.; Carreira, E. M. Cobalt-Catalyzed Hydroazidation of Olefins: Convenient Access to Alkyl Azides. *J. Am. Chem. Soc.* **2005**, *127* (23), 8294–8295.
- (209) Rosenau, C. P.; Jelier, B. J.; Gossert, A. D.; Togni, A. Exposing the Origins of Irreproducibility in Fluorine NMR Spectroscopy. *Angew. Chem. Int. Ed.* **2018**, *57* (30), 9528–9533.
- (210) Martiny, M.; Steckhan, E.; Esch, T. Cycloaddition Reactions Initiated by Photochemically Excited Pyrylium Salts. *Chem. Ber.* **1993**, *126* (7), 1671–1682.
- (211) Michaelides, M.; Hansen, T.; Dai, Y.; Zhu, G.; Frey, R.; Gong, J.; Penning, T.; Curtin, M.; McClellan, W.; Clark, R.; Torrent, M.; Mastracchio, A.; Kesicki, E. a; Kluge, A. F.; Patane, M. a; Van, D. J. H. J.; Ji, Z.; Lai, C. C.; Wang, C. Spirocyclic Hat Inhibitors and Methods for Their Use. WO2016044770 (A1).
- (212) Parsons, J. G.; Stachurska-Buczek, D.; Choi, N.; Griffiths, P. G.; Huggins, D. A.; Krywult, B. M.; Marino, S. T.; Nguyen, T.; Sheehan, C. S.; James, I. W.; Bray, A. M.; White, J. M.; Boyce, R. S. Chiral Building Blocks: Enantioselective Syntheses of Benzyloxymethyl Phenyl Propionic Acids. *Molecules* **2004**, *9* (6), 449–458.
- (213) Munday, R. H.; Martinelli, J. R.; Buchwald, S. L. Palladium-Catalyzed Carbonylation of Aryl Tosylates and Mesylates. *J. Am. Chem. Soc.* **2008**, *130* (9), 2754–2755.
- (214) Ritter, T.; Stanek, K.; Larrosa, I.; Carreira, E. M. Mild Cleavage of Aryl Mesylates: Methanesulfonate as Potent Protecting Group for Phenols. *Org. Lett.* **2004**, *6* (9), 1513–1514.
- (215) Lauber, M. B.; Stahl, S. S. Efficient Aerobic Oxidation of Secondary Alcohols at Ambient Temperature with an ABNO/NO_x Catalyst System. *ACS Catal.* **2013**, *3* (11), 2612–2616.

- (216) Frost, J. R.; Huber, S. M.; Breitenlechner, S.; Bannwarth, C.; Bach, T. Enantiotopos-Selective C-H Oxygenation Catalyzed by a Supramolecular Ruthenium Complex. *Angew. Chem. Int. Ed.* **2015**, *54* (2), 691–695.
- (217) Taylor, N. J.; Emer, E.; Preshlock, S.; Schedler, M.; Tredwell, M.; Verhoog, S.; Mercier, J.; Genicot, C.; Gouverneur, V. Derisking the Cu-Mediated 18F-Fluorination of Heterocyclic Positron Emission Tomography Radioligands. *J. Am. Chem. Soc.* **2017**, *139* (24), 8267–8276.
- (218) Chen, C.; Andreani, T.; Li, H. A Divergent and Selective Synthesis of Isomeric Benzoxazoles from a Single N–Cl Imine. *Org. Lett.* **2011**, *13* (23), 6300–6303.
- (219) Senaweera, S.; Weaver, J. D. S_NAr Catalysis Enhanced by an Aromatic Donor–Acceptor Interaction; Facile Access to Chlorinated Polyfluoroarenes. *Chem. Commun.* **2017**, *53* (54), 7545–7548.
- (220) Claudi, F.; Cardellini, M.; Cingolani, G. M.; Piergentili, A.; Peruzzi, G.; Balduini, W. Synthesis and Dopamine Receptor Affinities of 2-(4-Fluoro-3-Hydroxyphenyl)Ethylamine and N-Substituted Derivatives. *J. Med. Chem.* **1990**, *33* (9), 2408–2412.
- (221) Gao, M.; Sun, D.; Gong, H. Ni-Catalyzed Reductive C–O Bond Arylation of Oxalates Derived from α -Hydroxy Esters with Aryl Halides. *Org. Lett.* **2019**, *21* (6), 1645–1648.
- (222) Chen, H.; Yang, H.; Li, N.; Xue, X.; He, Z.; Zeng, Q. Palladium-Catalyzed C–N Cross-Coupling of NH-Heteroarenes and Quaternary Ammonium Salts via C–N Bond Cleavage. *Org. Process Res. Dev.* **2019**, *23* (8), 1679–1685.
- (223) Sato, T.; Yoshida, T.; Al Mamari, H. H.; Ilies, L.; Nakamura, E. Manganese-Catalyzed Directed Methylation of C(Sp²)–H Bonds at 25 °C with High Catalytic Turnover. *Org. Lett.* **2017**, *19* (19), 5458–5461.
- (224) Sinha, S.; Sikari, R.; Sinha, V.; Jash, U.; Das, S.; Brandão, P.; Demeshko, S.; Meyer, F.; Bruin, B. de; Paul, N. D. Iron-Catalyzed/Mediated C–N Bond Formation: Competition between Substrate Amination and Ligand Amination. *Inorganic Chemistry* **2019**.
- (225) Batchu, H.; Bhattacharyya, S.; Kant, R.; Batra, S. Palladium-Catalyzed Chelation-Assisted Regioselective Oxidative Dehydrogenative Homocoupling/Ortho-Hydroxylation in N-Phenylpyrazoles. *J. Org. Chem.* **2015**, *80* (15), 7360–7374.
- (226) Schneider, Y.; Prévost, J.; Gobin, M.; Legault, C. Y. Diazirines as Potent Electrophilic Nitrogen Sources: Application to the Synthesis of Pyrazoles. *Org. Lett.* **2014**, *16* (2), 596–599.

- (227) Alex, K.; Tillack, A.; Schwarz, N.; Beller, M. Zinc-Catalyzed Synthesis of Pyrazolines and Pyrazoles via Hydrohydrazination. *Org. Lett.* **2008**, *10* (12), 2377–2379.
- (228) Zhang, Q.; Meng, L.-G.; Wang, K.; Wang, L. NBu₃P-Catalyzed Desulfonylative [3 + 2] Cycloadditions of Allylic Carbonates with Arylazosulfones to Pyrazole Derivatives. *Org. Lett.* **2015**, *17* (4), 872–875.
- (229) Yang, N.; Yuan, G. A Multicomponent Electrosynthesis of 1,5-Disubstituted and 1-Aryl 1,2,4-Triazoles. *J. Org. Chem.* **2018**, *83* (19), 11963–11969.
- (230) Giel, M.-C.; Smedley, C. J.; Mackie, E. R. R.; Guo, T.; Dong, J.; Costa, T. P. S. da; Moses, J. E. Metal-Free Synthesis of Functional 1-Substituted-1,2,3-Triazoles from Ethenesulfonyl Fluoride and Organic Azides. *Angew. Chem. Int. Ed.* **2020**, *59* (3), 1181–1186.
- (231) Palanivel, A.; Mubeen, S.; Warner, T.; Ahmed, N.; Clive, D. L. J. Formation of Enol Ethers by Radical Decarboxylation of α -Alkoxy β -Phenylthio Acids. *J. Org. Chem.* **2019**, *84* (19), 12542–12552.
- (232) Zeitler, K.; Rose, C. A. An Efficient Carbene-Catalyzed Access to 3,4-Dihydrocoumarins. *J. Org. Chem.* **2009**, *74* (4), 1759–1762.
- (233) Li, Z.; Yu, H.; Bolm, C. Dibenzothiophene Sulfoximine as an NH₃ Surrogate in the Synthesis of Primary Amines by Copper-Catalyzed C–X and C–H Bond Amination. *Angew. Chem. Int. Ed.* **2017**, *56* (32), 9532–9535.
- (234) Yang, X.-Y.; Zhao, H.-Y.; Mao, S.; Zhang, S.-Q. Copper-Mediated Monochlorination of Anilines and Nitrogen-Containing Heterocycles. *Synth. Commun.* **2018**, *48* (20), 2708–2714.
- (235) Lin, D. W.; Masuda, T.; Biskup, M. B.; Nelson, J. D.; Baran, P. S. Synthesis-Guided Structure Revision of the Sarcodonin, Sarcoviolin, and Hydnellin Natural Product Family. *J. Org. Chem.* **2011**, *76* (4), 1013–1030.
- (236) Zhang, X.; Priestley, E. S.; Bates, J. A.; Halpern, O. S.; Reznik, S. K.; Richter, J. M. Bicyclic Heteroaryl Substituted Compounds, January 18, 2018.
- (237) Amant, A. H. S.; Frazier, C. P.; Newmeyer, B.; Fruehauf, K. R.; Alaniz, J. R. de. Direct Synthesis of Anilines and Nitrosobenzenes from Phenols. *Org. Biomol. Chem.* **2016**, *14* (24), 5520–5524.
- (238) Vo, G. D.; Hartwig, J. F. Palladium-Catalyzed Coupling of Ammonia with Aryl Chlorides, Bromides, Iodides, and Sulfonates: A General Method for the Preparation of Primary Arylamines. *J. Am. Chem. Soc.* **2009**, *131* (31), 11049–11061.

- (239) Hyodo, K.; Hasegawa, G.; Maki, H.; Uchida, K. Deacetylative Amination of Acetyl Arenes and Alkanes with C–C Bond Cleavage. *Org. Lett.* **2019**, *21* (8), 2818–2822.
- (240) Budén, M. E.; Guastavino, J. F.; Rossi, R. A. Room-Temperature Photoinduced Direct C–H-Arylation via Base-Promoted Homolytic Aromatic Substitution. *Org. Lett.* **2013**, *15* (6), 1174–1177.
- (241) Castro, L. C. M.; Sortais, J.-B.; Darcel, C. NHC-Carbene Cyclopentadienyl Iron Based Catalyst for a General and Efficient Hydrosilylation of Imines. *Chem. Commun.* **2011**, *48* (1), 151–153.
- (242) Lenze, M.; Martin, E. T.; Rath, N. P.; Bauer, E. B. Iron(II) α -Aminopyridine Complexes and Their Catalytic Activity in Oxidation Reactions: A Comparative Study of Activity and Ligand Decomposition. *ChemPlusChem* **2013**, *78* (1), 101–116.
- (243) Sreenath, K.; Yuan, Z.; Macias-Contreras, M.; Ramachandran, V.; Clark, R. J.; Zhu, L. Dual Role of Acetate in Copper(II) Acetate Catalyzed Dehydrogenation of Chelating Aromatic Secondary Amines: A Kinetic Case Study of Copper-Catalyzed Oxidation Reactions. *Eur. J. Inorg. Chem.* **2016**, *2016* (23), 3728–3743.
- (244) Tu, Y.; Yuan, L.; Wang, T.; Wang, C.; Ke, J.; Zhao, J. Palladium-Catalyzed Oxidative Carbonylation of Aryl Hydrazines with CO and O₂ at Atmospheric Pressure. *J. Org. Chem.* **2017**, *82* (9), 4970–4976.
- (245) Subramanian, K.; Yedage, S. L.; Bhanage, B. M. Electrodimerization of N-Alkoxyamides for Zinc(II) Catalyzed Phenolic Ester Synthesis under Mild Reaction Conditions. *Adv. Synth. Catal.* **2018**, *360* (13), 2511–2521.
- (246) Fuse, H.; Kojima, M.; Mitsunuma, H.; Kanai, M. Acceptorless Dehydrogenation of Hydrocarbons by Noble-Metal-Free Hybrid Catalyst System. *Org. Lett.* **2018**, *20* (7), 2042–2045.
- (247) Seni, A. A.; Kollár, L.; Mika, L. T.; Pongrácz, P. Rhodium-Catalysed Aryloxycarbonylation of Iodo-Aromatics by 4-Substituted Phenols with Carbon Monoxide or Paraformaldehyde. *Molecular Catalysis* **2018**, *457*, 67–73.
- (248) Herrmann, J. M.; Untergehrer, M.; Jürgenliemk, G.; Heilmann, J.; König, B. Synthesis of Phenyl-1-Benzoxepinols Isolated from Butcher's Broom and Analogous Benzoxepines. *Eur. J. Org. Chem.* **2014**, *2014* (15), 3170–3181.
- (249) Worthy, A. D.; Joe, C. L.; Lightburn, T. E.; Tan, K. L. Application of a Chiral Scaffolding Ligand in Catalytic Enantioselective Hydroformylation. *J. Am. Chem. Soc.* **2010**, *132* (42), 14757–14759.

- (250) Sakai, N.; Hori, H.; Ogiwara, Y. Copper(II)-Catalyzed [4+1] Annulation of Propargylamines with N,O-Acetals: Entry to the Synthesis of Polysubstituted Pyrrole Derivatives. *Eur. J. Org. Chem.* **2015**, 2015 (9), 1905–1909.
- (251) Ding, X.; Huang, M.; Yi, Z.; Du, D.; Zhu, X.; Wan, Y. Room-Temperature CuI-Catalyzed Amination of Aryl Iodides and Aryl Bromides. *J. Org. Chem.* **2017**, 82 (10), 5416–5423.
- (252) Tu, X.-S.; Zeng, N.-N.; Li, R.-Y.; Zhao, Y.-Q.; Xie, D.-Z.; Peng, Q.; Wang, X.-C. C2-Symmetric Bicyclic Bisborane Catalysts: Kinetic or Thermodynamic Products of a Reversible Hydroboration of Dienes. *Angew. Chem. Int. Ed.* **2018**, 57 (46), 15096–15100.
- (253) Renzi, P.; Hioe, J.; Gschwind, R. M. Decrypting Transition States by Light: Photoisomerization as a Mechanistic Tool in Brønsted Acid Catalysis. *J. Am. Chem. Soc.* **2017**, 139 (19), 6752–6760.
- (254) Luu, Q. H.; Guerra, J. D.; Castañeda, C. M.; Martinez, M. A.; Saunders, J.; Garcia, B. A.; Gonzales, B. V.; Aidunuthula, A. R.; Mito, S. Ultrasound Assisted One-Pot Synthesis of Benzo-Fused Indole-4,9-Dinones from 1,4-Naphthoquinone and α -Aminoacetals. *Tet. Lett.* **2016**, 57 (21), 2253–2256.
- (255) Moon, H. K.; Sung, G. H.; Kim, B. R.; Park, J. K.; Yoon, Y.-J.; Yoon, H. J. One for Many: A Universal Reagent for Acylation Processes. *Adv. Synth. Catal.* **2016**, 358 (11), 1725–1730.
- (256) Wang, W.; Liu, H.; Xu, S.; Gao, Y. Esterification Catalysis by Pyridinium P-Toluenesulfonate Revisited—Modification with a Lipid Chain for Improved Activities and Selectivities. *Synth. Commun.* **2013**, 43 (21), 2906–2912.
- (257) A. Miranda, M.; Rosa Diaz-Mondar, M. Photolysis of 2-Aryloxy- or 2-Arylthio-1,3-Benzodioxan-4-Ones. *Heterocycles* **1984**, 22 (5), 1125.
- (258) Kitano, H.; Ito, H.; Itami, K. Palladium-Catalyzed Esterification of Carboxylic Acids with Aryl Iodides. *Org. Lett.* **2018**, 20 (8), 2428–2432.